αPS3βPS1 INTEGRIN AND ITS ADAPTOR TALIN ARE ESSENTIAL FOR *DROSOPHILA* EMBRYONIC HEART TUBULOGENESIS

αPS3βPS1 INTEGRIN AND ITS ADAPTOR TALIN ARE ESSENTIAL FOR *DROSOPHILA* EMBRYONIC HEART TUBULOGENESIS

BY

JESSICA LYNN VANDERPLOEG, B. Sc.

A thesis

Submitted to the School of Graduate Studies

in Partial Fulfillment of the Requirements

for the Degree

Doctor of Philosophy

McMaster University

DOCTOR OF PHILOSOPHY (2014) McMaster University

(Biology) Hamilton, Ontario

TITLE: αPS3βPS1 Integrin and its adaptor Talin are essential for *Drosophila* embryonic heart tubulogenesis

AUTHOR: Jessica Lynn Vanderploeg, B. Sc. (Trinity Western University)

SUPERVISOR: Dr. J. Roger Jacobs

NUMBER OF PAGES: xviii, 278

ABSTRACT

Formation of a tubular organ, such as the heart, requires cells to integrate positional and polarity signals in order to enclose a fluid or gas transporting lumen. Developing tubes must establish a site for lumen initiation, demarcate membrane domains, and modulate cell polarization and morphology. The *Drosophila melanogaster* embryonic heart is a mesodermal tube model displaying a unique polarity, reminiscent of vertebrate vasculature. We have characterized a role for the transmembrane adhesion receptor αPS3βPS1 integrin and its cytoplasmic adaptor Talin in heart tubulogenesis. βPS1 and Talin are early indicators of the luminal site and Talin-mediated integrin function is essential for cardioblast polarization and morphology prior to and during lumen development. Careful analysis of hearts in embryos homozygous for a null allele of *rhea*, the gene encoding Talin, reveals that Talin is required to correctly orient the heart cell polarity such that a continuous central open lumen is enclosed. Without proper integrin or Talin function, the luminal determinants Slit and its receptor Robo are not stabilized within the heart, a central lumen fails to form, and the midline is instead marked by continuous adhesion. Furthermore, although Talin is essential for proper βPS1 integrin localization within the heart, either of Talin's two integrin binding sites are sufficient to stabilize βPS1 along the luminal domain and establish an open cardiac tube. Taken together, our findings reveal an instructive role for integrins and Talin in communicating polarization cues central to heart tubulogenesis.

ACKNOWLEDGEMENTS

First of all, I would like to extend a most sincere thank-you to my supervisor and mentor, Dr. Roger Jacobs. Throughout my time here at McMaster, you have guided, encouraged, and challenged me to achieve and surpass my research, graduate education, and career goals. Thank you for believing in your students and giving so much of your time and energy, often at a moment's notice, whenever we needed your help.

Thank you also to my committee members, Dr. Ana Campos and Dr. Juliet Daniel. You have both sought to challenge and motivate me, not only through your scientific critiques at committee meetings, but through informal meetings as you mentored me along my research and career paths, offering unique perspectives along the way. In addition, I extend my appreciation to Dr. Bhagwati Gupta for taking the time to fill in for Dr. Campos in the latter stages of my degree and at my defense examination.

To those past and present members in the Jacobs' lab and extended McMaster Biology community, thank you for your incredible support and encouragement these past five years. Lulu Vazquez Mitchell and Dr. Mihaela Georgescu, thank you for taking me under your wing when I first started in the lab, training me and encouraging me in my studies. Qamber Syed, my partner in crime since the beginning – thanks for the many stories, laughter, camping memories, and often lengthy afternoon conversations about science, overseas politics, and other random topics. Xioali, although not an official member of the Jacobs' lab crew, thank you for our many "fly room" conversations, for

sharing your fly pushing tricks, research and career advice, and, of course, your tasty spring rolls!

Lastly, I would like to thank my friends and family who have supported me throughout this journey. To my family out west, who never complained about the short visits squeezed between stock flips, thank you for encouraging me and supporting me in so many ways! To my Kuizenga “adopted” family, thank you for welcoming me into your home and putting up with an often frazzled and busy grad student. To my friends, thank you for trying to understand what I do (and for feigning interest even if you didn’t!), and for encouraging me to take time away from the lab when school was overwhelming.

TABLE OF CONTENTS

		PAGE
Title Page		i
Descriptive Note		ii
Abstract		iii
Acknowledgements		iv
Table of Contents		vi
List of Figures		xi
List of Tables		xv
List of Abbreviations		xvi
1.0	**CHAPTER ONE**: **INTRODUCTION**	**1**
1.1	The structure of the tubular *Drosophila melanogaster* embryonic heart	5
1.2	How do lumen-enclosing vessels develop?	6
	1.2.1 Morphological diversity in development of tubular organs	6
	1.2.2 Basic design principles common to diverse tubulogenesis events	10
	Determine the site of lumen formation	11
	Establish polarity and specify membrane domains	12
	Develop a luminal space	13
	Expand the lumen diameter	14
	1.2.3 Importance of studying the diverse mechanisms underlying basic design principles	15
1.3	The *Drosophila melanogaster* heart as a model of vertebrate cardiogenesis	16
	1.3.1 Importance of cardiac research	16
	1.3.2 Conservation of cardiac disease genes in *Drosophila*	17
	1.3.3 Benefits of studying cardiac tubulogenesis in the *Drosophila* model	18
1.4	Key stages of *Drosophila* embryonic heart development	19
	1.4.1 Specification and alignment of heart progenitors	19
	1.4.2 Migration of cardial cells to the dorsal midline	23
	1.4.3 Lumen formation	26
1.5	Cardioblast polarization during lumen formation	27
	1.5.1 A central role for Robo & Slit	27
	1.5.2 Additional luminal domain factors	29
	Unc5 and Netrin	29

Syndecan 29
Dystroglycan 30
Extracellular matrix 30
1.5.3 Dorsal and ventral midline adhesion 31
1.5.4 Lateral adhesion between neighboring cardioblasts 31
1.5.5 Basal cardioblast surfaces 32
1.6 The integrin heterodimer as an intriguing candidate to play an instructive role in *Drosophila* embryonic heart development 32
1.7 Integrin based adhesion and signaling 34
1.7.1 The integrin adhesome 34
Talin 37
Scaffold adaptor proteins and actin regulators 38
Signaling or regulatory proteins 39
1.7.2 Extracellular matrix integrin ligands 40
1.7.3 *In vitro* cell culture studies highlight a role for integrins in ECM adhesion 41
1.7.4 Integrin adhesion is essential in developing tissues 43
Integrin adhesion is essential in mice 43
Integrin adhesion is essential in *Drosophila melanogaster* 45
1.8 Thesis objectives 48

2.0 **CHAPTER TWO**: **METHODS** **49**
2.1 Acknowledgments 50
2.2 Fly maintenance 51
2.3 Genetic strains 51
2.4 Antibody production 55
2.4.1 Rabbit anti-MEF 55
2.4.1a Induction of His-dMEF2 fusion protein 55
2.4.1b Purification of His-dMEF2 fusion protein 56
2.4.1c Preparation of His-dMEF antiserum 57
2.4.1d Collection of His-dMEF antiserum 58
2.4.2 Chicken anti-βGal 58
2.4.2a Generation of egg yolk antibodies (IgY) against βGal 58
2.4.2b Collection of eggs 59
2.4.2c Isolation of chicken immunoglobulins (IgY) against βGal 59
2.4.3 Rabbit anti-Dystroglycan 60
2.4.3a Induction of GST-Dystroglycan (Dg) fusion protein 60
2.4.3b Purification of GST-Dg fusion protein 61

2.4.3c Preparation of GST-Dg antiserum 62
2.4.3d Collection of GST-Dg antiserum 62
2.4.4 Generation of LanA monoclonal antibody (Mouse anti-LamininA) 63
2.5 Immunohistochemistry 63
2.5.1 Embryo collection 63
2.5.2 Fixation 64
2.5.3 Immunolabeling 64
2.5.4 Imaging and image processing 66
2.5.5 Antibodies used 66
2.6 Live imaging 69
2.6.1 Imaging 70
2.6.2 Processing and quantification 70
2.7 Electron microscopy 70
2.8 Maternal and zygotic mutant embryos 71
2.9 Rescues 72
2.10 Embryo scoring 72
2.11 Western blots 73
2.11.1 Embryo collections 73
2.11.2 Sample prep 73
2.11.3 Western Blot procedure 74
2.11.4 Quantification 74

3.0 CHAPTER THREE: INTEGRINS ARE REQUIRED FOR CARDIOBLAST POLARIZATION IN *DROSOPHILA*. 75
3.1 Preface and explanation of contributions 76
3.2 Introduction 77
3.3 Results 78
3.3.1 αPS3βPS1 integrin is required for apical and basal polarity of cardioblasts. 78
3.3.2 Integrins are required for heart lumen formation 84
3.3.3 Integrins are required for CB polarization 89
3.3.4 Integrins are required for robust leading edge motility 95
3.3.5 Integrins interact genetically with genes for adhesion signaling 98
3.4 Discussion 102
3.5 Conclusions 104

4.0 CHAPTER FOUR: TALIN-MEDIATED INTEGRIN ADHESION IN *DROSOPHILA* EMBRYONIC HEART ASSEMBLY **106**
4.1 Introduction 107
4.1.1 Talin is an intriguing candidate to mediate integrin adhesion in *Drosophila* embryonic heart development 107
4.1.2 Talin is essential for integrin adhesion in *Drosophila melanogaster* 108
4.1.3 The Talin protein has two binding sites for β-integrin 109
4.2 Results 113
4.2.1 Talin localization during *Drosophila* embryonic heart development 113
4.2.2 Mutations in the gene *rhea* deplete the embryo of Talin 118
4.2.3 βPS Integrin is disrupted in *rhea* mutant embryos 122
4.2.4 Talin is required for normal localization of extracellular and intracellular integrin-related proteins 122
4.2.5 Loss of Talin disrupts cardioblast polarity 130
4.2.6 Talin is required for formation of an open lumen 136
4.2.7 Talin is required during cardioblast migration 137
4.2.8 *rhea*^{79} interacts genetically with mutations in genes for integrin adhesion 147
4.2.9 Neither IBS1- nor IBS2-mediated integrin binding is essential for Talin's role in tubulogenesis 151
4.3 Discussion 163
4.4 Conclusion 167

5.0 CHAPTER FIVE: DISCUSSION **168**
5.1 Integrin and Talin in *Drosophila* heart development 169
5.2 *Drosophila* heart tubulogenesis as an *in vivo* model to study the mechanism of integrin adhesions 175
5.3 *Drosophila* heart development as a unique model of tubulogenesis 183
5.4 Conclusion 187

REFERENCES **188**

APPENDIX A: SUPPLEMENTAL METHODS INFORMATION **219**

APPENDIX B: SUPPLEMENTAL INTEGRIN INFORMATION **230**

APPENDIX C: SUPPLEMENTAL TALIN INFORMATION **233**

APPENDIX D: *SRC42A* IS REQUIRED FOR CARDIOBLAST MIGRATION, BUT NOT LUMEN FORMATION **246**

D.1 Introduction 247
- **D.1.1** Src42A and Src64B 248
- **D.1.2** Fak56D 249

D.2 Results and Discussion 250
- **D.2.1** Loss of Src42A, but not Src64B, results in incomplete cardioblast migration 250
- **D.2.2** Mutations in *fak56D* do not enhance the *src42A*^{E1} phenotype 253
- **D.2.3** Heart specific disruption of Src42A does not prevent cardioblast migration 256
- **D.2.4** Src42A is required for leading edge membrane activity in the posterior heart 259
- **D.2.5** In *src42A*^{E1} embryos, amnioserosa cells at the midline inhibit cardioblast migration 262
- **D.2.6** Src42A is not essential for lumen formation 265

D.3 Conclusion 271

APPENDIX E: RECIPES FOR COMMON REAGENTS **272**

APPENDIX F: TIMELAPSE MOVIES **277**

LIST OF FIGURES

Figure 1.1 *Drosophila* embryonic heart development as a model of tubulogenesis

Figure 1.2 Shared basic design principles underlie diverse tubulogenesis events

Figure 1.3 *Drosophila* heart development shares key similarities with early vertebrate cardiogenesis

Figure 1.4 *Drosophila* heart tubulogenesis

Figure 1.5 Integrins interact with the ECM, cytoplasmic adhesome, and actin cytoskeleton

Figure 3.1 αPS3 integrin is required for apicalization of cardioblasts

Figure 3.2 αPS3 integrin is required for lumen formation

Figure 3.3 Expression of an αPS3 transgene in the cardioblasts restores apicalization of Robo

Figure 3.4. Integrins apicalize early during cardioblast polarization

Figure 3.5. Integrins concentrate at the presumptive luminal domain

Figure 3.6. Leading edge membrane activity requires integrin function

Figure 3.7. αPS3 integrin interacts with mutations in genes for adhesion and adhesion signaling

Figure 4.1 Talin has multiple integrin and adhesome-protein binding domains

Figure 4.2 Talin localization in the developing *Drosophila* embryonic heart

Figure 4.3 Mutations in the gene *rhea* deplete the embryo of Talin

Figure 4.4 Talin is required for βPS1 stabilization along the luminal and basal cardioblast surfaces

Figure 4.5 ECM components and cytoplasmic integrin adhesome proteins are abnormally distributed in *rhea* mutant embryos

Figure 4.6 Talin is required for continuous midline localization of Slit and Robo

Figure 4.7 *rhea* mutants have ectopic lateral accumulations of characterized luminal markers

Figure 4.8 *rhea* mutants lack an open lumen between opposing cardioblast rows

Figure 4.9 Talin is required for maximal membrane leading edge activity

Figure 4.10 Cardioblasts in *rhea* mutant embryos undergo aberrant morphogenesis during migration

Figure 4.11 $rhea^{79}$ interacts with mutations in genes encoding integrin-related proteins

Figure 4.12 Expression levels of transgenic talin rescue constructs

Figure 4.13 Either of Talin's integrin-binding-sites is sufficient to stabilize βPS integrin in the heart

Figure 4.14 $Talin^{IBS1-}$ and $Talin^{IBS2-}$ can mediate integrin-dependent lumen formation

Figure 5.1 Proposed model of integrin function during heart tubulogenesis

Figure 5.2 Talin-integrin adhesion in *Drosophila* embryonic development

Figure A.1 LanA is detected in multiple tissues in the *Drosophila* embryo

Figure A.2 Genetic scheme to generate maternal and zygotic *rhea* null embryos

Figure A.3 Genetic scheme to create strain for live imaging experiments

Figure A.4 Genetic schemes to express Talin transgenes in *rhea*^{79} homozygous embryos

Figure B.1 Heart phenotype in embryos homozygous for mutant alleles of integrin-related genes

Figure C.1 Range of heart phenotypes in *rhea* zygotic and germ-line clone mutant embryos

Figure C.2 Talin localization is disrupted in *mys* (βPS1 integrin) mutants

Figure C.3 CAP partially co-localizes with Talin along the apical and basal cardioblast surfaces

Figure C.4 In *rhea* mutants, ectopic Dg lateral accumulations are devoid of junctional Discs-large

Figure C.5 Talin localization in *rhea* zygotic mutants expressing transgenic Talin rescue constructs

Figure C.6 Talin^{IBS2b-} and Talin$^{IBS1-, IBS2-}$ are unable to rescue heart development in *rhea* mutant embryos

Figure D.1 Loss of Src42A, but not Src64B, results in incomplete cardioblast migration

Figure D.2 Mutations in *fak56D* do not enhance the *src42A*^{E1} phenotype

Figure D.3 Disrupting the kinase activity of Src42A in the cardioblasts does not disrupt cell migration

Figure D.4 In *src42A* mutant embryos, cardioblasts with stalled migration lack leading edge membrane activity

Figure D.5 Amnioserosa cells remain at the midline in late stage *src42A*^{E1} embryos

Figure D.6 In *src42A*^{E1} embryos amnioserosa cell invagination from the dorsal midline is incomplete

Figure D.7 Cardioblasts at the midline of *src42A*^{E1} embryos are capable of developing an open lumen between contralateral cells

LIST OF TABLES

Table 2.1a Alleles used in this thesis

Table 2.1b Balancer and/or marked chromosomes used in this thesis

Table 2.1c Stocks used in this thesis

Table 2.2a Polyclonal antibodies used for immunohistochemistry

Table 2.2b Monoclonal antibodies used for immunohistochemistry

Table 2.2c Secondary antibodies used for immunohistochemistry

Table 3.1 Leading edge polarization deficits in the heart region of the dorsal vessel

LIST OF ABBREVIATIONS and SYMBOLS

α	alpha- or anti-
ABD	**A**ctin **b**inding **d**omain
AMIS	**A**pical **m**embrane **i**nitiation **s**ite
aPKC	**a**typical **p**rotein **k**inase **C**
β	beta
βGal	**β**-**Gal**actosidase
βTub	**βTub**ulin
Bio	**Bio**tinylated
BMP	**B**one **m**orphogenic **p**rotein
CA	**C**onstitutively **a**ctive
CAP	**C**bl-**a**ssociated **p**rotein
CB	**C**ardio**b**last
Ch	**Ch**icken
DAB	3,3-**Dia**mino**b**enzidine Tetra hydrochloride
DCC	**D**eleted in **c**olorectal **c**ancer
Dg	**D**ystro**g**lycan
Dlg	**D**iscs-**l**ar**g**e
DN	**D**ominant **n**egative
E-cad	**E-cad**herin
ECM	**E**xtra**c**ellular **m**atrix

FAK **F**ocal **a**dhesion **k**inase

FLPase **Fl**i**p**p**ase** recombinase

FRT **F**LPase **r**ecognition **t**arget

GFP **G**reen **f**luorescent **p**rotein

GLC **G**erm-**l**ine **c**lone (identifies maternally and zygotically *rhea* or *mys* deficient embryos)

Gt **G**oa**t**

Hnt **H**i**n**dsigh**t**

hsFLP **h**eat-**s**hock inducible **FLP**ase

IBS **I**ntegrin **b**inding **s**ite

IgY Egg **y**olk **i**mmuno**g**lobulins

ILK **I**ntegrin **l**inked **k**inase

IPP **I**ntegrin-**P**inch-**P**arvin

IPTG **i**so**p**ropyl-beta-D-**t**hio**g**alactopyranoside

LanA **La**mini**n A** (α 3, 5)

M **M**ouse

MDCK **M**adine-**D**arby **c**anine **k**idney

Mef2 **M**yocyte **E**nhancing **F**actor **2**

MET **m**esenchymal-**e**pithelial **t**ransition

MMP **M**atrix **m**etallo**p**roteinase

Moe **Moe**sin

Mys **my**o**s**pheroid (βPS1 integrin gene)

NGS **N**ormal **g**oat **s**erum

PAK **p**21 **a**ctivated serine-threonine **k**inase

PAP **p**re-**a**pical **p**atch

PBS **P**hosphate **B**uffer **S**aline

PIP2 **P**hosphatidyl**i**nositol 4,5-bis**p**hosphate or PI(4,5)P2

PIP3 **P**hosphatidyl**i**nositol (3,4,5)-tri**p**hosphate

PIPIγ **P**hosphatidyl**i**nositol **p**hosphate kinase Type **I γ**

Prc **P**e**ric**ardin

PTEN **P**hosphatase and **ten**sin homolog

Rb **R**a**b**bit

Rt **Rat**

Scb **sc**a**b** (αPS3 integrin gene)

Svp **S**e**v**en-u**p**

TLN **T**a**l**i**n** (vertebrate)

TUP **T**ail-**up**

UAS **U**pstream **a**ctivation **s**equence

Vkg **Vik**in**g**

WT **W**ild**t**ype

YFP **Y**ellow **f**luorescent **p**rotein

Zfh1 **Z**n **f**inger **h**omeodomain **1**

Introduction

CHAPTER ONE

Growing up in a vegetable farming family, terms such as crop rotation, soil nutrients, and water content were a regular part of our conversation. During the hot dry weeks of summer, essential to maintaining healthy crops was a sprinkler water delivery system. Hour upon hour was spent assembling, disassembling, moving, and reassembling the many parts. Despite the complexity and numerous system components, none were more important than the basic hoses or pipes transporting the water to each sprinkler. Although simple in appearance and cumbersome to work with, the pipes were carefully crafted to their task: the water within the pipe was separated from the ground and air by a thick metal exterior, each pipe had a sufficient diameter to transport a high volume of water, and each pipe was diligently maintained to avoid cracks and water leakage. Having a carefully constructed quality hose was absolutely indispensable to deliver water to all the vegetable crops in the garden.

Looking beyond the garden analogy, intricately designed tubes are also essential in living organisms, including our own bodies. From the kidney to the lung, the mammary gland to blood vessels, the digestive tract to the pancreas, without similar tubular characteristics as seen in garden hoses, these organs would be unable to function. As biological tubes they enable the delivery of not simply water, but the transport, exchange, and secretion of many fluids and gases between tissues.

While tubular organs vary in size, specific function, and development, it is increasingly becoming clear that the basic structure of these tubes involves common features shared by a diverse set of organs across species (Figure 1.1B; reviewed by Hogan

Figure 1.1 – *Drosophila* embryonic heart development as a model of tubulogenesis

(**A**) The mature heart is a linear tube positioned along the dorsal midline of the stage 17 embryo. It is comprised of two cell types, the cardioblasts (green) and the flanking pericardial cells (pink). At the posterior (to the right) is the pumping heart proper ("h"). Hemolymph is pumped from the heart proper through the aorta outflow tract ("a") near the anterior of the embryo. (Figure adapted from http://flyembryo.nhlbi.nih.gov/images with permission not required, and Tao and Schultz 2007 with permission from Elsevier). (**B-C**) Tubular organs are enclosed by epithelial cells that display tight lateral cell-cell adhesion and strong luminal-basal polarity (**B**), characteristics shared by the *Drosophila* embryonic heart (**C**). (Figure adapted from Bryant and Mostov 2008 with permission from Nature Publishing Group).

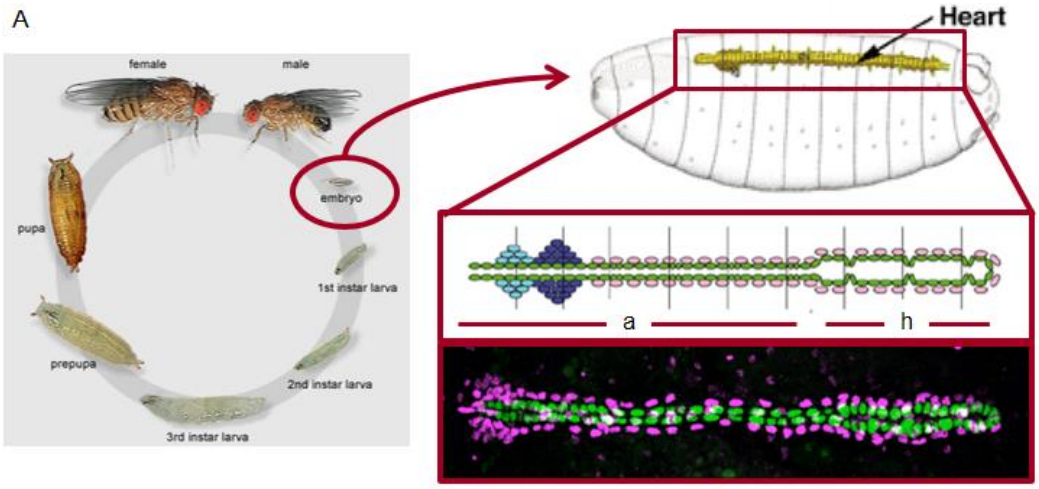
A
female
male
embryo
1st instar larva
2nd instar larva
3rd instar larva
prepupa
pupa
Heart
a
h

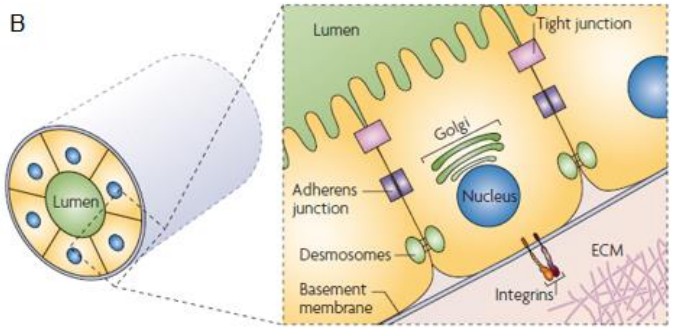
B
Lumen
Lumen
Tight junction
Golgi
Nucleus
Adherens junction
Desmosomes
Basement membrane
ECM
Integrins

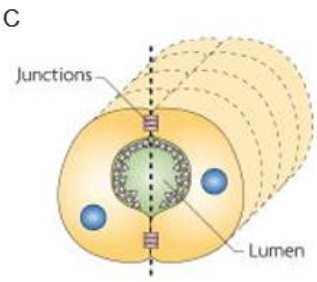
C
Junctions
Lumen

and Kolodziej 2002, Lubarsky and Krasnow 2003). As seen in the inner lining of our garden hose analogy, all tubes enclose a fluid or gas transporting lumen; this requires a defined luminal-basal polarity with the luminal domain facing the inside and the basal surface exposed to the surrounding tissues. Maintaining this polarity and the overall tube integrity requires control of the surrounding cells' shape or morphology, delineation of the specific domains, as well as the formation of intercellular junctions or adhesions connecting the neighboring cells that enclose the lumen.

In the following chapters, we explore tubulogenesis through the lens of the *Drosophila melanogaster* embryonic heart (Figure 1.1A, 1.1C). As described more extensively below, *Drosophila* embryonic heart development involves each of the common aspects of tube formation. Furthermore, despite its relative structural and developmental simplicity, many parallels have been and continue to be made to tubulogenesis in higher order organisms and humans (reviewed by Medioni *et al.* 2009). With its simple genetics, the numerous mutant and transgenic strains available, and the feasibility of assessing the heart in both immunolabeled fixed and transgenic living embryos, the *Drosophila* heart serves as an excellent model to elucidate the underlying mechanisms driving tubulogenesis.

1.1 The structure of the tubular *Drosophila melanogaster* embryonic heart

The *Drosophila* embryonic heart is a linear vessel enveloped by parallel rows of cardial cells linked pairwise across the midline (Figure 1.1A). The inner-lining contractile

cardioblasts (CBs) are flanked by non-contractile pericardial cells (Figure 1.1A). The posterior third of the heart forms the pumping heart proper ("h" in Figure 1.1A), while the anterior end forms the aorta or outflow tract ("a"). The luminal diameter is larger in the heart proper than in the aorta. The most anterior aorta is surrounded by the ring and lymph glands. Along the anterior-posterior axis, the heart is divided into six-cell segments which align with the embryo segment boundaries. In each segment, four cells expressing the transcription factor Tinman are followed by two Seven-up (Svp) expressing cells (Bryantsev and Cripps 2009). The Svp cells are more narrow than the Tinman cells; following embryogenesis these cells develop into the in-flow ostia tracts present in the larval and adult heart (Molina and Cripps 2001).

The simple tubular nature of the *Drosophila* embryonic heart is apparent when the heart is viewed in cross-section (Figure 1.1C). The CBs in the contralateral rows are crescent shaped, wrapping into a single cell-layered tube wall enclosing a central lumen through which hemolymph is pumped. Junctions or regions of adhesion dorsal and ventral to the lumen connect the cardial cells from the two contralateral rows.

1.2 How do lumen-enclosing vessels develop?

1.2.1 Morphological diversity in development of tubular organs

Consistent with the diversity seen in the shape, size, and function of tube-based organs, at first glance, tube development appears to vary greatly between species and organs. At least five general tubulogenesis categories have been described (eg. Lubarsky

and Krasnow 2003, Datta *et al.* 2011), some which initiate from existing polarized epithelial layers and others which require a mesenchymal-epithelial transition (MET) to generate polarity as tube formation progresses. Vertebrate neural tube development is a classic example of *wrapping*: a linear region of cells within an existing epithelial sheet invaginates, eventually curling into a tube and pinching off from the surrounding epithelial cells (Copp and Greene 2010). *Budding* involves cells protruding out from the plane of an epithelial layer, enclosing and extending a lumen as the bud lengthens. Tracheal tube branches in *Drosophila* form through budding (Ghabrial *et al.* 2003). *Cavitation*, as observed in mammary gland branching (Mailleux *et al.* 2008; Figure 1.2C), requires cell elimination or death: central cells are removed and surrounding cells develop a luminal-basal polarity to seal the new open (luminal) space. *Hollowing* is similar to cavitation, however it does not involve cell elimination, but rather creation of a lumen in the middle of a group of cells via vesicle-mediated deposition of luminal components. Hollowing can occur between several cells (eg. mouse aorta, Strilić *et al.* 2009; Figure 1.2B) or in the cytoplasm of a single cell (eg. initial zebrafish cranial vasculature, Lenard *et al.* 2013). As will be discussed further, *Drosophila* heart development occurs via *focalized contact*, in which neighboring cells connect and adhere only at specific domains and a non-adhesive luminal region forms between (Figure 1.2A).

In addition to the differences highlighted by these categories, the diversity of tube development is increased when events prior to and after the actual lumen-forming process are considered. For example, tube-forming cells originate from all three of the

Figure 1.2 – Shared basic design principles underlie diverse tubulogenesis events

Tubulogenesis in diverse contexts involves several basic principles of development: determination of the site of lumen formation through spatial environmental and neighboring cell cues, establishment of luminal-basal polarity and specification of membrane domains, and development and expansion of the lumen itself. These common features can be seen in tubes that form via focalized contact (**A**), hollowing (**B**, exocytosis of luminal components), and cavitation (**C**, apoptosis of inner cells). (Figure adapted from Datta *et al.* 2011 with permission from Elsevier).

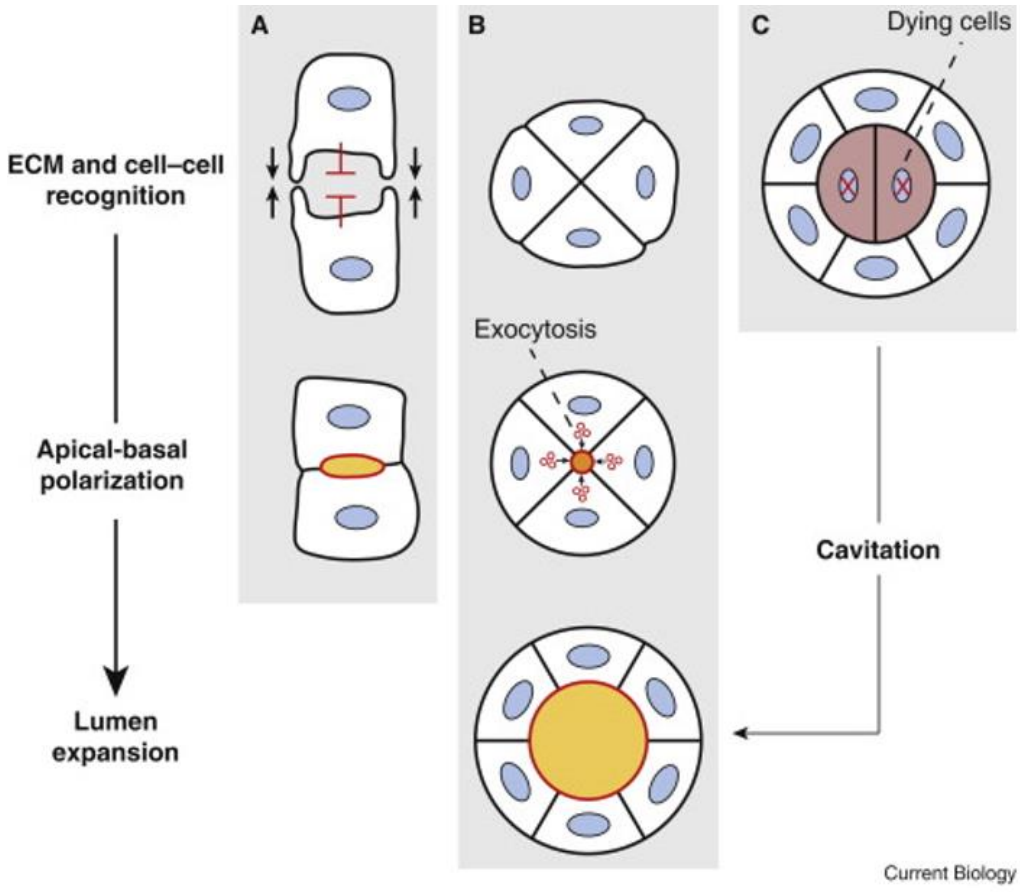
A
B
C
Dying cells
ECM and cell–cell recognition
Apical-basal polarization
Lumen expansion
Exocytosis
Cavitation
Current Biology

germ-layers; in *Drosophila* the salivary glands and trachea originate from the ectoderm, the malphigian tubules and gut from the endoderm, and the heart from mesodermal tissue. Following tubulogenesis, cell proliferation may (eg. vertebrate intestines) or may not (*Drosophila* heart) occur. In many tissues, such as the muscle-enveloped intestines, tubes must recruit or organize additional cell layers surrounding them. In each example of tubulogenesis that has been studied, intricate details differing from other systems have been identified.

1.2.2 Basic design principles common to diverse tubulogenesis events

Despite this diversity, as underlying cellular mechanisms are discovered it is becoming increasingly clear that tube-forming processes share several basic design principles. These include: recognition of neighboring cells (cell-cell) and the environment (cell-matrix) to determine the site of lumen formation, coordination with neighboring cells to establish luminal-basal polarity and luminal, junctional, and lateral cell domains, formation or enclosure of the luminal space, and expansion of the lumen (Figure 1.2; Ferrari *et al.* 2008, Datta *et al.* 2011). While these principles are often not discrete but rather overlapping and interdependent processes, identifying these fundamental principles provides a framework through which to study a variety of tubulogenesis models and apply this combined knowledge back to the individual context.

Determine the site of lumen formation

Establishing a central lumen amongst a tissue of cells requires directionality and identification of a common site for lumen formation. The extracellular matrix (ECM) is important in providing this spatial orientation, with the basal, ECM-interacting, cell surface and the obverse luminal domain forming on opposite cell surfaces. In some cases, such as between hepatocytes, the lumen may instead form laterally, perpendicular to the ECM-interacting surface (Treyer and Müsch 2013). While an early lumen or apical membrane initiation site (AMIS), or the more developed pre-apical patch (PAP), was first described in Madine-Darby canine kidney (MDCK) cell culture (Ferrari *et al.* 2008, Bryant *et al.* 2010), similar sites have been observed in other, *in vivo*, examples as well. For example, in zebrafish neural tube development, polarity proteins such as Pard3 localize to the cleavage furrow of dividing cells, a site which specifies lumen position (Tawk *et al.* 2007). During formation of the mouse aorta, the lumen site is initially identified by CD34 glycoprotein localized between adjacent endothelial cells (Strilić *et al.* 2009).

Both *in vitro* and *in vivo* studies demonstrate that the integrin family of transmembrane proteins is key to transducing ECM signals into the cell to promote a single lumen formation site. For example, when integrin expression or function is prevented, oxygen-transporting tracheal terminal branches in *Drosophila* fail to maintain a single central lumen and multiple mini-lumens develop instead (Levi *et al.* 2006). Furthermore, in mice with a late-embryonic endothelial-specific β1-integrin knock-out,

arterial vascular lumens were frequently non-continuous and luminal and junctional markers were mis-localized (Zovein *et al.* 2010).

In addition to cell-ECM interaction, neighboring cells must also coordinate with one another to establish one common site of lumenogenesis. When plated in collagen or laminin-rich 3D media, MDCK cells proliferate, eventually assembling into a spherical cyst structure consisting of an epithelial monolayer surrounding a central lumen. In this *in vitro* model, a failure to maintain E-cadherin (E-cad) mediated adhesion because of defective recycling results in multiple small lumens (Jung *et al.* 2013). Similar examples are seen in *in vivo* models. During tracheal tube cell fusion in *Drosophila*, establishment of E-cad at the site of fusion is essential for a continuous lumen branch (Tanaka-Matakatsu *et al.* 1996). Knock-out of E-cad in mice thyroid follicles results in irregular shaped lumens of reduced size (Calì *et al.* 2007), while a similar loss in *Drosophila* prevents lumen formation in the heart due to a lack of contralateral cell adhesion (Santiago-Martínez *et al.* 2008).

Establish polarity and specify membrane domains

Once the site of lumen formation has been established, all cells within the tissue must initiate, or continue to acquire, the appropriate polarity. The spatial orientation of the ECM and neighboring cells contribute to establishing the axis of cell polairty, as outlined above. Polarization involves reorganization of the cytoskeleton and assembling or demarcating the luminal, lateral, and basal membrane domains (Figure 1.1B).

In the MDCK cyst model, the epithelial polarity markers Par3 and atypical protein kinase C (aPKC) are early luminal-domain determinants, aggregating at the AMIS before relocalizing to apical-lateral tight junctions as lumen formation proceeds (Bryant *et al.* 2010). Upon loss of Par3 or aPKC, the early apical-scaffold protein Podocalyxin/gp135 (Meder *et al.* 2005) does not accumulate at the luminal domain and no lumen forms (Bryant *et al.* 2010). Not only is the luminal membrane disrupted, loss of Par3 or aPKC also disrupts lateral and basal domains: in cells expressing aPKC shRNA the basolateral β-catenin remains at the cyst center where apical lumenogenesis would usually proceed (Bryant *et al.* 2010). Inhibited β1-integrin function results in inverted polarity, with Podocalyxin remaining on the outer/basal surface of the MDCK cell aggregates and the apical-lateral tight-junction component Occludin present towards the basal surface (Yu *et al.* 2005). While the actin cytoskeleton was intensely labeled around the lumen in normal cells, inhibition of β1-integrin resulted in a disorganized actin pattern (Yu *et al.* 2005). Similarly, in mammary gland acini, β1-integrin knock-out resulted in loss of aPKC accumulation at the AMIS, tight junctions present near the outer edges of the cell aggregates, disorganized and improperly aligned microtubules, and a lack of lumen formation (Akhtar and Streuli 2013).

Develop a luminal space

Once a group or tissue of cells has identified a site for lumen formation and has become polarized, an open luminal space must be formed. The MDCK cyst model

highlights a central role for vesicle trafficking in this process. Knock-down of FIP5, a binding partner of the important trafficking GTPase Rab11, or loss of association between Rab11 and the vesicle-binding myosin motor Myo5B disrupted Podocalyxin accumulation and lumen formation (Willenborg *et al.* 2011, Roland *et al.* 2011). Furthermore, not only is exocytosis required for deposition of luminal factors, it is also important for junction establishment and the localization of numerous polarity proteins. In further study of MDCK cysts, Desclozeaux *et al.* highlighted an essential role for Rab11 in E-cad recycling and targeting to lateral junctions (2008). Byrant *et al.* found that Rab11a controls trafficking of Par3 to the AMIS, while Par3 was conversely required for localizing the $Rab11^{+}$ vesicle-tethering exocyst components Sec8 and Sec10 proteins (2010). In the *in vivo C. elegans* intestine tubulogenesis model, loss of the clathrin adaptor AP-1 resulted in not only deformed and ectopic lumens, but mislocalization of numerous apical polarity factors (including Par6) and actin disorganization (Zhang *et al.* 2012). Taken together, these and other studies suggest that vesicle trafficking and polarity mechanisms have an interdependent or positive-feedback relationship during lumen formation.

Expand the lumen diameter

In many systems, once lumens are formed they undergo further diameter expansion. This may involve continued apical targeting of lumen components and extension of the apical and junctional domains. For example, when secretion vesicle-coating COPII complex is disrupted, the tracheal branch system in *Drosophila* form

lumens, but they have markedly reduced diameters (Förster *et al.* 2010). Other processes involved include cell division and ion and water transport mediated by membrane-bound pumps or channels (Bagnat *et al.* 2007, Datta *et al.* 2011).

1.2.3 Importance of studying the diverse mechanisms underlying basic design principles

Despite the numerous studies and mechanistic insights that we have gained about tube formation, in particular from the *in vitro* MDCK model, much still remains to be discovered about the mechanisms underlying tubulogenesis models and their application to vertebrate development and disease. While the basic principles of design are shared by all tubes, it remains unclear if the cell signaling pathways and mechanisms regulating these principles are the same. Applying our insights from the MDCK model to other systems presupposes a similar establishment of apical-basal polarity and mechanism of lumenogenesis, however it is clear that this is not always the case. For example, while vesicle trafficking may be essential for multiple tubulogenesis processes, its role would necessarily be different in the tubes formed via central-cell elimination through apoptosis (ie. cavitation) than in exocytosis-driven hollowing. Furthermore, not all tubes have classical epithelial apical-basal polarity, with a lumen-facing apical surface. Vertebrate vasculature is lined by endothelial cells, which, although they have the basic polarity determinants Par3 and aPKC, are not known to require additional polarity proteins such as Discs-large (Dlg) nor Crumbs (Iruela-Arispe and Davis 2009). This polarity difference is

apparent also in the lumen itself which, unlike MDCK cysts, initially has basal-like characteristics (Strilić *et al.*, 2009, Davis and Senger 2005). Similarly, in the invertebrate lancelet family, it is the basal, rather than apical, cell surface that faces the heart tube lumen (Kucera *et al.* 2009). Further research of these different characteristics is necessary to understand and appreciate the full breadth of tubulogenesis events and differentiate between conserved mechanisms and those that are type specific. The *Drosophila* embryonic heart, a pumping tubular organ that encloses a midline lumen with basal-like characteristics (this thesis; see also Lehmacher *et al.* 2012), serves as a fascinating model to study numerous aspects of tubulogenesis including the role of collective cell migration, adhesion, cell morphology dynamics, and polarization of a non-classical epithelial-like tube (Medioni *et al.* 2008).

1.3 The *Drosophila melanogaster* heart as a model of vertebrate cardiogenesis

1.3.1 Importance of cardiac research

In humans, disruptions in heart tube development and vasculogenesis are critical, as these can lead to congenital heart defects and later-onset cardiovascular-related diseases (eg. reviewed by Fahed *et al.* 2013). In infants, cardiovascular defects are the most common congenital disorder, affecting close to 1% of all newborn children and 1.35 million newborns worldwide each year (van der Linde *et al.* 2011). While medical advances have greatly increased the survival rate of these children, later-onset complications are frequent in adulthood (van der Bom *et al.* 2011, Greutmann and Tobler

2012). Studying the biology of the cardiovascular system in both healthy and diseased individuals can, and has, greatly enhanced our ability to diagnose and treat these disorders (Nemer 2008, Greutmann and Tobler 2012). Despite these advances, our understanding about the contributing genetic and development factors is limited and further research is hindered by the complex and multifactorial nature of these disorders.

1.3.2 Conservation of cardiac disease genes in *Drosophila*

Despite its relative simplicity when compared to the vertebrate heart and many other tubular organs, the *Drosophila* heart is an excellent model to study heart development, function, and aging (initially suggested by Bodmer 1995, more recently reviewed by Bier and Bodmer 2004, Tao and Schulz 2007, Reim and Frasch 2010, Seyres *et al.* 2012). This is underscored by the shared cardiac-related genes in *Drosophila* and humans: mutations identified in human cardiovascular diseases have been found in at least thirty-four genes with known orthologues in flies (Bier and Bodmer 2004), consistent with the general finding that 75% of human disease genes have orthologues in flies (Reiter *et al.* 2001). In particular, several studies have suggested a role for integrins in disease progression (Ross 2002), and integrins have been gaining recognition as potential therapeutic targets to combat such diseases (Haverslag *et al.* 2008, Israeli-Rosenberg *et al.* 2014). This conservation of genes linked to vascular development and disease illustrates the influence that *Drosophila* studies may have for heart and general vascular research applications (Bier and Bodmer 2004, Hartenstein and Mandal 2006). While alleles or

specific mutations in genes may be correlatively linked to heart and vascular diseases in humans, it is through model organism research that normal function of these genes can be established and the etiology of the correlated diseases understood.

1.3.3 Benefits of studying cardiac tubulogenesis in the *Drosophila* model

Drosophila melanogaster is the only well-studied invertebrate model system with a heart comparable to vertebrates, and thus is a unique system, valuable because of its simplicity and the powerful genetic manipulations and analysis possible (reviewed by Bier and Bodmer 2004). Unlike the complex human heart, the *Drosophila* dorsal vessel is a simple and linear tube comprised of only two cell types that are easily tracked at a single-cell resolution using molecular markers both in fixed and living tissues (Figure 1.1A). Following cardiac specification, cells do not undergo further cell division nor complex rearrangements. This facilitates careful analysis of cell morphology and polarity changes directly required for tubulogenesis. The heart tube develops immediately ventral to the ectoderm, just under the dorsal cuticle, permitting direct imaging of the heart. This overlying ectoderm and the underlying transient amnioserosa tissue are the primary tissues that surround and potentially interact with the developing embryonic heart (Figure 1.4C, D). Furthermore, as the *Drosophila* heart is not necessary for oxygen transportation throughout the body (accomplished via diffusion during embryogenesis and through the tracheal system later in development; Wu and Sato 2008, Ghabrial *et al.* 2003), defects in cardiac function often do not result in embryonic lethality as they would in vertebrate

systems. This allows for very thorough examinations of mutant phenotypes, providing more information about the specific pathway being studied. More importantly however, the *Drosophila*-based system utilizes many simple but powerful techniques that facilitate straightforward analysis of gene and protein function. The techniques utilized in this thesis include numerous mutant alleles, tissue specific or ubiquitous expression of wildtype or mutant transgenes, double-stranded RNA-mediated knock-downs, immunolabeling of specific cell types and domains, and live imaging using fluorescent-tagged proteins.

1.4 Key stages of *Drosophila* embryonic heart development

Development of the *Drosophila* embryonic heart entails a series of steps reminiscent of early vertebrate heart morphogenesis (Figure 1.3; Bier and Bodmer 2004, Markwald *et al.* 1996). After gastrulation, the cardial cells originate from the lateral mesoderm and align into two bilateral rows. These rows then migrate towards each other and meet at the midline where they adhere and enclose a central lumen (Figure 1.3).

1.4.1 Specification and alignment of heart progenitors

The initial step in *Drosophila melanogaster* heart formation is specification and differentiation of the cardiac cells, a step requiring an intricate genetic hierarchy shared with vertebrates, including the genetic models of *Mus musculus* (mouse) and *Danio rerio* (zebrafish; Figure 1.3; Bryantsev and Cripps 2009). Early evidence of the remarkable

Figure 1.3 - *Drosophila* heart development shares key similarities with early vertebrate cardiogenesis

Embryonic heart assembly in mouse (*Mus musculus*), fish (*Danio rerio*), and fly (*Drosophila melanogaster*). Tubulogenesis proceeds by lateral alignment of cardiac progenitors, collective medial cell migration, and subsequent lumen formation at the midline. Progenitors are labeled for Myosin Light Chain (mouse and fish) or Hand-GFP (fly). (Figure adapted from Moorman *et al.* 2003 with permission from BMJ Publishing Group Ltd., Holtzman *et al.* 2007 and Han *et al.* 2006 with permissions not required under the Creative Commons Attribution CC-BY License, and Tao and Schulz 2007 with permission from Elsevier).

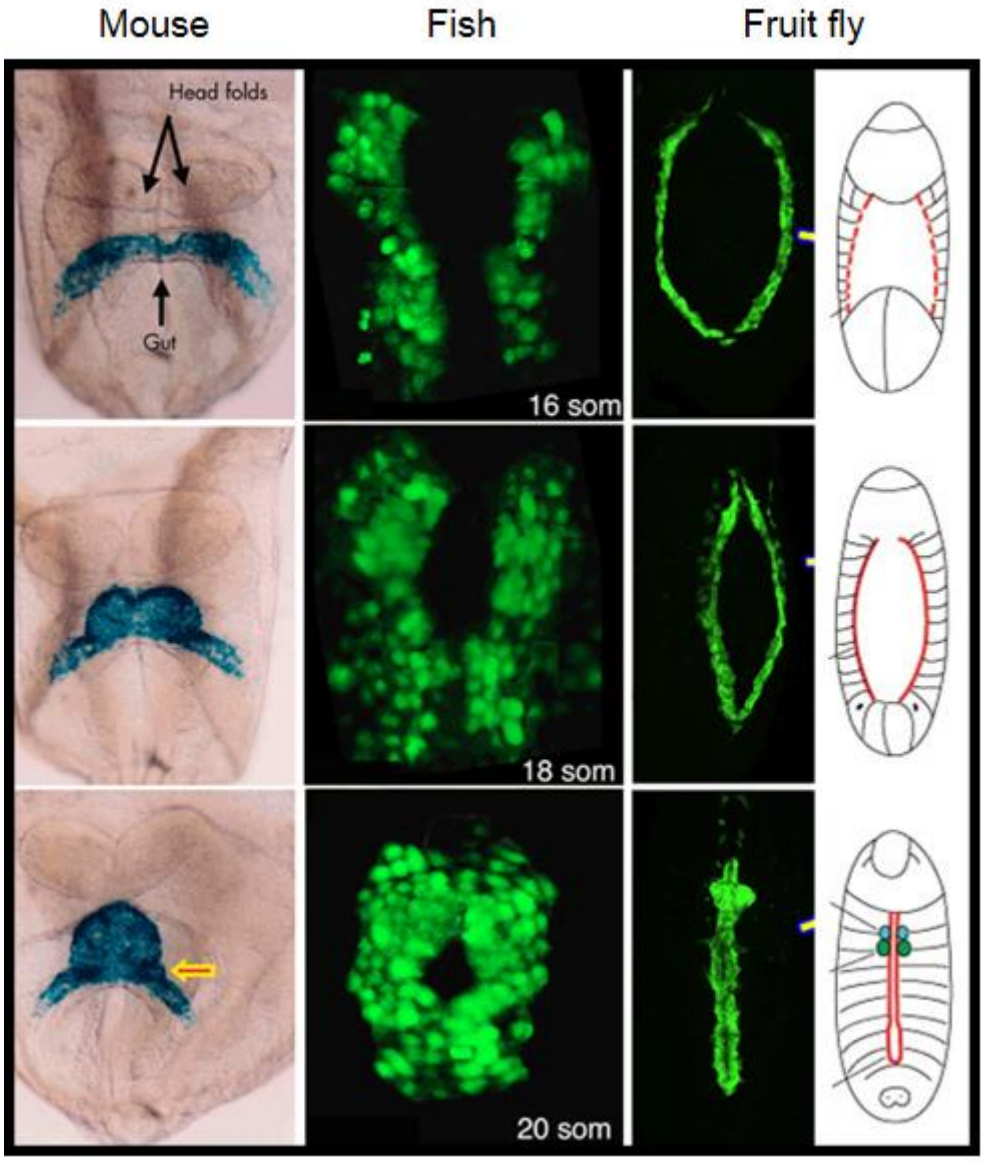
Mouse
Fish
Fruit fly
Head folds
Gut
16 som
18 som
20 som

similarity was found with the transcription factor Tinman (NKX2 in vertebrates) and *tinman*-like genes (Chen and Fishman 2000) required for heart precursor specification in vertebrates and flies (Bodmer 1993; Fu *et al.* 1998; Grow and Krieg 1998). In *Drosophila*, *pannier*, a GATA gene, co-regulates heart formation with Tinman (Gajewski *et al.* 1999). In vertebrates, GATA genes, such as *gata4* in zebrafish and mice, are expressed in heart progenitor tissues (Evans 1997; Reifers *et al.* 2000). Induction and maintenance of Tinman also involves Bone Morphogenic Protein (BMP) signaling. *decapentaplegic*, a BMP orthologue, and its receptor *thickveins* are required for maintenance of *tinman* expression in flies (Frasch 1995; Xu *et al.* 1998). Bmp2 and related proteins in the chick and zebrafish act similarly (Schultheiss *et al.* 1997; Kishimoto *et al.* 1997). Cardiac cell fate is maintained through Fibroblast Growth Factor signaling in both vertebrates and invertebrates, including *Drosophila* (Marques *et al.* 2008, Cota *et al.* 2014, Bryantsev and Cripps 2009). Following specification, the cardial cells are aligned in two parallel rows along the sides of the developing *Drosophila* or vertebrate embryo (Figure 1.3). Taken together, these and related findings demonstrate that not only are individual signaling factors homologous in the fly and vertebrate heart, but the pathway networks and regulation are also shared (Seyres *et al.* 2012, Olson 2006). This realization was key to establishing the relatively simple *Drosophila* cardiogenesis as an important model of vertebrate vascular tubulogenesis. Since these initial studies, the noted similarities have been extended to other stages in fly heart development, function, and aging (Ocorr *et al.* 2007).

1.4.2 Migration of cardial cells to the dorsal midline

Similar to the process in vertebrates, prior to the heart forming a tube, the two rows of cardiac precursors, or CBs, must migrate through the embryo and meet at the midline (Figure 1.3). Cardial cell migration is a coordinated event; cardiac progenitors undergo collective cell migration in which a population of cells, exhibiting an intermediate mesenchymal-epithelial state, migrate together through other tissues (Rørth 2009). In *Drosophila*, CB migration occurs simultaneously with dorsal closure, a process whereby the ectoderm migrates towards the dorsal midline, covering a gap in the epidermis left after germband retraction (Figure 1.4). Prior to dorsal closure, this gap is temporarily covered by an extraembryonic epithelium, the amnioserosa (green in Figure 1.4C). During the early stages of migration, the rows of CB cells follow the ectodermal leading edge, migrating one to two cell diameters behind (Figure 1.4 C and D, stage 15). Later, the CBs migrate between the ectoderm and amnioserosa to reach the dorsal midline (Figure 1.4 C and D, stage 16); for this to occur, the amnioserosa must detach from the ectoderm and be internalized, eventually undergoing programmed cell death (Figure 1.4 C, D, stage 17; Mohseni *et al.* 2009).

As mesenchymal-epithelial intermediates, migrating cardial cells in both vertebrates and *Drosophila* have polarized epithelial characteristics including distinct lateral, basal, and leading edge domains (Figure 1.4B; Medioni *et al.* 2008; Zhong 2005; Knox *et al.* 2011). Lateral domains contain cell-cell adhesion molecules, such as cadherins, which maintain the connection between the cells. Basal and pre-luminal surfaces interact

Figure 1.4 – *Drosophila* heart tubulogenesis

Frontal (**A**) and transverse (**B-D**) schematic images of the heart during the cardioblast (CB) migration (stage 15, top panels), midline attachment (stage 16, middle) and lumen formation (stage 17, bottom).

(B) Our lab has identified several membrane domains that are established in migrating CBs, prior to lumen formation. The pre-luminal domain (blue) is marked early during migration by βPS1 integrin and Talin and persists through cardiogenesis. Pericardin localizes to the basal surface of CBs (yellow). The dorsal leading edge of migrating CBs extends highly dynamic filopodia processes (green). Once the CBs contact their contralateral partner at the midline, cell-cell adhesions (red) form dorsally and, later, ventrally.

(C) In electron microscopy transverse sections, migrating cardial cells (yellow) follow the dorsal ectoderm leading edge (blue) and contact the amnioserosa (green) ventrally (stage 15). As CBs approach the midline, they migrate between the ectoderm and amnioserosa to reach their contralateral partner at the midline (asterisk, stage 16). Once at the midline, the CBs adopt a crescent-shape morphology and enclose the lumen (stage 17).

(D) The CBs and surrounding tissues visualized in fluorescently immunolabeled fixed-tissue embryo samples.

as, amnioserosa; ec, ectoderm; cc, cardial cells.

Images in (A) are adapted from Tao and Schulz 2007 with permission from Elsevier.

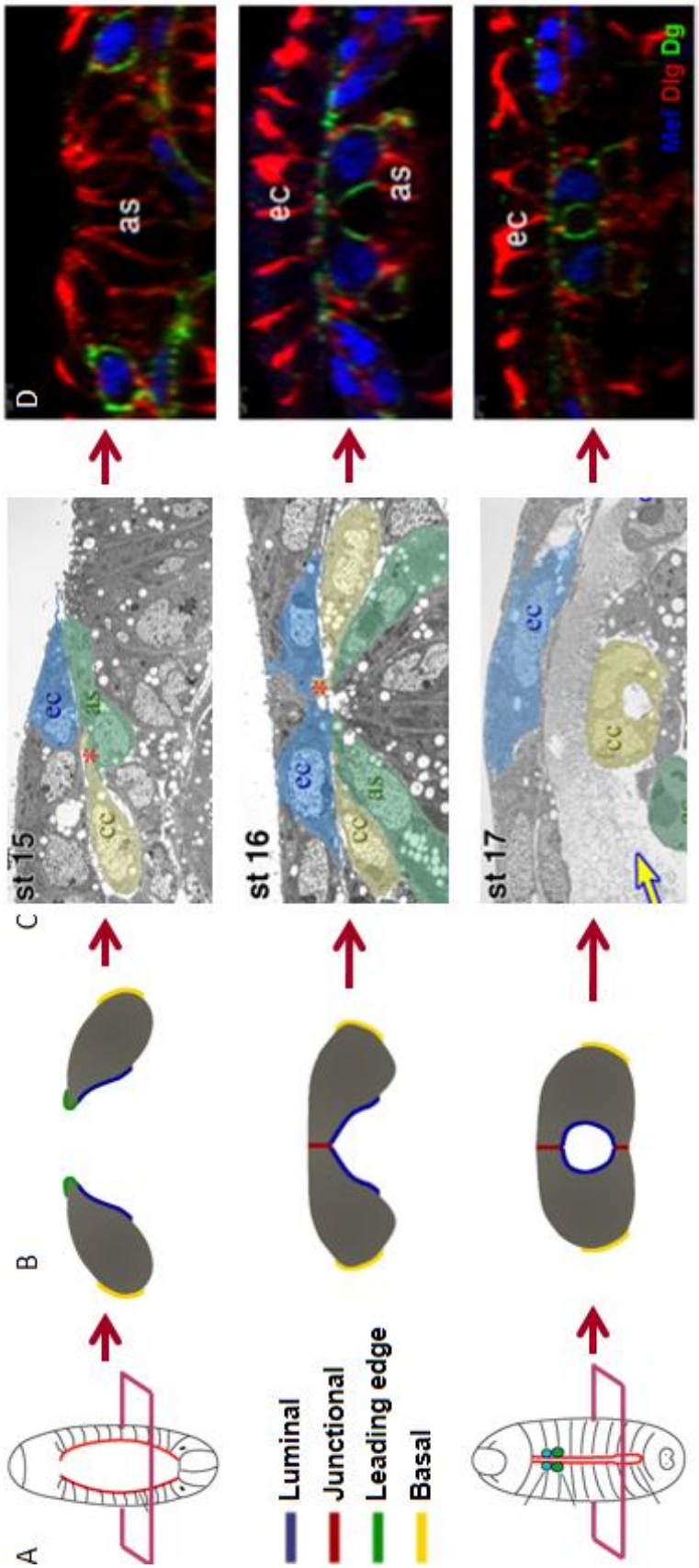
A
B
C st 15
st 16
st 17
D
ec
as
cc
Luminal
Junctional
Leading edge
Basal
Mud Dlg Dg

with the ECM, primarily through integrin transmembrane dimers. The leading edge domain extends highly dynamic actin-based protrusions in the direction of the migration, towards the dorsal midline in the developing embryo (Syed, 2012). In *Drosophila*, delineation of these domains becomes pronounced in the latter stages of cell migration, when the cuboidal CBs constrict and become triangular (Figure 1.4 B-D, stage 15). Following migration, the CBs complete the mesenchymal-epithelial transition and enclose the lumen.

1.4.3 Lumen formation

Near the end of migration, an initial dorsal contact is made between contralateral CBs (Figure 1.4, stage 16). CBs become crescent-shaped and adhere ventrally to wrap around and fully enclose the inner lumen and complete tubulogenesis (Figure 1.4, stage 17). Although somewhat different from a classical epithelial structure, the polarized nature of the CBs has been recognized as an important prerequisite for proper organization of the heart in *Drosophila* (MacMullin and Jacobs 2006; Medioni *et al.* 2008). However, the spatial demarcation of these polarized domains, and the dynamic morphogenesis of the CBs as they undergo MET to complete lumen formation have only recently begun to be appreciated (Medioni *et al.* 2008; Knox *et al.* 2011; rev. by Brandt and Paululat 2013). Our current understanding of lumen formation is summarized in Section 1.5.

1.5 Cardioblast polarization during lumen formation

Although the general morphological cell and tissue processes during *Drosophila* heart development were well characterized almost two decades ago (Rugendorff *et al.* 1994), it is only more recently that the molecular pathways governing these processes, specifically the latter lumenogenesis steps, have been investigated. What follows is a summary of the currently known factors involved in *Drosophila* heart lumen formation. While much attention has been given to the ligand-receptor pair, Slit and Robo, it appears that additional cell-surface factors must also work together to complete lumen formation.

1.5.1 A central role for Robo & Slit

Central to the models proposed by several labs is the ligand-receptor pair Slit and Robo (Qian *et al.* 2005; MacMullin and Jacobs 2006; Medioni *et al.* 2008; Santiago-Martinez *et al.* 2008). Slit is a secreted glycoprotein which binds to one or more of the immunoglobulin-family Robo transmembrane receptors. Although originally identified as producing a chemo-repulsive signal during axonal guidance in the nervous system, Slit and Robo are expressed by numerous tissues and organs in both vertebrates and invertebrates. In the *Drosophila* heart, Slit and Robo are both expressed by the CBs (MacMullin and Jacobs 2006; Qian *et al.* 2005) and by late stages of embryogenesis localize apically to the lumen (Slit) or luminal membrane (Robo). In the absence of Slit and Robo, a lumen fails to form (MacMullin and Jacobs 2006; Santiago-Martinez *et al.* 2008; Medioni *et al.* 2008). Moreover, a close examination of the CB morphology during the

latter stages of heart development suggests that Slit and Robo are required for the shape changes that occur during lumen formation; in contrast to wildtype embryos, the CBs in *slit* and *robo*, *robo2* mutants keep their initial round shape and do not extend a dorsal protrusion towards the midline (Medioni *et al.* 2008). As *slit* and *robo*, *robo2* mutants have an extended E-cad rich junctional domain while embryos over-expressing Slit have extra ectopic lumens, one model of lumen formation suggests that Slit-Robo signaling at the midline restricts adhesion between opposing CBs to the dorsal and ventral contact points leaving a non-adhesive open luminal domain (Santiago-Martinez *et al.* 2008). Such a mechanism is similar to lumen formation in the mouse aorta, a process dependent on the glycoprotein protein CD34-sialomucin which prevents adhesion along the luminal surface (Strilić *et al.* 2009). Indeed, several recent studies have highlighted a role for Slit and Robo function in heart and vascular formation in vertebrates, suggesting that the similarities between vertebrate and fly heart development extend beyond the early cardial cell specification networks. Not only do vertebrate hearts express Slit and Robo (Medioni *et al.* 2010, Fish *et al.* 2011), but an inhibition or loss of Slit-Robo signaling leads to developmental abnormalities in multiple heart tissues including the lumen-lining endocardium, the musculature forming myocardium, and the surrounding pericardium (Fish *et al.* 2011, Mommersteeg *et al.* 2013, Liu *et al.* 2003) as well as other non-heart endothelial-lined vasculature (Small *et al.* 2010; Fish *et al.* 2011).

1.5.2 Additional luminal domain factors

While Slit and Robo are essential for lumen formation, additional studies reveal the importance of numerous other cell-surface or extracellular factors that localize to the apical luminal membrane or the lumen itself. Interestingly, as several other research groups have recently highlighted, these factors do not include some of the well-characterized apical epithelial markers such as Crumbs, Bazooka/Par3, nor aPKC (Qian *et al.* 2005, Medioni *et al.* 2008, Brandt and Paululat 2013). In contrast, several of the proteins that do localize to the lumen are characteristic of basal surfaces.

Unc5 and Netrin

Similar to Slit and Robo, the ligand-receptor pair Netrin-Unc5 is also required for development of a continuous lumen, possibly in a pathway independent of Slit and Robo (Albrecht *et al.* 2011). However, the phenotype of null mutant alleles for these genes is less severe than seen for *slit* and *robo* mutants and few cell polarization defects are present (Albrecht *et al.* 2011).

Syndecan

Recently, our lab implicated a second Slit receptor, Syndecan, in lumen formation (Knox *et al.* 2011). Similar to its known role in the nervous system (Johnson *et al.* 2004), it is possible that Syndecan functions as a co-receptor for Slit, concentrating it to enhance signaling through Robo. Indeed, in embryos mutant for *syndecan*, a heart lumen is unable

to form as Slit and Robo are not restricted to the lumen, but are ectopically distributed both laterally and basally (Knox *et al.* 2011).

Dystroglycan

Dystroglycan (Dg), a component of the widely conserved actin-connecting Dystrophin complex, is another extracellular matrix receptor that is present along both the luminal and basal CB surfaces. In hypomorphic *dg* mutants, the luminal domain is absent or reduced and an extended junctional domain is observed (Medioni *et al.* 2008).

Extracellular matrix

In addition to secreted ligands such as Slit and Netrin, the lumen of the mature embryonic heart also contains several basement membrane components such as CollagenIV α2 (Drechsler *et al.* 2013), the heparin sulphate proteoglycan Trol/Perlecan (Medioni *et al.* 2008, Drechsler *et al.* 2013), the Nidogen glycoprotein (Drechsler *et al.* 2013), and the Collagen XV/XVIII Multiplexin (Harpaz *et al.* 2013). Detailed analysis of these lumen factors is lacking as most studies have been limited to determining their presence and localization, rather than their specific function. An exception to this is Multiplexin, which has been implicated in regulating the lumen size in the heart (Harpaz *et al.* 2013). In embryos mutant for *multiplexin*, a lumen of significantly decreased diameter develops, whereas Multiplexin overexpression leads to formation of a lumen of greater size than in wildtype embryos (Harpaz *et al.* 2013).

1.5.3 Dorsal and ventral midline adhesion

Immediately dorsal and ventral to the lumen are midline cell-cell adhesions, enclosing and sealing the lumen. Several known junctional proteins localize to these domains, including E-cad, Armadillo/β-catenin, Frazzled/Deleted in colorectal cancer (DCC), and Dlg (Santiago-Martínez *et al.* 2008, Medioni *et al.* 2008, Macabenta *et al.* 2013). E-cad and Armadillo mark the site of adherens junctions. As discussed above (1.5.1), this adherens junction domain is restricted and excluded from the lumen through Slit and Robo signaling (Santiago-Martínez *et al.* 2008). Similarly, Netrin signals through Frazzled, concentrated at the developing junctional domains, to modulate the lumen-sealing adhesion sites (Macabenta *et al.* 2013). Extension of these adhesions towards the middle of the contralateral CBs prevents formation of an open lumen (eg. in *slit*, *robo*, or *dystroglyan* mutant embryos; MacMullin and Jacobs 2006, Qian *et al.* 2005, Santiago-Martínez *et al.* 2008, Medioni *et al.* 2008). While the role of Dlg in *Drosophila* heart development is not known, as a member of the Scribble polarity complex, it is a classical basolateral marker, and clearly labels the CB adhesions (Medioni *et al.* 2008).

1.5.4 Lateral adhesion between neighboring cardioblasts

Cell-cell adhesion is not only required between contralateral CBs to enclose the lumen, it is also required between neighboring ipsilateral cells allowing for proper alignment and cohesion during collective CB migration and subsequent lumen formation. Thus, throughout all stages of embryonic heart development, cell junction proteins such

as E-cad and Dlg also localize laterally between the specified CBs (Haag *et al.* 1999, Medioni *et al.* 2008). When lateral adhesion is disrupted early in heart development (for example in embryos lacking Slit or the lateral transmembrane Toll), CBs are frequently misaligned or separated from each other (MacMullin and Jacobs 2006, Santiago-Martínez *et al.* 2006, Wang *et al.* 2005). This affects the CB rows not only during lumen formation, but also in the prior stages as the CBs are migrating (1.4.2).

1.5.5 Basal cardioblast surfaces

In addition to the luminal and junctional factors, there are also proteins known to localize to the basal surface of the CBs. Some of these, such as Collagen IV α2 and Trol are shared with the luminal basement membrane, while others such as the CollagenIV-like Pericardin, the thrombospondin-repeat containing Lonely heart, or Robo2 are specific to this outer domain (Chartier *et al.* 2002, Drechsler *et al.* 2013, Qian *et al.* 2005, Santiago-Martínez *et al.* 2006).

1.6 The integrin heterodimer as an intriguing candidate to play an instructive role in *Drosophila* embryonic heart development

While Slit-Robo signaling is essential for generating an anti-adhesive luminal pocket, Slit and Robo are unable to instruct the position of this lumen. This is illustrated through Slit overexpression studies: while extra Slit is sufficient to promote additional lumen formation, these ectopic lumens are generated at the basal surface between CBs

and the flanking pericardial cells, between CBs and the underlying amnioserosa, or at lateral surfaces between ipsilateral rather than contralateral CBs (Santiago-Martínez *et al.* 2008). Therefore, although factors in addition to Slit and Robo have also been identified, what remains unclear is the underlying mechanism identifying the site of lumen formation and establishment of the initial polarization cue. Why does a central continuous lumen develop at the midline? Why, in the absence of Slit, do open lateral pockets persist between neighboring CBs or between CBs and the flanking pericardial cells? What guides Robo, Dg, Syndecan, and Unc5 to the proper luminal domain? The mechanism guiding or promoting proper localization of the essential luminal components remains an open question.

Currently, our understanding of tubulogenesis is largely based on a classical epithelial tube model, with the lumen-facing apical membrane opposite to the ECM-interacting basal cell surface. As highlighted previously, this model suggests a leading role for the ECM and the primary ECM receptor, the integrin heterodimer, in orienting the cell or tissue and identifying the site of lumenogenesis and establishing polarity (1.2.2). However, in this thesis, we study a unique model of tubulogenesis, one in which the lumen has basal-like rather than classical apical features. Despite the attention given to *Drosophila* heart tubulogenesis, in large part because of its similarities with vertebrate cardiogenesis and vasculature (Medioni *et al.* 2008, Brandt and Paululat 2013), the role of integrins in this developmental model has not been established.

1.7 Integrin based adhesion and signaling

Integrins are heterodimeric transmembrane receptors that mediate a physical link between the extracellular matrix and cytoplasmic signaling adaptors and the cytoskeleton (Figure 1.5). Each integrin dimer is comprised of one alpha (α) and one beta (β) subunit. Binding of an ECM ligand to the integrin receptor triggers a conformational change which exposes binding sites within the integrin cytoplasmic tails. These sites mediate specific protein-protein interactions between the integrin subunits and numerous cytoskeletal adaptors or signaling proteins (Figure 1.5). Thus, integrins serve as a physical connection to the outside of the cell and also as a signaling hub within the cell, controlling adhesion, cytoskeletal dynamics, cell migration, differentiation, survival, and polarization (Berrier and Yamada 2007). However, not only are extracellular cues communicated to cytoplasmic machinery via integrins (termed “outside-in” signaling), but integrins can also transmit intracellular signals to the ECM (termed “inside-out” signaling). Signals delivered to integrins via phosphorylation of one of the subunit tails or through binding of adaptor proteins can increase or decrease the affinity of integrins for specific ECM ligands (Calderwood *et al.* 2002, Anthis *et al.* 2009a, Takala *et al.* 2008).

1.7.1 The integrin adhesome

Integrins are enzymatically inactive receptors. They mediate adhesion and signaling through complex interactions with the integrin adhesome, a collection of

Figure 1.5 – Integrins interact with the ECM, cytoplasmic adhesome, and actin cytoskeleton

Integrins are heterodimeric proteins comprised of one alpha (α) and one beta (β) subunit that span the cell membrane. Outside the cell (bottom), the integrin dimer binds to ligands within the extracellular matrix. Within the cell (top), primarily the β-integrin cytoplasmic tail binds to numerous adhesome proteins which mediate interactions with the actin cytoskeleton and a diverse array of signal cascades. Key adhesome proteins depicted here include Talin, FAK, the IPP (ILK, Pinch, Parvin), CAP, and Vinculin. Figure adapted from Gunst and Zhang 2008 with permission not required.

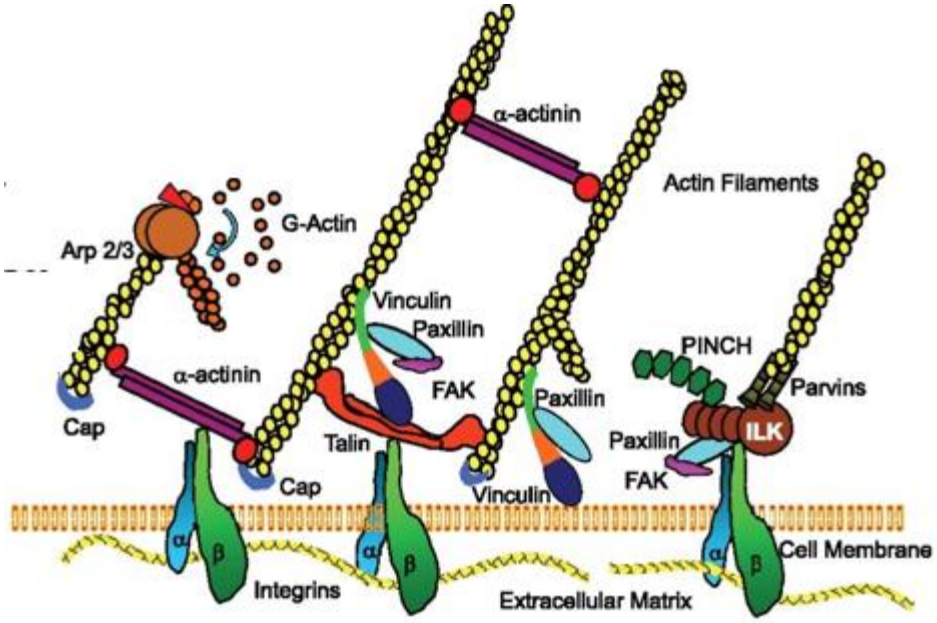
α-actinin
Actin Filaments
G-Actin
Arp 2/3
Vinculin
Paxillin
PINCH
α-actinin
FAK
Paxillin
Parvins
Cap
Talin
ILK
Paxillin
Cap
FAK
Vinculin
α
β
α
β
α
β
Integrins
Extracellular Matrix
Cell Membrane

numerous cytoskeletal adaptors and signaling proteins and enzymes which are recruited when an ECM ligand binds (Figure 1.5; Zaidel-Bar *et al.* 2007a).

Talin

Key to integrin-based adhesion and signaling is the adaptor protein Talin (eg. in mice Monkley *et al.* 2000, in nematodes Cram *et al.* 2003, in flies Brown *et al.* 2002b). While there are numerous signaling molecules downstream of integrins, Talin is unique for its requirement in both inside-out and outside-in integrin function (see review by Das *et al.* 2014). Binding of Talin to the β-integrin tail activates integrins, increasing the affinity for ECM ligands (Calderwood *et al.* 2002). Inside the cell, Talin directly and indirectly (eg. via Vinculin) links integrins to the actin cytoskeleton (Calderwood and Ginsberg 2003). These interactions are possible because of the unique structure of Talin: Talin is a large ~250kDa protein comprised of a small N-terminal, FERM-domain containing, head and an extended C-terminal rod (Ziegler *et al.* 2008). In both the head and rod regions there are binding sites for β-integrin (Integrin Binding Site or IBS1 and IBS2; Calderwood *et al.* 2002, Moes *et al.* 2007, Rodius *et al.* 2008). In addition, binding sites exist for F-actin (Hemmings *et al.* 1996, Lee *et al.* 2004), Vinculin (Gingras *et al.* 2005), Focal Adhesion Kinase (FAK, Chen *et al.* 1995), and several other proteins (reviewed in Das *et al.* 2014).

Scaffold adaptor proteins and Actin regulators

In addition to Talin, there are numerous other scaffolding and adaptor proteins that mediate the connection from integrins to the actin cytoskeleton (Figure 1.5; Zaidelbar *et al.* 2007a). Some, like Talin, are able to directly link integrins to actin (eg. Tensin/Blistery and α-actinin), but most interact with additional proteins to form this linkage (Zaidelbar *et al.* 2007a). Wech, a multi-domain protein recently identified in *Drosophila*, functions downstream of Talin to localize Integrin Linked Kinase (ILK) at sites of integrin adhesion in muscles (Löer *et al.* 2008). Contrary to its name, ILK is likely unable to catalyze phosphorylation (Wickström *et al.* 2010, Fukuda *et al.* 2011). However, through its numerous protein-binding domains, it acts as a scaffold for proteins such as Parvin and Pinch to mediate the integrin-actin connection (Qin and Wu 2012; Ghatak *et al.* 2013). Ponsin or Cbl-associated protein (CAP) is another adaptor protein that localizes to integrin adhesion sites (Zhang *et al.* 2006, Bharadwaj *et al.* 2013). CAP binds to Paxillin and Vinculin and modulates cytoskeletal organization, possibly through a Vinculin-CAP complex or through other proteins that bind to one or more of its SH3 domains (Zhang *et al.* 2006, Bharadwaj *et al.* 2013). Vinculin is recruited by Talin and is important in anchoring actin at sites of stable integrin adhesion (Humphries *et al.* 2007, Carisey *et al.* 2013).

Signaling or regulatory proteins

While some proteins mediate the integrin-actin link, others are kinases, phosphatases, proteases, or GTPases involved in signaling from the site of integrin adhesion into the cell or in regulation of the integrin adhesome itself (Zaidel-bar *et al.* 2007a). Often the distinction between scaffolding and regulatory proteins is blurred, as many of the scaffolding proteins also have catalytic activity or are indirectly involved in signaling through enzyme recruitment. Calpain is a protease with numerous cleavage targets within the adhesome, including Talin (Franco *et al.* 2004, Bate *et al.* 2012), the integrin activator Kindlin (Zhao *et al.* 2012), FAK (Chan *et al.* 2010), Paxillin (Cortesio *et al.* 2011), as well as the β-integrin cytoplasmic tail itself (Pfaff *et al.* 1999, Flevaris *et al.* 2007). Src is a tyrosine kinase, involved in cell migration and integrin E-cad cross-talk (Avizienyte and Frame 2005). Src often forms a functional complex with FAK, which has both a central kinase domain and protein binding domains for Talin and Paxillin, among others (Zhao and Guan 2011). Paxillin, another scaffolding protein that directly binds the β-Integrin tail (Liu *et al.* 1999), regulates the actin cytoskeleton in part by coordinating Rac and RhoA GTPases and recruiting p21-activated serine-threonine kinase (PAK; Chen *et al.* 2005, Brown *et al.* 2002a, Deakin and Turner 2008). The GTPases Rac and Cdc42 regulate early formation of integrin adhesions and related actin dynamics while the RhoA GTPases involve the actin-associated Myosins especially during adhesion maturation and stabilization (Price *et al.* 1998, Clark *et al.* 1998; Begum *et al.* 2004, Filipenko *et al.* 2005, Abreu-Blanco *et al.* 2014).

1.7.2 Extracellular matrix integrin ligands

The extracellular matrix is a complex environment that includes numerous integrin ligands which vary depending on the cell type and spatiotemporal situation. The ability of integrins to interact with ECMs of varying composition allow them to "sense" the environment and transmit these cues into the cell. Integrin ligands present in the ECM of both vertebrates and flies include Laminin heterotrimeric glycoproteins (eg. LanA and Wing Blister comprise the alpha chains in *Drosophila;* Belkin and Stepp 2000), the triple-helical structural Type IV collagen proteins (eg. CollagenIV α1, CollagenIV α2, and Pericardin in *Drosophila;* Singhal and Martin 2011), the heparan sulfate proteoglycan Perlecan (eg. Trol in *Drosophila;* Whitelock *et al.* 2008), and the homotrimeric Thrombospondin glycoproteins (Calzada *et al.* 2003). Notably, Fibronectin, an ECM ligand of integrins found in vertebrates, is likely not present in *Drosophila* (Gratecos *et al.* 1988, Broadie *et al.* 2011).

Furthermore, just as integrins can bind to multiple ligands, ECM components often are ligands for several different receptors. For example, as in vertebrates, *Drosophila* Laminins bind to the integrin receptor, but also to Dg and Syndecan (Schneider *et al.* 2006, Narita *et al.* 2004, Yamashita *et al.* 2004), which notably are also present in the developing *Drosophila* heart (Medioni *et al.* 2008, Knox *et al.* 2011). Dg is also a primary receptor for Perlecan (Peng *et al.* 1998). Therefore, while the ECM-receptor network is complex, much of the basic network is similar in flies and vertebrates. The reduced number of redundant

ligands and receptors in *Drosophila* makes it a relatively simple model in which to study Interin-ECM requirements.

1.7.3 *In vitro* cell culture studies highlight a role for integrins in ECM adhesion

While many of the earliest studies on integrin-ECM interactions were in animal developmental models, cancer studies, and immunology (Eg. Duband *et al.* 1986, Mentzer *et al.* 1988, Sonnenberg *et al.* 1988, Saga *et al.* 1988; Overviews in Hynes 1987, Ruoslahti and Pierschbacher 1987), more recently the feasibility of maintaining, genetically or chemically manipulating, and imaging cells in culture has led to incredible insights being gained from *in vitro* molecular biology and biochemistry studies. Integrins are now recognized as being essential to "sense" the composition and structure of the ECM environments and transduce these signals into the cell to control cell shape, migration or motility, polarization, survival, and proliferation, and even to regulate the ECM itself (Wolfenson *et al.* 2013, Miranti and Brugge 2002).

Numerous studies on integrin structure and function have identified unique characteristics allowing integrins to serve as this sensing and signaling "hub". As mentioned previously, integrin dimers can bind to a variety of ECM ligands allowing them to identify both chemical (eg. secreted signals from neighboring cells or tissues) and physical (eg. mechanical force or structural differences in the ECM) changes in the environment. In vertebrates, the response is further refined through the cell or tissue specific expression of up to 24 different heterodimer combinations formed by eighteen

alpha and eight beta subunits (Hynes 2002). Through the complex and dynamic adhesome protein interactions within the cell, integrins can activate diverse signal cascades, many of which have been elucidated and analyzed in detail (Harburger and Calderwood 2009). Additional transmembrane proteins and receptors such as Syndecans and Cadherins can also directly or indirectly interact with integrins and further fine-tune the signals (Streuli and Akhar 2009, Weber *et al.* 2011, Morgan *et al.* 2007). Furthermore, integrins are capable of forming different types of adhesions, allowing for both transient and longer-lasting stable connections. For example, in migrating cells, transient nascent adhesions, involving only a few integrin molecules, form at the tip of the lamellipodia, assembling and disassembling within seconds (Choi *et al.* 2008). If they do not disassemble, these integrin clusters can mature into focal complexes (one to two minute turnover rate) or larger and longer lasting stable focal adhesions lasting tens of minutes which recruit and involve additional adhesome proteins (Choi *et al.* 2008, Zaidel-Bar *et al.* 2007b). Cell culture systems allow the study of the intricate mechanisms underlying the changes and signaling that occur during integrin adhesion formation and maturation.

Although many insights into integrin function have been made using cell culture models, it is important to know if these mechanisms of integrin adhesion and signaling are representative of *in vivo* integrin requirements as well. Recent advances using a variety of *in vitro* systems, including culturing cells on a variety of ECM substrates and in 3D matrices, have aimed to bridge this knowledge gap. And, indeed, much of what we know does appear to translate. However, in some contexts, there are differences as well

(discussed in Wolfenson *et al.* 2013). For example, when comparing developing tissues to cell cultures or when comparing varying cell culture conditions, a general theme is that smaller or less concentrated adhesions form when the ECM surface is less rigid (Wolfenson *et al.* 2013, Prager-Khoutorsky *et al.* 2011, Ghassemi *et al.* 2012). Thus, it is essential to use a combination of approaches to elucidate the full mechanism of integrin function.

1.7.4 Integrin adhesion is essential in developing tissues

Consistent with *in vitro* findings, integrin studies in both vertebrates and invertebrates highlight an essential and complex requirement of integrins in establishing cell-ECM adhesion. Following is a brief overview of studies in mice (mammalian vertebrate) and flies (invertebrate) highlighting some of the insights gained and some of the difficulties encountered.

Integrin adhesion is essential in mice

Whole organism gene knock-out studies for the individual integrin alpha and beta subunits demonstrate that integrin adhesion is essential, although not every subunit is individually necessary for development (reviewed Beauvais-Jaouneau and Thiery 1997, Sheppard 2000, Bouvard *et al.* 2001, Chen and Sheppard 2007, Israeli-Rosenberg *et al.* 2014). The β1 subunit is broadly expressed during development and serves as the β-integrin subunit for about half of all known vertebrate heterodimers. Thus, it is not

surprising that β1-null mice die very early in development prior to embryo implantation (at E5.5; Fässler and Meyer 1995, Stephens *et al.* 1995). It is likely that a contributing factor to the inviability of these embryos is a failure to generate a normal ECM, as mice lacking the ECM glycoprotein Laminin share similar developmental defects (Bouvard *et al.* 2001, Smyth *et al.* 1999). Furthermore, tissue-specific loss of β1 reveals roles for development of multiple organs, including the heart (Valencik *et al.* 2002, Keller *et al.* 2001). Knock-out mice for α4 or α5, two of the β1 partners, also exhibit early embryonic lethality (by E8-10; Goh *et al.* 1997, Yang *et al.* 1993, Yang *et al.* 1995), with a lack of adhesion between the mesoderm and endoderm germ layers (α4), prominent defects in the epicardium of the heart (α4), and reduced blood vessel integrity (α4 and α5; Yang *et al.* 1993, Yang *et al.* 1995). Similar studies disrupting ECM-encoding genes also affect cardiac development and vasculogenesis consistent with an essential requirement for integrin-ECM adhesions during vascular tubulogenesis (Gustafsson and Fässler 2000). However, knock-out models of additional integrin subunits suggest that not all integrin heterodimers are essential for development or viability. For example, embryos lacking α3, α8, or α6 often survive until birth while mice with disrupted α10, β5, or β6 genes are both viable and fertile (Bouvard *et al.* 2001). However, even within these viable or late-lethal examples there is some disruption in cell-ECM adhesion. For example, loss of either α3, α6, or β4 leads to skin blistering, due to disorganization of the underlying ECM (DiPersio *et al.* 1997, Georges-Labouesse *et al.* 1998, van der Neut *et al.* 1996). Similarly, lack of a

proper ECM in α3 knock-out mice leads to abnormal development of the tubular kidney organ (Kreidberg *et al.* 1996)

Taken together, it is clear that integrins are essential for multiple stages and processes of mouse development. As in cell culture models, integrins are required for establishment of a linkage between cells or tissues and the ECM. However, these studies also highlight several of the difficulties when studying integrins in mice or other vertebrates. The early lethality phenotype of many integrin knock-out models prevents detailed analyses of tissue development, let alone the underlying subcellular and molecular processes. Studies of viable or late-lethality gene knock-out models are often complicated by functional redundancy or compensation by remaining subunits. Even just within the heart, at least three integrin dimers and two Talin genes are expressed (Bouvard *et al.* 2001, Brancaccio *et al.* 1998, Ben-Yosef and Francomano 1999, Monkley *et al.* 2011). While some studies have addressed this by generating multiple-gene knock-outs, this is genetically cumbersome, expensive, and time consuming.

Integrin adhesion is essential in Drosophila melanogaster

Another *in vivo* system is the genetically amenable *Drosophila melanogaster*. In contrast to the eighteen alpha and eight beta integrin subunits found in vertebrates, this invertebrate model has only two beta and five alpha integrin genes (βPS1 and βv, αPS1-αPS5), and only one heterodimer has been detected in the heart (αPS3βPS1; Brower 2003, Stark *et al.* 1997). Consistent with what is known of integrin function in cell culture and in

other animal models, *Drosophila* integrins are essential for dynamic adhesion required during development of numerous tissues and organs and for maintainance of stable, long-lasting adhesions. Longer-lasting adhesion are required in the wing epithelium (Wilcox *et al.* 1989, Brower and Jaffe 1989) and in the musculature system to prevent muscle-muscle and muscle-tendon cell detachment during muscle contraction (Martin-Bermudo and Brown 1996; Perkins *et al.* 2010). Dynamic morphogenetic processes such as germ-band retraction, dorsal closure, and salivary gland and tracheal tubulogenesis during embryogenesis also require integrins (Roote and Zusman 1995, Stark *et al.* 1997, Bradley *et al.* 2003, Levi *et al.* 2006). During heart assembly, embryos lacking either αPS3, βPS1, or the integrin ECM ligand LanA had misplaced or missing pericardial cells (Stark *et al.* 1997, Yarnitzky and Volk 1995). Furthermore, during our lab's previous studies on Slit, genetic dosage sensitive screens implicated αPS3 and βPS1, as well as integrin ECM ligands and second messengers, in working with Slit to coordinate heart development (MacMullin and Jacobs 2006). Although a detailed analysis of the heart development defects was not done for these studies, together they support a role for integrin adhesion during this tubulogenesis event.

More recently, benefiting from insights gained through *in vitro* models, *Drosophila* studies have begun to elucidate the molecular mechanisms and signaling pathways essential for tissue morphogenesis and maintenance. Several studies have identified specific domains or amino acids as crucial for integrin activation or protein binding in development or tissue maintenance (Li *et al.* 1998, Jannuzi *et al.* 2004; Pines *et al.* 2011).

Other studies focused on the adhesome components including Talin, FAK, ILK, Src, Paxillin, and Kindlin. The lack of gene redundancy in *Drosophila* negates the possibility of compensation in knock-out studies and facilitates the analysis of integrin networks during development (eg. one Talin compared to two in vertebrate). Combined with the numerous genetic tools and mutants readily available, this permits a more simple and effective approach to test for the requirement of particular genes and their physical or functional interactions with each other. For example, consistent with the IPP complex found in cell culture, triple-mutant analysis suggests that ILK, Pinch, and Parvin function synergistically at muscle-epidermis attachment sites (Vakaloglou *et al.* 2012). Several recent studies have assessed the requirement for the integrin adaptor Talin in embryonic development, suggesting that Talin is essential for all integrin-dependent processes (see 4.2.1; Brown *et al.* 2002b, Ellis *et al.* 2011).

Taken together, studies on integrins and integrin-related proteins in *Drosophila* confirm a conserved basic ECM-integrin-adhesome network which, similar to in cell culture and vertebrate models, is essential for cell-ECM interactions in multiple contexts including organogenesis. Our lab has recently focused on understanding the underlying molecular mechanisms governing *Drosophila* embryonic heart development. As integrins have the ability to interact with the surrounding environment and transmit these cues into the cell to control cytoskeletal dynamics and numerous signaling pathways, they are an intriguing candidate to play an initiating role in the cell polarization and morphogical changes required for heart tubulogenesis.

1.8 Thesis objectives

The thesis experimental research plan was designed to determine the role of integrins during *Drosophila* heart cell migration, polarization, and lumen formation. The first research focus was to establish a requirement for the integrin αPS3βPS1 heterodimer itself (Chapter 3). Using genetic and immunohistochemical approaches (including several novel antibody heart markers), we found that integrin localization is an early indicator of the luminal site and that both αPS3 and βPS1 are required for the CB polarization and shape changes required for lumen formation. Following this, to identify adhesome proteins required for integrin adhesion in the heart, the tools and insights gained were further applied to the essential integrin activator and adaptor Talin (Chapter 4) and downstream integrin targets Src and FAK (Appendix D). I demonstrate that while Src function is required in the embryo for CB migration to proceed, it is unlikely to be an essential downstream target of integrins in heart development. Rather, it appears that lack of Src function inhibits internalisation of the amnioserosa, which secondarily results in stalled CB migration. In contrast, Talin is essential for heart tubulogenesis. Talin is localized along the luminal domain during tubulogenesis and the disrupted heart development observed in mutants for *rhea*, the gene encoding Talin, is reminiscent of the phenotype in embryos lacking integrin. Furthermore, although Talin is essential for proper βPS1 integrin localization within the heart, either of Talin's integrin binding sites are sufficient to stabilize βPS1 along the luminal domain and establish an open cardiac tube.

Methods

CHAPTER TWO

Recipes for reagents shown in **bold** can be found in Appendix E.

2.1 Acknowledgements

We thank the following investigators for providing *Drosophila* strains used in thesis: E. Bier (B2-3-20), A. Brand (UAS-rpr), C. Chien (fak56D^{N30}, fak56D^{K24}, and the kr-GFP balancer), M. Freeman (GMR-Gal4), C. Goodman (lanA$^{9-32}$), C. Klämbt (lea$^{54-14}$), T. Kojima (src42A$^{26-1}$, UAS-Src42A^{CA}, UAS-Src42A^{DN}), B. McCabe (dMEF-Gal4), N. McGinnis (vkg$^{p1003-83}$), T. Millard (UAS-moesin-mCherry), B. Reed (YET1), R. Schulz (TUP-GFP), G. Tanentzapf (Talin rescue strains, rhea^{2}, rhea^{79}, mys^{XG43}, and yw; hsFLP; Dr/TM3, Sb), and T. Xu (UAS-Src42A^{WT}). All other stocks were provided by the Bloomington Stock Centre, the Vienna *Drosophila* RNAi Centre, and the *Drosophila* Genetic Resource Centre (Kyoto). The LanA monoclonal antibody was produced by Abmart (ab-mart.com). All other monoclonal antibodies were obtained from the Developmental Studies Hybridoma Bank developed under the auspices of the NICHD. Polyclonal antibodies were generously supplied by M. Beckerle (Pinch), W. Deng (Dystroglycan), A. Kolodkin (CAP), and Z. Lai (Zfh1). The pRSETB-dMEF2 and pGEX-5X-1-Dg-cyto plasmids were kindly provided by H. Nguyen and W. Deng, respectively. A special thanks to Qamber Syed and Megan Collie for performing the embryo heart phenotype blind scoring. Research was funded by OGS, NSERC CGS-D, and CIHR.

2.2 Fly maintenance

Fly stocks were maintained under standard conditions at room temperature (23-25°C). Stock flies were transferred to fresh **fly food** every 15 days; adults were cleared from vials seven days after transfer. Crosses were performed at 25°C unless otherwise noted; to maximize the number of eggs laid, adults were transferred to fresh food two times per week (Monday and Thursday).

2.3 Genetic strains

For all experiments, y^1w^{1118} ("*yw*") was used as a wildtype control unless otherwise noted. Table 2.1a lists all alleles used in this thesis. Each allele was crossed into a *yw* background and maintained over β-galactosidase (βGal), Green fluorescent protein (GFP), or Yellow fluorescent protein (YFP) marked balancers (Table 2.1b). All other fly strains used in this thesis are listed in Table 2.1c. *UAS-scb* was constructed using 5'-TGG CGT AGA ATT CAT CTG TTG-3' (EcoRI site) and 5'-TCA CGA TCT AGA GGA CAT TC-3' (XbaI site) as primers for a PCR reaction to amplify the full length protein ScabA from the original EST clone (RE41844, Berkeley *Drosophila* Genome Project). The lacZ enhancer trap line B2-3-20 was used to visualize the cardial cell nuclei in Chapter 3 experiments (Bier *et al.* 1989).

Table 2.1a: A list of all alleles used in this thesis

Stock	Full gene name	Source (Stock #*)
dab$^{M54\text{-}R}$	*disabled*	Bloomington
fak56D^{KG00304}	*fak56D (focal adhesion kinase)*	Bloomington (#13080)
fak56D^{K24}	*fak56D (focal adhesion kinase)*	Tsai *et al.* 2008
fak56D^{N30}	*fak56D (focal adhesion kinase)*	Tsai *et al.* 2008
ilk^{1}	*integrin linked kinase*	Bloomington (#4861)
ilk^{2}	*integrin linked kinase*	Bloomington
lanA$^{9\text{-}32}$	*laminin A (α3,5)*	Henchcliffe *et al.* 1993
lea$^{54\text{-}14}$	*leak (robo2)*	C. Klämbt
mys^{1}	*myospheroid (βPS1)*	Bloomington (#59)
mys^{XG43}	*myospheroid (βPS1)*	Wieschaus *et al.* 1984
rhea^{1}	*rhea*	Bloomington (#2296)
rhea^{2}	*rhea*	Prout *et al.* 1997
rhea^{79}	*rhea*	Brown *et al.* 2002b
robo^{1}	*robo1*	Bloomington (#8755)
scb^{2}	*scab (αPS3)*	Bloomington (#3098)
scb^{01288}	*scab (αPS3)*	Bloomington (#11035)
sli^{2}	*slit*	Bloomington (#3266)
src42A^{E1}	*src42A*	Bloomington (#6408)
src42A^{k10108}	*src42A*	Bloomington (#10969)
src42A$^{26\text{-}1}$	*src42A*	Takahashi *et al.* 2005
src64B^{P1}	*src64B*	Bloomington (#7379)
stck$^{3R\text{-}17}$	*steamerduck (pinch)*	Bloomington (#2302)
vinc^{1}	*vinculin*	Bloomington (#6030)
vkg $^{p1003\text{-}83}$	*viking (collagen IV α2)*	N. McGinnis
wb^{SF11}	*wing blister (laminin α1,2)*	Bloomington (#3409)
wech^{K08815a}	*wech*	Bloomington (#10818)

*Stock from which allele originated. All alleles were maintained in a *yw* background and over a marked balancer.

Table 2.1b: A list of balancer and/or marked chromosomes used in this thesis

	Full name	**Source (stock #)**
Y Chromosome		
Y, Act-GFP	*Dp(1;Y)y^{+} P{ry+11} P{w+mC=ActGFP}JMR1*	Kyoto (#109661)
X Chromosome		
FM7c, Kr-GFP	*FM7c, P{w[+mC]=GAL4-Kr.C}DC1, P{w[+mC]=UAS-GFP.S65T}DC5, sn[+]*	Bloomington (#5193)
Chromosome 2		
CyO, En-lacZ	*CyO, engrailed-lacZ*	Jacobs' central stocks
CyO, Kr-GFP	*CyO, kruppel-GFP*	C. Chien
Chromosome 3		
TM3, Ftz-lacZ	*TM3, fushi tarazu-lacZ*	Jacobs' central stocks
TM6, GMR-YFP	*TM6B, P{Dfd-GMR-nvYFP}4, Sb1 Tb1 ca1*	Bloomington (#23232)
TM3, GMR-YFP	*TM3, P{Dfd-GMR-nvYFP}3, Sb[1]*	Bloomington (#23231)

Table 2.1c: A list of all stocks used in this thesis

Stock	Full name (additional information)	Source (Stock #)
yw	*y^1w^{1118}*	Bloomington (#6598)
dMEF-Gal4		Ranganayakulu *et al.* 1996
GMR-Gal4	*Glass multiple promoter-Gal4*	Freeman 1996
*UAS-rpr**	*UR4-UAS-rep #133 (z-UAS-rpr)*	A. Brand
*UAS-CD8GFP**	*y[1] w[*]; Pin[Yt]/CyO; P{w[+mC]=UAS-mCD8::GFP.L}LL6*	Bloomington (#5130)
UAS-moe-mCherry	*UAS-moesin-mCherry*	Millard and Martin 2008
B2-3-20	*Expresses lacZ in cardioblast nuclei*	Bier *et al.* 1989
tup-GFP	*tup-F4-GFP*	Tokusumi *et al.* 2007
YET1	*Expresses YFP in AS perimeter cells*	Mohseni *et al.* 2009
UAS-scb		A. MacMullin
UAS-mys-RNAi		Vienna (#103704)
UAS-scb-RNAi		Vienna (#100949)
UAS-Trip-scb-RNAi	*y^1 v^1; P{y[+t7.7]v[+t1.8]=TRiP.JF02696}attP2*	Bloomington (#27545)
UAS-Trip-mys-RNAi	*y^1 v^1; P{y[+t7.7]v[+t1.8]=TRiP.HMS00043}attP2*	Bloomington (#33642)
UAS-$src42^{WT}$	*(2nd chr), "Rod3-65"*	Pedraza *et al.* 2004
UAS-$Src42A^{CA}$	*UAS-$Src42A^{Y2-13}$*	Takahashi *et al.* 2005
UAS-$Src42A^{DN}$	*UAS-$Src42A^{KR5-1}$*	Takahashi *et al.* 2005
ubi-$Talin^{WT}$	*pUBI-Talin[EGFP] on X*	Yuan *et al.* 2010
ubi-$Talin^{IBS1-}$	*pUBI-$Talin[EGFP]^{R367A}$ on III*	Tanentzapf and Brown 2006
ubi-$Talin^{IBS2-}$	*pUBI-$Talin[EGFP]^{KS>DD}$ on II*	Ellis *et al.* 2011
ubi-$Talin^{IBS2b-}$	*pUBI-$Talin[EGFP]^{LI>AA}$ on X*	Ellis *et al.* 2011
ubi-$Talin^{IBS1- IBS2-}$	*pUBI-$Talin[EGFP]^{R367A, LI>AA}$ on II*	Ellis *et al.* 2011
ubi-$Talin^{IBS1- IBS2-}$	*pUBI-$Talin[EGFP]^{R367A, LI>AA}$ "4F" on II*	Ellis *et al.* 2011
ubi-$Talin^{IBS1- IBS2-}$	*pUBI-$Talin[EGFP]^{R367A, LI>AA}$ "2M" on II*	Ellis *et al.* 2011
hsFLP; Dr/TM3	*yw; hsFLP; Dr/TM3, Sb*	Chou and Perrimon 1996
ovo^{D1}, FRT2A/TM3	*w*; P{w[+mC]=ovoD1-18}3L P{w[+mW.hs]= FRT(w^{hs})}2A/st^1betaTub85D^D ss^1 e^s/TM3, Sb^1*	Bloomington (#2139)
ovo^{D1}, FRT101; hsFLP	*w* ovo^{D1} v^{24} P{w[+mW.hs]=FRT(w^{hs})}101/ C(1)DX, y^1 f^1/Y; P{ry[+t7.2]=hsFLP}38*	Bloomington (#1813)

* No data shown in thesis – used to confirm presence and expression pattern of Gal4 lines

2.4 Antibody production

2.4.1 Rabbit anti-MEF

The *Drosophila* heart is comprised of two cell types, the lumen enclosing cardioblasts and the flanking pericardial cells (Figure 1.1A). A rabbit polyclonal antibody against *Drosophila* Myocyte enhancing factor 2 (MEF2), a muscle transcription factor, was generated to label the cardioblast nuclei (and other somatic muscles) in fixed tissue. Both anti-MEF (cardioblasts) and anti-Zinc finger homeodomain 1 (anti-Zfh1; pericardial cells) label the cell nuclei (eg. Figure 3.1), allowing approximate cell position and number to be easily assessed.

2.4.1a Induction of His-dMEF2 fusion protein

Rabbit polyclonal antibody, Rabbit anti-MEF, was designed to a His-dMEF2 fusion protein (amino acids 1-168). The pRSETB-dMEF2 plasmid was kindly provided by H. Nguyen (Bour *et al.* 1995; Pennsylvania State University). The plasmid was transformed into competent BL21 cells (Invitrogen 44-0048) using standard procedures and positive transformants were identified using ampicillin-selective plates. **LB (with 0.1 mg/mL ampicillin)** was inoculated with a single transformed colony and cultured at 37°C until log-phase was achieved (OD600 ~0.4). His-dMEF2 Protein expression was induced with 1mM isopropyl-beta-D-thiogalactopyranoside (IPTG; final concentration) for four hours with constant shaking at 37°C. Cells were harvested by centrifugation (10,000g for ten minutes

at 4°C) and the supernatant was removed. Harvested cells were stored at -20°C until protein purification.

2.4.1b Purification of His-dMEF2 fusion protein

His-dMEF2 was purified using native or denatured conditions. Buffers for native purification included the lysis buffer (50 mM sodium phosphate pH 8, 300 mM NaCl, 0.1% TritonX-100, 5 mM imidazole + 1 protease inhibitor tablet/50 mL buffer), the wash buffer (50 mM sodium phosphate pH 8, 500 mM NaCl, 1% TritonX-100, 40 mM imidazole), and the elution buffer(50 mM sodium phosphate pH 8, 500 mM NaCl, 250 mM imidazole). Buffers used for denatured protein purification were the lysis buffer (50 mM sodium phosphate pH 8, 300 mM NaCl, 10 mM imidazole, 8 M urea), the wash buffer (50 mM sodium phosphate pH 6.3, 500 mM NaCl, 30 mM imidazole, 8 M urea), and the elution buffer (50 mM sodium phosphate pH 5, 300 mM NaCl, 8 M urea, 500 mM imidazole). To collect purified His-dMEF2, harvested cells were thawed on ice, resuspended in lysis buffer (1/10 volume of original cell culture), sonicated, and then centrifuged (10 min at 4°C at 14,000 rpm) to remove cellular debris. Supernatant was applied to a His-Select Nickel Affinity Gel column (Sigma P6611; column volume 1/1000 of induced culture volume) following standard manufacturer protocols. Following multiple washes (10-15 column volumes), protein was eluted in ten column volumes of elution buffer (500 µl/fraction) and stored at -20°C until dialysis. Samples collected under native conditions were concentrated in 1x Phosphate buffer saline (PBS; Amicon Ultra Centrifugal Filter Device,

Millipore UFC801008). To remove urea in the eluted denatured sample, dialysis was performed overnight in 1xPBS with Membra-Cel MD25-14 dialysis membrane (14,000 kDa cut-off).

Final protein concentration was determined using a Bradford assay (Sigma B6916). The presence of His-dMEF2 in the purified sample was confirmed using a western blot probed with mouse anti-His(C-terminal) (1:5,000; Invitrogen 46-0693; data not shown).

2.4.1c Preparation of His-dMEF antiserum

Polyclonal anti-MEF antibodies were generated by injecting purified protein into two male New Zealand White rabbits age >12 weeks old (Rabbit #9753 or "A" and Rabbit #9874 or "B"). A total volume of approximately 500 µl was injected in 3 subcutaneous sites (services performed by the Central Animal Facility, McMaster University). Approximately 110 µg of total protein (in 50% Freund's complete adjuvant, Sigma F5881) was used for the initial injection per rabbit. Four subsequent boosters were provided at three week intervals; approximately 65 µg of total protein (in 50% Freund's incomplete adjuvant, Sigma F5506) was used per rabbit. Since purification in native conditions resulted in low protein yields, injected protein included a mix of denatured and native protein (Rabbit A) or only denatured protein (Rabbit B).

2.4.1d Collection of His-dMEF antiserum

Eleven days following the fourth booster, a final terminal bleed was collected. To induce clotting, the bleed was incubated in a 37°C water bath for 30-60 minutes and then placed at 4°C overnight to allow the clot to settle. Following centrifugation of resulting liquid (ten minutes at 4°C at 10,000g), the serum was collected and stored at -20°C. Serum was tested at a range of concentrations (1/100-1/1,000,000) for the ability to immunolabel dMEF2 in fixed embryos. An optimal concentration was determined to be ~1/10,000 for serum collected from both Rabbit A and Rabbit B.

2.4.2 Chicken anti-βGal

Several common balancer chromosomes (Table 2.1b) carry a βGal gene. To differentiate between homozygous embryos and heterozygous embryos carrying these balancers, a chicken polyclonal antibody was generated against βGal.

2.4.2a Generation of egg yolk antibodies (IgY) against βGal

Egg yolk immunoglobulins (IgY) against βGal were generated by injecting purified βGal (Sigma G3153) into two female Leghorn chickens of egg-laying age (Chicken B and Chicken C). A total volume of 1000 µl was injected in four subcutaneous sites (services performed by the Central Animal Facility, McMaster University). For each chicken, 80 µg of βGal rehydrated in 1xPBS (in 50% Freund's complete adjuvant; Sigma F5881) was used for the initial injection. Four subsequent boosters were provided at two week intervals,

and approximately 60 µg of βGal rehydrated in 1xPBS (in 50% Freund's incomplete adjuvant; Sigma F5506) was injected per chicken.

2.4.2b Collection of eggs

Beginning one week after the second booster, eggs were collected daily and stored at 4°C until isolation of IgY's from egg yolk. Each day, one to two eggs per chicken were collected.

2.4.2c Isolation of chicken immunoglobulins (IgY) against βGal

Egg yolk immunoglobulins were isolated using polyethylene glycol precipitation (Goldring and Coetzer 2003). Egg yolks were separated from egg whites and the yolk sac was removed. Two volumes of phosphate buffer (100 mM, pH 7.6) were mixed with the egg yolks and then 3.5% (w/v) PEG6000 was mixed in until fully dissolved. Following centrifugation to eliminate yolk debris (4420g for 20 minutes at room temperature), the lipid fraction was removed by filtering the supernatant through a cotton wool plug (absorbent type). The filtrate was collected and PEG6000 was added to a final concentration of 12% (ie. 8.5% more than the initial 3.5%). IgY's were pelleted by centrifugation (12,000g for 10 minutes at room temperature) and resuspended in one egg yolk volume of phosphate buffer (100 mM, pH 7.6). PEG6000 was added to a final concentration of 12% and the IgY's were pelleted a second time by centrifugation (12,000g for 10 minutes at room temperature). The final pellet was resuspended in 1/6

egg yolk volume of phosphate buffer (100 mM, pH 7.6), with 0.01% sodium azide to inhibit bacterial and fungal growth. IgY samples were stored at -80°C.

Isolated IgY antibodies were tested at a range of concentrations for the ability to immunolabel βGal in fixed embryos (1/100-1,000,000). Samples collected from post-second booster eggs were optimal at a concentration of ~1/100,000 while later samples (post-third or fourth booster) were optimal at ~$1/10^6$.

2.4.3 Rabbit anti-Dystroglycan

To assess the size and shape of the cardioblasts as they migrate and form a lumen, a rabbit polyclonal antibody was generated against Dystroglycan (Dg). Dg is a transmembrane protein that is present in numerous tissues, including the cardioblast cells. The antibody labels the cell membrane of the cardioblasts and can be used to visualize the heart in both frontal (eg. Figure 4.7) and transverse (eg. Figure 4.8) confocal images.

2.4.3a Induction of GST-Dg fusion protein

Rabbit polyclonal antibody, Rabbit anti-Dg, was designed to a GST-Dg fusion protein (102 C-terminal amino acids corresponding to the cytoplasmic domain). The pGEX-5X-1-Dg-cyto plasmid was kindly provided by W. Deng (Deng *et al.* 2003; Florida State University). Presence of the appropriate insert was confirmed by DNA sequencing of the plasmid from a pGEX 5' primer (sequencing performed by MOBIX, McMaster University).

The plasmid was transformed into competent BL21 cells (Invitrogen 44-0048) using standard procedures and positive transformants were identified using ampicillin-selective plates. **LB (with 0.1 mg/mL ampicillin)** was inoculated with a single transformed colony and cultured at 37°C until log-phase was achieved (OD600 ~0.7). GST-Dg-cyto protein expression was induced with 1 mM IPTG (final concentration) for five hours with constant shaking at 37°C. Cells were harvested by centrifugation (10,000g for ten minutes at 4°C) and the supernatant was removed. Harvested cells were stored at -20°C until protein purification.

2.4.3b Purification of GST-Dg fusion protein

Harvested cells were thawed on ice, resuspended in 1xPBS with added protease inhibitor (Roche applied sciences 5056489001; 1xPBS volume used was 1/20 volume of original cell culture), sonicated, and then centrifuged (10 minutes at 4°C at 14,000 rpm) to remove cellular debris. A Glutathione Sepharose 4B affinity gel column was prepared following standard manufacturer protocols (GE Healthcare 17-0756-05; column volume 1/1000 of volume of induced culture). The supernatant was applied to the column and the flow-through was applied to the column two additional times to ensure maximum protein binding. Following multiple washes with 1xPBS (three washes each of five column volumes), protein was eluted in eight column volumes of elution buffer (50 mM Tris-HCl, 10 mM reduced glutathione – Sigma G4251) and stored at -20°C until dialysis. Samples were dialyzed overnight in 1xPBS with Membra-Cel MD25-14 dialysis membrane (14,000

kDa cut-off). Final protein concentration was determined using a Bradford assay (Sigma B6916).

2.4.3c Preparation of GST-Dg antiserum

Polyclonal anti-Dg antibodies were generated by injecting purified GST-Dg-cyto protein into two male New Zealand White rabbits age >12 weeks old (Rabbit #9802 or "A" and Rabbit #9803 or "B"). A total volume of 500 µl was injected in 3 subcutaneous sites (services performed by the Central Animal Facility, McMaster University). For each rabbit, 120 µg of total protein (in 50% Freund's complete adjuvant, Sigma F5881) was used for the initial injection. Four subsequent boosters were provided at three week intervals, and approximately 77 µg of total protein (in 50% Freund's incomplete adjuvant, Sigma F5506) was used per rabbit.

2.4.3d Collection of GST-Dg antiserum

Fourteen days following the fourth booster, a final terminal bleed was collected. To induce clotting, the bleed was incubated in a 37°C water bath for 30-60 minutes and then placed at 4°C overnight to allow the clot to settle. Following centrifugation of resulting liquid (ten minutes at 4°C at 10,000g), the serum was collected and stored at -20°C. Serum was tested at a range of concentrations (1/100-1/10,000) for the ability to immunolabel Dg in fixed embryos. An optimal concentration was determined to be ~1/100 for serum collected from both Rabbit A and Rabbit B. However, only anti-serum from

Rabbit B was used in further immunolabeling experiments, as anti-serum A resulted in high background.

2.4.4 Generation of LanA monoclonal antibody (Mouse anti-LamininA)

To detect Laminin A (α 3,5; LanA), a monoclonal antibody was generated against the peptide sequence ANTEHDHIDYSV, corresponding to amino acids 59-70 (of 3,712 total amino acids comprising LanA). Peptide generation, immunization, myeloma-spleen cell fusion, cell line selection, and antibody collection and lyophilisation were performed by Abmart (ab-mart.com). Lyophilized antibody was rehydrated overnight in ddH_20 (with 0.1% sodium azide) at 4°C. Glycerol was added to 50% final concentration and the solution was stored at -20°C. The antibody was tested at a range of concentrations (1/5-1/1,000) for the ability to immunolabel LanA in fixed embryos (Appendix A.1; Figure 4.5). An optimal concentration was determined to be ~1/10-1/50.

2.5 Immunohistochemistry

2.5.1 Embryo collection

Flies (30-60 females and 15-30 males) were placed in houses (100 ml plastic tri-corner beakers with added air-exchange pinholes) and allowed to lay eggs on **apple juice agar plates** with a dab of **yeast paste** for eight to 16 hours. After the flies were removed, the embryos were aged to a total of 20-22 hours from the start time of initial egg-laying and then stored at 4°C for a maximum of 72 hours. Cooled embryos were placed at room

temperature for 90 minutes prior to fixation. For RNAi experiments, the embryo collection protocol was modified to three hours of egg laying at room temperature, 16-20 hours of aging at 29°C, followed by immediate fixation.

2.5.2 Fixation

Embryos were dechorionated in 50% bleach for three to five minutes, collected on sieves, and rinsed with ddH_2O. Collected embryos were fixed for 20 to 30 minutes (0.5 mL 37% formaldehyde, Caledon 5300-1; 4.5 mL PBS; 5 mL heptane, Fisher O3008-4) and then methanol cracked. Embryos were washed with methanol to remove fixative and then immediately washed in **PBT** (or **PBS + Tween** if using anti-Robo) to rehydrate for immunolabeling. Occasionally, embryos were stored in methanol (Caledon 6700-1) at 4°C for up to two weeks prior to rehydration in PBT.

2.5.3 Immunolabeling

Immunolabeling protocols were adapted from Patel (Patel, 1994). After rehydration in PBT, fixed embryos were blocked with 1/15 Normal Goat Serum (NGS) in PBT for 30 minutes. Embryos were incubated with primary antibody overnight or over the weekend at 4°C. Following this incubation, the embryos were rotated in PBT for four to six hours, washing with fresh PBT every 30 to 45 minutes. Embryos were re-blocked in 1/15 NGS in PBT for 30 minutes and then incubated in secondary antibody for 2 hours at room temperature. Embryos prepared for confocal imaging were labeled with fluorescent

secondary antibodies (Alexa, Molecular Probes) and protected from light using tinfoil wrapped labeling tubes, while embryos prepared for light microscopy imaging were incubated with biotinylated (bio-) secondary antibodies (Table 2.2c).

Following five washes in PBT and a final overnight rotation in PBT at 4°C, fluorescently labeled embryos were stored in 70% glycerol in PBS (Caledon 5350-1). If immunolabeling was performed using multiple primary antibodies generated in the same animal species, sequential reactions were used and antibody concentrations were modified to prevent cross-labeling (see 2.5.5). Prior to imaging, embryos were mounted onto a modified glass slide. Modified glass slides were prepared using two No. 1 coverslips (VWR 48366-067) placed side-by-side on a glass microscope slide (VWR 48323-185) with a 5 mm gap between (held in place with a dab of nail-polish placed on the outer edge of each coverslip). Approximately 20 µl of 70% glycerol-embryo mixture was mounted in the created chamber and then covered with a No. 1.5 coverslip (VWR 48366-227).

Following the final overnight PBT wash, embryos labeled with a biotinylated secondary antibody were incubated with the avidin and biotinynlated peroxidase containing Vectastain ABC system for one hour (Vector Laboratories PK-6100). Following multiple washes in PBT, embryos were immersed in a 0.5 mg/ml 3,3-Diaminobenzidine Tetra hydrochloride (DAB) in 1xPBS solution and 0.05% (final concentration) hydrogen peroxide was added. The peroxidase catalyzed oxidation of DAB produced a dark-brown precipitate at the sites of antibody binding. Labelled embryos were dehydrated using a 50-100% ethanol gradient and then stored in methyl salicylate (Sigma 37616) at room

temperature. Prior to imaging, embryos were mounted in D.P.X. neutral mounting media (Sigma 317616) on glass microscopes slides and covered with a No. 1 coverslip (VWR 48366-067).

2.5.4 Imaging and image processing

DAB-reacted embryos were imaged using a Zeiss Axioskop microscope (with a Qimaging RETIGA 1300i digital camera) and OpenLab software. Fluorescent-labelled embryos were imaged on a Leica SP5 confocal microscope. Frontal images displayed in this thesis are maximum projections of 3-10 slice stacks taken 1 µm apart in the heart proper. Images of embryo z-sections (transverse images) are single slice images of heart proper Tinman-expressing cardioblasts. All images were processed with ImageJ and figures were assembled using Adobe Photoshop CS4.

2.5.5 Antibodies used

Polyclonal primary antibodies (Table 2.1a)

Polyclonal primary antibodies were used at the following dilutions: rabbit anti-MEF (1:5,000; this thesis), rabbit anti-Dg (1:600; Deng *et al.* 2003; used for Chapter 3 experiments), rabbit anti-Dg (1:100-1:200; this thesis; used for Chapter 4, Appendix D experiments), rat anti-Zfh1 (1:150; Lai *et al.* 1991), rabbit anti-CAP (1:1,000; Bharadwaj *et al.* 2013), rabbit anti-Pinch (1:500; Clark *et al.* 2003), rabbit anti-GFP (1:600, Invitrogen), chicken anti-GFP (1:1,000, Cedarlane), chicken anti-βGal (1:150; MacMullin and Jacobs

Table 2.2a: A list of all polyclonal antibodies used for immunohistochemistry

Antibody	Dilution	Host animal	Source	Catalogue #
α-CAP	1:1,000	Rabbit	Bharadwaj *et al.* 2013	
α-dMEF	1:5,000	Rabbit	This thesis	
α-Dg	1:100-1:200	Rabbit	This thesis	
α-Dg	1:600	Rabbit	Deng *et al.* 2003	
α-βGal	1:150	Chicken	MacMullin and Jacobs 2006	
α-βGal	~1:100,000	Chicken	This thesis	
α-GFP	1:600	Rabbit	Invitrogen	A6455
α-GFP	1:1,000	Chicken	Cedarlane	ab13970
α-Pinch	1:500	Rabbit	Clark *et al.* 2003	
α-Zfh1	1:150	Rat	Lai *et al.* 1991	

2006; used for Chapter 3 experiments), chicken anti-βGal (1:100,000; this thesis; used for Appendix D experiments). When both rabbit anti-MEF and another rabbit-derived primary antibody were used to label the same embryos, sequential labeling was used with anti-MEF added second at a high concentration (1:500).

Monoclonal primary antibodies (Table 2.1b)

In addition, the following mouse monoclonal antibodies were obtained from the Developmental Studies Hybridoma Bank and used at a 1:30 dilution: anti-βPS1, anti-Talin, anti-Slit, anti-Robo, anti-Dlg, anti-Hindsight (Hnt), anti-Pericardin (Prc; used at 1:60). A mouse monoclonal antibody against LanA was used at 1:10-1:50 (this thesis).

Secondary antibodies (Table 2.1c)

The following fluorescent secondary antibodies were used: Alexa 488 anti-Chicken (Ch), Alexa 488 anti-Rabbit (Rb), Alexa 546 anti-Mouse (M), Alexa 546 anti-Rb, Alexa 594 anti-M, Alexa 594 anti-Rb, Alexa 594 anti-Rat (Rt), Alexa 647 anti-Ch, Alexa 647 anti-Rb

(Molecular Probes, Invitrogen). For embryos prepared for light microscopy the following biotinynlated secondary antibodies were used: goat (Gt) anti-chicken, Gt anti-Rb, and Gt anti-Rt (Jackson ImmunoResearch). All secondary antibodies were used at a 1:150 dilution. Both primary and secondary antibodies were added directly to the block solution (10 µl NGS in 140 µl PBT).

Table 2.2b: A list of all monoclonal antibodies used for immunohistochemistry

Antibody	Dilution	Full name	Source	Name/Catalogue #
α-βPS	1:30	α-βPS1 integrin	D. Brower	DF.6G11-s
α-Dlg	1:30	α-Discs large	C. Goodman	4F3 anti-discs large
α-Hnt	1:30	α-Hindsight	H. D. Lipshitz	1G9-s
α-LanA	1:10-1:50	α-Laminin A	This thesis	
α-Prc	1:60	α-Pericardin	D. Gratecos	EC11 anti-Pericardin
α-Robo	1:30	α-Robo	C. Goodman	13C9 anti-Robo-s
α-Slit	1:30	α-Slit	S. Artavanis-Tsakonas	C555.6D-s
α-Talin	1:30	α-Talin	R. White	Talin E16B-s

Table 2.2c: A list of all secondary antibodies used for immunohistochemistry

Antibody	Dilution	Source	Catalogue #:
Alexa 488 α-Ch	1:150	Invitrogen	A11039
Alexa 488 α-Rb	1:150	Invitrogen	A11034
Alexa 488 α-Rt	1:150	Invitrogen	A11006
Alexa 546 α-M	1:150	Invitrogen	A11030
Alexa 546 α-Rb	1:150	Invitrogen	A11010
Alexa 594 α-M	1:150	Invitrogen	A11032
Alexa 594 α-Rb	1:150	Invitrogen	A11037
Alexa 594 α-Rt	1:150	Invitrogen	A11007
Alexa 647 α-Rb	1:150	Invitrogen	A21245
Alexa 647 α-Ch	1:150	Invitrogen	A21449
Bio α-Ch	1:150	Jackson ImmunoResearch	103-065-155
Bio α-Rb	1:150	Jackson ImmunoResearch	111-065-003
Bio α-Rt	1:150	Jackson ImmunoResearch	112-065-003

2.6 Live imaging

Live imaging of embryos was performed using the hanging drop method adapted from Reed *et al.* 2009. Flies (20-30 females and 10-15 males) were placed in houses and allowed to lay eggs on **apple juice agar plates** with a dab of **yeast paste** for 24 hours. Embryos of the desired stage were selected, manually dechorionated using double-sided tape, and placed on a No. 1 coverslip (VWR 48393-048) with the dorsal side facing the coverslip. Each embryo was submerged in a drop of halocarbon oil (Halocarbon Products Corp, 700 Series) and the coverslip was placed embryo-side-down on the mounting chamber. The mounting chamber consisted of a 5 mm deep well, padded with a moist Kimwipe.

Imaged embryos expressed Tailup (TUP)-GFP in the cardial cell nuclei (Tao *et al.* 2007, Tokusumi *et al.* 2007) and UAS-moe-mCherry (Millard and Martin 2008) under control of the muscle-specific dMEF-Gal4 (Ranganayakulu *et al.* 1996). Moesin (Moe), an actin-plasma membrane cross-linker protein, localizes to filopodia. These three genetic elements (TUPGFP, dMEF-Gal4, and UAS-moe-mCherry) were recombined onto one chromosome for *mys*, *scb*, *src42A*, and RNAi live imaging (Appendix A.3). For Talin experiments, these elements were further recombined onto a $rhea^{79}$ containing chromosome (Appendix A.3).

2.6.1 Imaging

Embryos were imaged on a Leica SP5 confocal microscope. Embryos were imaged every two minutes for 30 to 60 minutes. Stacks of 20-30 images 1 µm apart were maximum projected.

2.6.2 Processing and quantification

Quantification of leading edge activity in integrin-related live image experiments (Chapter 3) was calculated as a percentage: the summed length of active membrane (with filopodia extensions) was divided by the total cardioblast row length and presented as a percentage. For Talin experiments (Chapter 4), leading edge activity was quantified by counting the number of filopodia per six-cell segment. Since the leading edge becomes more active as the cardioblast rows approach one another (Syed 2012), only late stage embryos were quantified (defined as less than 13 µm from the cardioblast nuclei to the midline). A minimum of twelve cardioblast rows (integrin) or 30 six-cell segments (Talin) were assessed per genotype. The non-parametric Mann Whitney-U was used to test for significant differences.

2.7 Electron microscopy

Dechorionated embryos were fixed in heptane equilibrated with 25% glutaraldehyde (Fluka) in 0.1 M Sodium Cacodylate. Embryos were manually devitellinated in 4% paraformaldehyde and 2.5% glutaraldehyde in cacodylate buffer, post-fixed in 1%

osmium tetroxide, and stained in uranyl acetate before embedding in Epon-Araldite (Jacobs and Goodman 1989). Lead stained 0.1 µm sections were examined on a JEOL 1200EXII microscope. We examined over 120 sections from specimens of each genotype.

2.8 Maternal and zygotic mutant embryos

During the cellularization stage of *Drosophila* embryogenesis, no transcription occurs. Rather, the embryo relies on mRNA deposited into the egg during oogenesis by the mother's nurse cells. While most zygotic transcription starts around the mid-blastula transition, the maternally contributed mRNA often persists in low levels through embryogenesis. While this process is essential for proper development of the embryo, it hinders generating an embryo that completely lacks an essential protein. Typically crossing two heterozygous parents will result in one-quarter of the progeny being homozygous mutant. However, if mRNA of the protein of interest is deposited maternally, the homozygous mutant progeny will have low levels of wildtype mRNA from the heterozygous mother. For example, compared to wildtype, Talin is markedly reduced in *rhea*^{1}*, rhea*^{2}*, and rhea*^{79} homozygous embryos, however low levels of Talin remain (Figure 4.3). To provide a true *rhea* null embryo devoid of both maternal and zygotic Talin contributions, *rhea* mutant germ-line clones were generated by triggering mitotic recombination in a heterozygous female fly (Appendix A.2). Since these mutant clones cannot deposit *rhea* mRNA into the egg, there is no maternal contribution of Talin and any homozygous mutant progeny embryos lack both maternal and zygotic Talin (Figure 4.3E;

termed germ-line clone or GLC embryos). A similar cross scheme (not shown) was used to produce *mys* GLC mutant embryos completely devoid of βPS1 integrin (eg. as used in Appendix C.2).

2.9 Rescues

To express Talin transgenes in *rhea*^{79} embryos, fly strains containing Talin rescue constructs were obtained from G. Tanentzapf (Ellis *et al.* 2011). These flies ubiquitously express Talin transgenes via the *ubiquitin-E63* gene promoter (Tanentzapf and Brown 2006). Rescue transgenes included wildtype Talin (Talin^{WT}), IBS1 mutant R367A (Talin^{IBS1-}), IBS2 mutants KS>DD (Talin^{IBS2-}) and LI>AA (Talin^{IBS2b-}), and IBS1-IBS2 double mutant R367A, LI>AA (Talin$^{IBS1-IBS2-}$; Figure 4.1). Since fly strains carrying these constructs ubiquitously and continuously overexpress Talin, flies may be prone to accumulate modifying mutations countering the excess Talin. Therefore, to remove potential modifiers, each strain was outcrossed to *yw* three times prior to being crossed into a *rhea*^{79} background (Appendix A.4a-c). Rescue crosses were set up to ensure that all transgenes were inherited maternally and present in a single copy in the embryos (Appendix A.4a-c).

2.10 Embryo scoring

For experiments with quantitative scoring of the heart phenotype (Chapter 4), twenty or more stage 17 embryos of each genotype were labeled with anti-MEF and blindly assessed by two independent researchers. The heart proper of each embryo was

assessed for lumen size and cardial cell row blistering. Lumen size was scored on an ordinal scale from zero to two for increasing space between opposing cardioblast rows (0 for no apparent lumen, 2 for a full or normal luminal space). Blisters (lateral displacement of seven-up cells away from the midline; eg. see *rhea/lanA* panel in Figure 4.11) were counted in each heart proper. The average score for each genotype was calculated and genotypes were compared using a Mann-Whitney U test.

2.11 Western blots

2.11.1 Embryo collections

Flies (80-100 females and 40-50 males) were placed in houses and allowed to lay eggs on **apple juice agar plates** with a dab of **yeast paste** for two hours. These eggs were then further aged at room temperature for 22-24 hours. *rhea*^{79} heterozygous embryos or homozygous *rhea*^{79} embryos with a single copy Talin transgene (wildtype, IBS1^{-}, IBS2^{-}, IBS2b^{-}, or IBS1^{-}IBS2b^{-}) were individually selected using –GFP or –YFP marked chromosomes. Ten stage 17 embryos (staging confirmed using gut morphology) were collected for each genotype.

2.11.2 Sample prep

Collected embryo samples were immediately homogenized in 30 µl ice cold 1X sample buffer with 1x protease cocktail inhibitor (Cell signaling technology 5871S), boiled

for four minutes (96°C heatblock), and centrifuged (10 min at 4°C at 14,000rpm) to remove cellular debris. Samples were stored at -20°C for up to one week.

2.11.3 Western Blot procedure

20 µl of sample was electrophoresed on a 6% Tris-glycine SDS-polyacrylamide gel for 75 minutes at 110 V. The samples were transferred to an Immobilon-P PVDF transfer membrane (EMD Millipore IPVH00010) at 100 V for 120 minutes at 4°C. Following the transfer, the membrane was blocked in 5% milk for one hour and subsequently washed for 30 minutes in **PBS + 0.1% Tween 20**. The membrane was incubated with mouse anti-Talin (1:500; DSHB Talin A22A or Talin E16B) or mouse anti-βTubulin (βTub; 1:1,000; DSHB E7) in 3% milk overnight at 4°C. Following three ten-minute washes in PBS + 0.1% Tween 20, the membrane was incubated with a horseradish peroxidase-conjugated anti-mouse secondary antibody (1:5,000; Jackson ImmunoResearch 115-035-166) for one hour at room temperature, washed with PBS + 0.1% Tween 20 and prepared for developing using Pierce ECL Western Blotting Substrate (Thermo Scientific 32106) and Amersham Hyperfilm ECL (GE Healthcare 28906838).

2.11.4 Quantification

Western blots were analyzed and quantified using ImageJ, with βTub used as a loading control reference. Graph images show the average band intensity values (relative to *rhea*^{79} heterozygote levels) of 5-7 independent Western Blots.

Integrins are required for cardioblast polarization in *Drosophila*

CHAPTER THREE

3.1 Preface and explanation of contributions

This chapter is adapted from an article published in BMC Developmental Biology. Revisions were made to minimize redundancy and to maintain formatting consistency with other chapters. Significant revisions include modifications to the introduction (3.2; reduce repetition of literature reviewed in Chapter 1), elimination of the methods section (details are presented in Chapter 2), and removal of the reference list (included in a combined thesis list on pp. 188-218). One additional figure, not in the published article (Appendix B.1), is presented and discussed.

Adapted from:

Vanderploeg, J., Vazquez Paz, L. L., MacMullin, A. and Jacobs, J. R. (2012). Integrins are required for cardioblast polarisation in Drosophila. *BMC Dev. Biol.* **12**, 8.

Contributions:

J. Vanderploeg performed experiments for Figure 3.1 (anti-Pericardin images), Table 3.1, Figure 3.4, Figure 3.5, and Figure 3.6. L. L. Vazquez Pas provided the immunohistochemical data as presented in Figure 3.1 (excluding the anti-Pericardin labels) and Figure 3.3, A. MacMullin completed Figure 3.7, and Dr. R. Jacobs performed the electron microscopy imaging experiments in Figure 3.2.

Permissions:

Permission for re-use granted through Open Access, BioMed Central Ltd.

3.2 Introduction

Integrins are transmembrane receptors comprised of pairs of alpha (α) and beta (β) subunits, which link the extracellular matrix (ECM) to the cell cytoskeleton, and mediate cell locomotion, adhesion and signals that affect differentiation and survival (Reynolds *et al.* 2002, Hynes 2007). There are at least seven integrin dimers expressed in the vascular system, implicated in vascular cell migration, and subsequently in lumen formation (Hynes 2007). Reduced β1-integrin function in endothelia, by β1-integrin antibody in quail (Drake *et al.* 1992) or by knockout of β1-integrin function restricted to mouse endothelia (Zovein *et al.* 2010) result in a reduced or lost vascular lumen. In other contexts, reduced integrin function is not sufficient to prevent lumen formation, possibly due to the contributions of other ECM factors (Davis and Senger 2005).

Drosophila affords multiple models of lumen formation, such as the salivary gland, trachea, and heart. Here, we focus on the role of integrins in the formation of the lumen of the *Drosophila* heart. As with vertebrates, the *Drosophila* heart precursors arise from lateral mesoderm, which migrate medially after specification, to meet their contralateral partners, and then assemble a midline vessel (Medioni *et al.* 2009, Haag *et al.* 1999). The regulators of this collective cell migration event have not been characterised, however genetic and developmental studies illustrate that the precursors (called cardioblasts, CBs) maintain a close association with the migrating ectodermal cells that provide the inductive signals that establish cardiac fate. Reduced Cadherin function does not affect CB alignment or migration, but the sole integrin dimer expressed by the CBs (αPS3, βPS), and

ligand (LanA) are required for CB alignment (Haag *et al.* 1999, Stark *et al.* 1997). Significantly, the timely migration and alignment of CBs requires the Slit morphogen and Robo receptor, a requirement that interacts genetically with the αPS3 gene *scb*, and the Laminin genes *lanA* and *wing blister* (MacMullin and Jacobs 2006, Santiago-Martinez *et al.* 2006, Qian *et al.* 2005). Furthermore, the subsequent formation of a lumen in the *Drosophila* heart requires integrated function of cell surface Robo, E-cadherin (E-cad), Dystroglycan (Dg), Syndecan, and NetrinB to complete cell polarization and establish the luminal ECM (Haag *et al.* 1999, Albrecht *et al.* 2010, Medioni *et al.* 2008, Knox *et al.* 2011). However, it is not clear whether integrins function upstream to apicalize the migrating CBs, or as co-factors with Robo, to help assemble the luminal ECM. Here we characterise changes in CB polarization and heart morphogenesis subsequent to genetically altered integrin function. We identify a role for the αPS3βPS1 integrin dimer in both the early establishment of the apical, pre-luminal domain, as well as a requirement upon Robo for maintained apicalization of proteins required for lumen formation. This suggests that Robo dependent lumen formation acts downstream of other cell polarizing signals.

3.3 Results

3.3.1 αPS3βPS1 integrin is required for apical and basal polarity of cardioblasts.

The *Drosophila* heart vessel is formed by the dorsal and medial migration of lateral somatic mesodermal cardioblasts. The migration of this mesoderm is linked to dorsal closure, which is the tandem dorsal migration of lateral ectoderm to envelop the gut, and

replacing a transient embryonic tissue, the amnioserosa on the dorsal surface of the embryo (Jacinto *et al.* 2002). Previous studies have established a role for the αPS3βPS1 integrin dimer in the displacement and involution of the amnioserosa, as well as the assembly of the heart vessel (Stark *et al.* 1997). Involution of the amnioserosa, and dorsal closure is incomplete in embryos lacking zygotic function of either αPS3 (*scab* or *scb*) or βPS1 (*myospheroid* or *mys*), complicating an assessment of heart morphogenesis. We have assessed the mutant heart in two manners, in zygotic mutants, and after dsRNA mediated reduction of integrin levels. Zygotic mutants for the amorph scb^2 had complete dorsal closure of abdominal segments 6 to 8, which contains most of the heart chamber, so our analysis focused on these segments. In wildtype embryos, and embryos heterozygous for scb^2, two rows of CB were aligned across the midline, and the morphogen, Slit was restricted to the heart lumen (Figure 3.1A). Embryos mutant for αPS3 (scb^2), in contrast, revealed less regular alignment of CB nuclei, with displaced CBs forming blisters across or beside the midline being a common feature (Figure 3.1D). Levels of Slit were reduced, and were not concentrated apically. Similarly, zygotic mutants for βPS1 (mys^1) had blisters and gaps in the CBs, and reduced Slit accumulation (Figure 3.1J, Table 3.1), although apicalization was better preserved.

We found that βPS1 integrin was concentrated in the luminal domain of wildtype stage 17 hearts (Figure 3.1B, arrow) with lower levels on the basal surface of the CBs. In the absence of α-integrin, β-integrin is not properly targeted to the cell surface (Leptin *et al.* 1989). Accordingly, in *scb* mutants, levels of βPS1 were reduced, with relatively more

Figure 3.1. αPS3 integrin is required for apicalization of cardioblasts.

Slit is located in the heart lumen (arrow) in stage 17 wildtype embryos (**A**). The level of immuno-detected Slit (red) is much lower in *scb*^{2} mutants (**D**), and *mys*^{1} mutants (**J**) or if α- or β-integrin levels are reduced by dsRNA knockdown (scbRNAi in **G** and mysRNAi in **M**, directed by dMEF-GAL4). Residual Slit is not apicalized, and is found on lateral cell surfaces (arrowheads in insets of **D** and **M**). Most of the immunolabel for βPS1 integrin is concentrated on the luminal surface in wildtype (red, **B**). Levels of βPS1 are reduced in *scb* mutants (**E**) and subsequent to scbRNAi expression (**H**), however, some luminal label remains. No βPS1 is detected in *mys*^{1} mutants (**K**), and trace levels of βPS1 remain after mysRNAi expression (**N**). Pericardin, synthesized by the pericardial cells (labeled with Zfh-1 antibody, blue in **C, F, I, L, O**) is restricted to the basal surface of the CBs in wildtype (red, **C**). Reduced integrin function in *scb* and *mys* mutants (**F, L**), or subsequent to scbRNAi (**I**) or mysRNAi (**O**) expression results in Pericardin re-distribution around the entire pericardial cell perimeter (arrowheads, **F, L, O**), as well as between some CBs (arrowhead in **I**), and less at the basal surface of the CBs. Midline Pericardin marks medially displaced pericardial cells (asterisk in **F, L**). The CB nuclei here and subsequent fluorescence images are identified with antibody to dMEF2 (green), unless otherwise noted. In G, H, M, N, I, and O, CB nuclei are labeled with βGal for the B2-3-20 enhancer trap. Posterior is to the right in all panels here and in subsequent figures, unless otherwise noted. The arrow marks the dorsal midline. All images were generated at the same gain. The gain in the insets is adjusted to visualise low intensity immuno-label signals.

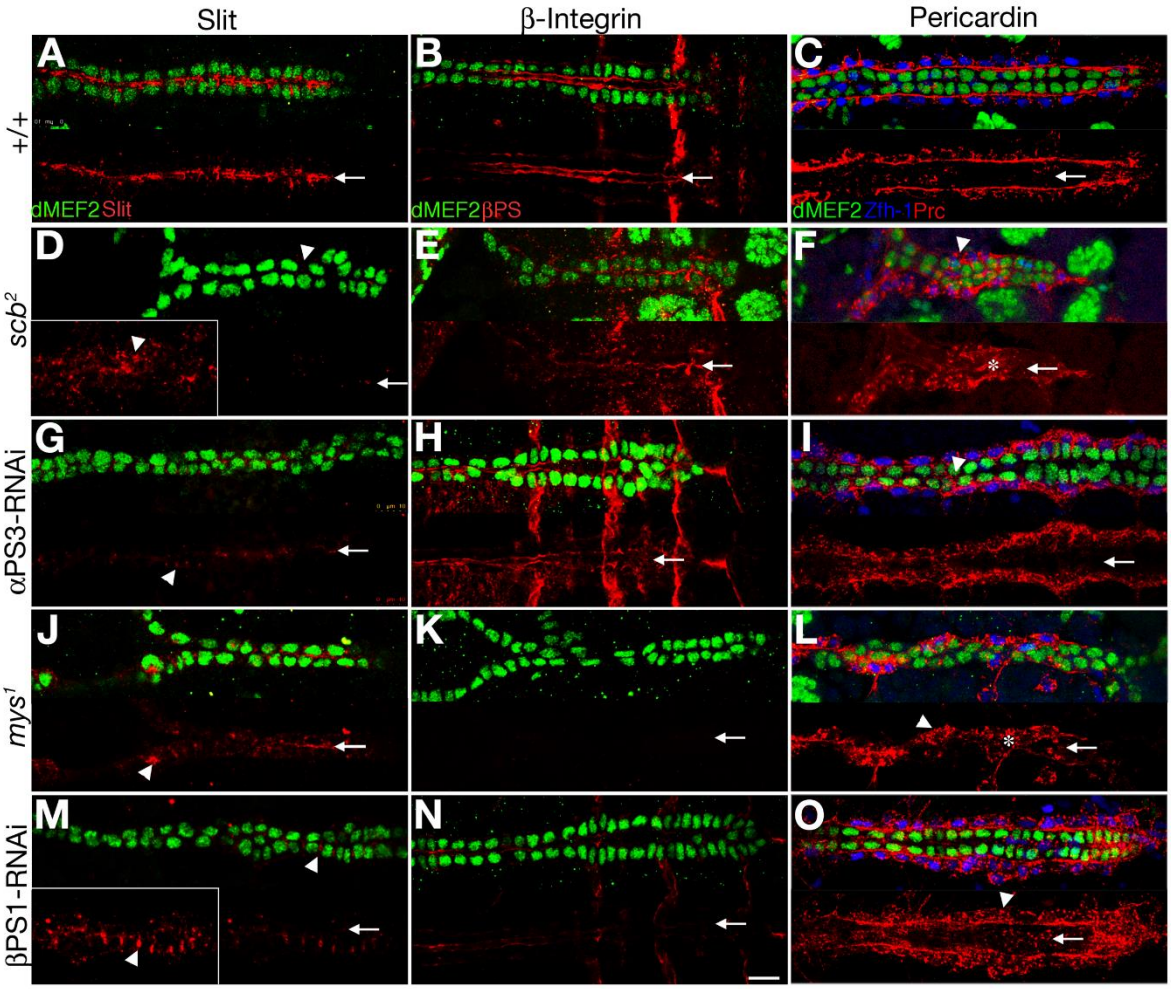
Slit
β-Integrin
Pericardin
+/+
scb2
αPS3-RNAi
mys1
βPS1-RNAi
A
B
C
D
E
F
G
H
I
J
K
L
M
N
O
dMEF2 Slit
dMEF2 βPS
dMEF2 Zfh-1 Prc

Table 3.1. Leading edge polarization deficits in the heart region of the dorsal vessel.

Genotype	*yw*	*mys*[1]	*scb*[2]	*mys RNAi*	*scb RNAi*	n (per genotype)
Embryos with CB displacement	4	**16**	**12**	10	**12**	*20 embryos*
Apical/Non-Apical Slit	8.6±1.2	***2.6±0.3***	***1.8±0.1***	***2.2±0.2***	***2.1±0.1***	*9 embryos*
Leading Edge Activity, %	41±3	***12±2***	***16±3***	42±2	36±3	*12 LEs*

Slit apicalization is expressed as a ratio of the average immunofluorescence intensity in the apical region, divided by the intensity of non- apical heart fluorescence. Means shown ±standard error. Data sets significantly different from *yw* or *yw*, *UAS-moesin-mCherry/+, tup-GFP, dMEF-GAL4/+* controls are in bold italic if p<0.001 and in bold if p<0.05 by Mann-Whitney U test.

immunolabel outside the luminal domain (Figure 3.1E). βPS1 antigen was not detected on CBs of zygotic *mys*[1] mutants (Figure 3.1K).

Pericardin (Prc) is a collagen-like protein secreted by the pericardial cells, which concentrates at the CB-pericardial cell interface (Chartier *et al.* 2002). In wildtype, Prc labeling marked a continuous structure at the base of the CBs (Figure 3.1C). In *scb* mutants, Prc label more frequently surrounded the pericardial cell (arrowhead, Figure 1F), and was distributed discontinuously on the CB surface. Embryos mutant for *mys* have Prc distributed irregularly over the pericardial cell surface, and pericardial cells were displaced towards the midline (asterisk, Figure 3.1L).

As an independent approach to assessing integrin function in the CB, we have reduced αPS3 and βPS1 protein levels in the mesoderm, with targeted expression of dsRNA (in *dMEF2-GAL4/ UAS-scbRNAi* embryos in Figure 3.1G-I, and in *dMEF2-GAL4/ UAS-*

mysRNAi embryos in Figure 3.1M-O). We obtained qualitatively similar results with two *scbRNAi* strains and two *mysRNAi* strains (see Methods and Table 3.1). Dorsal closure was normal after integrin knockdown in the mesoderm, and CBs from all segments met their contralateral partners. However, small gaps or clumps in alignment are observed (Figure 3.1G, M). As in the mutant, the level of Slit was reduced (Table 3.1), and strikingly, Slit was detected between ipsilateral cells, a membrane domain from which it is normally excluded (arrowheads, Figure 3.1G, M; Haag *et al.* 1999, Santiago-Martinez *et al.* 2008). We further assessed the distribution of βPS1 integrin (Figure 3.1H, N) and Pericardin (Figure 3.1I, O) and *scb* encountered phenotypes intermediate between wildtype and scb^2. Lower levels of βPS1 were observed subsequent to *RNAi* knockdown, possibly because of some perdurant αPS3 protein. Very low levels of βPS1 labeling subsequent to mysRNAi (Figure 3.1N) suggests that quantities of maternally contributed βPS1 are limited. Nevertheless, for both integrin knockdown genotypes, Slit and Pericardin distribution was abnormal (Figure 3.1G, I, M, O).

Considered together with the data from the zygotic mutants, we conclude that integrin function is required for orderly alignment of the CBs, is essential for establishing an apical or luminal domain for CBs, and polarizes Pericardin on the pericardial cells. The reduction in the level and apical deposition of Slit in mutants indicates that integrins are required to target or stabilise this morphogen apically.

3.3.2 Integrins are required for heart lumen formation

Previous studies have established that apicalization of Slit is required to establish a lumen in the *Drosophila* heart (MacMullin and Jacobs 2006, Qian *et al.* 2005). Given the mislocalisation and reduced levels of Slit subsequent to reduced integrin function, we sought to determine if lumen formation was similarly affected. A well developed lumen was visualised in cross-sections of stage 17 hearts, and no lumen was detected between contralaterally apposed CBs in the heart region of scb^2 mutants (Figure 3.2A, B). However, expression of an αPS3 transgene in the CB of scb^2 mutants partially restored lumen formation (Figure 3.2C). These data are consistent with a model wherein integrin acts to apicalize Slit binding and signaling, which is a pre-requisite for lumen formation. We addressed this model directly by determining whether restoring αPS3 expression to the CBs in a *scb* mutant would restore apicalization of the Slit receptor, Robo. In contrast to wildtype (Figure 3.3A), Robo levels are reduced and incompletely apicalized in *scb* mutants (Figure 3.3B and inset). As expected, mesodermal expression of αPS3 in *scb* mutants did not restore normal dorsal closure. However, Robo, was concentrated apically (Figure 3.3C), and no longer laterally as seen in scb^2 mutants. Truncation of the short cytoplasmic domain of αPS2 locks the integrin into an "excessively active" high affinity receptor, forming ectopic adhesions (Martin-Bermudo *et al.* 1998). Rescue of *scb* mutants with a similarly truncated transgene was sufficient to restore apicalization of Robo, also expanding the apical area of Robo expression (Figure 3.3D).

Figure 3.2. αPS3 integrin is required for lumen formation.

The lumen of the *Drosophila* heart is developed in stage 17 wildtype embryos (arrow), between contralaterally apposed cardioblasts ("c"; **A**). No lumen develops between cardioblasts in *scb*^{2} mutant embryos (**B**), however, there is partial restoration of the lumen (arrow, **C**) in *scb*^{2} mutant embryos expressing an αPS3 transgene (*scb*^{2}*/scb*^{2}*; dMEF-GAL4/UAS-*α*PS3*). Sections were sampled within the posterior heart proper. Ectodermal cells ("e") and amnioserosa cells (asterisk) are identified. Calibration: 5 microns.

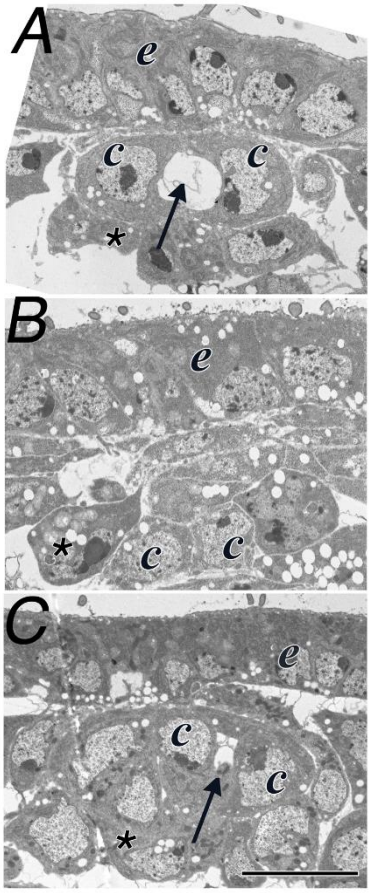
A
e
c
c
*
B
e
*
c
c
C
e
c
c
*

Figure 3.3. Expression of an αPS3 transgene in the cardioblasts restores apicalization of Robo.

Like the ligand Slit, its receptor Robo is apicalized in wildtype embryos (red, **A**). In *scb*^{2} homozygotes, Robo levels are dramatically reduced (**B**, unadjusted gain shown in inset), however at increased gain, Robo at the midline (arrow) and between ipsilateral cells (arrowhead) is detected. In *scb*^{2}*/scb*^{2}; *dMEF-GAL4/UAS-scb* embryos, expression of αPS3 only in somatic mesoderm is sufficient to restore apical restriction of Robo (**C**). Rescue of *scb*^{2}*/scb*^{2} with a cytoplasmically truncated αPS3 transgene yields partial restoration of midline Robo (arrow, **D**), although Robo between ipsilateral cells is detected (arrowheads). Calibration: 10 microns.

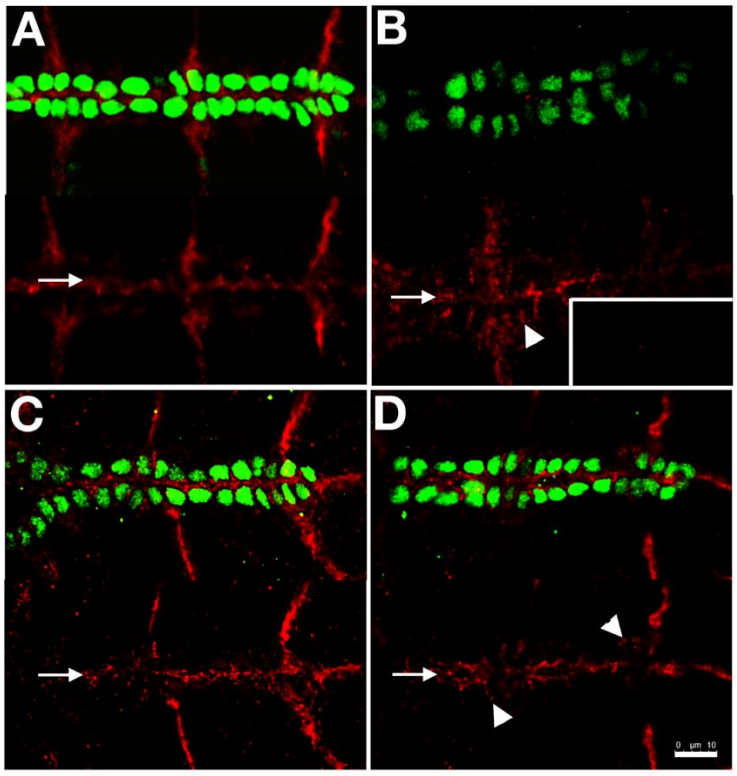
A
B
C
D
0 µm 10

3.3.3 Integrins are required for cardioblast polarization

During their medial migration, the CBs are in an intermediate state of polarization. The CBs adhere to their ipsilateral neighbours, which is likely cadherin based (Haag *et al.* 1999), and the advancing and trailing edges interact with the ECM, which is likely integrin based. However, when the CBs meet their contralateral partners, the leading edge of the cells will develop a luminal domain that concentrates Slit and Robo. Given that a luminal domain fails to develop in *scb* mutants, and that luminal markers require *scb* function to apicalize, we speculated that integrins may be instructive in establishing the location of the luminal domain. We therefore sought to determine how the distribution of integrins reflected the transition from a migratory phenotype to epithelial differentiation. In stage 15 embryos, before the leading processes of the CBs make contact across the midline, the βPS1 integrin was localized primarily on the leading edge of the migrating CBs (Figure 3.4A, arrow) while much less label was detected on the trailing edge (Figure 3.4A, arrowhead). The preponderantly apical distribution was not significantly altered once the lumen was formed (Figure 3.4D). In contrast, Robo protein was located on apical, lateral and basal surfaces of the CB during migration (Figure 3.4B), and is entirely luminal by stage 17 (Figure 3.4E). Dystroglycan, another apical membrane protein required for lumen formation, was also excluded from lateral membrane domains at both stages, although more basal labeling was evident during migration that was reduced after lumen formation (Figure 3.4C, F, arrowheads).

Figure 3.4. Integrins apicalize early during cardioblast polarization.

During CB migration, integrins (βPS1 immunolabel) are predominantly located on the advancing apical edge (**A**, arrow), with low levels on the basal trailing edge (arrowhead). Integrin is not detected on lateral CB surfaces, yet at the same stage, Robo is detected on apical, lateral and basal membrane domains (**B**). Dystroglycan (Dg) is excluded from lateral cell surfaces, and is concentrated at both apical and basal membranes (**C**). At stage 17, migration is complete, and the heart lumen is formed. The apical and basal distribution of βPS1 has not changed (**D**), however, Robo (**E**) and Dg (**F**) are now almost entirely apical. Apicalization of integrin is reduced in *robo, lea* mutants at stage 15 (**G**) and 17 (**H**). The inset in (**G**) shows the intensity of immuno-labeling at the same gain as the other βPS1 panels. Dg apicalization is similarly affected in *robo, lea* mutants (**I**). The asterisks in stage 15 panels identifies βPS1 label in the amnioserosa. Arrows mark apical surfaces, and arrowheads mark basal surfaces of the CBs. Calibration: 10 microns.

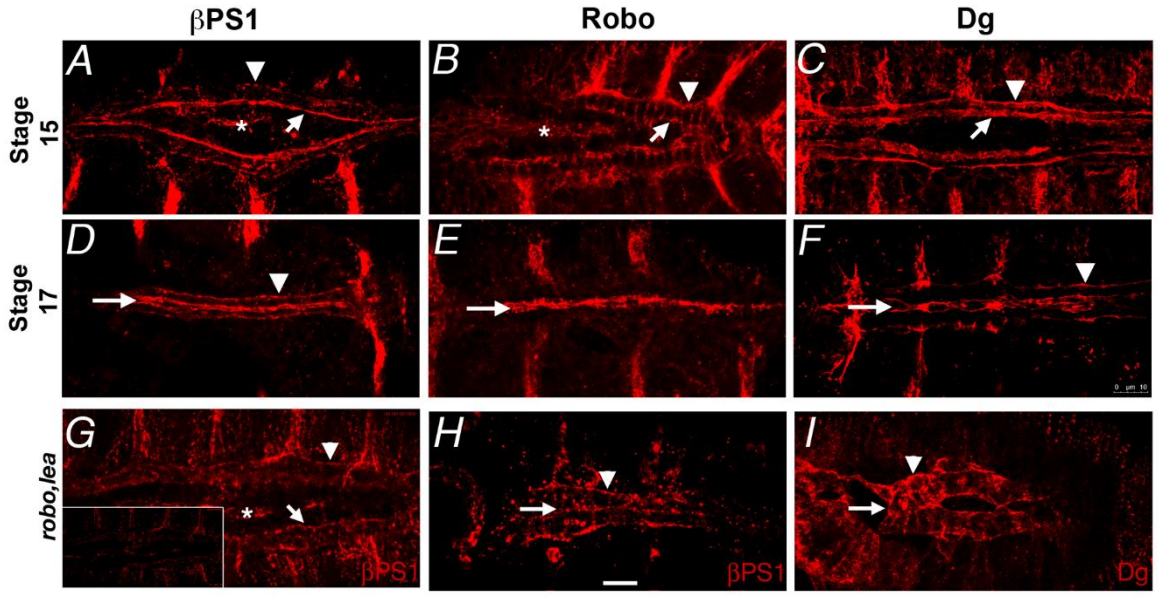
βPS1
Robo
Dg
Stage 15
Stage 17
robo,lea
A
B
C
D
E
F
G
H
I
βPS1
βPS1
Dg

Previous studies demonstrate that the apical surface of mature CBs are subdivided into a junctional (J) domain and a luminal (L) domain (1.5.1-1.5.3; Medioni *et al.* 2008). We sought to determine whether formation of these domains required integrin function, and whether early integrin apicalization reflected early establishment of the luminal domain. We therefore examined migrating CBs in cross-sectional view to determine whether βPS1 integrin was spatially restricted to a subdomain of the leading edge membrane before midline fusion. The dorsal limit of a wildtype CB at stage 16 extended Dg labeled membrane towards the midline (Figure 3.5A, arrowhead), yet this extension was missing in *scb* mutants (Figure 3.5D, arrowhead). βPS1 integrin accumulated immediately ventral to the dorsal extension during migration, and this domain contributed to the integrin rich luminal membrane at stage 17 (Figure 3.5A, B, arrowheads). The accumulation of integrin was reduced in *scb* mutants, but a presumptive luminal domain was still apparent (Figure 3.5D, E, arrowheads). At stage 17, Dg labeling outlined the heart lumen (L domain; Figure 3.5B, C, arrowhead), and Discs-large (Dlg) accumulated at the adhesive junction between contralateral CBs (J domain; Figure 3.5C, arrow). When integrin function was reduced, the Dlg domain is uninterrupted, and a small domain expressing both Dlg and Dg was observed (Figure 3.5F).

These data suggest that early integrin aggregation presages the formation of the luminal domain during CB migration, and integrin may therefore be instructive in localizing factors like Robo, also required to establish the lumen. These data do not exclude the possibility that other apical signals work in concert with integrin. We also

Figure 3.5. Integrins concentrate at the presumptive luminal domain.

Transverse optical sections from the heart proper of immunolabeled embryos reveal that βPS1 integrin (red) is concentrated ventral to the leading edge of migrating CBs (arrowhead, **A, A'**), where the lumen forms at stage 17 (arrowhead, **B, B'**). Dystroglycan (green) outlines most of the cell surface during migration, and concentrates at the lumen surface later than Integrin (**A, B**). However, Dg is excluded from the cell junction between contralateral CBs, which instead accumulates Dlg (arrow, red) at stage 17 (**C, C'**). Zygotic *scb*^{2} mutants accumulate lower levels of βPS1 integrin apically during migration (arrowhead, **D, D'**). Integrin and Dg are both located apically at stage 17, but lumen formation fails (arrowhead, **E,E'**). An adherent domain marked by continuous Dlg labeling (arrow, **F, F'**) indicates that no lumen forms, although a pocket of apical Dg labeling is still seen (arrowhead, **F**). The dorsal leading process apparent in *yw* migrating CBs (arrow, **A**) is missing in *scb*^{2} mutants (arrow, **D**). Dorsal at top; asterisks label approximate location of CB nucleus. Calibration: 5 microns.

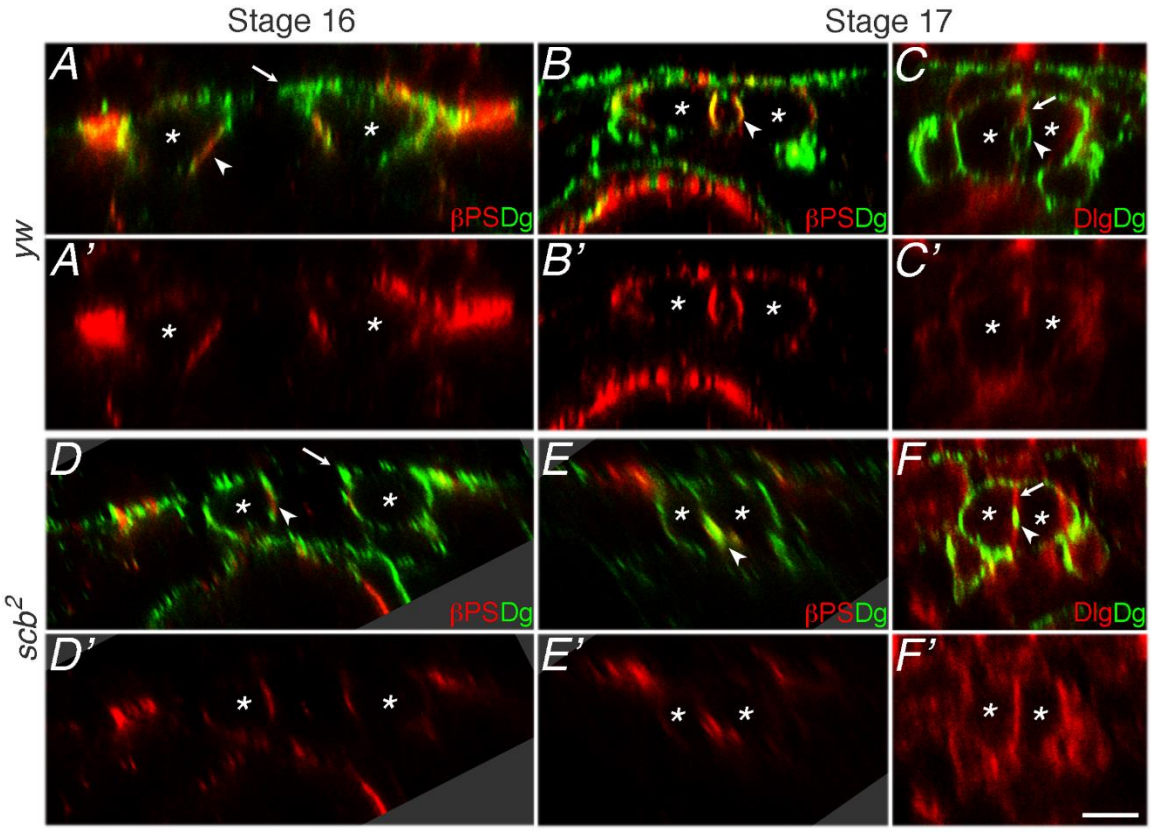
Stage 16
Stage 17
A
B
C
βPSDg
βPSDg
DlgDg
yw
A'
B'
C'
D
E
F
βPSDg
βPSDg
DlgDg
scb2
D'
E'
F'

explored the possibility that Robo signaling augments apical signaling. In embryos lacking function of both Robo1 and Robo2 (*robo*^{1}*lea*$^{54-14}$), βPS1 and Dg distribution were remarkably less polarized at both stages 15 and 17 (Figure 3.4G, H, I), even though Robo was not normally apically concentrated until stage 17 (Figure 3.4E). At stage 15 it is unlikely that CBs can detect contralateral Slit. Therefore, autocrine Slit signaling may contribute to CB polarization during migration.

3.3.4 Integrins are required for robust leading edge motility

Cell migration requires polarized membrane and cytoskeletal trafficking, and instructive polarizing signals may require outside-in signals from integrins (Ulrich and Heisenberg 2009, Caswell *et al.* 2009). Of the apical markers examined, only βPS1 integrin is concentrated at the apical leading edge before stage 16. Embryos mutant for *scb*^{2} appear to lack a leading membrane process (Figure 3.5D). We therefore sought to determine whether the exploratory activity of the leading edge required normal integrin function. Leading edge activity is effectively assessed with fluorescently tagged Moesin, which binds to submembrane actin, outlining lamellipodia and filopodia (Millard and Martin 2008). We compared the density and length of membrane processes of wildtype CBs (Figure 3.6A) with those of zygotic *mys* (Figure 6B) and *scb* mutants (Table 3.1). Although leading edge activity was clearly present in *mys* mutant, only 12% of the leading edge was active, while in contrast, membrane activity was more vigorous in wildtype, incorporating 41% of the leading edge of CBs (Table 3.1). A phenocopy of this effect

Figure 3.6. Leading edge membrane activity requires integrin function.

The dynamic activity of the leading edge of migrating CBs was monitored in living embryos, labeling membrane actin with *dMEF-GAL4* regulated *UAS-moesin-mCherry* (red), while marking the CBs with *tup-F4-GFP* (green). In early stage 16, wildtype CBs within the heart proper are 20 microns apart, and extend highly dynamic lamellipodial and filopodial processes to contact their contralateral partners (arrows in **A**). Although zygotic mutants of *mys*^{1} generate similar cell processes (arrows in **B**), most of the leading edge is quiescent (asterisks), and medial migration is slower. Images are taken at 2 minute intervals; the dorsal midline at t=0 is marked with a dotted line. Calibration: 25 microns.

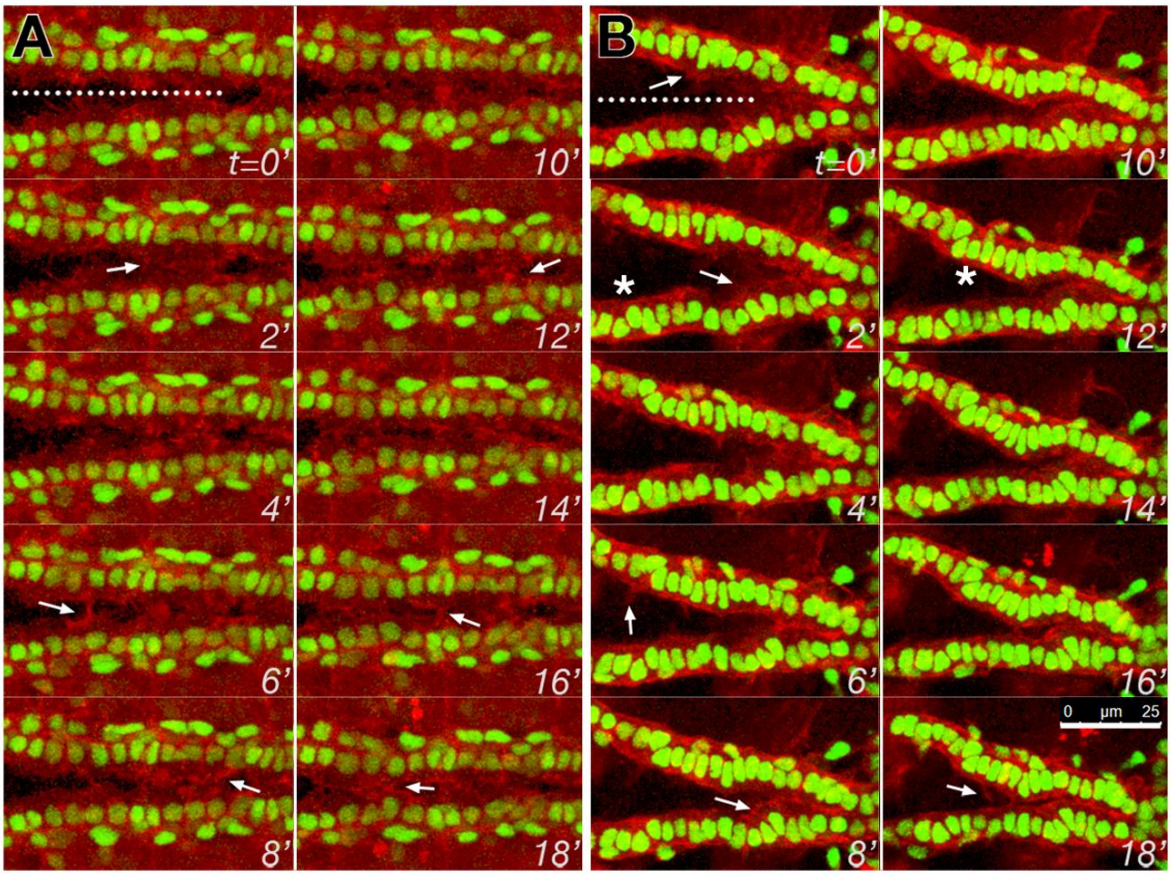
A
t=0'
10'
2'
12'
4'
14'
6'
16'
8'
18'
B
t=0'
10'
2'
12'
4'
14'
6'
16'
8'
18'
0 µm 25

subsequent to dsRNA interference of *mys* or *scb* could not be generated, possibly due to the presence of an additional UAS target (UAS-moesin-mCherry). The low level of leading edge activity in integrin mutants may reflect maternally contributed integrin function, or compensation by other apicalizing signals. It remains to be resolved whether integrin signaling from the pre-luminal domain affects leading edge activity, or whether integrins function in the leading processes, but are not detectable after histochemical processing.

3.3.5 Integrins interact genetically with genes for adhesion signaling

A contribution by integrin function to CB migration or polarization can be revealed through genetic interactions between *scb* and mutations in genes that act in the same, or a converging pathway. We have surveyed possible interactions with genes coding components of the ECM, and with genes that act to mediate adhesive or morphogenetic signals. Similar phenotypes were observed in embryos heterozygous for scb^2, and also heterozygous for mutations in βPS1 or known integrin ligands Collagen IV (*viking or vkg*), Laminin chains α3,5 and α1,2 (*lanA*, *wb*), and Tiggrin (*tig,* not shown) (Figure 3.7B, C, D, E respectively). Phenotypic interactions were characterised by interruptions in the continuity of each CB leading edge, evidenced by either small gaps (Figure 3.7, asterisks) or spans or clumps of CBs, 3 or more cells across (Figure 3.7 arrows). We also screened for interactions between *scb* and genes for intracellular factors that mediate cytoskeletal responses to signals from the membrane. Interestingly, embryos doubly heterozygous for *scb* and Talin (*rhea*) had a phenotype similar to that seen for the ECM gene interactions,

Figure 3.7. αPS3 integrin interacts with mutations in genes for adhesion and adhesion signaling.

Cardioblast position at stage 17 is visualised for embryos zygotically and maternally heterozygous for both *scb*^{2} and zygotically heterozygous for an interacting gene. Embryos heterozygous for *scb* have normal heart assembly (**A**). If additionally heterozygous for the gene for βPS1 integrin (*mys*^{1}), the continuity (asterisks) and alignment (arrows) of the CBs is disrupted (**B**). A similar phenotype is seen in embryos also heterozygous for collagen IV (*vkg*$^{[p1003-8]}$, **C**), whereas mutation in two Laminin chains (*LanA* $^{9-32}$, **D** and *Laminin* α*2* or *wb*^{SF11} , **E**) affect CB alignment, but without effect on continuity. Genetic interactions are revealed with a reduced gene copy of adhesion second messengers associated with integrin, such as Talin (*rhea*^{1}, **F**) and Integrin linked kinase (ILK; **G**), as well with second messengers associated with guidance signaling, such as Disabled (*dab*$^{M54-R1}$, **H**). CBs labeled with the B2-3-20 enhancer trap. Posterior is at the bottom.

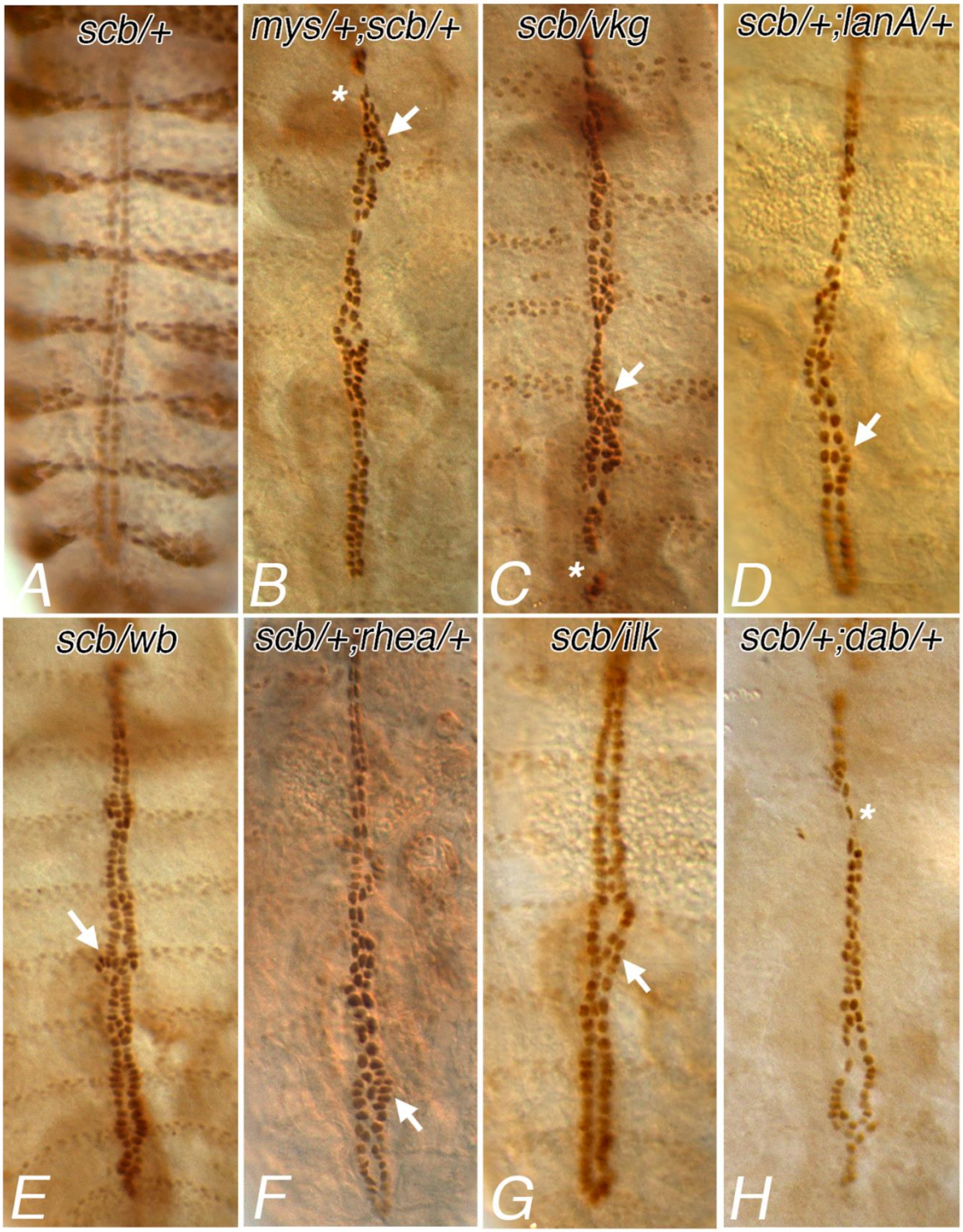
scb/+
mys/+;scb/+
scb/vkg
scb/+;lanA/+
A
B
C
D
scb/wb
scb/+;rhea/+
scb/ilk
scb/+;dab/+
E
F
G
H

suggesting that Talin, which links integrins to the actin cytoskeleton, mediates the effects of adhesion to the ECM (Figure 3.7F). In contrast, perturbations in heart morphology were less stereotyped for genes believed to affect actin remodeling, and acting downstream of Robo (*dab*, *dock*, and *abl*; Figure 3.7 H, and data not shown) or integrin (*ilk*, Figure 3.7G). These data suggest that integrin function in CB alignment is more sensitive to factors affecting adhesion than to changes in cytoskeletal signaling.

Since the scb^2/+ sensitized screen revealed only subtle genetic interactions with genes encoding cytoplasmic proteins that act downstream of integrin, embryos homozygous for mutant alleles of several adhesome genes were assessed to directly test for their requirement in heart development (Appendix B.1). In *rhea* homozygous embryos, the space between contralateral CB rows was narrow and Robo failed to apicalize (Appendix B.1, compare B to A), accordant with a putative role in mediating integrin function in heart tubulogenesis. Consistent with the subtle genetic interaction observed between *scb* and integrin downstream targets, minor disruptions in cardioblast migration or alignment, but not Robo localization, were observed in embryos homozygous for mutant alleles of *ilk*, *wech*, *stck* (*pinch*), *vinc*, and *fak56D* (Appendix B.1C-G). This suggests that these genes are not essential for *Drosophila* heart development, although it is also possible that low levels of perdurant maternally loaded protein may mask a requirement. In contrast, *src42A* mutants displayed a severe delayed or stalled migration phenotype in the posterior region of the heart and had mislocalized punctate, lateral accumulations of

Robo (Appendix B.1H). This is intriguing, as Src is a kinase capable of modulating integrin E-cad crosstalk to promote cell migration (Avizienyte and Frame 2005).

3.4 Discussion

Morphogenesis of the *Drosophila* heart provides an accessible genetic model to dissect the signals that orient migrating mesenchymal cells, and enable the cells to transform to a differentiated, stable epithelial structure with luminal and basal identity. A diversity of genes has been identified that are required for lumen formation in the heart. They include genes encoding ECM proteins such as Laminin A, homophilic adhesion receptors such as Cadherin, and genes associated with mediating cell guidance, such as Slit or NetrinB (Haag *et al.* 1999, Albrecht *et al.* 2010, Medioni *et al.* 2008, Knox *et al.* 2011). This work establishes that integrins are also required for CB polarization- during cell migration, for apical leading edge motility, and during lumen formation. A lumen fails to develop in the hearts of embryos lacking *scb* function, but the luminal domain can be restored by expression of αPS3 in the CBs of a *scb* mutant.

Although Robo is believed to be key to the establishment of the luminal domain, the mechanisms that localize Robo function are unclear (Medioni *et al.* 2008, Santiago-Martinez *et al.* 2008). Our previous studies establish a close functional relationship between Robo function and integrins, in both axon guidance, and in heart morphogenesis (MacMullin and Jacobs 2006, Stevens and Jacobs 2002). Apical accumulation of βPS1 integrin precedes apicalization of the proposed lumen determinants, Slit and its receptor,

Robo. Furthermore, in *scb*^{2} mutants, Robo and Slit do not accumulate apically, and in fact, are found on lateral cell surfaces, associated with Cadherin based adhesion. Restoring *scb* function with either normal or high affinity αPS3 restores Robo apicalization- suggesting that regulating integrin affinity for the ECM is not critical for its apical signal.

Robo signaling prevents local accumulation of Cadherin in both neurons and CBs – and in the heart, it has been proposed that this is the basis of generating an non-adherent luminal domain (Santiago-Martinez *et al.* 2008, Emerson and Van Vactor 2002). Our data suggest that Robo signaling must act in concert with integrin to restrict Cadherin from the apical domain. In the salivary gland model of lumen development, Cadherin is removed from the luminal domain by endocytosis, employing Rho family GTPases and p21 activated kinase 1 (Pak1; Pirraglia *et al.* 2010), which in turn, are downstream of integrin and Robo signals (Gupton and Gertler 2010, Wong *et al.* 2001).

Given that mutation of any one of seven cell surface receptors (Cadherin, Integrin, Robo, Neurexin, Syndecan, Dystroglycan and Unc5) is sufficient to block lumen formation, it is likely that cooperative signaling defines the luminal domain and luminal differentiation (Haag *et al.* 1999, Santiago-Martinez *et al.* 2006, Albrecht *et al.* 2010, Medioni *et al.* 2008, Knox *et al.* 2011). Of the seven required receptors, Robo, Syndecan, Dystroglycan, Integrin and Unc5 locate to the luminal domain. Integrin, its ligand Laminin (Harpaz and Volk 2012), and Unc5 (Albrecht *et al.* 2010) concentrate in the presumptive luminal domain before the others, and likely are instructive. Our data also suggest that the

presumptive luminal domain is defined by βPS1 integrin accumulation during migration, and before contact with contralateral CBs.

At stages 15 and 16, βPS1 integrin localizes apically when Robo is still expressed on all membrane domains. Nevertheless, at this stage, polarized integrin distribution requires Robo function. It is possible that integrins suppress Robo turnover at the apical surface only, and Robo signaling stabilises the integrins, culminating in the apical aggregation of Robo seen by late stage 16. Leading edge membrane motility becomes most pronounced during stage 16. Loss of integrin function reduces the fraction of the membrane leading edge that is active. In contrast, loss of *robo* function reduces leading edge activity uniformly, and filopodia are rare (Medioni *et al.* 2008, Santiago-Martinez *et al.* 2008, Syed 2012), suggesting that integrin dependent accumulation of Robo augments membrane activity.

3.5 Conclusions

We have characterised the contribution of integrin function to cell migration and lumen formation in a mesodermal organ, the *Drosophila* heart. Integrins are required to maintain the alignment of the migrating CB leading edge cells, and are also required for normal levels of leading edge motile membrane activity. A pre-luminal domain, first revealed by early integrin accumulation, is defined before the CBs meet their contralateral partners. Integrin accumulation is required to stabilise the morphogen Slit, and its receptor Robo, to the pre-luminal domain. This is consistent with Robo signaling

contributing to leading edge membrane activity. Even through Robo does not aggregate apically in migratory CBs, its expression is required to stabilise integrins in the pre-luminal domain.

We confirm an earlier report that αPS3 integrin is required for heart lumen formation (Stark *et al.* 1997). The genetic interaction of *scb* with *rhea* (Talin) further suggests that assembly of a complex of ligand-bound integrin, linked to the actin cytoskeleton through Talin, both stabilises the apical membrane domain, and enables Robo accumulation (Chapter 4). Additionally, the phenotype observed in homozygous *src42A*^{E1} embryos alludes to a putative role for Src-mediated integrin control of collective cardioblast migration (Appendix D).

Talin-mediated integrin adhesion in *Drosophila* embryonic heart assembly

CHAPTER FOUR

4.1 Introduction

4.1.1 Talin is an intriguing candidate to mediate integrin adhesion in *Drosophila* embryonic heart development

While it is clear that integrins and other cell surface factors are required for heart development, it is less apparent how signals from or through these receptors modulate cardioblast (CB) morphogenesis, polarity, and adhesion dynamics. Although only one of numerous proteins that interact with the β-integrin cytoplasmic tail, Talin is unique as it is a requisite for both integrin activation (increasing integrin adhesivity) and signaling (linking to actin and numerous other adhesome factors). During our lab's study on *slit*, a genetic dosage sensitive screen highlighted a possible role for *rhea*, the gene encoding Talin, in *Drosophila* heart tubulogenesis (MacMullin and Jacobs 2006). A similar interaction was observed when we reduced the gene dosage of *rhea* in an *αPS3* integrin (scb^2/+) sensitized background (Figure 3.7).

In vertebrates, there are two *tln* genes encoding Talin1 (TLN1) and Talin2 (TLN2), sharing 74% sequence identity and 86% similarity (Monkley *et al.* 2001). While TLN1 is expressed in all tissues studied (Ben-Yosef and Francomano 1999; Monkley *et al.* 2001), TLN2 is primarily found at high levels in the heart (Monkley *et al.* 2001). Despite its presence in the heart, few studies have focused on TLN2. One study by Conti *et al.* (2008) looked at skeletal muscle, another tissue where TLN2 is the major isoform expressed (Conti *et al.* 2009). Although loss of TLN2 is likely partially compensated by TLN1, TLN2 deficient mice showed defects in the myotendinous junctions (Conti *et al.* 2008).

Furthermore, TLN localizes together with Vinculin in the costamere of cardiac muscle (Anastasi *et al.* 2009), and Vinculin has been implicated in numerous studies on heart-related diseases (reviewed by Zemljic-Harpf *et al.* 2009). Therefore, given its likely, but uncharacterized, role in the complex vertebrate heart, Talin is a fascinating candidate to study in a much simpler tubulogenesis model such as the *Drosophila* cardiac tube.

4.1.2 Talin is essential for integrin adhesion in *Drosophila melanogaster*

In *Drosophila*, *rhea* was first discovered through a genetic screen designed to identify genes required for integrin-mediated adhesion in the wing (Prout *et al.* 1997). *rhea* mutant clones within the wing do not express Talin; lack of Talin led to wing blisters, the result of a failure of integrin adhesion between the two wing epithelial layers (Prout *et al.* 1997). Talin is similarly required for stable integrin adhesion to prevent somatic muscle detachment (Brown *et al.* 2002b) and to establish stem cell anchorage to the underlying intestinal basement membrane (Lin *et al.* 2013). In addition, Talin is required for dynamic and transient integrin adhesion such as during germ-band retraction, dorsal hole closure (Brown *et al.* 2002b, Ellis *et al.* 2011), and haemocyte/macrophage migration (Comber *et al.* 2013). In these wide-ranging studies, *rhea* mutant tissues phenocopy tissues deficient in one or more of the integrin alpha or beta subunits, suggesting that Talin is essential for integrin adhesion in *Drosophila*.

Consistent with the dual role of Talin in outside-in and inside-out integrin signaling characterized *in vitro*, *Drosophila* Talin is required for both integrin activation and integrin-

actin linkage. Activation of integrins results in a high affinity interaction with extracellular matrix (ECM) ligands. However, null *rhea* embryos expressing a Talin transgene lacking the first of two integrin binding sites (see 4.1.3) are unable to activate integrins, resulting in reduced ECM affinity and a physical separation from the ECM at muscle-muscle segment boundaries (Tanentzapf and Brown 2006). The integrin-actin linkage is mediated by Talin's actin-binding domain (ABD) near its C-terminus. Mutations within this domain prevented direct actin binding in both *in vitro* and *in vivo* assays (Franco-Cea *et al.* 2010). In flies expressing an ABD-disrupted Talin transgene, developmental processes that require transient and dynamic integrin adhesion were disrupted suggesting that direct Talin-actin interaction is required for such adhesion (Franco-Cea *et al.* 2010). In *in vitro* models of stable force-transmitting adhesions, Talin indirectly strengthens the integrin-actin linkage by recruiting the actin-binding Vinculin (Humphries *et al.* 2007, Goult *et al.* 2013a, Lee *et al.* 2013). As *Drosophila* Talin has multiple Vinculin binding domains (Brown *et al.* 2002b), it is likely that its indirect, yet robust, actin-linking role is similar in *Drosophila*.

4.1.3 The Talin protein has two binding sites for β-integrin

Talin is a large ~250kDa protein comprised of a small N-terminal, FERM-domain containing, head and an extended C-terminal rod. In both the head and rod regions there are binding sites for the β-integrin cytoplasmic tail (Integrin Binding Site or IBS1 and IBS2 respectively; Figure 4.1). Although either β-integrin-binding domain is sufficient to bind Talin to the membrane-proximal part of the β-integrin tail, the binding motif is different in

Figure 4.1 – Talin has multiple integrin and adhesome-protein binding domains

(**A**) Talin binds to the β-integrin cytoplasmic tail through two integrin binding sites (IBSs). Talin-integrin binding activates integrins (inside-out signaling) and connects integrins to actin and the cytoplasmic integrin adhesome network (outside-in signaling). In the *Drosophila* embryo, the IBS1 has been implicated in supporting a strong integrin-ECM connection and maintaining long-lasting stable adhesions, while the IBS2 mediates the sustained recruitment of the integrin adhesome and is essential for both transient and stable adhesions (Ellis *et al.* 2011). (Figure adapted from Vicente-Manzanares *et al.* 2009 with permission from Nature Publishing Group.)

(**B**) The *rhea* gene encodes for the multi-domain adaptor protein Talin. In addition to the two integrin binding sites, Talin has domains which interact with several adhesome proteins, directly bind to actin, and permit homodimerization. Red arrows indicate the site of null point mutations (*rhea*^{1} and *rhea*^{2}) or the deletion span (*rhea*^{79}). Blue arrows highlight the site-directed mutations in the Talin transgenes that result in abrogated IBS1 or IBS2 function. (Figure adapted from Roberts and Critchley 2009 with permission from Springer.)

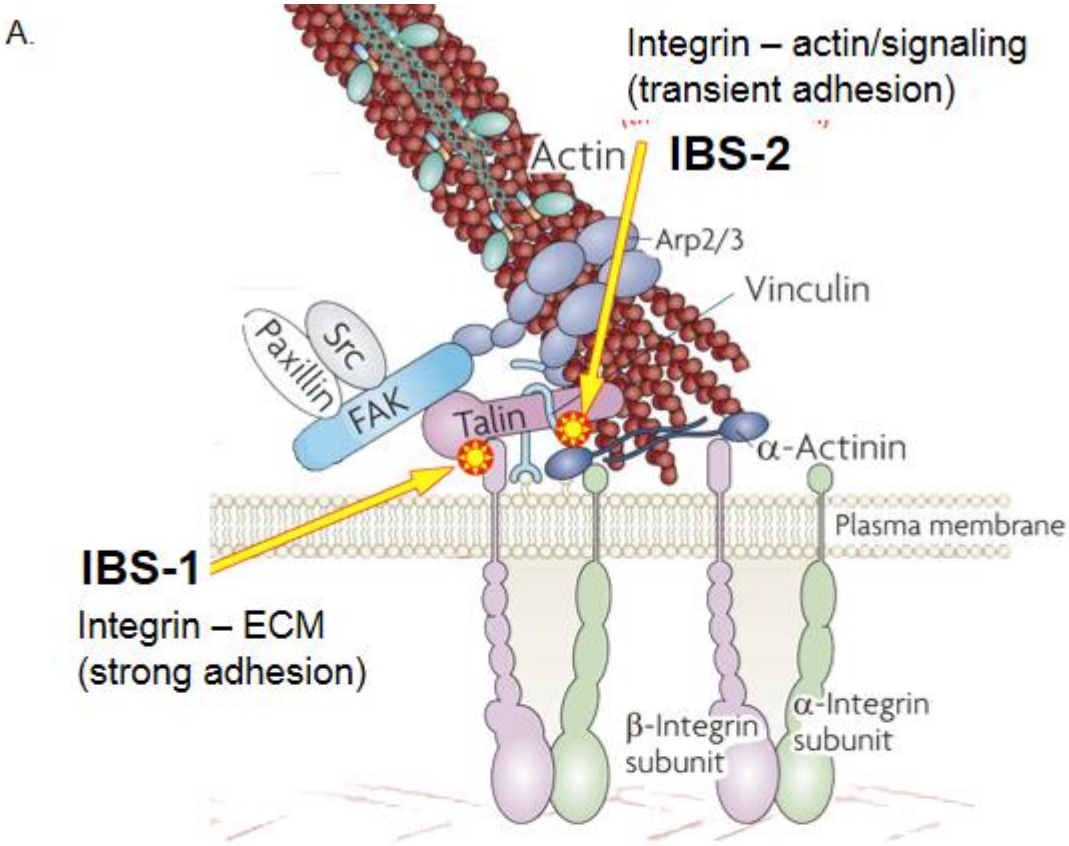
A.
Integrin – actin/signaling
(transient adhesion)
Actin
IBS-2
Arp2/3
Vinculin
Paxillin
Src
FAK
Talin
α-Actinin
Plasma membrane
IBS-1
Integrin – ECM
(strong adhesion)
β-Integrin
subunit
α-Integrin
subunit

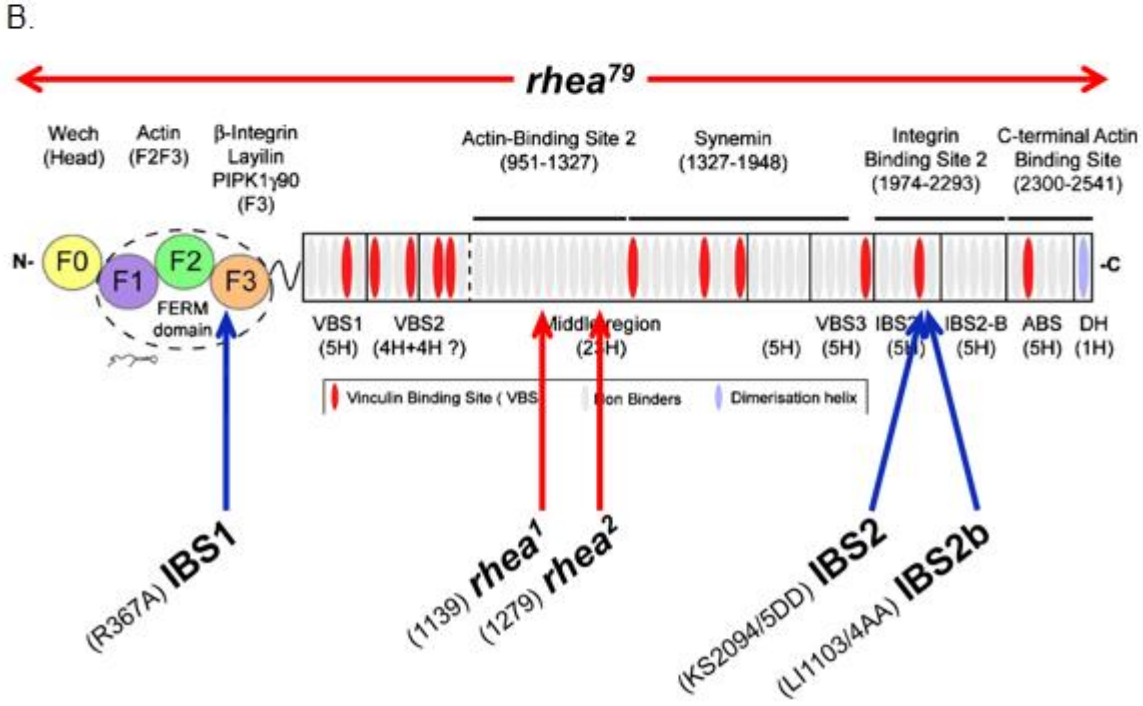
B.
rhea79
Wech
(Head)
Actin
(F2F3)
β-Integrin
Layilin
PIPK1γ90
(F3)
Actin-Binding Site 2
(951-1327)
Synemin
(1327-1948)
Integrin
Binding Site 2
(1974-2293)
C-terminal Actin
Binding Site
(2300-2541)
N-
F0
F1
F2
F3
FERM
domain
-C
VBS1
(5H)
VBS2
(4H+4H ?)
VBS3
(5H)
IBS2-B
(5H)
ABS
(5H)
DH
(1H)
Vinculin Binding Site (VBS
Dimerisation helix
(R367A) IBS1
(1139) rhea1
(1279) rhea2
(KS2094/5DD) IBS2
(LI1103/4AA) IBS2b

each case. IBS1 interacts with the NPxY sequence (Calderwood *et al.* 2002; García-Alvarez *et al.* 2003; Anthis *et al.* 2009b), a site also bound by the integrin-activating Kindlin (Yates *et al.* 2012; Mathew *et al.* 2012). It is binding by IBS1 to the NPxY region that induces integrin conformational changes, activating them and increasing the affinity for extracellular matrix ligands (Calderwood *et al.* 2002; Wegener *et al.* 2007; Tadokoro *et al.* 2003). While the IBS2 binding is less studied, it is known to bind to β-integrin via an alpha-helix region distinct from the NPxY sequence (Xing *et al.* 2001, Rodius *et al.* 2008; Tremuth *et al.* 2004; Gingras *et al.* 2009). IBS2 is not involved in integrin activation (Tremuth *et al.* 2004), consistent with sequence analysis of the IBS2–β-integrin binding region which suggests that integrins must be activated (conformational change) prior to IBS2 binding (Rodius *et al.* 2008). Several *in vitro* studies suggest that without the IBS2 domain, Talin is unable to link integrins to the cytoskeleton or to focal adhesion proteins such as FAK (Moes *et al.* 2007, Tremuth *et al.* 2004, Wang *et al.* 2011).

In *Drosophila*, the differential binding of IBS1 and IBS2 has been similarly connected to distinct adhesion-dependent processes. Although either IBS is capable of binding to β-integrin and recruiting cytoplasmic adhesome proteins to integrin, different tissues highlight context specific roles for each site. Consistent with a role in integrin activation, IBS1 binding increases integrin affinity for the ECM and induces long-lasting and stable adhesions. For example, it is essential at sites of muscle-muscle or muscle-tendon connections which require strong adhesion during muscle contractions (Tanentzapf and Brown 2006; Ellis *et al.* 2011). In contrast, IBS2 reinforces the linkage to

cytoplasmic factors within the integrin adhesome and is additionally required for the dynamic developmental processes such as germ-band retraction and dorsal closure (Ellis *et al.* 2011). Thus, genetic manipulation of each of these binding sites provides unique tools to independently assess the role of integrin-ECM affinity and the integrin-adhesome linkage in *Drosophila* development.

Although we have established that integrins are required for tubulogenesis of the *Drosophila* heart, it remains unclear which proteins may mediate this function. Here I demonstrate that the integrin adaptor Talin is essential for multiple aspects of heart formation. Consistent with Talin being required for integrin function, *rhea* mutant embryos largely phenocopy *αPS3* and β*PS1* mutants. Using embryos lacking zygotic or both maternal and zygotic Talin, I demonstrate that Talin is required for CB dynamics during collective cell migration. Following migration, the CBs in *rhea* null embryos fail to concentrate βPS1 and Robo at the luminal domain and are unable to enclose the heart tube. This *rhea* null loss-of-lumen phenotype can be rescued by expressing either full-length Talin or Talin lacking one of the integrin binding sites, suggesting that either site is sufficient for Talin-mediated integrin function during heart development.

4.2 Results

4.2.1 Talin localization during *Drosophila* embryonic heart development

Following cardial cell specification, the CBs align in two rows, adjacent to the amnioserosa. Immediately lateral to the CBs are the pericardial cells (Figure 4.2A'). During

dorsal closure, the overlying ectoderm migrates to cover the dorsal hole transiently filled by the amnioserosa. Coincident to this process, the CBs and pericardial cells collectively move towards the dorsal midline (Figure 1.4). Following dorsal closure, the cardial cells complete their migration by wedging between the ectoderm and the internalising amnioserosa cells so that the CBs meet their contralateral partners at the midline (Figure 1.4 stage 16). Throughout CB migration, Talin localizes specifically to the apical and basal CB domains (Figure 4.2A-F arrow and arrowheads respectively), but is not detected laterally between neighboring CBs within each row. Talin expression is not restricted to the heart, but is also detected in surrounding tissues including the amnioserosa and gut (Figure 4.2A-F). Following migration, high levels of Talin remain at the basal surface and apically, at the midline (Figure 4.2G). Furthermore, recruitment or stabilization of Talin at the luminal and basal surface is βPS1 (*mys*) dependent, consistent with Talin binding to the β-integrin cytoplasmic tail at sites of integrin adhesion (Appendix C.2; Calderwood *et al.* 2002, Rodius *et al.* 2008). Embryos homozygous for the null mys^{XG43} allele have reduced concentration of Talin along the midline and some instances of diffuse lateral accumulation (Appendix C.2B, C). In embryos that lack both zygotic and maternally deposited βPS1, Talin localization is further disrupted and there is no consistent apical or basal pattern of Talin accumulation (Appendix C.2D).

As first suggested by Medioni *et al.* (2008) and further supported by research presented in Chapter 3, the apparent "apical" cell surface opposite to the basal surface in a frontal heart image is not a single domain, but can be more correctly described as a

Figure 4.2 – Talin localization in the developing *Drosophila* embryonic heart

Part 1. Frontal images of the *Drosophila* heart at stage 14, 15, 16, and 17 of embryogenesis.

During early (**A, B**), mid (**C, D**), and late (**E, F**) CB migration, Talin is localized along the advancing apical domain (arrow) and the trailing basal surface along the CB-pericardial cell interface (arrowhead), but is excluded laterally. Talin immunolabel can also be detected in the gut (g) and amnioserosa (as). Following migration, during heart tube enclosure at stage 17, the apical (arrow) and basal (arrowhead) distribution of Talin remains unchanged (**G**). CBs here and in subsequent figures are labeled with αMEF. Pericardial cells are labeled with αZfh1. Calibration: 10 microns.

Part 2. Transverse images of the *Drosophila* heart at stages 16 and 17 of embryogenesis. During cardial cell migration, the triangular cardioblasts (outlined with Dystroglycan, Dg) extend dorsally towards the midline (arrowhead). Talin immunolabel is concentrated ventral to the leading edge (arrow), marking the pre-luminal domain (**H, I**). Following migration, the cardioblasts adopt a crescent shape to enclose the Talin-lined lumen (**J**). Dorsal is to the top in all panels. Calibration: 5 microns.

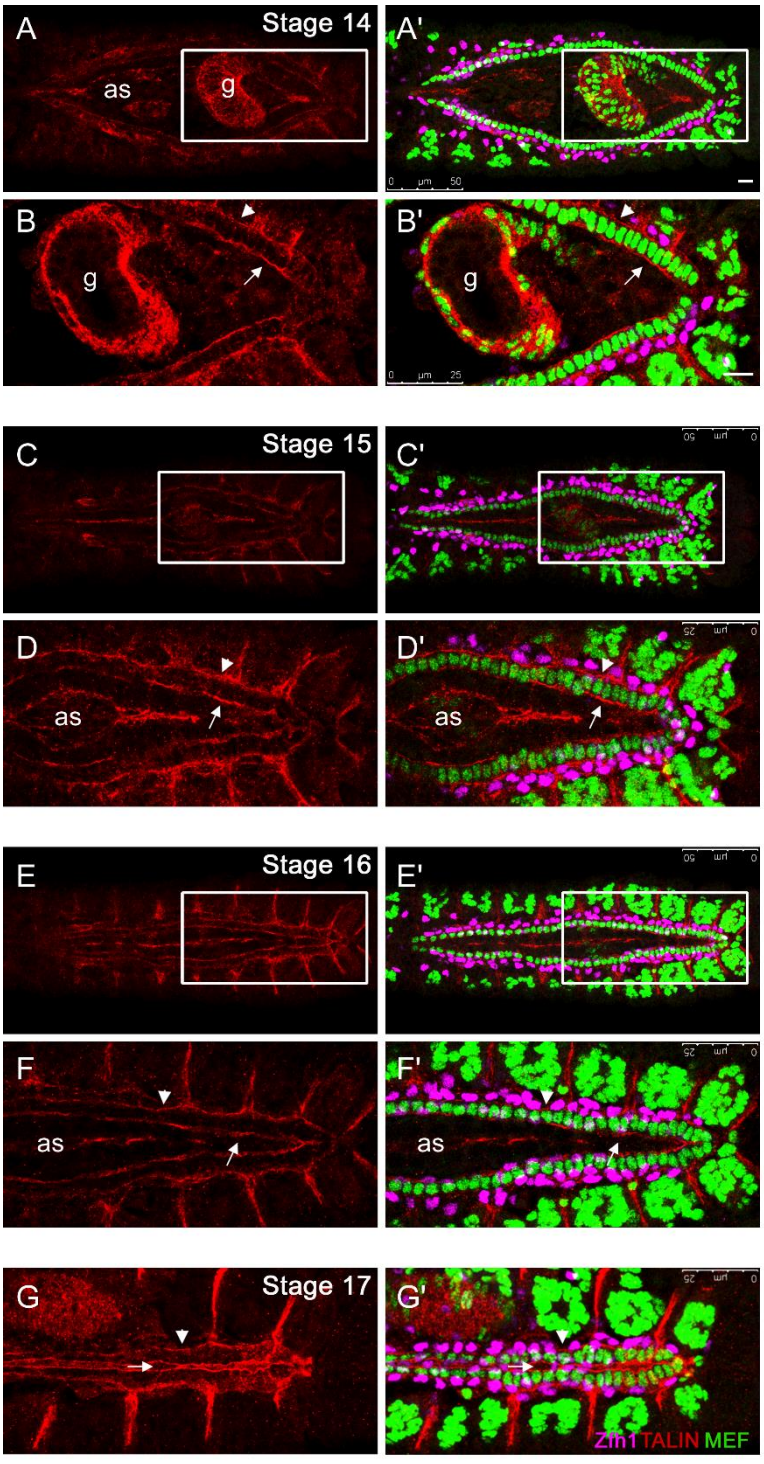
A
Stage 14
as
g
A'
B
g
B'
g
C
Stage 15
C'
D
as
D'
as
E
Stage 16
E'
F
as
F'
as
G
Stage 17
G'
Zip1 TALIN MEF

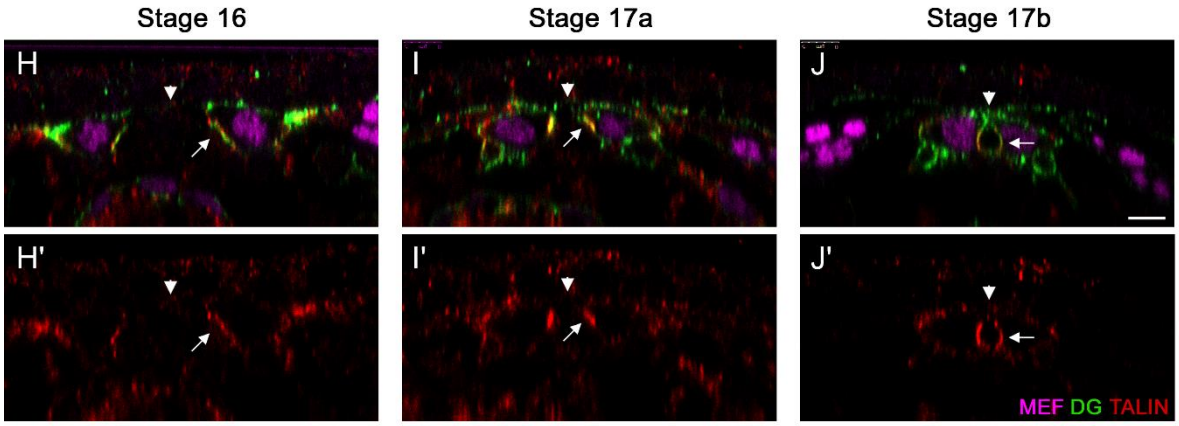
Stage 16
Stage 17a
Stage 17b
H
I
J
H'
I'
J'
MEF DG TALIN

central luminal (L) domain sealed dorsally and ventrally by two junctional (J) or adherent regions. This is most apparent when a transverse image of the heart is viewed (eg. Figure 1.4). In the mature embryonic heart, Talin accumulates along the luminal domain (arrow), but is excluded from the sites of adhesion (arrowhead; Figure 4.2J). However, Talin is a marker for the luminal domain well before tubulogenesis occurs. Already as the CBs are migrating, Talin localizes to the pre-luminal or lumen initiation site (Figure 4.2H, I), suggesting that Talin, like integrins, may be an early site-determinant for lumen formation.

4.2.2 Mutations in the gene *rhea* deplete the embryo of Talin

To test the hypothesis that Talin is required for *Drosophila* heart tubulogenesis, embryos homozygous for a null $rhea^{79}$ allele were generated. The $rhea^{79}$ allele contains a deletion spanning the entirety of *rhea* plus two flanking genes *ergic-53* and *CG6638* (Brown *et al.* 2002b). Compared to wildtype, $rhea^{79}$ embryos have markedly reduced Talin (Figure 4.3A, B); however, when the gain was increased, low levels of Talin were still detected in basal and apical punctate accumulations (Figure 4.3B''). Similar results were obtained when additional null alleles of *rhea* were tested (Figure 4.3C-D). Both $rhea^{1}$ and $rhea^{2}$ contain point mutations which result in stop codons in the middle region of Talin; embryos homozygous for $rhea^{1}$ or $rhea^{2}$ had markedly reduced, but still detectable, Talin. This residual Talin is consistent with previous studies of Talin during *Drosophila* embryogenesis: hindering our analysis is a maternal contribution of Talin to the

Figure 4.3 – Mutations in the gene *rhea* deplete the embryo of Talin

Compared to wildtype (**A**), *rhea* zygotic mutants have reduced Talin, with low levels detected in punctate accumulations along the apical and basal cardioblasts domains (**B-D**). In germ-line clone mutant embryos lacking both maternal and zygotic Talin, no Talin immunolabel is detected (**E**). All center panels were images with identical settings, while the gain in the right panels was adjusted to visualize low intensity immunolabel signals. Arrows indicate the midline. Calibration: 10 microns.

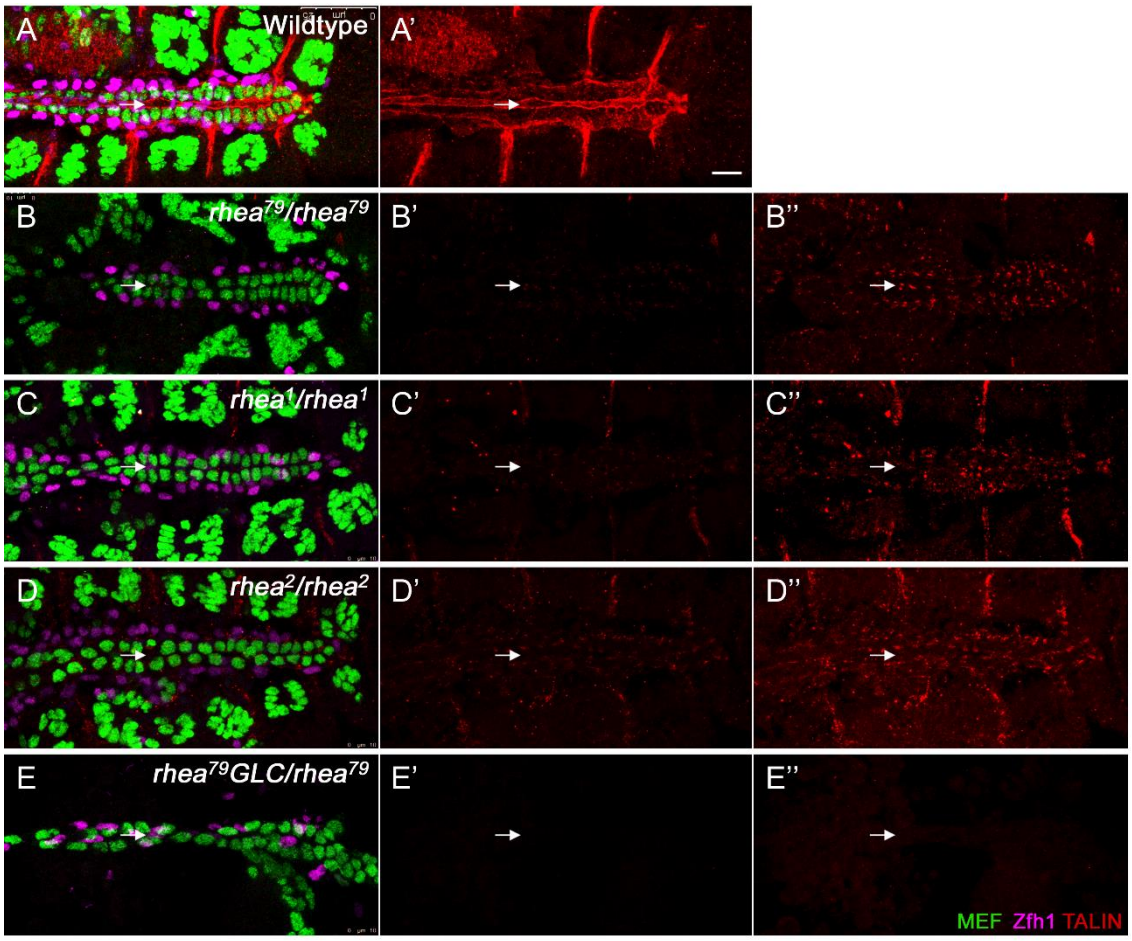
A
Wildtype
A'
B
rhea79/rhea79
B'
B''
C
rhea1/rhea1
C'
C''
D
rhea2/rhea2
D'
D''
E
rhea79GLC/rhea79
E'
E''
MEF Zfh1 TALIN

developing embryo (see Methods 2.8; Brown *et al.* 2002b). Although maternal contribution is essential for proper embryonic development, it makes it difficult to experimentally generate and analyze embryos completely devoid of Talin. To provide a true *rhea* null embryo, embryos without either maternally or zygotically contributed Talin were generated using the dominant female-sterile germ-line clone technique (2.8; Appendix A.2; Chou and Perrimon 1996).

Germ-line clone (GLC) *rhea* mutant embryos allow us to differentiate between developmental processes that require low levels of Talin from those that do not require Talin at all. For example, dorsal closure fails in *rhea* GLC mutants, demonstrating that Talin is required for this process (eg. see Appendix C.1; Ellis *et al.* 2013). However, most zygotic *rhea* mutants had complete dorsal closure (Appendix C.1B), suggesting that low levels of maternally contributed Talin are sufficient. Similarly, unlike wildtype or zygotic *rhea* mutants, *rhea* GLC embryos exhibited displacement of pericardial cells from the CB basal surface. This suggests that while Talin is essential for CB-pericardial cell attachment, low maternal levels are sufficient to maintain adhesion (Figure 4.3). These examples illustrate that a complete understanding of Talin's function in *Drosophila* heart development requires assessment of *rhea* GLC embryos. However, analysis of the heart in these embryos is complicated by earlier developmental defects, such as the failure to complete germ-band retraction and dorsal closure (Brown *et al.* 2002b; Appendix C.1C). These phenotypes are not observed in zygotic mutant embryos (Appendix C.1B). Therefore, to

thoroughly examine the role of Talin in *Drosophila* heart development, a combination of zygotic and maternal-and-zygotic mutant analysis have been utilized.

4.2.3 βPS1 integrin is disrupted in *rhea* mutant embryos

Talin is required to activate integrins and increase their affinity for ECM ligands. Studies in both vertebrates and flies suggest that Talin is required for focal adhesion assembly and stabilization of integrins at sites of adhesion (Liu *et al.* 2011, Brown *et al.* 2002b). This appears to be true also in the *Drosophila* heart. Wildtype embryos have apicalized βPS1 integrin at the luminal surface and lower levels basally (Figure 4.4A). In comparison, *rhea* mutants have reduced and mislocalized βPS1 (Figure 4.4). In zygotic mutants, βPS1 integrin accumulates in a punctate pattern, similar to that seen with maternal Talin localization (Figure 4.4B-D, compare to Figure 4.3B''-D''). Maternal-and-zygotic mutant embryos have a more diffuse pattern of βPS1 (Figure 4.4E), consistent with Talin being required for integrin stabilization at sites of adhesion.

4.2.4 Talin is required for normal localization of extracellular and intracellular integrin-related proteins

One role of integrins is to promote proper establishment and maintenance of the ECM. For example, Laminin polymerization and network anchorage, crucial initiating steps in basement membrane assembly, are facilitated by integrin binding (Colognato *et al.* 1999, Yurchenco 2011). Integrins can also regulate ECM remodeling by promoting the

Figure 4.4 – Talin is required for βPS1 stabilization along the luminal and basal cardioblast surfaces

βPS1 localization in wildtype (**A**), *rhea* zygotic mutants (**B-D**), and *rhea* maternal-and-zygotic mutants (**E**). In wildtype embryos, βPS1 immunolabel is detected at high levels along the midline luminal surface and at lower levels basally (**A**). *rhea* zygotic and germ-line clone mutant embryos have reduced βPS1 that accumulates in a punctate (**B-D**) or diffuse (**E**) localization pattern, respectively. All βPS label was imaged using identical settings. Arrows indicate the midline. Calibration: 10 microns.

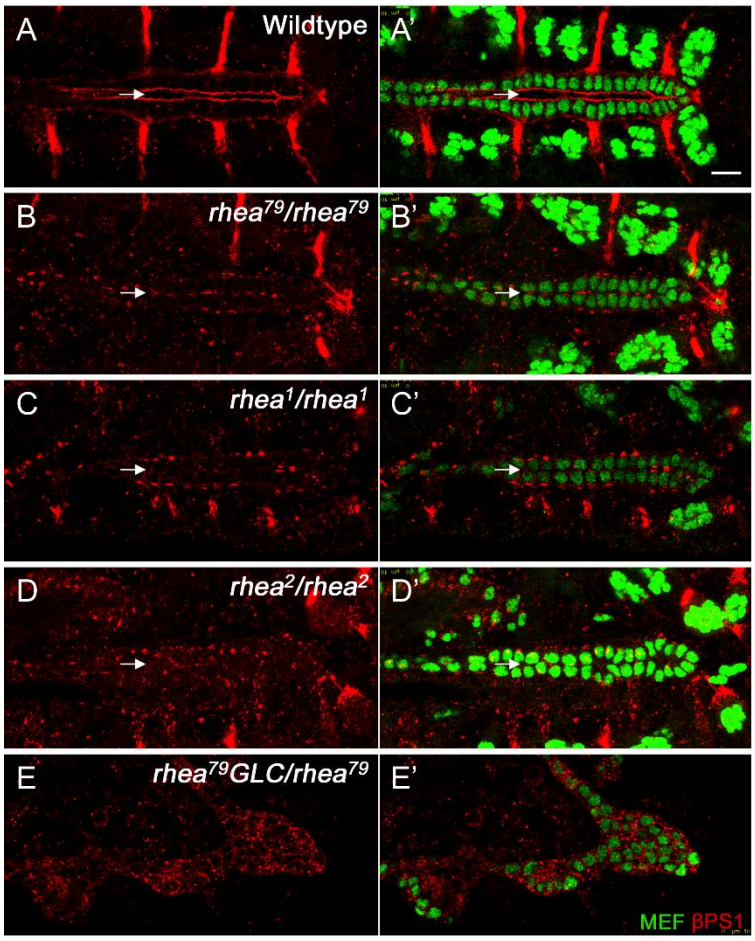
A
Wildtype
A'
B
rhea79/rhea79
B'
C
rhea1/rhea1
C'
D
rhea2/rhea2
D'
E
rhea79GLC/rhea79
E'
MEF βPS1

Figure 4.5 – ECM components and cytoplasmic integrin adhesome proteins are abnormally distributed in *rhea* mutant embryos

Part 1 – Localization of ECM components

(**A-C**) In heterozygous *rhea* embryos, LamininA (LanA) accumulates contiguous to the apical and basal cardioblast surfaces. *rhea*^{79} embryos have reduced LanA, with apical cardioblast surfaces often devoid of any detectable LanA.

(**D-F**) In heterozygous *rhea* embryos, Pericardin (Prc) is restricted to CB basal surface, along the CB-pericardial cell interface (arrowhead). In zygotic *rhea* mutant embryos, Prc remains basal, often surrounding the pericardial cells (arrowhead), but is also detected apically (horizontal arrow) and laterally (vertical arrow) between neighboring cardioblasts. Germ-line clone *rhea* mutant embryos have severely disrupted Prc distribution. Basal accumulation is frequently interrupted and non-continuous (arrowhead), while mislocalized Prc completely surrounds individual cardioblasts (arrow).

Part 2 – Localization of integrin adhesome proteins

(**G-H**) The pattern of Pinch in *rhea* heterozygotes is highly polarized, with strong apical and basal immunolabel and low levels laterally. In contrast, Pinch does not accumulate at any specific domain in *rhea*^{79} embryos, but is diffusely distributed around each cardioblast.

(**I-J**) Both *rhea*^{79} heterozygous and homozygous embryos have punctate accumulations of CAP present both apically and basally, although fewer apical accumulations are visible in mutant embryos. Calibration: 10 microns.

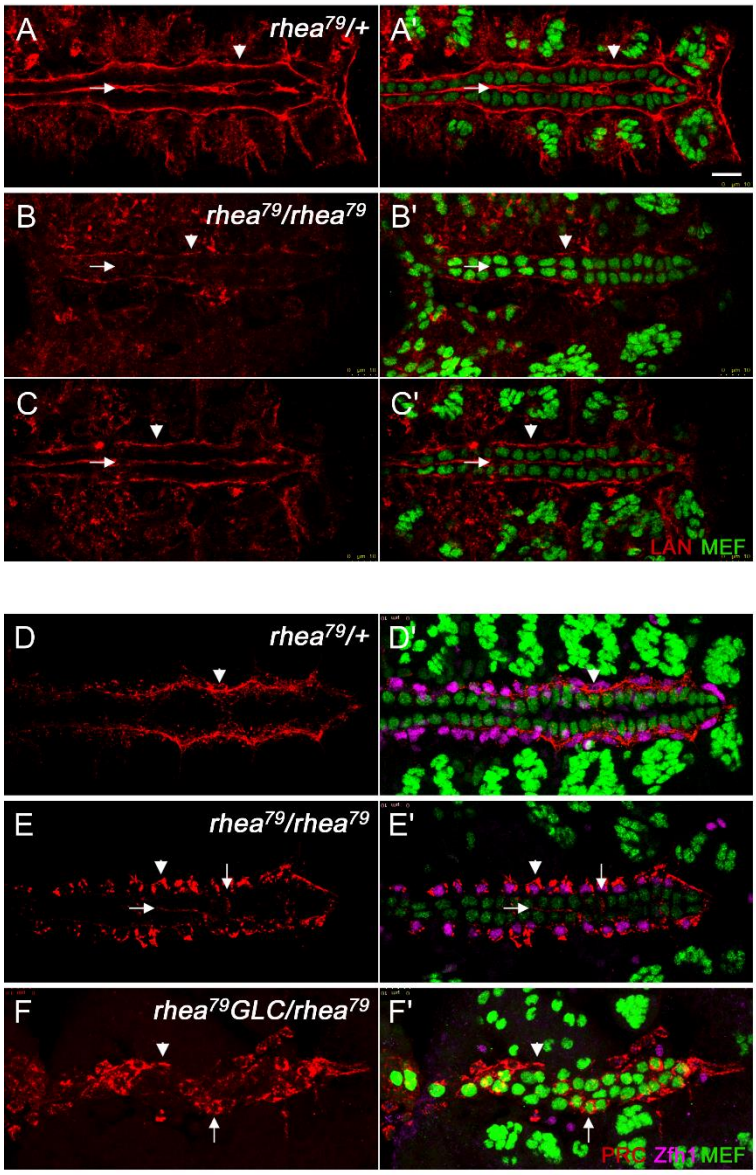
A
rhea79/+
A'
B
rhea79/rhea79
B'
C
C'
LAN MEF
D
rhea79/+
D'
E
rhea79/rhea79
E'
F
rhea79GLC/rhea79
F'
PTC Zfh1 MEF

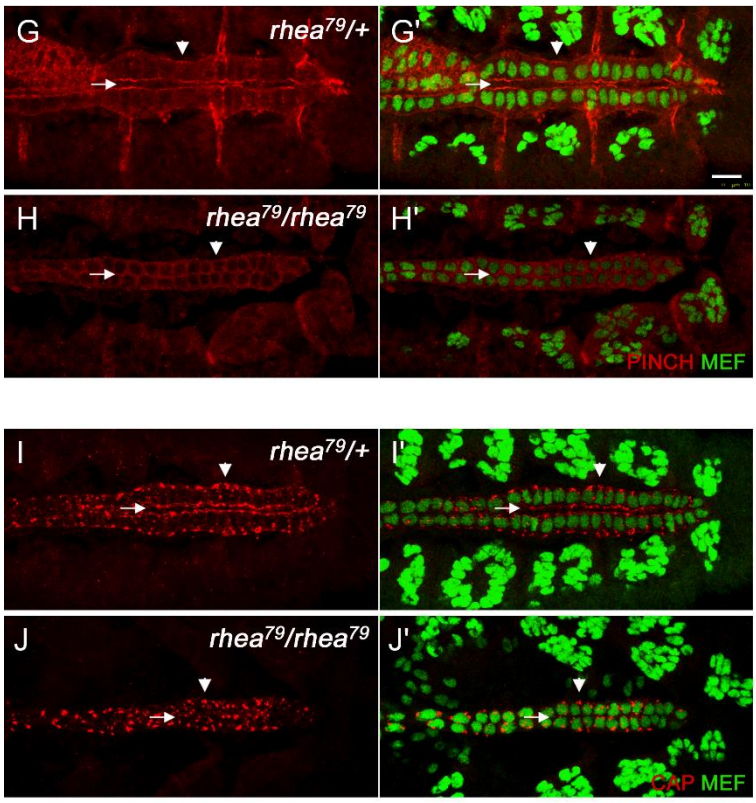
G
rhea79/+
G'
H
rhea79/rhea79
H'
PINCH MEF
I
rhea79/+
I'
J
rhea79/rhea79
J'
CAP MEF

activation of matrix metalloproteinases (MMPs) such as the membrane bound MT1-MMP or the secreted MMP2 (Gonzalo *et al.* 2010, Jiao *et al.* 2012, reviewed in Yue *et al.* 2012). Since Talin is essential for proper localization of integrin in the *Drosophila* heart, we sought to determine if Talin is similarly required to localize ECM factors surrounding the heart. Laminin, a likely αPS3βPS1 ligand (Stark *et al.* 1997), is a heterotrimeric ECM glycoprotein. To observe the localization pattern of Laminin, a mouse monoclonal antibody against LanA, one of two *Drosophila* laminin alpha chains, was generated (2.4.4, Appendix A.1). Consistent with it being an integrin ligand, in wildtype embryos, LanA immunolabel mirrored that of βPS1 and Talin with strong immuno-label detected along the apical and basal CB surfaces (Figure 4.5A). In *rhea* zygotic mutant embryos, LanA was reduced or absent apically (arrows) and detected at lower levels along the basal domain (arrowheads; Figure 4.5B, C). A second *Drosophila* heart ECM component is the Type IV collagen-like Pericardin (Prc), secreted by the pericardial cells and seven-up CBs (Singhal and Martin 2011, Chartier *et al.* 2002). Unlike LanA, in wildtype embryos Prc is excluded from the apical CB surface (Figure 4.5D). Rather, Prc is restricted to the basal surface, lining the CB-pericardial cell interface, and *pericardin* mutants are marked by pericardial cell detachment (Chartier *et al.* 2002, Drechsler *et al.* 2013). This localization pattern is disrupted in both zygotic and GLC *rhea* mutant embryos (Figure 4.5E, F). In zygotic mutants, Prc was mislocalized, often surrounding the pericardial cells (arrowhead) and detected within the heart, both apically (horizontal arrow) and laterally between neighboring CBs (vertical arrow; Figure 4.5E). In embryos devoid of all maternal and

zygotic contributions of Talin, this mislocalization phenotype was more severe, as Prc surrounded numerous CBs (arrow) and was absent from much of the basal CB surface (arrowhead; Figure 4.5F). This phenotype enhancement upon loss of maternal Talin is consistent with Talin being required for CB-pericardial adhesion, a process for which maternal Talin is sufficient (Figure 4.3). In contrast, maternal Talin is not sufficient to properly establish the ECM along the lumen-forming apical surface, as LanA is reduced and Prc fails to be excluded in *rhea* zygotic mutant embryos.

Since Talin also mediates the integrin-adhesome link, we assessed the localization pattern of Pinch and Cbl-associated protein (CAP), two cytoplasmic proteins recruited by Talin to integrin-mediated muscle attachment sites in *Drosophila* (Clark *et al.* 2003, Zervas *et al.* 2011, Bharadwaj *et al.* 2013). In *Drosophila* musculature, CAP is not present at initial sites of integrin adhesion, but is gradually recruited to muscle attachment sites (Bharadwaj *et al.* 2013). Furthermore, larval, but not embryonic, musculature is disrupted in *cap* mutants (Bharadwaj *et al.* 2013). Thus, CAP is likely involved in integrin adhesion stabilization or maintenance, but not initial assembly. Similarly, during early stages of heart cell migration, CAP immunolabel is initially weak, but increases as heart development proceeds (data not shown). By late stage embryogenesis, punctate accumulations of CAP line the basal and apical CB surface (Figure 4.5I). This punctate pattern overlaps with Talin immunolabel, but is more restricted (Appendix C.3), suggesting that Talin is not sufficient to recruit CAP. In addition, CAP localization is not sensitive to reduced Talin levels: in *rhea* zygotic mutants, the punctate apical and basal pattern of CAP

remains, despite perturbations in the heart itself (Figure 4.5J). In contrast, Pinch localization is dependent on Talin. Pinch, encoded by *Drosophila steamerduck* (*stck*), functions together with Integrin linked kinase (ILK) and Parvin (the IPP complex) to maintain adhesion between muscles and the epidermal tendon cells and to maintain an organized actin cytoskeleton at these adhesion sites during embryogenesis (Clark *et al.* 2003, Vakaloglou *et al.* 2012). In the *Drosophila* heart, Pinch is recruited to sites of integrin and Talin, accumulating most prominently along the apical and basal CB surfaces (Figure 4.5G; Clark *et al.* 2003). This recruitment is Talin dependent; in *rhea* zygotic mutants, Pinch is no longer restricted in its localization, but is found more diffusely around each CB (Figure 4.5H). This Talin-dependent heart pattern is more sensitive than in embryonic muscles, as maternal Talin was sufficient for Pinch recruitment to muscle attachment sites (Zervas *et al.* 2011). Taken together, it appears that ECM factors and core cytosplasmic adhesome proteins are dependent on Talin for proper localization patterns, although CAP, a protein required for adhesion stabilization, is not as sensitive.

4.2.5 Loss of Talin disrupts cardioblast polarity

Since Talin is required for correct localization of integrin-related factors within the heart, we wondered if Talin was essential for other aspects of heart cell polarity as well. Several labs, including our own, have established a critical role for the apicalization of Slit and Robo in generating a non-adherent luminal membrane surface (MacMullin and Jacobs 2006; Medioni *et al.* 2008). We have further shown that this apicalization is disrupted in

scb (αPS3) or *mys* (βPS) integrin mutants (3.3.1). In wildtype embryos, both Slit and Robo localize along the apical midline surface of the CBs (arrows) and are excluded from the lateral domains in stage 17 embryos (Figure 4.6A, D). In contrast to this, both zygotic and GLC *rhea* mutant embryos have a disrupted Slit and Robo pattern; rather than a continuous localization along the apical CB surface, Slit and Robo accumulate in small lateral pockets between two neighboring CBs (arrowheads) or apically at the site of intersection between four cells (arrows, Figure 4.5 B, C, E, F). Similar to Robo, the transmembrane Dystroglycan (Dg) receptor is present along the apical CB surface in wildtype embryos (arrows, Figure 4.7A, C). However, it is largely excluded from this region in *rhea* mutant embryos and is rather detected in small lateral accumulations and apically only at tetra-cellular intersections (arrows; Figure 4.7B, D). Importantly, Dg localization does not overlap with the junctional marker Discs-large (Dlg) in either wildtype or mutant embryo hearts. In frontal images of the heart in wildtype embryos, Dlg does not colocalize with Dg at the midline, but is primarily found along the lateral adhesions between neighboring CBs (Appendix C.4A; Medioni *et al.* 2008). In contrast, in *rhea* mutants, Dlg is observed along the midline between the contralateral CB rows (Appendix C.4B). Furthermore, it is excluded from the ectopic Dg-rich lateral sites suggesting these are pockets lacking neighboring cell adhesion (arrows, Appendix C.4B, C). Thus ectopic Dg lateral pockets are reminiscent of the Dg-rich midline CB surface along which a lumen forms in wildtype embryos. Consistent with this, Slit and Robo, required for an open luminal space at the midline, colocalize with the ectopic Dg lateral accumulations in *rhea*

Figure 4.6 – Talin is required for continuous midline localization of Slit and Robo

In wildtype embryos, Robo (**A**) and Slit (**D**) localize apically, along the midline between the cardioblasts rows (arrow). *rhea* mutant embryos are characterized by a loss of apical Robo and Slit, with punctate accumulations detected laterally or at the site of tetra-cellular intersections (arrowheads, **B, E**). Although the overall heart structure is more severely disrupted in *rhea* germ-line clone embryos, the punctate Robo and Slit accumulations are similar to those in zygotic mutants (**C, F**). Calibration: 10 microns.

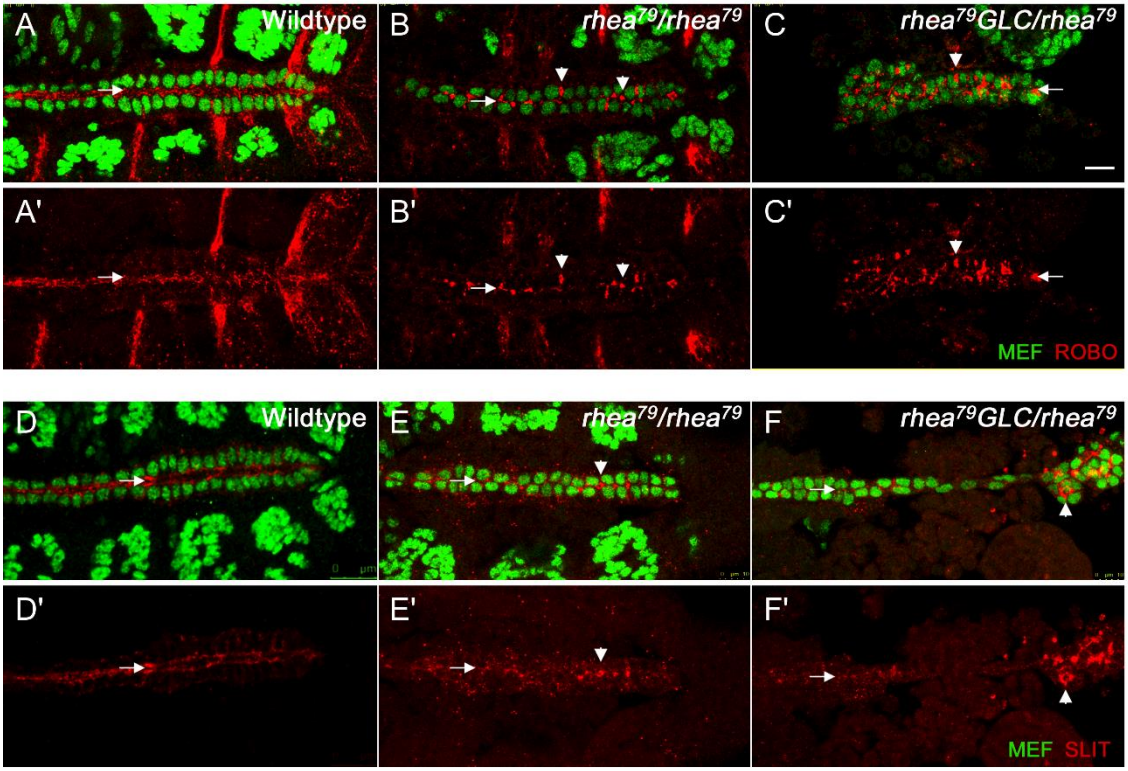
A
Wildtype
B
rhea79/rhea79
C
rhea79GLC/rhea79
A'
B'
C'
MEF ROBO
D
Wildtype
E
rhea79/rhea79
F
rhea79GLC/rhea79
D'
E'
F'
MEF SLIT

Figure 4.7 – *rhea* mutants have ectopic lateral accumulations of characterized luminal markers

Dystroglycan and Robo or Slit double-labeled stage 17 wildtype (**A, C**) or zygotic *rhea* mutant (**B, D**) embryos. Slit and Robo overlap with the membrane-bound Dg receptor along the heart midline in wildtype embryos. Embryos lacking zygotic Talin have Dg-rich ectopic open pockets which overlap with the lateral punctate accumulations of Slit and Robo. In all panels, right panels are enlarged images of framed sections on the left. Double-primed (") images were edited to enhance the detected signals; yellow indicates red-green signal overlap. Vertical arrows point to lateral or tetra-cellular Dg pockets, while horizontal arrows indicate normal midline accumulations. Calibration: 10 microns.

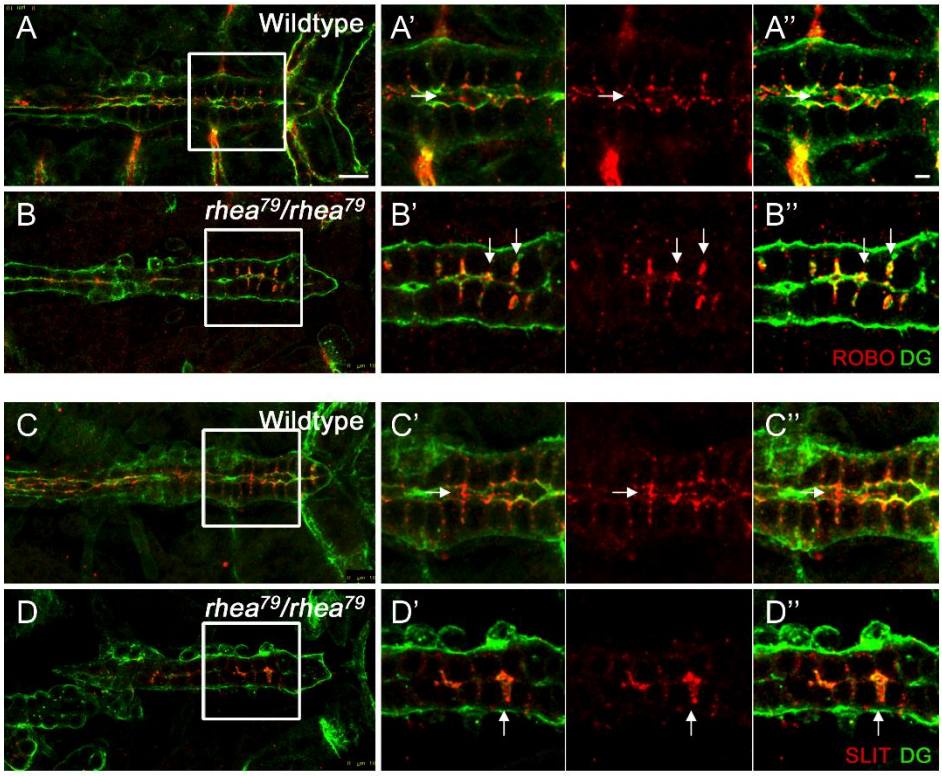
A
Wildtype
A'
A''
B
rhea79/rhea79
B'
B''
ROBO DG
C
Wildtype
C'
C''
D
rhea79/rhea79
D'
D''
SLIT DG

mutants (Figure 4.7B, D). Taken together, it appears that Talin, similar to αPS3βPS1 integrin (3.3.1), is not required for Slit and Robo expression, but is required to restrict these known luminal determinants to the apical CB surface.

4.2.6 Talin is required for formation of an open lumen

During *Drosophila* heart tube formation, CBs gain several polarized domains, including an apical luminal surface enclosed by two junctional regions and an abluminal basal domain. In the absence of Slit-Robo or integrin signaling, this polarity is disrupted and an open lumen does not form (Qian *et al.* 2005, MacMullin and Jacobs 2006, Medioni *et al.* 2008, Santiago-Martinez *et al.* 2008, Chapter 3). Since *rhea* mutants have disrupted localization not only of βPS1 integrin, but also of Slit and Robo, it is likely that Talin is required for proper heart tubulogenesis. Initial assessment of frontal images of the heart demonstrated a reduced space between the contralateral CB rows in *rhea* mutant embryos, suggesting a small or absent lumen (arrows, Figure 4.3). This was apparent both in zygotic (Figure 4.3B-D) and GLC *rhea* mutant embryos (Figure 4.3E). Furthermore, as noted above, this reduced space was accompanied by Dlg lining the midline and a loss of apical Dg (Figure 4.7 B, D, Appendix C.3).

To directly test if Talin is required for lumen formation, transverse images of the heart were acquired in *rhea* mutant embryos (Figure 4.8). In wildtype embryos, along the heart midline (arrow) the lumen boundaries were clearly demarcated by Dg immunolabel (green) while small dorsal and ventral regions of adhesion enclosing the lumen were

marked with Dlg (red, Figure 4.8A). Dg also outlined most of the basal CB surface as well as flanking pericardial cells. In *rhea* zygotic mutants, CBs were still clearly outlined by Dg. Consistent with the lateral open pockets observed in frontal images of *rhea* mutant embryos, ectopic pockets of Dg were detected within the CBs, presumably near the lateral cell membrane (eg. arrowhead in Figure 4.8E). However, no open luminal space was observed between contralateral CBs, but rather the midline was marked by a continuous adherent region (arrow; Figure 4.8B-E). Embryos lacking both maternal and zygotic Talin similarly did not exhibit an open lumen between CBs at the midline (Figure 4.8F, G). However, careful analysis of the heart was hindered by gross developmental defects, often leaving the embryo dorsal surface without an overlying ectoderm (Figure 4.8F), with residual and disorganized amnioserosa cells, and cardial cell clumping (Figure 4.8G). Maternally contributed Talin rescues these processes, as these ectoderm and amnioserosa defects are rare in zygotic mutants. However, importantly, maternal Talin is not sufficient for proper CB polarity nor lumen formation, facilitating a study of the role of Talin during tubulogenesis in zygotic *rhea* mutant embryos.

4.2.7 Talin is required during cardioblast migration

In both *in vitro* and *in vivo* models of tubulogenesis, an early luminal or apical membrane initiation site (AMIS) has been identified prior to establishment of the open lumen itself (1.2.2; Bryant et al 2010, Tawk *et al.* 2007). Similarly, prior to lumen enclosure during *Drosophila* cardiogenesis, the migrating CBs establish a pre-luminal domain marked

Figure 4.8 – *rhea* mutants lack an open lumen between opposing cardioblast rows

Transverse images of the heart in stage 17 embryos. Dystroglycan (green) outlines the cardioblasts basal and luminal surfaces, but is excluded from junctional domains. At the midline (arrowheads), Discs-large (red) labels the junctional domains between opposing cardioblasts and also outlines the overlying ectoderm. Wildtype embryos (**A**) have a circular open lumen (outlined by Dg) at the midline, sealed by dorsal and ventral junctions (in red, above and below the lumen). In contrast, *rhea* mutants lack an open lumen, but have an extended junctional domain (Dlg) at the midline between opposing cardioblasts (**B-G**). Germ-line clone mutant embryos additionally have ectoderm and amnioserosa defects (**F, G**). Arrowheads identify ectopic lateral mini-lumens. Calibration: 10 microns.

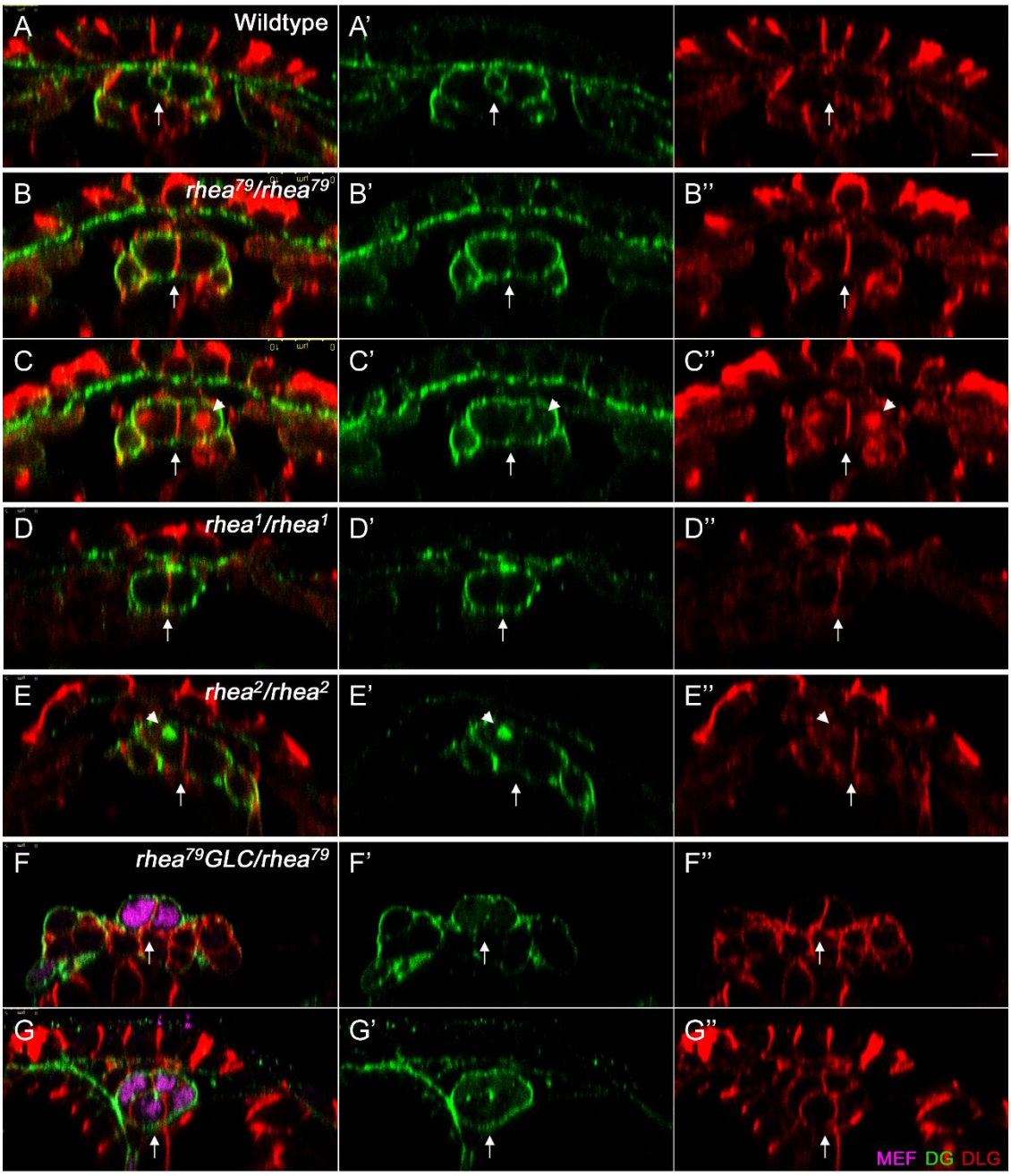
A
Wildtype
A'
B
rhea79/rhea79
B'
B''
C
C'
C''
D
rhea1/rhea1
D'
D''
E
rhea2/rhea2
E'
E''
F
rhea79GLC/rhea79
F'
F''
G
G'
G''
MEF DG DLG

by βPS1 integrin (3.3.3) and Talin (Figure 4.2H-J). Since Talin is required for development of a single, continuous midline lumen, we hypothesized that it may also be required for earlier establishment of CB polarity. It addition to the pre-luminal accumulation of integrin and Talin, CB migration is marked by several other defining polarization events, including a dynamic membrane leading edge (Figure 4.9) and changes to the CB morphology (Figure 4.10).

During the latter stages of CB migration, the CBs extend highly dynamic membrane processes towards the dorsal midline (Syed, 2012). These leading edge membrane protrusions, characteristic of migrating cells (reviewed by Ridley 2011), can be visualized using fluorescently tagged moesin, an actin-plasma membrane cross-linker protein (Millard and Martin 2008). CBs in wildtype and heterozygous *rhea* embryos rapidly extend and retract numerous filopodia (arrows, Figure 4.9A, D). In contrast, embryos lacking zygotic or maternal and zygotic Talin have reduced leading edge activity: fewer filopodia are generated and there are regions of membrane quiescence (asterisks, Figure 4.9B, C, D). Notably, although reduced, there is some membrane activity even in GLC *rhea* mutants, suggesting that there may be partially redundant or compensating factors, in addition to Talin, that promote leading edge activity.

In addition to extending dorsal membrane processes, migratory CBs also begin a dynamic morphogenesis required for complete enclosure of the lumen (Medioni *et al.* 2008). As dorsal closure commences, the increasingly triangular-shaped migrating CBs follow the leading ectodermal cells, protruding dorsally towards the midline (Figure

Figure 4.9 – Talin is required for maximal membrane leading edge activity

Part 1 - Live imaging of the cardioblast leading edge visualized with *dMEF-Gal4* regulated *UAS-moesin-mCherry* (red) and cardiac nuclei marker *tup-GFP* (green). In wildtype embryos (**A**), numerous filopodial protrusions are extended towards the midline (arrows) and they dynamically extend and retract as the cardioblasts migrate (compare processes at 0, 14, and 28 minutes). In *rhea* zygotic (**B**) or germ-line clone (**C**) mutant embryos, there are fewer protrusions extended towards the midline (arrows) and large regions of membrane quiescence (asterisks). Posterior is to the right in all images. Calibration: 15 microns.

Part 2 (D) - Quantification of the number of filopodial extensions per six-cell segment of the heart proper in each genotype listed. *rhea* heterozygotes have a similar number of filopodia per segment to wildtype (yw) embryos, while *rhea* zygotic and germ-line clone mutant embryos have fewer filopodia. Since the number of filopodia increase as the distance to the midline decreases (Syed, 2012), only segments within 13µm of the midline were scored. Numbers within each column designate sample size in number of segments. P-values were calculated using an unpaired t-test (*$p<0.01$, **$p<1.0x10^{-13}$; blue * compared to yw, red * compared to heterozygotes). Plus-minus bars represent standard deviation.

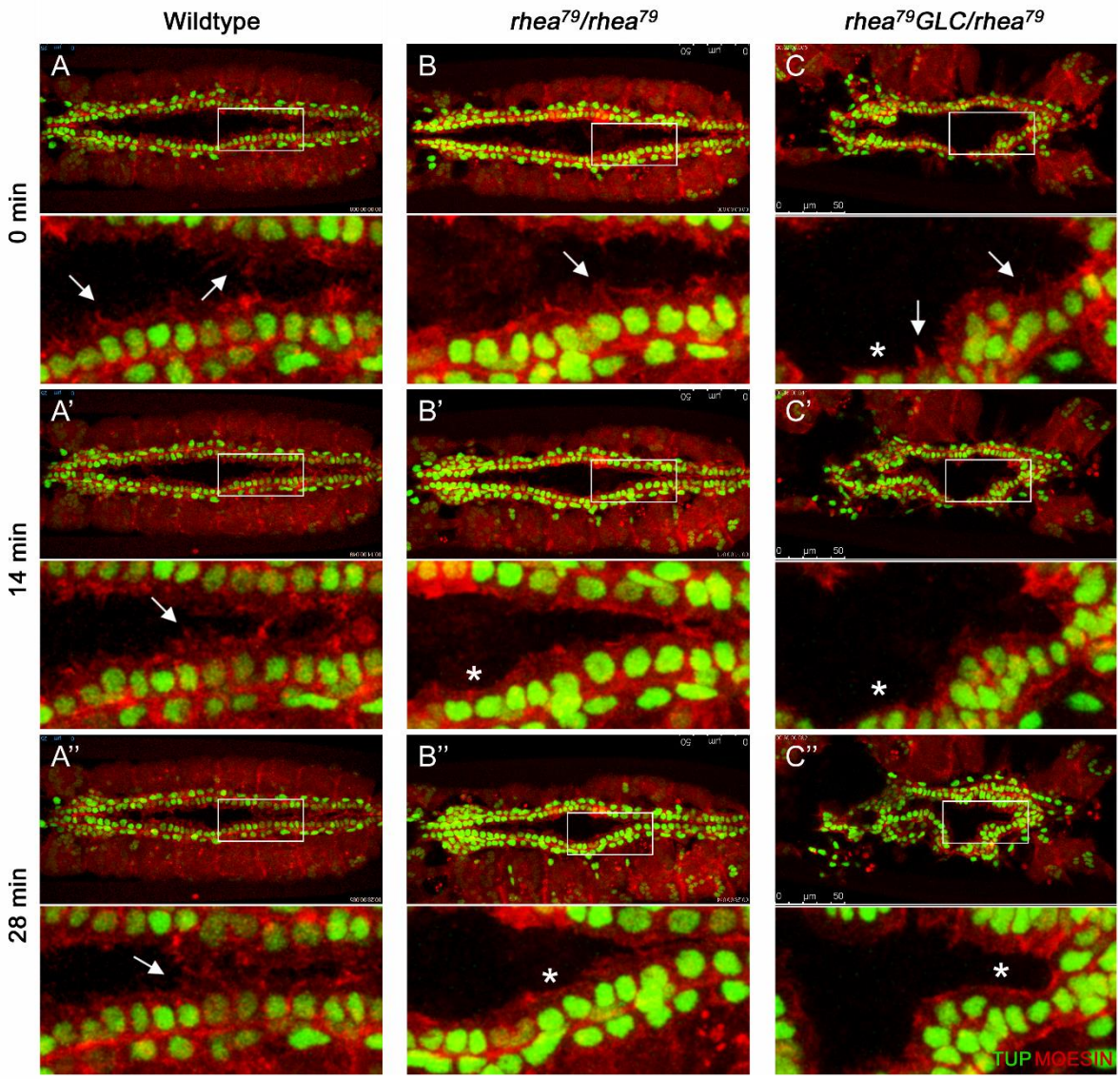
Wildtype
rhea79/rhea79
rhea79GLC/rhea79
0 min
14 min
28 min
A
B
C
A'
B'
C'
A''
B''
C''
TUP MOESIN

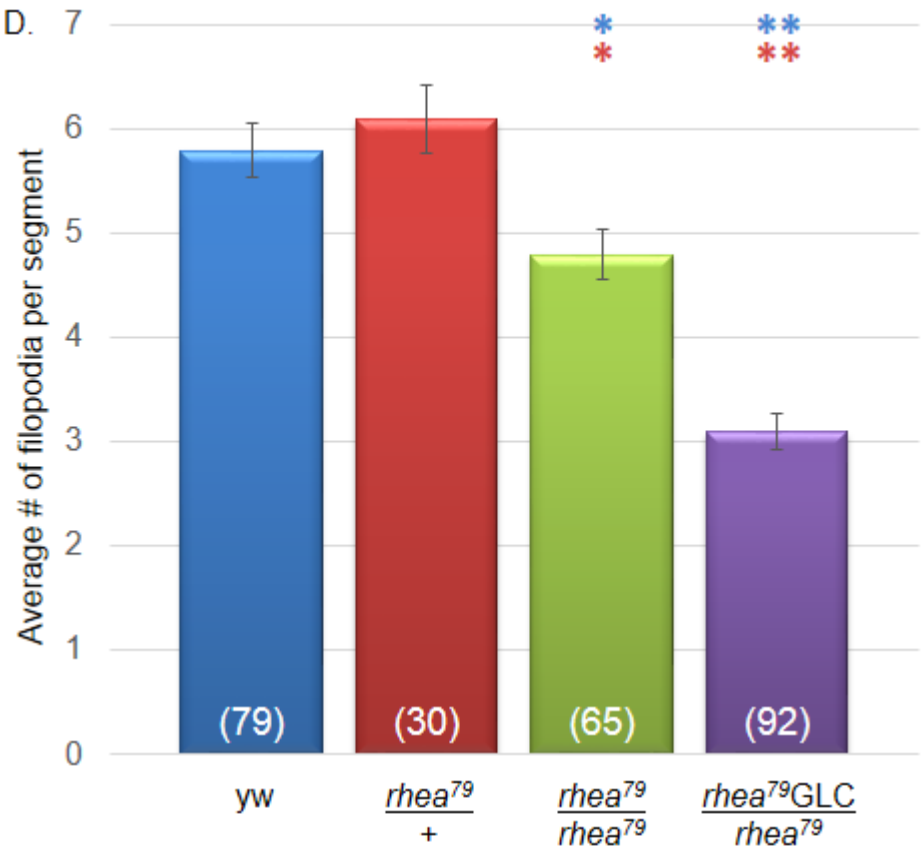
D.
Average # of filopodia per segment
0
1
2
3
4
5
6
7
(79)
(30)
(65)
(92)
yw
rhea79 / +
rhea79 / rhea79
rhea79GLC / rhea79

Figure 4. 10 – Cardioblasts in *rhea* mutant embryos undergo aberrant morphogenesis during migration

Transverse images of the dorsal midline at stage 15, stage 16, and early and late stage 17 of embryogenesis. In wildtype embryos (**A-A'''**), migrating CBs become triangular-shaped and extend dorsally towards the midline (stage 15, 16), eventually adhering (stage 17a) and enclosing a lumen (stage 17b). Early in migration, CBs in *rhea* zygotic mutants frequently adopt a triangular shape similar to those in wildtype embryos (**B-B'**). However, rather than continue to extend a narrow dorsal protrusion towards the midline, CBs in *rhea* zygotic mutants are typically more rounded (**B'** and **B''**) and contact contralateral partners along a large dorsal region (**B''**). Following migration, the CBs do not adopt a crescent shape to enclose a lumen (**B'''**). In germ-line clone rhea mutant embryos (**C-C'''**), the CBs are abnormally shaped throughout migration and no lumen forms at the midline. MEF identifies the CB nuclei (magenta, C panels only) while Dystroglycan (green) outlines their shape. Discs-large (red) highlights the ectoderm (ec) and amnioserosa (as), as well as the cardioblast junctions at stage 17. Arrowheads indicate the midline. Dorsal is to the top in all panels. Calibration: 10 microns.

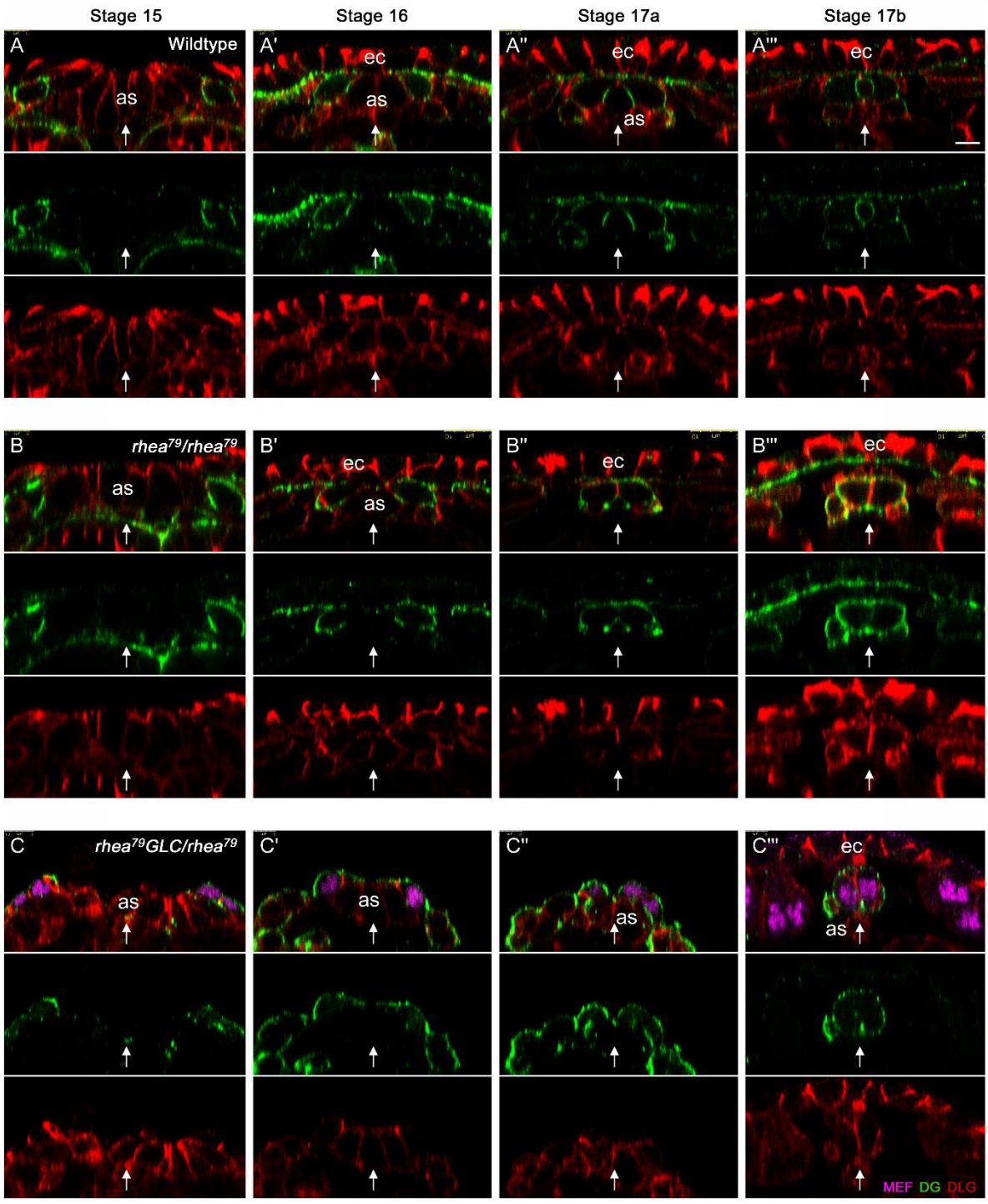
Stage 15
Stage 16
Stage 17a
Stage 17b
A
Wildtype
A'
A"
A'"
B
rhea79/rhea79
B'
B"
B'"
C
rhea79GLC/rhea79
C'
C"
C'"
ec
as
MEF DG DLG

4.10A). Once dorsal closure completes, the CBs migrate between the ectoderm and the internalizing amnioserosa and adhere dorsally to the opposing CBs (Figure 4.10A'-A''). Following the initial dorsal attachment, the CBs adopt a crescent shape and adhere ventrally to fully enclose the lumen (Figure 4.10A'''). In GLC *rhea* mutant embryos, this entire process is disrupted. As previously documented (Brown *et al.* 2002b, Ellis *et al.* 2011), dorsal closure and the internalization of the amnioserosa are abnormal in maternal and zygotic *rhea* mutants (Figure 4.8F, G, Figure 4.10C-C'''). Furthermore, the CBs do not adopt the expected triangular shape extending towards the midline and do not have a Dg-rich pre-luminal domain (Figure 4.10C-C'''). This suggests that Talin is required for these aspects of CB polarization during migration. However, it is possible that these polarization defects are not heart cell specific, but are caused indirectly by the dorsal closure failure. Indeed, the CBs in *rhea* zygotic mutant embryos do adopt a triangular shape similar to that observed in wildtype (Figure 4.10B, B'), and it is only during the latter stages of CB morphogenesis that the process is disrupted (Figure 4.10B'', B'''). Following migration, CBs in zygotic mutants frequently form a larger dorsal attachment site and do not become crescent shaped (Figure 4.10B''), but rather form a continuous dorsal to ventral adhesion between opposing CB rows (Figure 4.10B'''). However, it remains unclear whether Talin is not required for the early shape changes or, rather, if maternal Talin is sufficient for the earlier, but not culminating, structural cell changes required for tubulogenesis.

4.2.8 *rhea*^{79} interacts genetically with mutations in genes for integrin adhesion

In *Drosophila*, many essential genes are sufficient when present in a single copy. For example, flies heterozygous for null alleles of *slit* or *scb* (*αPS3*) are viable and fertile. However, these animals are sensitive to a reduced dosage of genes that act in the same, or a converging, pathway (MacMullin and Jacobs 2006, 3.3.5). For example, halving the gene dosage of both *slit* and *scb* in the same embryo results in abnormal nervous system and heart development (Stevens and Jacobs 2002, MacMullin and Jacobs 2006). Similarly, *rhea* heterozygotes are viable, are fertile, and have normal heart development (Figure 4.11A). However, embryos with a single gene copy of both *rhea* and *scb* have disrupted heart development, consistent with Talin and integrins functioning together in this process; these doubly heterozygous embryos exhibit a reduced space between CB rows and frequent blistering or puckering of the seven-up CBs (Figure 4.11E). These phenotypes were quantified using a blind scoring system (Figure 4.11H, I). Similar defects were observed in embryos doubly heterozygous for *rhea* and the ECM *lanA* gene, further highlighting a role for Talin in mediating integrin-ECM adhesion during heart development (Figure 4.11C, H, I). In contrast, this genetic dosage approach was not sensitive to genes encoding cytoplasmic factors. *rhea* heterozygotes with reduced gene copies of *ilk* or both *robo1* and *lea* (*robo2*) have normal heart development, with few embryos exhibiting reduced luminal space or blisters (Figure 4.11D, F, H, I). As Talin is required for proper localization of both Robo and the ILK-interacting Pinch, it is unlikely that *rhea* and *ilk* or *robo* do not work together to mediate heart development. Rather, it may reflect a

Figure 4.11 – *rhea*^{79} interacts with mutations in genes encoding integrin-related proteins

Cardioblasts at stage 17 are visualised in embryos zygotically and maternally heterozygous for both *rhea*^{79} and zygotically heterozygous for an interacting gene (termed transheterozygotes)

Part 1. Qualitative analysis - Embryos singly heterozygous for *rhea*^{79} have normal heart assembly (**A**), while *rhea*^{79} homozygotes are characterized by a reduced space between cardioblast rows (**B**). If *rhea*^{79} heterozygotes additionally have reduced gene dosage of αPS3 integrin (*scb*^{2}, **E**) or Laminin (*lanA*$^{9\text{-}32}$, **C**), heart defects are observed (including seven-up cell blisters, asterisks, and disruptions in alignment). Embryos doubly heterozygous for *rhea* and alleles of *ilk* (*ilk*^{1}) or both *robo1* (*robo*^{1}) and *robo2* (*lea*$^{54\text{-}14}$) have few disruptions in heart assembly (**D, F**). Calibration: 10 microns.

Part 2. Quantitative analysis - Average lumen size (**H**) and the number of seven-up cell blisters per embryo (**I**). *rhea*^{79} homozygotes and *rhea*^{79} heterozygotes with a reduction in *lanA* or *scb* gene dosage had significantly reduced average lumen size, and the latter two genotypes also had frequent blistering of the seven-up cells. Numbers within each column designate number of embryos scored. P-values were calculated using the non-parametric Mann-Whitney U test (*$p<0.05$, ** $p<0.000001$ from *rhea*^{79}/+). Error bars represent standard deviation.

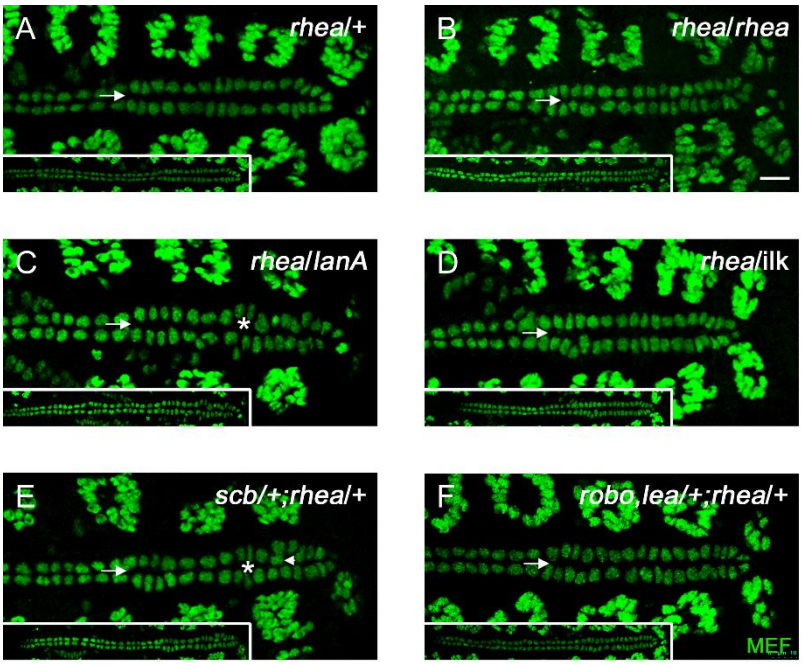
A
rhea/+
B
rhea/rhea
C
rhea/lanA
D
rhea/ilk
E
scb/+;rhea/+
F
robo,lea/+;rhea/+
MEF

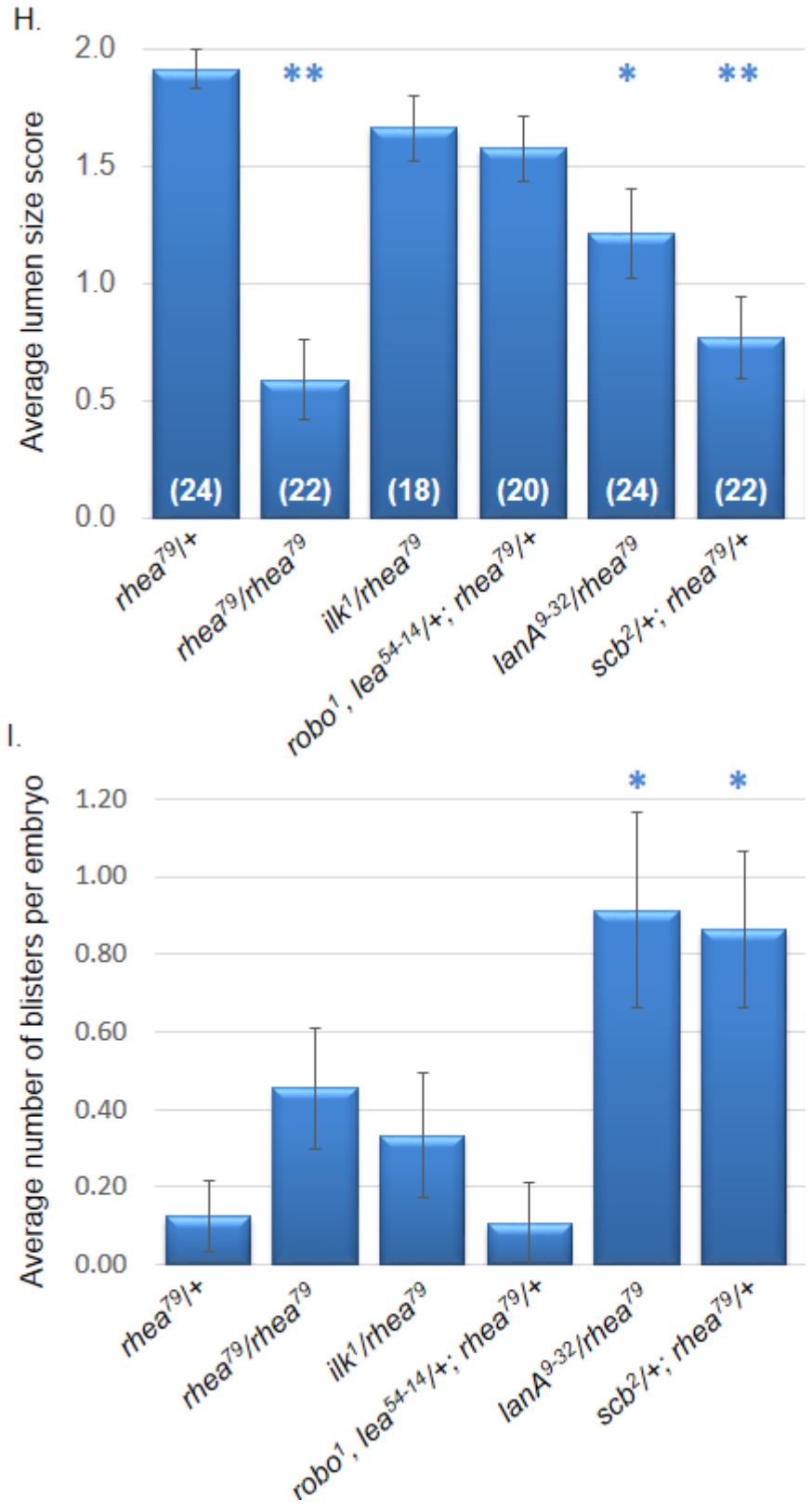
H.
Average lumen size score
2.0
1.5
1.0
0.5
0.0
**
*
**
(24)
(22)
(18)
(20)
(24)
(22)
rhea79/+
rhea79/rhea79
ilk1/rhea79
robo1, lea54-14/+; rhea79/+
lanA9-32/rhea79
scb2/+; rhea79/+
I.
Average number of blisters per embryo
1.20
1.00
0.80
0.60
0.40
0.20
0.00
*
*
rhea79/+
rhea79/rhea79
ilk1/rhea79
robo1, lea54-14/+; rhea79/+
lanA9-32/rhea79
scb2/+; rhea79/+

high sensitivity threshold for this assay. Therefore, although this approach was initiated with hopes of using it to identify cytoplasmic downstream mediators of Talin function, its effectiveness was limited to confirming previously established interactions between Talin and integrin-ECM adhesion.

4.2.9 Neither IBS1 nor IBS2 mediated integrin binding is essential for Talin's role in tubulogenesis

In *Drosophila* and vertebrates, Talin binds to integrin via two distinct binding sites. *In vivo* studies in *Drosophila* suggest that these two sites are partially redundant, as either site is sufficient to bind to integrin and knockout of either IBS1 or IBS2 produces less severe phenotypes than a double knockout (Tanentzapf and Brown 2006, Ellis *et al.* 2011). However, these sites are not fully redundant, as, for example, IBS2 but not IBS1 is required for dynamic developmental events such as germ-band retraction and dorsal closure (Ellis *et al.* 2011). Therefore, we sought to determine if heart development requires both of the integrin binding sites, or if either is sufficient during this morphogenetic event.

$Talin^{IBS1-}$ and $Talin^{IBS2-}$ are present in high levels in zygotic $rhea^{79}$ mutant embryos

To assess the importance of each of the integrin binding sites, we utilized ubiquitously expressed Talin transgenes (under control of the *ubiquitin-E* promoter) that had mutations designed to abrogate the integrin-binding function of each site (Figure 4.1B; constructed and validated by Tanentzapf and Brown 2006 and Ellis *et al.* 2011).

When expressed in zygotic *rhea* mutant embryos, wildtype Talin ($Talin^{WT}$), the IBS1 mutant $Talin^{R367A}$ ($Talin^{IBS1-}$), and the IBS2 mutant $Talin^{KS>DD}$ ($Talin^{IBS2-}$) were detected in abundance, at levels above those of endogenous Talin in *rhea* heterozygotes (Figure 4.12). In contrast, *rhea* zygotic mutant strains with the IBS2 mutant $Talin^{LI>AA}$ ($Talin^{IBS2b-}$) or with an IBS1 and IBS2 double mutant $Talin^{R367A, LI>AA}$ ($Talin^{IBS1- IBS2-}$) were detected at levels similar to those in *rhea* zygotic mutants, suggesting little or no ectopic protein was present (Figure 4.12). It is possible that the lack of detectable protein is due to a breakdown or contamination of the original strain, as Ellis *et al.* found relatively comparable protein levels using all these transgenes (Ellis *et al.* 2011). However, as two independent $Talin^{IBS1- IBS2-}$ strains were tested, this is unlikely for this particular construct. Rather, it is possible that since $Talin^{IBS1- IBS2-}$ is unable to bind to integrins, it is unstable and rapidly degraded. The apparent discrepancy with Ellis *et al.* (2011) may be explained by a difference in experimental set-up: protein levels were quantified by Ellis *et al.* in adult flies expressing both endogenous and ectopic Talin (2011), perhaps suggesting that $Talin^{IBS1- IBS2-}$ is stabilized in the cytoplasm by endogenous Talin. Indeed, although detected in whole adult flies, when analyzed within embryonic tissues, $Talin^{IBS1- IBS2-}$ was not highly enriched at sites of integrin adhesion in muscles or the ectoderm (Ellis *et al.* 2011).

Although $Talin^{IBS1-}$ and $Talin^{IBS2-}$ protein was detected at high levels in whole embryos, to confirm the protein was present in the heart itself and localizing properly, immunolabel experiments were used to mark Talin within the developing embryo (Appendix C.5). In zygotic $rhea^{79}$ embryos, $Talin^{WT}$ localized to the apical and basal CB

Figure 4.12 – Expression levels of transgenic talin rescue constructs

Talin transgenic protein levels determined by western blot. Lysate from stage 17 embryos were probed with two independent Talin antibodies. *rhea*^{79} mutant embryos expressing full-length wildtype Talin or Talin with modified IBS1 (R267A, Talin^{IBS1-}) or IBS2 (KS>DD, Talin^{IBS2-}) domains had similar high levels of Talin, above those detected in *rhea* heterozygous embryos. In contrast, embryos expressing transgenes harbouring mutations in both IBS1 and IBS2 (Talin$^{IBS1- IBS2-}$) or a single LI>AA mutation in the IBS2 (Talin^{IBS2b-}) had low levels of Talin, similar to those detected in *rhea* zygotic mutants. Graphs are averages of three to four western blots, with band pixel intensity (density) used as a proxy of protein level. βTubulin (βTub) was used an a loading control. All densities are relative to *rhea*^{79}/+ Talin levels. Error bars represent standard deviation.

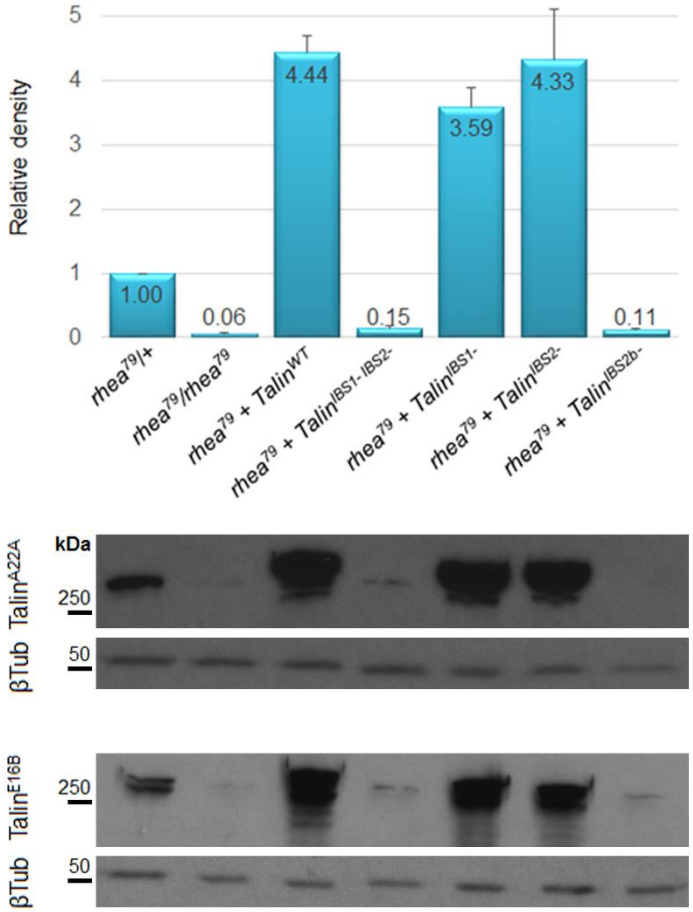
Relative density
5
4
3
2
1
0
1.00
0.06
4.44
0.15
3.59
4.33
0.11
rhea79/+
rhea79/rhea79
rhea79 + TalinWT
rhea79 + TalinIBS1-IBS2-
rhea79 + TalinIBS1-
rhea79 + TalinIBS2-
rhea79 + TalinIBS2b-
kDa
TalinA22A
250
βTub
50
TalinE16B
250
βTub
50

surfaces (Appendix C.5B), similar to endogenous Talin in wildtype embryos (Figure 4.3). A similar pattern was seen in embryos expressing Talin^{IBS1-} and Talin^{IBS2-} (Appendix C.5C, D). In contrast, minimal Talin was present in the heart in *rhea*^{79} strains with Talin$^{IBS1- IBS2-}$ or Talin^{IBS2b-}. These results are consistent with Talin recruitment in the embryonic ectoderm during germ-band retraction and leading edge epidermis during dorsal closure: in these tissues Talin^{IBS1-} and Talin^{IBS2-}, but not Talin$^{IBS1- IBS2-}$, were detected in a similar pattern to Talin^{WT} (Ellis *et al.* 2011). Taken together, these data suggest that either binding site is sufficient to recruit Talin to sites of integrin adhesion in the developing heart.

Either of Talin's integrin-binding sites is sufficient to stabilize β*PS1 integrin in the heart*

Since both IBS1 and IBS2 are capable of binding to integrin (García-Alvarez *et al.* 2003, Rodius *et al.* 2008, Ellis *et al.* 2011), I hypothesized that either Talin^{IBS1-} or Talin^{IBS2-} would be sufficient for normal βPS1 localization in the *Drosophila* embryonic heart. In wildtype embryos or zygotic *rhea* mutants expressing the *talin*^{WT} transgene, βPS1 was localized along the apical CB surfaces with lower levels basally (Figure 4.4A, 4.13B). Similar to zygotic *rhea* mutants (Figure 4.13A), mutants with Talin$^{IBS1- IBS2-}$ or Talin^{IBS2b-} had little βPS1 immunolabel in the heart, with none or low levels detected apically (Appendix C.6A, C). However, Talin lacking either IBS1 or IBS2 was sufficient to stabilize βPS1 along the apical and basal CB domains (Figure 4.13C, D), suggesting that IBS1 and IBS2 are functionally redundant in this capacity.

Figure 4.13 - Either of Talin's integrin-binding-sites is sufficient to stabilize βPS integrin in the heart

Cardioblast position and βPS1 localization in stage 17 zygotic *rhea* null embryos ubiquitously expressing no rescue construct (**A**), wildtype Talin (**B**), or Talin with a non-functional IBS1 (**C**) or IBS2 (**D**). In contrast to the tight juxtaposition of the contralateral cardioblasts in zygotic *rhea* null embryos (arrow in **A**), the cardioblast rows in rescued embryos maintained an open space along the heart midline (arrows in **B, C**, and **D**). All three of the rescue constructs were sufficient for a strong and continuous distribution of βPS1 along the cardioblast apical surfaces (arrows). All βPS label was imaged using identical settings. Calibration: 10 microns.

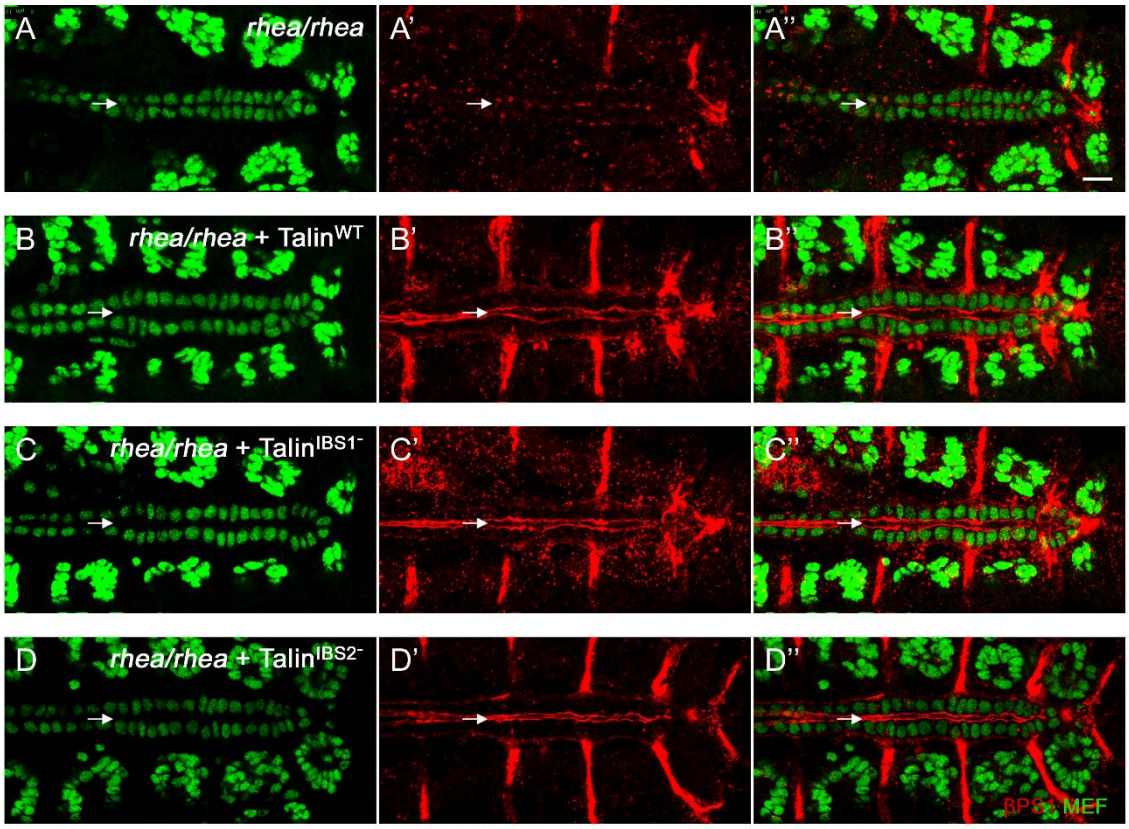
A
rhea/rhea
A'
A''
B
rhea/rhea + TalinWT
B'
B''
C
rhea/rhea + TalinIBS1-
C'
C''
D
rhea/rhea + TalinIBS2-
D'
D''
BPS1 MEF

Talin^{IBS1-} and Talin^{IBS2-} can mediate integrin-dependent lumen formation

In the *Drosophila* embryonic musculature, both Talin^{IBS1-} and Talin^{IBS2-} were essential for the strong integrin adhesions required during muscle contractions, although either was adequate for initial localization of ECM and integrin adhesome components (Tanentzapf and Brown 2006, Ellis *et al.* 2011). However, in the dramatic germ-band retraction and dorsal closure processes requiring rapidly changing integrin adhesions, Talin's IBS2 domain, but not IBS1, was sufficient for normal development (Ellis *et al.* 2011). In *Drosophila* heart development, although the Talin-marked early luminal domain remains throughout cardial cell migration, the CBs undergo a dynamic morphogenesis and become increasingly polarized. Therefore, I hypothesized that similar to germ-band retraction and dorsal closure, heart tubulogenesis would require IBS2, but not the strong-adhesion mediating IBS1. To test this, the ability of the heart to form an open tube was assessed in embryos in which endogenous zygotic Talin was replaced with ectopic full length Talin or Talin with abrogated integrin binding (Figure 4.14, Appendix C.6). Consistent with Talin being required for lumen formation, ectopic Talin^{WT} was able to rescue the loss-of-lumen phenotype of *rhea* zygotic mutant embryos. Whereas *rhea* mutants had continuous Dlg-rich adhesion between opposing CBs, those expressing Talin^{WT} had an open lumen lined with Dg (Figure 4.14A, B). The average luminal width in Talin^{WT} rescued embryos was significantly greater than in *rhea^{79}* homozygotes (Figure 4.14E).

Figure 4.14 - Talin^{IBS1-} and Talin^{IBS2-} can mediate integrin-dependent lumen formation

Part 1 - Transverse images of the heart in stage 17 zygotic *rhea* null embryos ubiquitously expressing no rescue construct (**A**), wildtype Talin (**B**), or Talin with a non-functional IBS1 (**C**) or IBS2 (**D**). Dg (green) outlines the cardioblasts basal and luminal surfaces, but is excluded from junctional domains. At the midline (arrowheads), Dlg (red) labels the junctional domains between opposing cardioblasts and also outlines the overlying ectoderm. In contrast to the loss-of-lumen phenotype in zygotic *rhea* null embryos, embryos expressing Talin^{WT}, Talin^{IBS1-}, or Talin^{IBS2-} have an open Dg-lined lumen and junctional regions restricted to small dorsal and ventral contact sites (above the vertical arrows in **B**, **C**, and **D**). Talin transgenes are tagged with GFP (**B'**, **C'**, and **D'**). Dorsal is to the top in all panels. Calibration: 5 microns.

Part 2 - Average lumen size (**E**) as scored from frontal images of the heart (eg. as Figure 4.13), and the number of seven-up cell blisters per embryo (**F**). zygotic *rhea* null embryos ubiquitously expressing Talin^{WT}, Talin^{IBS1-}, or Talin^{IBS2-} had significantly higher average lumen scores than those without rescue construct expression (**E**). Although no statistically significant difference was apparent, compared to *rhea* heterozygous embryos a consistent trend of increased seven-up cell blistering was observed in rescued embryos ubiquitously expressing the Talin constructs (**F**). Numbers within each column designate number of embryos scored. P-values were calculated using the non-parametric Mann-Whitney U test (*$p<0.05$, ** $p<0.01$ from $rhea^{79}/rhea^{79}$). Error bars represent standard deviation.

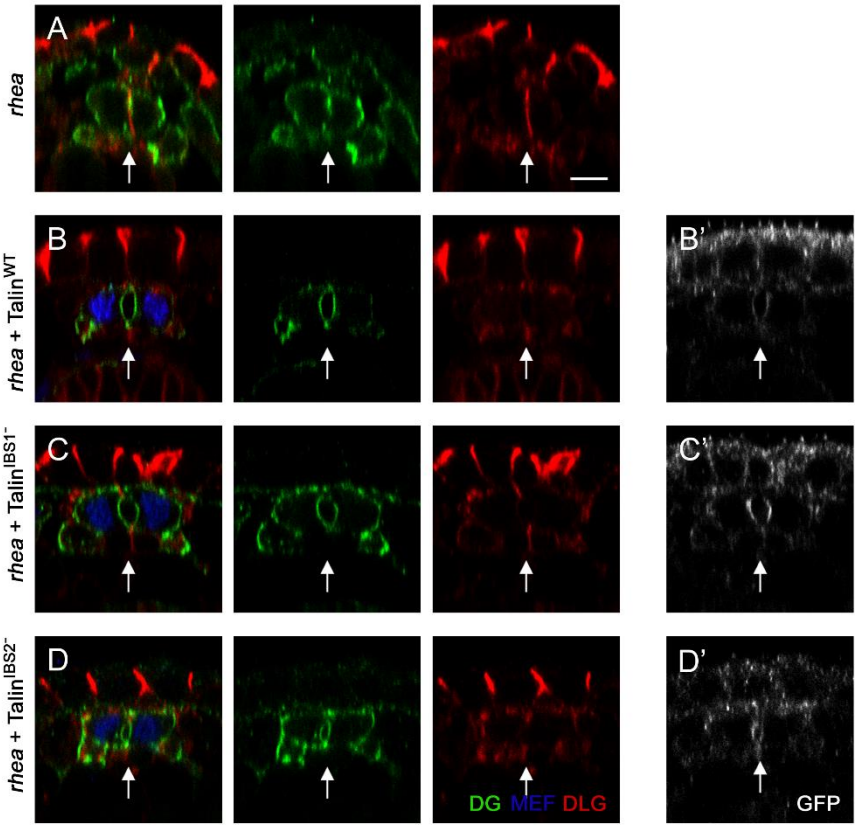
A
rhea
B
rhea + TalinWT
B'
C
rhea + TalinIBS1-
C'
D
rhea + TalinIBS2-
D'
DG MEF DLG
GFP

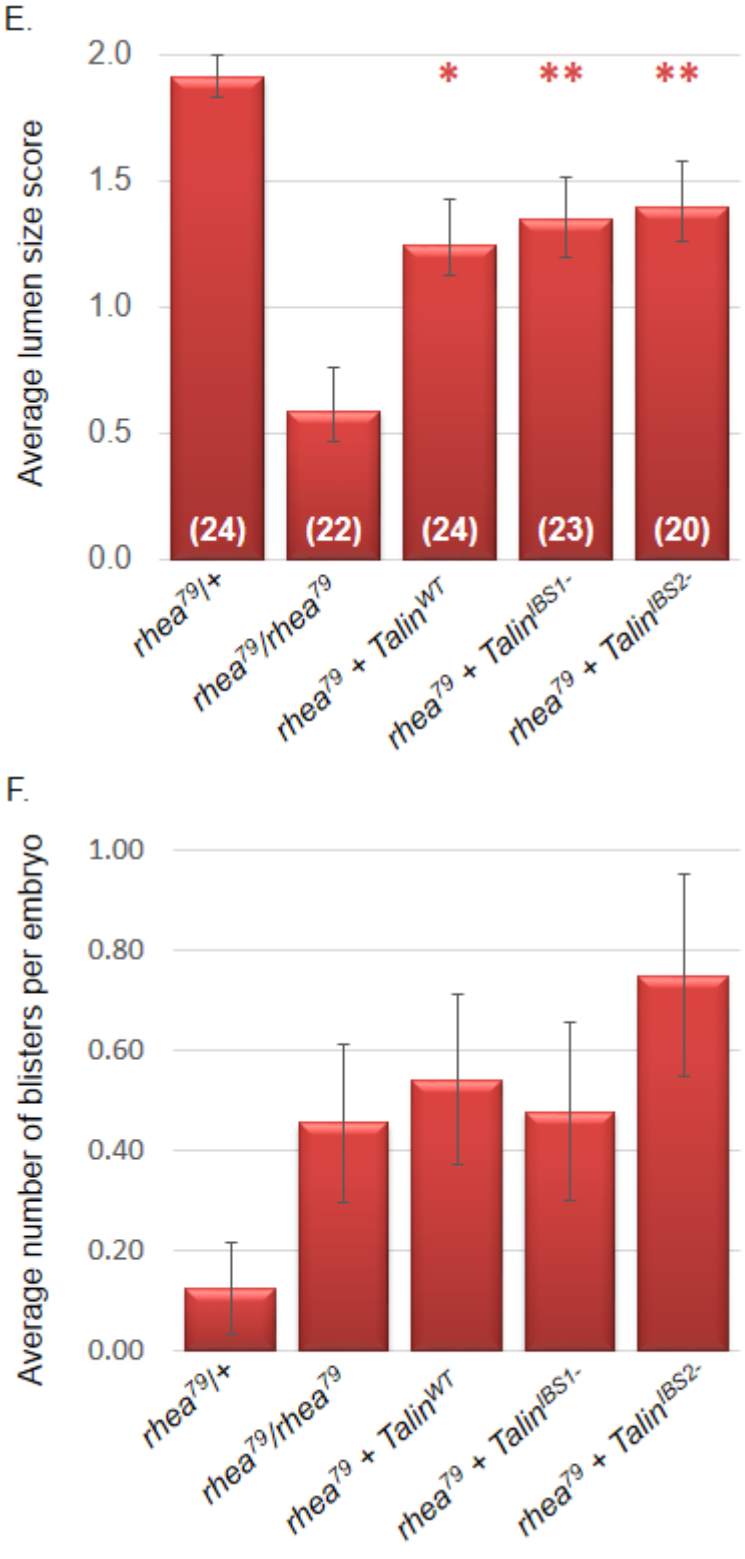
E.
Average lumen size score
2.0
1.5
1.0
0.5
0.0
*
**
**
(24)
(22)
(24)
(23)
(20)
rhea79/+
rhea79/rhea79
rhea79 + TalinWT
rhea79 + TalinIBS1-
rhea79 + TalinIBS2-
F.
Average number of blisters per embryo
1.00
0.80
0.60
0.40
0.20
0.00
rhea79/+
rhea79/rhea79
rhea79 + TalinWT
rhea79 + TalinIBS1-
rhea79 + TalinIBS2-

Interestingly however, many of the hearts in these *rhea*^{79} with *Talin*^{WT} embryos had lateral puckering or blisters of the seven-up cells (Figure 4.14F), reminiscent of embryos with reduced integrin (eg. Figure 3.1D, Figure 4.11C, see also Figure 4.4D'). Since *Talin*^{WT} is detectable at levels well above endogenous Talin levels (Figure 4.12), it is unlikely that reduced levels of Talin are the cause. However, it is possible that the full length Talin is unable to fully substitute for the endogenous Talin, perhaps due to the large GFP tag or subtle differences in localization. Another possibility is that the level of Talin must be tightly controlled, and that either high or low levels disrupt integrin-mediated adhesion. Indeed, in the adult wing, overexpression of αPS1 or αPS2 integrin produces blisters, a phenotype associated with loss of integrin adhesion (Brabant *et al.* 1996, Prout *et al.* 1997). This possibility could be tested by overexpressing Talin^{WT} in a wildtype background or varying the levels of ectopically expressed Talin and seeing if the blister penetrance correlates with increasing Talin levels. However, although the reason for these blisters is unclear, this does not negate that Talin^{WT} is able to significantly rescue the ability of the CBs to enclose an open lumen.

Furthermore, as hypothesized, Talin^{IBS1-} was also able to rescue lumen formation (Figure 4.14C, E). Consistent with the lack of properly localized βPS1 (Appendix C.6A, C), zygotic *rhea* mutants expressing Talin$^{IBS1- IBS2-}$ and Talin^{IBS2b-} were also unable to establish an open lumen, nor did they promote seven-up cell blisters (Appendix C.6B, D-G). However, in contrast to the requirement of IBS2 during germ-band retraction and dorsal closure, Talin^{IBS2-} was sufficient to promote integrin-dependent lumen formation (Figure

4.14D, E). Both the Talin^{IBS1-} and Talin^{IBS2-} rescued embryos displayed blisters, similar to those observed in the full length Talin rescues (Figure 4.14). These data support a model whereby neither IBS1 nor IBS2 is essential in the heart, but either of these domains is capable of mediating the Talin-integrin interaction required to promote heart tubulogenesis.

4.3 Discussion

The results presented here clearly demonstrate an essential role for Talin in *Drosophila melanogaster* heart tubulogenesis. During CB migration, Talin is required for maximal membrane leading edge activity and changes in CB morphology. Once CBs are aligned at the dorsal midline, embryos lacking Talin are unable to enclose a continuous lumen between the bilateral CB rows. Rather, ectopic open pockets occur atypically, often between neighboring cardial cells, along the lateral domains. Thus, Talin is not only an early marker of the lumen initiation domain, but it is essential to determine this site. The inability of *rhea* mutants to properly target the heart lumen correlates with a loss of CB polarization and proper establishment of membrane domains. In particular, the luminal determinants Slit and Robo fail to accumulate along the midline and other markers characteristic of the luminal (eg. Dg), junctional (eg. Dlg), and basal (eg. Prc) domains also display altered localization patterns. This lumen phenotype is rescued when a Talin transgene is expressed in *rhea*^{79} null embryos, confirming the requirement for Talin in lumen formation.

Previous studies on *Drosophila* Talin identified a critical role for Talin in early embryonic development: embryos lacking maternally and zygotically contributed Talin had a failure of germ-band retraction and dorsal closure (Brown *et al.* 2002b). As such phenotypes impact the ectoderm and amnioserosa, two tissues which surround the heart, cardiogenesis is indirectly, yet severely disrupted in these embryos (eg. Figure 4.10C-C''' and Appendix C.1). Importantly, here we establish that zygotic *rhea* null embryos, which retain maternal Talin, complete germ-band retraction and dorsal closure, yet still fail to establish an open cardiac tube lumen. Thus, Talin is also essential for heart cardiogenesis, and maternal Talin is insufficient for lumen formation. This may reflect a higher threshold level of Talin required for heart tubulogenesis than for germ-band retraction or dorsal closure, or it may be due to dwindling levels of maternal Talin remaining at late stage embryogenesis when the heart lumen is enclosed. This latter case is likely, as earlier heart development events such as pericardial-CB adhesion, CB shape changes, and leading edge activity are greatly disrupted in germ-line clone *rhea* null mutants, but display only subtle phenotypes in zygotic mutant embryos.

Analysis of *rhea* zygotic mutant embryos permitted a careful and in depth analysis of the heart in embryos with disrupted integrin signaling. Numerous *in vitro* and *in vivo* studies have suggested that Talin is essential for integrin function as it both activates integrins and modulates outside-in integrin signaling. Consistent with this, I demonstrate that Talin is essential for integrin promoted *Drosophila* heart development. In the heart, *rhea* null mutants phenocopy embryos expressing mutant alleles for *scb* (αPS3) and *mys*

(βPS1; Chapter 3). This is similar to other aspects of integrin-dependent *Drosophila* development and maintenance (eg. germ-band retraction and musculature - Brown *et al.* 2002b, trachea – Levi *et al.* 2006, hemocyte migration – Comber *et al.* 2013 and Moreira *et al.* 2013, intestinal stem cell anchorage – Lin *et al.* 2013). Furthermore, Talin and βPS1 are mutually dependent on one another for stabilization within the heart; null mutations in *rhea* or *mys* disrupt the localization pattern of βPS1 and Talin, respectively. Consistent with Talin activating the integrin-ECM binding and the integrin-adhesome link, *rhea* mutants also have abnormal patterns of LanA (ECM) and luminal domain accumulation of Pinch (cytoplasmic adhesome component) within the heart. Genetic gene dosage data is also consistent with Talin mediating integrin function during heart development.

Several lines of evidence suggest that the role of integrins during heart tubulogenesis is to transmit polarizing and lumen-initiating cues, but not to establish longer-lasting stable adhesions. First of all, although Talin is required for normal Pinch localization, CAP, a protein recruited to more mature muscle adhesions, does not accumulate along the entire luminal surface and remains correctly localized in $rhea^{79}$ homozygous embryos. Furthermore, unlike during the dynamic events of germ-band retraction and dorsal closure or in strong muscle adhesions (Ellis *et al.* 2011), either of Talin's two integrin binding sites is sufficient to promote heart tube assembly. It is possible that an essential role for either IBS1 or IBS2 is masked by the persisting maternal Talin in zygotic mutants. As Talin has a C-terminal dimerization domain (Goult *et al.* 2013a), $Talin^{IBS1-}$ and $Talin^{IBS2-}$ may bind to residual maternal Talin to form functional homodimers

which are sufficient to rescue heart development. However, functional redundancy of these domains is consistent with *in vitro* and *in vivo* studies suggesting that either IBS is capable of binding to integrins and mediating Talin's function as an adaptor protein, even though in certain contexts one or both of IBS1 and IBS2 may be especially relied upon for specialized roles (Calderwood *et al.* 2002, Wegener *et al.* 2007, Tremuth *et al.* 2004, Tanentzapf and Brown 2006, Ellis *et al.* 2011). The ability of the heart to form in the absence of IBS1 suggests that, unlike in the embryonic musculature, strong long-lasting integrin-mediated adhesions are unnecessary. This is not unexpected as *Drosophila* heart lumen formation involves rapid cell shape changes which complete within an hour of dorsal closure (data not shown); it is likely that dynamic transient adhesions would be sufficient. The functional redundancy of IBS1 and IBS2 also suggests that heart tubulogenesis does not require a strong integrin-adhesome linkage, as this interaction is promoted by Talin's IBS2. In cell culture, *talin*-/- cells were rescued with Talin lacking a functional IBS2 domain; these cells displayed aberrant cytoskeletal organization suggesting that the IBS2 is required to mediate the integrin-adhesome-actin linkage (Moes *et al.* 2007). Consistent with this, in *Drosophila* musculature, although either IBS was sufficient to initially recruit adhesome proteins such as Pinch and Paxillin, only IBS2 was able to prevent integrins from subsequently detaching from the adhesome (Ellis *et al.* 2011). Taken together, here I illustrate a developmental event in which either IBS1 or IBS2 is sufficient to not only stabilize integrin along the luminal domain, but also to develop an open lumen and complete heart tubulogenesis.

4.4 Conclusion

Here we have established Talin function as essential for several key aspects of tubulogenesis in the *Drosophila* embryonic heart, a mesodermal tube model displaying a unique polarity with a basal-like luminal surface. As an early luminal-site marker, Talin promotes the CB shape changes and integrin adhesion required for lumen formation. Talin is required to stablize the luminal determinants Slit and Robo along the apical CB surface and restrict the junctional membrane domains to seal the non-adherent luminal surfaces. Thus, loss of Talin during *Drosophila* cardiogenesis disrupts several basic tubular organ design principles: determination of the lumen formation site, establishment of tube cell polarity and specified membrane domains, and development of the luminal space (reviewed by Ferrari *et al.* 2008, Datta *et al.* 2011).

Discussion

CHAPTER FIVE

5.1 Integrin and Talin in *Drosophila* heart development

The experiments reported here establish an essential function for the αPS3βPS1 integrin heterodimer and its adaptor Talin in *Drosophila* embryonic heart tube assembly. Prior to lumen enclosure, the cardioblasts (CB) collectively migrate towards the dorsal midline becoming increasingly polarized. They adopt a triangular shape oriented towards the dorsal midline and extend highly active leading edge processes in the direction of migration. During this migratory phase, βPS1 and Talin localize along the CB apical surface, immediately ventral to the extended leading edge. As this βPS1 and Talin rich domain persists throughout embryonic heart assembly, eventually surrounding the lumen of the open cardiac tube, we have termed this surface the presumptive or pre-luminal domain. αPS3βPS1 and Talin are both essential for the dynamic cell morphology and leading edge features that characterise collective cardial cell migration. Furthermore, following migration, αPS3, βPS1, and Talin are required for correct luminal, junctional, and basal polarity. Importantly, without proper integrin or Talin function, the secreted ligand Slit and its receptor Robo are not stabilized along the heart midline and a lumen fails to form between the CB rows. Thus, integrins and Talin work upstream of Slit and Robo to promote lumen formation. Slit signaling during axon guidance and salivary gland migration is also sensitive to integrin function (Pirraglia and Myat 2010, Stevens and Jacobs 2002). Integrins may have a conserved role in establishing membrane domains rich in Robo to enable localised signaling.

Embryos mutant for both maternal and zygotic *rhea* or integrin and, to a slightly lesser extent, zygotic integrin mutants (ether *scb* or *mys*) are characterized by severe phenotypes during the early embryonic development. Developmental disruptions in germ-band retraction and dorsal closure secondarily interfere with heart development. However, maternally contributed Talin in *rhea* zygotic mutants is sufficient for these processes to complete, allowing a more thorough analysis of cardiac tubulogenesis in these mutants. Disrupted heart development in these zygotic mutant embryos confirms that the roles in CB polarity and lumen formation (outlined above) are not merely due to secondary effects that reflect the known requirement for integrin and Talin in early embryonic development (Nusslein-Volhard *et al.* 1984, Schöck and Perrimon 2003, Brown *et al.* 2002b, Ellis *et al.* 2013).

Careful analysis of late stage hearts in *rhea* zygotic mutants reveals that Talin is essential to correctly orient the CB polarity such that a continuous lumen is enclosed along the midline. In wildtype, many membrane receptors including Robo, Dystroglycan, Unc5, and Syndecan accumulate along the luminal domain (Medioni *et al.* 2008, Albrecht *et al.* 2011, Knox *et al.* 2011). As seen through our Robo and Dystroglycan (Dg) immunolabeling experiments, this luminal domain is absent or, at best, is discontinuous along the midline in *rhea* mutant embryos. However, these Robo and Dg enriched luminal domains are not completely absent in null *rhea* homozygotes, but are found ectopically along lateral membranes between neighboring CBs. Robo's secreted ligand Slit is also detected within these ectopic accumulations. As Slit-Robo signaling has been suggested to create the non-

adherent membrane surrounding the lumen (Santiago-Martinez *et al.* 2008), these ectopic pockets have characteristic luminal features. Thus, Talin and integrins are essential for proper luminal polarity and CB enclosure of a single, continuous midline lumen.

Integrin and Talin are not only essential for establishment of the luminal domain, but they are required to restrict the midline junctions to minimal contact sites dorsal and ventral to the lumen. Without *slit*, *robo1*, and its compensating *robo2*, CBs exhibit expanded junctional domains that span the midline between the contralateral CB rows (MacMullin and Jacobs 2006; Medioni *et al.* 2008; Santiago-Martinez *et al.* 2008). Where Slit and Robo accumulate, either along the midline in wildtype embryos or in lateral pockets in *rhea* mutants, cell-cell junctions are excluded. Thus, the extended adhesive contact observed in $rhea^{79}$ and scb^{2} (αPS3) embryo hearts is consistent with a model in which integrin and Talin act upstream to provide instructive localization or polarization cues to Slit and Robo. These cues are essential to correctly orient the lumen and to restrict the sealing adhesive regions. However, the presence of ectopic open pockets in *rhea* zygotic and GLC embryos suggests that integrin-Talin signaling by itself is not sufficient to confer non-adhesiveness. Rather, generation of non-adherent luminal domains requires integrin-instructed Slit-Robo signaling (Figure 5.1).

Although Talin-mediated integrin function is essential for CB polarity and lumen formation, other cell surface factors also modulate heart tubulogenesis. The luminal markers mentioned above (including Robo, Syndecan, Dg, and Unc5) and also the junctional E-cadherin (E-cad) and Frazzled/DCC are essential for proper heart assembly

Figure 5.1 – Proposed model of integrin function during heart tubulogenesis

In the latter stages of CB migration and during lumen enclosure, αPS3βPS1 integrin and Talin are required to define a site of lumen formation, polarize luminal determinants, and modulate CB morphology. Based upon evidence from our studies (bold numbers and arrows) and *in vitro* tubulogenesis models, we propose the following mechanism of heart tube formation. 1. Integrins receive instructive positional cues from the ECM (Turlo *et al.* 2012, Davis and Senger 2005) and likely also transmit back further assembly cues (Colognato *et al.* 1999, Yurchenco 2011). 2. Integrins recruit or stabilize luminal factors along the pre-luminal surface. In particular, here we highlight the importance of the Robo-Syndecan-Slit complex. 3. Integrins restrict cell-cell adhesions from the luminal surface. This may occur through Robo-Slit signaling (3b; Santiago-Martinez *et al.* 2008) or through other pathways (3a, 3c; Pirraglia *et al.* 2013, Canel *et al.* 2013). 4. The Slit-Robo-Syndecan complex promotes integrin along the luminal domain (Johnson *et al.* 2004, Beauvais and Rapreager 2010). 5-7. Integrins regulate actin dynamics to promote the cardioblast shape changes required during lumen formation. This may be through a direct interaction with the integrin adhesome (5, eg. Talin; Franco-Cea *et al.* 2010), or indirectly through Cdc42/Rac1 (6-7; Harden *et al.* 1996, Price *et al.* 1998). 8. We hypothesize that integrins also promote polarization of polarity determinants (eg. Par6 and aPKC) and phosphoinositols (eg. PIP2 and PIP3), possibly through Cdc42 (6) or through additional signaling molecules (not shown; Datta *et al.* 2011).

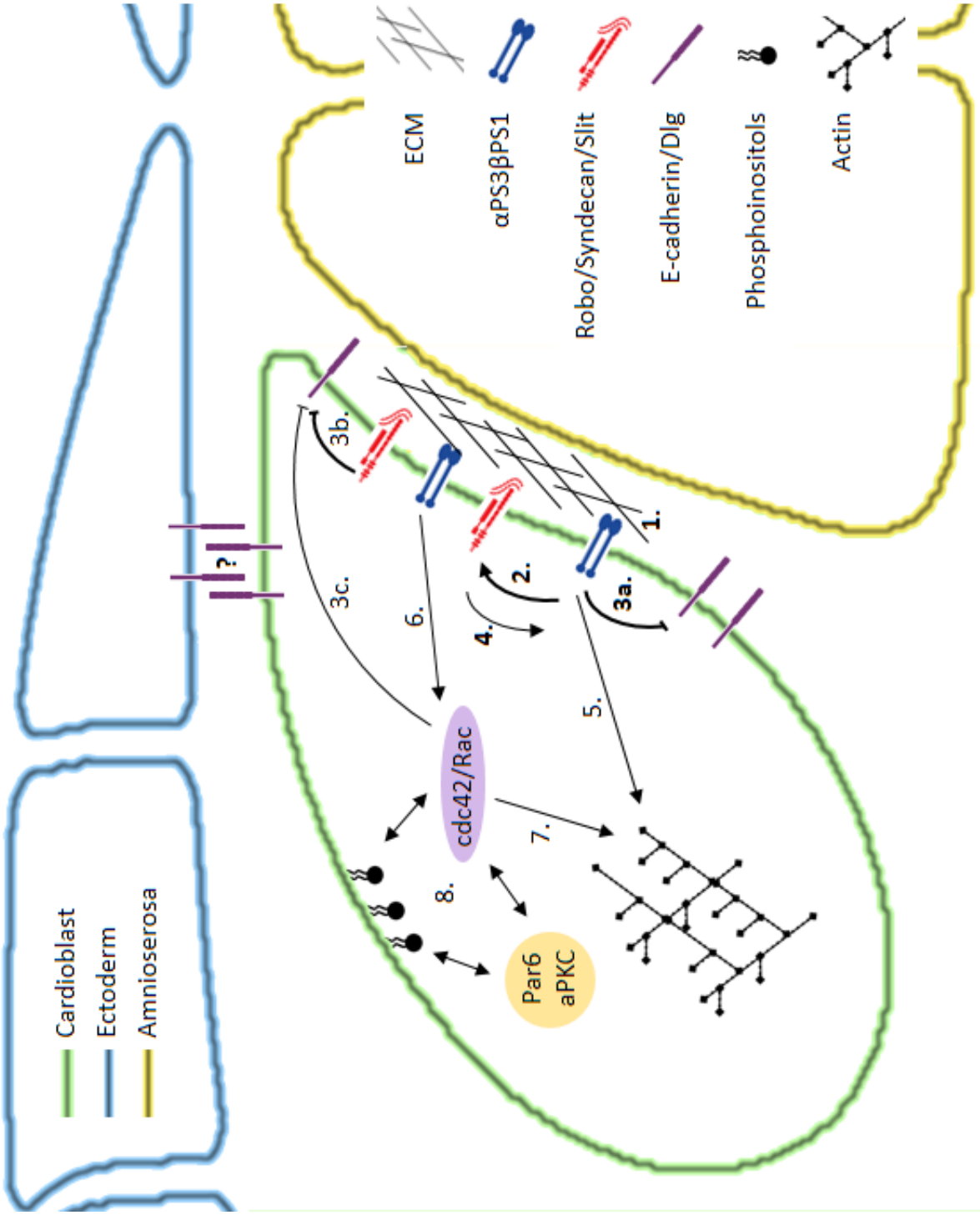
ECM
αPS3βPS1
Robo/Syndecan/Slit
E-cadherin/Dlg
Phosphoinositols
Actin
Cardioblast
Ectoderm
Amnioserosa
?
1.
2.
3a.
3b.
3c.
4.
5.
6.
7.
8.
cdc42/Rac
Par6
aPKC

(Santiago-Martínez *et al.* 2008, Macabenta *et al.* 2013). Loss of the luminal receptors, or their respective ligands, results in a small, discontinuous, or absent lumen (MacMullin and Jacobs 2006; Knox *et al.* 2011, Medioni *et al.* 2008; Santiago-Martinez *et al.* 2008, Albrecht *et al.* 2011). Embryos homozygous for mutant alleles of *frazzled* or *shotgun* (encoding *Drosophila* E-cad) exhibit reduced or absent midline adhesion respectively (Santiago-Martínez *et al.* 2008, Macabenta *et al.* 2013). Although we have established that integrins are instructive in defining the luminal domain, this does not exclude the possibility that other luminal signals work in concert with integrin. Indeed, although Robo is not restricted to the luminal domain until late stage embryogenesis, in the absence of Robo, βPS1 also fails to concentrate along the apical CB surface.

Interactions between cell-surface factors have been characterized in other systems, and these inform our model of lumen formation in the *Drosophila* heart (Figure 5.1). During *Drosophila* salivary gland development, E-cad, Robo, and integrins contribute to cell adhesion flexibility, interactions with surrounding tissues, and positional guidance cues that together promote gland extension and collective cell migration (Pirraglia and Myat 2010). Within this system, E-cad is downregulated by integrin-dependent Rac1 signaling (Pirraglia *et al.* 2013). Numerous cancer cell studies further demonstrate that not only Rac1, but also Src and Integrin linked kinase (ILK) control integrin – E-cad crosstalk (reviewed by Canel *et al.* 2013). Within the nervous system, Robo functions as part of a ternary complex with Syndecan and their shared ligand Slit (Johnson *et al.* 2004, Hohenester *et al.* 2006). This enhances repellent axon guidance signals (Johnson *et al.*

2004, Hohenester *et al.* 2006). Similarly, within the *Drosophila* heart, a Robo-Syndecan-Slit complex likely promotes sufficient Robo signaling to create a non-adherent luminal domain (Knox *et al.* 2011). This is significant, as Syndecan has been reported to physically interact with the integrin heterodimer (Wang *et al.* 2010, Beauvais *et al.* 2009) and promote integrin function either directly (Beauvais *et al.* 2009) or through other signaling or trafficking pathways (Hozumi *et al.* 2010, Morgan *et al.* 2013, Beauvais and Rapreager 2010). Within the heart, genetic interactions between *syndecan* and integrin (*scb* and *mys*) or extracellular matrix genes (eg. *lanA*) have been identified (Knox *et al.* 2011). We hypothesize that the Robo-Syndecan complex may stabilize or promote the function of integrins within the luminal domain (Figure 5.1).

5.2 *Drosophila* heart tubulogenesis as an *in vivo* model to study the mechanism of integrin adhesions

We have further established the heart as a feasible and effective *in vivo* model to study integrin adhesion and signaling in a dynamic developing system, a system well-suited to test and extend our *in vitro*-derived integrin models. Integrins are the core component of several cell-ECM adhesion structures, including long-lasting focal adhesions capable of withstanding strong forces (eg. during muscle contractions) and more transient adhesions that are flexible and dynamic (eg. at the leading edge of migrating cells; Choi *et al.* 2008, Zaidel-Bar *et al.* 2007b). The somatic musculature and adult wing are established *Drosophila* models used to study stable integrin-mediated adhesions (Martin-Bermudo

and Brown 1996, Wilcox *et al.* 1989, Brower and Jaffe 1989). More dynamic processes requiring integrins include dorsal closure, germ-band retraction, salivary gland and trachea development, and hemocyte migration (Brown *et al.* 2002, Bradley *et al.* 2003, Levi *et al.* 2006, Moreira *et al.* 2013). Cardiac development presents an excellent system in which cellular dynamics and protein localization can be easily assessed at a whole organ and individual cell resolution. Not only have we established the core integrin heterodimer and Talin proteins as essential for heart tubulogenesis, we have used genetic and immunohistochemical assays to further implicate other conserved factors, such as the ECM component LanA and the cytoplasmic IPP-complex. Figure 5.2 presents a comparative overview of Talin-mediated integrin adhesion during *Drosophila* heart tubulogenesis, muscle development, and dorsal closure and germ-band retraction. The following paragraphs explore the key aspects of integrin-Talin adhesion during heart development in more detail.

As integrins are enzymatically inactive receptors, they mediate their function through interactions with ECM ligands and with the cytoplasmic adhesome, a collection of many signaling and adaptor proteins (Figure 1.5). Although ECM components are known to localize to the heart lumen, a clear role for the ECM in providing spatial cues to integrins has not been studied in the *Drosophila* heart. Consistent with our genetic interaction experiments, previous studies suggest that the ECM is required for proper heart development (Martin *et al.* 1999, Haag *et al.* 1999, Yarnitzky and Volk 1995), but this

Figure 5.2 – Talin-integrin adhesion in *Drosophila* embryonic development

Talin-mediated integrin function can be simplified to focus on key aspects of integrin-ECM affinity, adhesome recruitment, and direct (Talin) or indirect (adhesome) actin binding. Here we present a comparison of relative contributions of each of these aspects during muscle development (requires strong, long-lasting adhesions), dorsal closure and germ-band retraction (dynamic events involving large morphogenic tissue movements), and heart tubulogenesis.

A. The somatic musculature requires strong IBS1 and IBS2 mediated integrin-Talin binding. Disruptions in this binding results in muscle detachment, and ECM and adhesome mislocalization (Ellis *et al.* 2011). However, loss of Talin's actin-binding domain (ABD) only subtly disrupts the muscle architecture (Franco-Cea *et al.* 2010).

B. High integrin-ECM affinity promoted by Talin's IBS1 is not essential for dorsal closure or germ-band retraction (Ellis *et al.* 2011). In contrast, Talin's IBS2 and ABD are critical for these processes (Franco-Cea *et al.* 2010).

C. Since either of Talin's integrin binding sites is sufficient for heart tubulogenesis, neither high integrin-ECM affinity nor strong adhesome linkage is essential. However, *scb* (αPS3) and *rhea* genetic interactions with *lanA* suggest that the ECM is important. Furthermore, adhesome components required for transient, but not stabilized, adhesions are recruited to the luminal domain in a Talin-dependent manner. Since Talin's ABD is essential for transient, dynamic integrin adhesions (Franco-Cea *et al.* 2010, Jiang *et al.* 2003), we hypothesize that direct Talin-actin binding may be important for heart tubulogenesis.

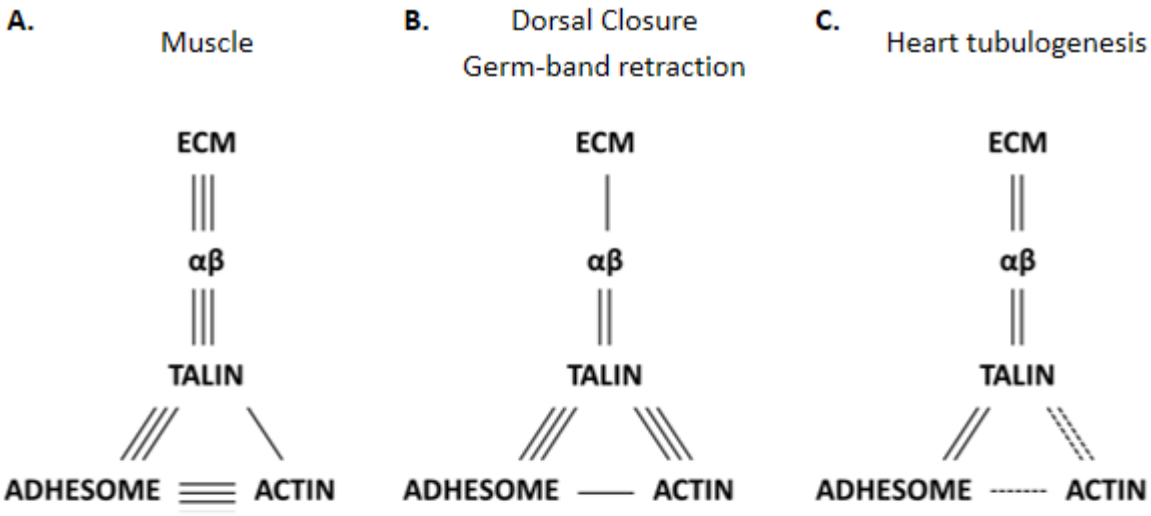
A.
Muscle
ECM
αβ
TALIN
ADHESOME
ACTIN
B.
Dorsal Closure
Germ-band retraction
ECM
αβ
TALIN
ADHESOME
ACTIN
C.
Heart tubulogenesis
ECM
αβ
TALIN
ADHESOME
ACTIN

requirement has not been characterized at the cellular level. However, in both *in vitro* and *in vivo* endothelial tube studies, proper ECM deposition is essential for vessel assembly (Turlo *et al.* 2012, Davis and Senger 2005).

Elucidating a role for factors downstream of integrins will provide important insights into the mechanism of integrin function in adhesions *in vivo*. As heart tubulogenesis involves dynamic morphogenetic events, it is likely that transient, but not long-lasting stable adhesions mediated by integrin are essential (Figure 5.2). In embryonic musculature, Cbl-associated protein (CAP) is a marker of long-lasting stable adhesions; it is recruited to mature muscle-attachment sites and is essential to maintain strong adhesions during muscle contractions (Bharadwaj *et al.* 2013). The late accumulation of CAP within the *Drosophila* heart and its punctate pattern in both wildtype and *rhea* mutant hearts is consistent with a minimal role for mature integrin adhesions during tubulogenesis. Another protein recruited to maturing integrin adhesions is Vinculin (Humphries *et al.* 2007, Carisey *et al.* 2013, Papagrigoriou *et al.* 2004). Embryos expressing an amorphic allele of *vinc* have normal heart assembly, suggesting that integrins do not require Vinculin to mediate their function. Additional proteins characteristic of mature integrin adhesion include Zyxin and Tensin. Zyxin is a common *in vitro* marker for mature integrin adhesions (Zaidel-bar *et al.* 2003). Tensin, encoded by *blistery* in *Drosophila*, is thought to strengthen integrin adhesions, for example in the adult wing (Torgler *et al.* 2004, Delon and Brown 2009). Analyzing protein recruitment and assessing heart development in embryos with

mutant alleles of these genes would allow us to further test if mature adhesions are dispensable for tubulogenesis (Figure 5.2).

Further insights into the mechanism of integrin function can be gained from studying specific integrin or Talin domains which mediate protein-protein interactions. We have performed rescue experiments using Talin transgenes with abrogated β-integrin binding to test the requirement for either of Talin's two integrin binding sites (IBSs). In contrast to *Drosophila* tissues that require long-lasting strong adhesions (eg. somatic muscles) or those that involve major morphological changes (eg. germ-band retraction and dorsal closure, Ellis *et al.* 2011), we found that heart development requires proper function of either IBS1 or IBS2. This suggests that while integrin-Talin interaction is essential for heart tubulogenesis, the specific mechanism of integrin-Talin binding is not important. Our findings are consistent with a model in which IBS1 and IBS2 are partially redundant, as they are both sufficient to bind to integrin, mediate initial recruitment of adhesome proteins, and promote heart tubulogenesis (Figure 5.2). However, other developmental or tissue maintenance processes may require additional aspects of Talin-mediated integrin adhesion which rely primarily on one or both of Talin's IBSs (Tanentzapf and Brown 2006, Ellis *et al.* 2011, Mathew *et al.* 2012).

Context-dependent mechanisms of integrin function are consistent with the differential recruitment of proteins to nascent and mature adhesion complexes. In addition to the integrin-Talin binding sites, both β-integrin and Talin have binding sites for other proteins whose requirement for heart development would be informative to our

understanding of integrin adhesions. For example, the β-integrin tail also binds the activator Kindlin. Kindlin has recently garnered interest for its role in working synergistically with Talin to promote integrin activation (Harburger *et al.* 2009, Margadant *et al.* 2012, Ye *et al.* 2013). However, few studies have explored an early role for the *Drosophila* kindlin orthologues *fermitin1* and *fermitin2* (Catterson *et al.* 2013). A second example are Talin's actin binding domains (ABDs). Talin connects to the actin cytoskeleton directly though several ABDs (McCann and Craig, 1997, Lee *et al.* 2004) or indirectly by recruiting other actin-binding proteins like Vinculin and Wech (Ziegler *et al.* 2008, Fillingham *et al.* 2005, Goult *et al.* 2013a, Löer *et al.* 2008). The C-terminal ABD (see Figure 4.1B, Gingras *et al.* 2008, Smith and McCann 2007) is particularly important for nascent transient integrin adhesions during development and thus would be a strong candidate domain to test our model that short-term adhesions are essential for heart tubulogenesis (Figure 5.2; Franco-Cea *et al.* 2010, Jiang *et al.* 2003).

One aspect of integrin and Talin function that has not been studied in our heart model is regulation of activity. While Talin and Kindlin are essential integrin activators, integrins in both nascent and long-term adhesions are also tightly regulated by phosphorylation and trafficking or recycling (Bledzka *et al.* 2010, Deshmukh *et al.* 2011, Rainero and Norman 2013). For example, lack of Dynamin2, a GTPase responsible for vesicle scission, decreased integrin endocytosis which resulted in large focal adhesions that inhibited cell migration and angiogenesis (Lee *et al.* 2014). Furthermore, the localization and activity of Talin itself must also be tightly controlled through lipid or

protein-mediated recruitment, proteolysis, phosphorylation, and release from autoinhibition. Two calpain-mediated cleavage sites are thought to trigger adhesion turnover through Talin inactivation and increased β-integrin binding affinity. The former occurs through cleavage near Talin's C-terminus (Bate *et al.* 2012), while the latter is promoted through Talin-head release following proteolysis within a linker region between the Talin head and rod domains (Franco *et al.* 2004, Yan *et al.* 2001). Phosphorylation of the Talin head by Cdk5, a cyclin dependent protein kinase, prevents degradation of this cleavage product: Talin harbouring a mutation at the Cdk5 target site is susceptible to ubiquitylation, which increases focal adhesion turnover (Huang *et al.* 2009). Recently*, in vitro* and *in vivo* studies have highlighted the importance of Talin autoinhibition. Intramolecular interactions between the Talin FERM domain (within the head) and the rod domain create a closed conformation, masking several key protein binding domains (Goksoy *et al.* 2008, Goult *et al.* 2013b). In *Drosophila*, *rhea* null embryos were rescued with a Talin transgene which lacked the Talin rod amino acid residues key to these intramolecular interactions. In these embryos, there was increased recruitment of Talin and βPS1, reduced Talin turnover, and delayed dorsal closure (Ellis *et al.* 2013). Membrane recruitment of Talin and release of the autoinhibition (ie. Talin activation) is promoted by phosphatidylinositol 4,5-bisphosphate (PI(4,5)P2 or PIP2), a phospholipid distributed throughout the cell membrane, but locally increased by PIP kinase Type I γ (PIPKIγ) or the lipid phosphatase PTEN (Legate *et al.* 2011, Martel *et al.* 2001, Song *et al.* 2012). Thus PIP2 is required for proper localization and function of Talin at sites of integrin adhesion, and

this is important for maintenance and clustering of Talin-bound integrin heterodimers (Martel *et al.* 2001, Saltel *et al.* 2009). Importantly for our study, phospholipid polarity is also critical for tubulogenesis (reviewed in Datta *et al.* 2011). Briefly, in the Madine-Darby canine kidney (MDCK) cell model, PIP2 localizes to apical or luminal membranes, while phosphatidylinositol (3,4,5)-triphosphate (PIP3) is enriched basolaterally (Martin-Belmonte and Mostov 2007). Exogenous addition of either PIP2 or PIP3 to the incorrect membrane domain induces abnormal cell polarity (Gassama-Diagne *et al.* 2006, Martin-Belmonte *et al.* 2008). As *Drosophila* heart tubulogenesis has atypical polarity compared to the MDCK model, it would be fascinating to study the localization of and requirement for these membrane components in heart development. Our studies characterizing the requirement for Talin and integrin in the heart have set a foundation on which to study in detail, not only phosphoinositols, but many aspects of the mechanism of activation, regulation, and function of Talin-mediated integrin adhesion.

5.3 *Drosophila* heart development as a unique model of tubulogenesis

The experimental approaches utilized and the data presented here highlight the importance of the *Drosophila* heart as a unique and tractable model of tubulogenesis. Traditionally, *Drosophila* cardiogenesis has been primarily compared to vertebrate heart development (eg. Bier and Bodmer 2004, Tao and Schulz 2007). *Drosophila* and early vertebrate heart development follow similar keys steps: cardial precursor specification from the lateral mesoderm, parallel alignment of the cells, collective cell migration to the

midline, and heart tube assembly (Markwald *et al.* 1996, Bier and Bodmer 2004). Several fly heart determinants discussed in this thesis are also involved in vertebrate heart development. Integrins and Talin are expressed in multiple heart layers and are essential for embryo viability and proper heart assembly and maintenance (Terraccio *et al.* 1991, Carver *et al.* 1994, Valencik *et al.* 2002, Keller *et al.* 2001, Yang *et al.* 1995). Moreover, Slit and Robo signaling has been identified during cardial cell alignment and morphology, heart field migration, and tube formation in both mice and zebrafish (Fish *et al.* 2011, Mommersteeg *et al.* 2013, Medioni *et al.* 2010).

However, more recently, parallels have been made to endothelial-lined blood vessels that develop de novo from endothelial precursors (vasculogenesis) or via branch sprouting from existing vessels (angiogenesis; Medioni *et al.* 2009, Brand and Paululat 2013). Indeed, Hartenstein and Mandel use comparative morphological and molecular data to suggest that insights into *Drosophila* heart development will be equally informative to vertebrate cardiogenesis and vasculogenesis (2006). Vertebrate studies support this view. For example, Robo-Slit signaling has received increasing attention during angiogenesis for its role in cell migration and tube formation (Jones *et al.* 2008, Paul *et al.* 2013, review in Yadav and Narayan 2014). Within the mouse aorta, the glycoprotein CD34-siolomucin is deposited into the luminal space to promote luminal wall repulsion (Strilić *et al.* 2009), reminiscent of the anti-adherent mechanism of Slit-Robo function during fly heart tube formation (Santiago-Martinez *et al.* 2008). Furthermore, although the ECM is rapidly excluded from the developing vertebrate vasculature, ECM

components of the interstitial matrix are initially present within the endothelia-lined lumen (Strilić *et al.* 2009, Davis and Senger 2005). This is comparable to the *Drosophila* heart as integrin is no longer present at high levels in the lumen during larval development (S. Bogatan, personal communication). Similarly, in invertebrate lancelets, an initial ECM filled heart lumen is later cleared by phagocytotic blood cells (Kucera *et al.* 2009).

Studying integrins and Talin in vertebrate blood vessel development is difficult, as embryos lacking β1 integrin or Talin1, the predominant isoforms expressed in endothelial cells, die early in embryogenesis (Fässler and Meyer 1995, Stephens *et al.* 1995, Monkley *et al.* 2000). More recently, limited endothelial tissue knock-outs have demonstrated that both β1 integrin and Talin1 are required for angiogenesis and blood vessel integrity (Monkley *et al.* 2011, Tanjore *et al.* 2008, Lei *et al.* 2008, Carlson *et al.* 2008). However, these knock-outs also result in early embryonic lethality, making careful analysis of mechanism impractical. Studies using endothelial cell culture models suggest that integrin function is required for endothelial polarity, migration, and lumen formation (Zovein *et al.* 2010, Malan *et al.* 2010). Thus, both *in vivo* and *in vitro* studies are consistent with our findings that integrin and Talin are key factors in specifying a lumen initiating site and developing an open tube. As classical epithelial models such as MDCK and mammary gland acini also rely on integrin-mediated signals to orient the cells (Yu *et al.* 2005, Akhtar and Streuli 2013), integrins may have a conserved function in establishing luminal polarity.

Additional mechanisms of tubulogenesis may also be shared between *Drosophila* heart development and vertebrate vessel formation. To date, most studies on the

Drosophila embryonic heart have focused on cell surface factors including receptors and their respective ligands; few studies have moved into the cell to establish the downstream signaling pathways involved. Insights from *in vitro* models suggest that polarity pathways and vesicle trafficking will be informative areas of study (Figure 5.1). In the epithelial MDCK model, the small GTPases Rab8a and Rab11a coordinate with the exocyst complex to deliver luminal factors to the pre-luminal apical membrane initiation site (AMIS; Bryant *et al.* 2010). In mouse endothelial cells lacking β1 integrin, excess vesicles accumulate in the cytoplasm and lumen formation fails (Zovein *et al.* 2010). In both the epithelial and endothelial models, vesicle trafficking is linked to establishment of polarity essential for lumen development. For instance, Zovein *et al.* additionally found that Par3 functions downstream of β1 integrin to promote lumen development (2010). In addition to Par3, key cytoskeletal regulators Cdc42, Rac1, and PAK, and core polarity proteins Par6 and atypical protein kinase C (aPKC) have all been implicated in lumen and tube formation (Koh *et al.* 2008, Qi *et al.* 2011, review in Domigan and Iruela-Arispe 2012). We propose a model whereby integrins initiate and provide instructive cues to the vesicle trafficking and polarity networks to establish luminal factors and restrict junctional components from the pre-luminal domain (Figure 5.1). For example, p21 activated kinase 1 (PAK1) is a target of Rac1 and Cdc42 which localizes to integrin adhesions (Harden *et al.* 1996). In the *Drosophila* salivary gland, PAK1 promotes E-cadherin endocytosis at the adherens junction to increase the luminal domain (Pirraglia *et al.* 2010). Although it is currently unclear which classical apical polarity proteins are maintained in the unique *Drosophila* heart,

epithelial and endothelial models suggest that the Cdc42-Par6-aPKC complex is a conserved master regulator of tube formation in both vertebrates and flies (eg. Bryant and Mostov 2008, Sacharidou *et al.* 2010, Pirraglia *et al.* 2010, Jones and Metzstein 2011).

5.4 Conclusion

Tube formation in vertebrates and invertebrates is a diverse phenomenon with respect to the tube size, function, and unique developmental requirements. Here we explore an *in vivo* tube model exhibiting a non-classical polarity. We have shown that the αPS3βPS1 integrin heterodimer and its adaptor Talin are essential for CB morphology and polarization during *Drosophila* heart formation. Taken together with information from endothelial and classical epithelial tubulogenesis models, Talin-mediated integrin adhesion likely has a conserved role in initiating luminal cues to define polarity and demarcate membrane domains essential for tube formation. It remains to be seen if downstream cytoplasmic mechanisms are shared between these different models, however it is likely that key polarity and vesicle trafficking factors are conserved. Furthermore, the regulation of integrins at the luminal surface is an intriguing topic for further study. This likely depends on a combination of ECM cues, cross-talk with other transmembrane receptors, and cytoplasmic inside-out signals perhaps promoted through Talin activation. As integrins are abundantly expressed, not only in tubular organs, but in migratory, developing, and established tissues, insights from the *Drosophila* heart are broadly informative.

REFERENCES

Abreu-Blanco, M. T., Verboon, J. M. and Parkhurst, S. M. (2014). Coordination of Rho Family GTPase Activities to Orchestrate Cytoskeleton Responses during Cell Wound Repair. *Curr. Biol.* **24**, 144-155.

Akhtar, N. and Streuli, C. H. (2013). An integrin-ILK-microtubule network orients cell polarity and lumen formation in glandular epithelium. *Nat. Cel Biol*. **15**, 17-27.

Albrecht, S., Altenhein, B. and Paululat, A. (2011). The transmembrane receptor Uncoordinated5 (Unc5) is essential for heart lumen formation in Drosophila melanogaster. *Dev. Biol.* **350**, 89-100.

Anastasi, G., Cutroneo, G., Gaeta, R., Di Mauro, D., Arco, A., Consolo, A., Santoro, G., Trimarchi, F. and Favaloro, A. (2009). Dystrophin-glycoprotein complex and vinculin-talin-integrin system in human adult cardiac muscle. *Int. J. Mol. Med.* **23**, 149-159.

Anthis, N.J., Haling, J. R., Oxley, C. L., Memo, M., Wegener, K. L., Lim, C. J., Ginsberg, M. H. and Campbell, I. D. (2009a). Beta integrin tyrosine phosphorylation is a conserved mechanism for regulating talin-induced integrin activation. *J. Biol. Chem.* **284**, 36700-36710.

Anthis, N. J., Wegener, K. L., Ye, F., Kim, C., Goult, B. T., Lowe, E. D., Vakonakis, I., Bate, N., Critchley, D. R., Ginsberg, M. H. and Campbell, I. D. (2009b). The structure of an integrin/talin complex reveals the basis of inside-out signal transduction. *J. EMBO* **28**, 3623-3632.

Avizienyte, E. and Frame, M. C. (2005). Src and FAK signalling controls adhesion fate and the epithelial-to-mesenchymal transition. *Curr. Opin. Cell Biol.* **17**, 542-547.

Bagnat, M., Cheung, I. D., Mostov, K. E. and Stainier, D. Y. (2007). Genetic control of single lumen formation in the zebrafish gut. *Nature Cell Biol.* **9**, 954–960.

Bate, N., Gingras, A. R., Bachir, A., Horwitz, R., Ye, F., Patel, B., Goult, B. T. and Critchley, D. R. (2012). Talin contains a C-terminal calpain2 cleavage site important in focal adhesion dynamics. *PLoS One* **7**, e34461.

Beauvais-Jouneau, A. and Thiery, J. P. (1997). Multiple roles for integrins during development. *Biol. Cell* **89**, 5-11.

Beauvais, D. M. and Rapraeger, A. C. (2010). Syndecan-1 couples the insulin-like growth factor-1 receptor to inside-out integrin activation. *J. Cell Sci.* **123**, 3796-3807.

Beauvais, D. M., Ell, B. J., McWhorter, A. R. and Rapraeger, A. C. (2009). Syndecan-1 regulates alphavbeta3 and alphavbeta5 integrin activation during angiogenesis and is blocked by synstatin, a novel peptide inhibitor. J. Exp. Med. **206**, 691-705.

Begum, R., Nur-E-Kamal, M. S. and Zaman, M. A. (2004). The role of Rho GTPases in the regulation of the rearrangement of actin cytoskeleton and cell movement. *Exp. Mol. Med.* **36**, 358-366.

Belkin, A M. and Stepp, M. A. (2000). Integrins as receptors for laminins. *Microsc. Res. Tech.* **51**, 280-301.

Ben-Yosef, F. and Francomano, C. A. (1999). Characterization of the human talin (TLN) gene: genomic structure, chromosomal localization, and expression pattern. *Genomics* **62**, 316-319.

Berrier, A. L. and Yamada, K. M. (2007). Cell-matrix adhesion. *J. Cell Physiol.* **213**, 565-573.

Bharadwaj, R., Roy, M., Ohyama, T., Sivan-Loukianova, E., Delannoy, M., Lloyd, T. E., Zlatic, M., Eberl, D. F. and Kolodkin, A. L. (2013). Cbl-associated protein regulates assembly and function of two tension-sensing structures in Drosophila. *Development* **140**, 627-638.

Bhoopathi, P., Gondi, C. S., Gujrati, M., Dinh, D. H. and Lakka, S. S. (2011). SPARC mediates Src-induced disruption of actin cytoskeleton via inactivation of small GTPases Rho-Rac-Cdc42. *Cell Signal*. **23**, 1978-1987.

Bodmer, R. (1993). The gene tinman is required for specification of the heart and visceral muscles in Drosophila. *Development* **118**, 719-729.

Bier, E. and Bodmer, R. (2004). Drosophila, an emerging model for cardiac disease. *Gene* **342**, 1-11.

Bier, E., Vaessin, H., Shepherd, S., Lee, K., McCall, K., Barbel, S., Ackerman, L., Carretto, R., Uemura, T., Grell, E., *et al.* (1989). Searching for pattern and mutation in the *Drosophila* genome with a P-lacZ vector. *Genes. Dev.* **3**, 1273-1287.

Bledzka, K., Bialkowska, K., Nie, H., Qin, J., Byzova, T., Wu, C., Plow, E. F. and Ma, Y. Q. (2010). Tyrosine phosphorylation of integrin beta3 regulates kindlin-2 binding and integrin activation. *J. Biol. Chem*. **285**, 30370-30374.

Bodmer, R. (1993). The gene tinman is required for specification of the heart and visceral muscles in *Drosophila*. *Development* **118**, 719-29.

Bodmer, R. (1995). Heart development in Drosophila and its relationship to vertebrates. *Trends Cardiovasc. Med.* **5**, 21-28.

Boggon, T. J. and Eck, M. J. (2004). Structure and regulation of Src family kinases. *Oncogene* **23**, 7918-7927.

Bour, B. A., O'Brien, M. A., Lockwood, W. L., Goldstein, E. S., Bodmer, R., Taghert, P. H., Abmayr, S. M. and Nguyen, H. T. (1995). Drosophila MEF2, a transcription factor that is essential for myogenesis. *Trends Cardiovasc. Med*. **5**, 21-28.

Bouvard, D., Brakebusch, C., Gustafsson, E., Aszódi, A., Bengtsson, T., Berna, A. and Fässler, R. (2001). Functional consequences of integrin gene mutations in mice. *Circ. Res.* **89**, 211-223.

Brabant, M. C., Fristrom, D., Bunch, T. A. and Brower, D. L. (1996). Distinct spatial and temporal functions for PS integrins during Drosophila wing morphogenesis. *Development* **122**, 3307-3317.

Bradley, P. L., Myat, M. M., Comeaux, C. A. and Andrew, D. J. (2003). Posterior migration of the salivary gland requires an intact visceral mesoderm and integrin function. *Dev. Biol.* **257**, 249-262.

Brancaccio, M., Cabodi, S., Belkin, A. M., Collo, G., Koteliansky, V. E., Tomatis, D., Altruda, F., Silengo, L. and Tarone, G. (1998). Differential onset of expression of alpha 7 and beta 1D integrins during mouse heart and skeletal muscle development. *Cell Adhes. Commun.* **5**, 193-205.

Brandt, R. and Paululat, A. (2013). Microcompartments in the Drosophila heart and the mammalian brain: general features and common principles. *Biol. Chem.* **394**, 217-230.

Broadie, K., Baumgartner, S. and Prokop, A. (2011). Extracellular matrix and its receptors in Drosophila neural development. *Dev. Neurobiol.* **71**, 1102-1130.

Brower, D. L. (2003). Platelets with wings: the maturation of Drosophila integrin biology. *Curr. Opin. Cell Biol.* **15**, 607-613.

Brower, D.L. and Jaffe, S. M. (1989). Requirement for integrins during Drosophila wing development. *Nature* **342**, 285-287.

Brown, M. C., West, K. A. and Turner, C. E. (2002a). Paxillin-dependent paxillin kinase linker and p21-activated kinase localization to focal adhesions involves a multistep activation pathway. *Mol. Biol. Cell* **13**, 1550-1565.

Brown, N.H., Gregory, S. L., Rickoll, W. L., Fessler, L. I., Prout, M., White, R. A. and Fristrom, J. W. (2002b). Talin is essential for integrin function in Drosophila. *Dev. Cell* **3**, 569-579.

Bryant, D. M. and Mostov, K. E. (2008). From cells to organs: building polarized tissue. *Nat. Rev. Mol. Cell Biol.* **9**, 887-901.

Bryant, D. M., Datta, A., Rodríguez-Fraticelli, A. E., Peränen, J., Martín-Belmonte, F. and Mostov, K. E. (2010). A molecular network for de novo generation of the apical surface and lumen. *Nat. Cell Biol*. **12**, 1035-1045.

Bryantsev, A. L. and Cripps, R. M. (2009). Cardiac gene regulatory networks in Drosophila. *Biochim. Biophys. Acta.* **1789**, 343-353.

Calderwood, D. A. and Ginsberg, M. H. (2003). Talin forges the links between integrins and actin. *Nat. Cell Biol.* **5**, 694-697.

Calderwood, D. A., Yan, B., de Pereda, J. M., Alvarez, B. G., Fujioka, Y., Liddington, R. C. and Ginsberg, M. H. (2002). The phosphotyrosine binding-like domain of talin activates integrins*. J. Biol. Chem.* **277**, 21749-21758.

Calì, G., Zannini, M., Rubini, P., Tacchetti, C., D'Andrea, B., Affuso, A., Wintermantel, T., Boussadia, O., Terracciano, D., Silberschmidt, D., *et al.* (2007). Conditional inactivation of the E-cadherin gene in thyroid follicular cells affects gland development but does not impair junction formation. *Endocrinology* **148**, 2737-2746.

Calzada, M. J., Sipes, J. M., Krutzsch, H. C., Yurchenco, P. D., Annis, D. S., Mosher, D. F. and Roberts, D. D. (2003). Recognition of the N-terminal modules of thrombospondin-1 and thrombospondin-2 by alpha6beta1 integrin*. J. Biol. Chem.* **278**, 40679-40687.

Canel, M., Serrels, A., Miller, D., Timpson, P., Serrels, B., Frame, M. C. and Brunton, V. G. (2010). Quantitative in vivo imaging of the effects of inhibiting integrin signaling via Src and FAK on cancer cell movement: effects on E-cadherin dynamics. *Cancer Res.* **70**, 9413-9422.

Canel, M., Serrels, A., Frame, M. C. and Brunton, V. G. (2013). E-cadherin-integrin crosstalk in cancer invasion and metastasis. *J. Cell Sci*. **126**, 393-401.

Carisey, A., Tsang, R., Greiner, A. M., Nijenhuis, N., Heath, N., Nazgiewicz, A., Kemkemer, R., Derby, B., Spatz, J., Ballestrem, C. (2013). Vinculin regulates the recruitment and release of core focal adhesion proteins in a force-dependent manner. *Curr. Biol.* **23**, 271-281.

Carlson, T. R., Hu, H., Braren, R., Kim, Y. H. and Wang, R. A. (2008). Cell-autonomous requirement for beta1 integrin in endothelial cell adhesion, migration and survival during angiogenesis in mice. *Development* **135**, 2193-2202.

Carver, W., Price, R. L., Raso, D. S., Terracio, L. and Borg, T. K. (1994). Distribution of beta-1 integrin in the developing rat heart. *J. Histochem. Cytochem*. **42**, 167-175.

Caswell, P. T., Vadrevu, S. and Norman, J. C. (2009). Integrins: masters and slaves of endocytic transport. *Nat. Rev. Mol. Cell Biol.* **10**, 843-853.

Catterson, J. H., Heck, M. M. and Hartley, P. S. (2013). Fermitins, the orthologs of mammalian Kindlins, regulate the development of a functional cardiac syncytium in Drosophila melanogaster. *PLoS One* **8**, e62958.

Chan, K. T., Bennin, D. A. and Huttenlocher, A. (2010). Regulation of adhesion dynamics by calpain-mediated proteolysis of focal adhesion kinase (FAK). *J. Biol. Chem.* **285**, 11418-11426.

Chang, J. H., Gill, S., Settleman, J. and Parsons, S. J. (1995). c-Src regulates the simultaneous rearrangement of actin cytoskeleton, p190RhoGAP, and p120RasGAP following epidermal growth factor stimulation. *J. Cell Biol*. **130**, 355-368.

Chartier, A., Zaffran, S., Astier, M., Semeriva, M. and Gratecos, D. (2002). Pericardin, a Drosophila type IV collagen-like protein is involved in the morphogenesis and maintenance of the heart epithelium during dorsal ectoderm closure. *Development* **129**, 3241-3253.

Chatzizacharias, N. A., Kouraklis, G. P. and Theocharis, S. E. (2010). The role of focal adhesion kinase in early development. *Histol. Histopathol*. **25**, 1039-1055.

Chen, J. N. and Fishman, M. C. (2000). Genetics of heart development. *Trends Genet* **16**, 383-8.

Chen, C. and Sheppard, D. (2007). Identification and molecular characterization of multiple phenotypes in integrin knockout mice. *Methods Enzymol*. **426**, 291-305.

Chen, H. C., Appeddu, P. A., Parsons, J. T., Hildebrand, J. D., Schaller, M. D. and Guan, J. L. (1995). Interaction of focal adhesion kinase with cytoskeletal protein talin. *J. Biol. Chem*. **270**, 16995-16999.

Chen, G. C., Turano, B., Ruest, P. J., Hagel, M., Settleman, J. and Thomas, S. M. (2005). Regulation of Rho and Rac signaling to the actin cytoskeleton by paxillin during Drosophila development. *Mol. Cell. Biol.* **25**, 979-987.

Choi, C. K., Vicente-Manzanares, M., Zareno, J., Whitmore, L. A., Mogilner, A. and Horwitz, A. R. (2008). Actin and alpha-actinin orchestrate the assembly and maturation of nascent adhesions in a myosin II motor-independent manner. *Nat. Cell Biol.* **10**, 1039-1050.

Chou, T. B. and Perrimon, N. (1996). The autosomal FLP-DFS technique for generating germline mosaics in Drosophila melanogaster. *Genetics* **144**, 1673-1679.

Clark, E. A., King, W. G., Brugge, J. S., Symons, M. and Hynes, R. O. (1998). Integrin-mediated signals regulated by members of the rho family of GTPases. *J. Cell Biol.* **142**, 573-586.

Clark, K. A., McGrail, M. and Beckerle, M. C. (2003). Analysis of PINCH function in Drosophila demonstrates its requirement in integrin-dependent cellular processes. *Development* **130**, 2611-2621.

Colognato, H., Winkelmann, D. A. and Yurchenco, P. D. (1999). Laminin polymerization induces a receptor-cytoskeleton network*. J. Cell Biol.* **145**, 619-631.

Comber, K., Huelsmann, S., Evans, I., Sánchez-Sánchez, B. J., Chalmers, A., Reuter, R., Wood, W., and Martín-Bermudo, M. D. (2013). A dual role for the βPS integrin myospheroid in mediating Drosophila embryonic macrophage migration. *J. Cell Sci.* **126**, 3475-3484.

Conti, F. J., Felder, A., Monkley, S., Schwander, M., Wood, M. R., Lieber, R., Critchley, D. and Müller, U. (2008). Progressive myopathy and defects in the maintenance of myotendinous junctions in mice that lack talin 1 in skeletal muscle. *Development* **135**, 2043-2053.

Conti, F. J., Monkley, S. J., Wood, M. R., Critchley, D. R. and Müller, U. (2009). Talin 1 and 2 are required for myoblast fusion, sarcomere assembly and the maintenance of myotendinous junctions. *Development* **136**, 3597-3606.

Cooper, J. A., Gould, K. L., Cartwright, C. A. and Hunter, T. (1986). Tyr527 is phosphorylated in pp60c-src: implications for regulation. *Science* **231**, 1431-1444.

Copp, A. J. and Greene, N. D. (2010). Genetics and development of neural tube defects*. J. Pathol.* **220**, 217-230.

Cortesio, C. L., Boateng, L. R., Piazza, T. M., Bennin, D. A. and Huttenlocher, A. (2011). Calpain-mediated proteolysis of paxillin negatively regulates focal adhesion dynamics and cell migration. *J. Biol. Chem.* **286**, 9998-10006.

Cota, C. D., Segade, F. and Davidson, B. (2014). Heart genetics in a small package, exploiting the condensed genome of Ciona intestinalis. *Brief Funct. Genomics* **13**, 3-14.

Cram, E. J., Clark, S. G. and Schwarzbauer, J. E. (2003). Talin loss-of-function uncovers roles in cell contractility and migration in C. elegans*. J. Cell Sci.* **116**, 3871-3878.

Das, M., Subbayya Ithychanda, S., Qin, J. and Plow, E.F. (2014). Mechanisms of talin-dependent integrin signaling and crosstalk. *Biochim. Biophys. Acta.* **1838**, 579-588.

Datta, A., Byrant, D. M. and Mostov, K. E. (2011). Molecular regulation of lumen morphogenesis. *Curr. Biol.* **21**, R126-136.

Davis, G. E. and Senger, D. R. (2005). Endothelial extracellular matrix: biosynthesis, remodeling, and functions during vascular morphogenesis and neovessel stabilization. *Circ. Res.* **97**, 1093-1107.

DiPersio, C. M., Hodivala-Dilke, K. M., Jaenisch, R., Kreidberg, J. A., Hynes, R. O. (1997). alpha3beta1 Integrin is required for normal development of the epidermal basement membrane*. J. Cell Biol.* **137**, 729-742.

Deakin, N.O. and Turner, C. E. (2008). Paxillin comes of age*. J. Cell Sci.* **121**, 2435-2444.

Delon, I. and Brown, N. H. (2009). The integrin adhesion complex changes its composition and function during morphogenesis of an epithelium*. J. Cell Sci*. **122**, 4363-4374.

Deng, W. M., Schneider, M., Frock, R., Castillejo-Lopez, C., Gaman, E. A., Baumgartner, S. and Ruohola-Baker, H. (2003). Dystroglycan is required for polarizing the epithelial cells and the oocyte in Drosophila. *Development* **130**, 173-184.

Desclozeaux, M., Venturato, J., Wylie, F. G., Kay, J. G., Joseph, S. R., Le, H. T. and Stow, J. L. (2008). Active Rab11 and functional recycling endosome are required for E-cadherin trafficking and lumen formation during epithelial morphogenesis. *Am. J. Physiol. Cell Physiol.* **295**, 545-556.

Deshmukh, L., Meller, N., Alder, N., Byzova, T. and Vinogradova, O. (2011). Tyrosine phosphorylation as a conformational switch: a case study of integrin β3 cytoplasmic tail*. J. Biol. Chem*. **286**, 40943-40953.

Dodson, G. S., Guarnieri, D. J. and Simon, M. A. (1988). Src64 is required for ovarian ring canal morphogenesis during Drosophila oogenesis. *Development* **125**, 2883-2892.

Domigan, C. K. and Iruela-Arispe, M. L. (2012). Recent advances in vascular development. *Curr. Opin. Hematol*. **19**, 176-183.

Drake, C. J., Davis, L. A. and Little, C. D. (1992). Antibodies to beta 1-integrins cause alterations of aortic vasculogenesis, in vivo. *Dev. Dyn*. **193**, 83-91.

Drechsler, M., Schmidt, A. C., Meyer, H. and Paululat, A. (2013). The conserved ADAMTS-like protein lonely heart mediates matrix formation and cardiac tissue integrity. *PLoS Genet*. **9**, e1003616.

Duband, J. L, Rocher, S., Chen, W. T., Yamada, K. M. and Thiery, J. P. (1986). Cell adhesion and migration in the early vertebrate embryo: location and possible role of the putative fibronectin receptor complex*. J. Cell Biol.* **102**, 160-178.

Eide, B. L., Turck, C. W. and Escobedo, J. A. (1995). Identification of Tyr-397 as the primary site of tyrosine phosphorylation and pp60src association in the focal adhesion kinase, pp125FAK. *Mol. Cell Biol*. **15**, 2819-2827.

Ellis, S. J., Pines, M., Fairchild, M. J. and Tanentzapf, G. (2011). In vivo functional analysis reveals specific roles for the integrin-binding sites of talin. *J. Cell Sci.* **124**, 1844-1856.

Ellis, S. J., Goult, B. T., Fairchild, M. J., Harris, N. J., Long, J., Lobo, P., Czerniecki, S., Van Petegem, F., Schöck, F., Peifer, M. and Tanentzapf, G. (2013). Talin autoinhibition is required for morphogenesis. *Curr. Biol.* **23**, 1825-1833.

Emerson, M. M. and Van Vactor, D. (2002). Robo is Abl to block N-Cadherin function. *Nat. Cell Biol.* **4**, E227-230.

Evans, T. (1997). Regulation of cardiac gene expression by GATA-4/5/6. *TCM* **7**, 75–83.

Fahed, A. C., Gelb, B. D., Seidman, J. G. and Seidman, C. E. (2013). Genetics of congenital heart disease: the glass half empty. *Circ. Res.* **112**, 707-720.

Fässler, R. and Meyer, M. (1995). Consequences of lack of b1 integrin gene expression in mice. *Genes Dev*. **9**, 1896-1908.

Ferrari, A., Veligodskiy, A., Berge, U., Lucas, M. S. and Kroschewski, R. (2008). ROCK-mediated contractility, tight junctions and channels contribute to the conversion of a preapical patch into apical surface during isochoric lumen initiation. *J. Cell Sci.* **121**, 3649-3663.

Fillingham, I., Gingras, A. R., Papagrigoriou, E., Patel, B., Emsley, J., Critchley, D. R., Roberts, G. C. and Barsukov, I. L. (2005). A vinculin binding domain from the talin rod unfolds to form a complex with the vinculin head. *Structure* **13**, 65-74.

Fincham, V. J., Brunton, V. G. and Frame, M. C. (2000). The SH3 domain directs acto-myosin-dependent targeting of v-Src to focal adhesions via phosphatidylinositol 3-kinase. *Mol. Cell Biol*. **20**, 6518-6536.

Fish, J. E., Wythe, J. D., Xiao, T., Bruneau, B. G., Stainier, D. Y., Srivastava, D. and Woo, S. (2011). A Slit/miR-218/Robo regulatory loop is required during heart tube formation in zebrafish. *Development* **138**, 1409-1419.

Filipenko, N. R., Attwell, S., Roskelley, C. and Dedhar, S. (2005). Integrin-linked kinase activity regulates Rac- and Cdc42-mediated actin cytoskeleton reorganization via alpha-PIX. *Oncogene* **24**, 5837-5849.

Flevaris, P., Stojanovic, A., Gong, H., Chishti, A., Welch, E. and Du, X. (2007). A molecular switch that controls cell spreading and retraction. *J. Cell Biol.* **179**, 553-565.

Förster, D., Armbruster, K. and Luschnig, S. (2010). Sec24-dependent secretion drives cell-autonomous expansion of tracheal tubes in Drosophila. *Curr. Biol*. **20**, 62-68.

Fox, G. L., Rebay, I. and Hynes, R. O. (1999). Expression of DFak56, a Drosophila homolog of vertebrate focal adhesion kinase, supports a role in cell migration in vivo. *Proc. Natl. Acad. Sci. U S A* **96**, 14978-14983.

Franco, S. J., Rodgers, M. A., Perrin, B. J., Han, J., Bennin, D. A., Critchley, D. R. and Huttenlocher, A. (2004). Calpain-mediated proteolysis of talin regulates adhesion dynamics. *Nat. Cell Biol.* **6**, 977-983.

Franco-Cea, A., Ellis, S. J., Fairchild, M. J., Yuan, L., Cheung, T. Y. and Tanentzapf, G. (2010). Distinct developmental roles for direct and indirect talin-mediated linkage to actin. *Dev. Biol*. **345**, 64-77.

Frasch, M. (1995). Induction of visceral and cardiac mesoderm by ectodermal Dpp in the early *Drosophila* embryo. *Nature* **374**, 464-7.

Freeman, M. (1996). Reiterative use of the EGF receptor triggers differentiation of all cell types in the Drosophila eye. *Cell* **87**, 651-660.

Fu, Y., Yan, W., Mohun, T. J. and Evans, S. M. (1998). Vertebrate tinman homologues XNkx2-3 and XNkx2-5 are required for heart formation in a functionally redundant manner. *Development* **125**, 4439-49.

Fukuda, K., Knight, J. D., Piszczek, G., Kothary, R. and Qin, J. (2011). Biochemical, proteomic, structural, . and thermodynamic characterizations of integrin-linked kinase (ILK): cross-validation of the pseudokinase. *J. Biol. Chem.* **286**, 21886–21895.

Fujimoto, J., Sawamoto, K., Okabe, M., Takagi, Y., Tezuka, T., Yoshikawa, S., Ryo, H., Okano, H. and Yamamoto, T. (1999). Cloning and characterization of Dfak56, a homolog of Focal Adhesion Kinase, in Drosophila melanogaster. *J. Biol. Chem*. **274**, 29196-29201.

Gajewski, K., Fossett, N., Molkentin, J. D. and Schulz, R. A. (1999). The zinc finger proteins Pannier and GATA4 function as cardiogenic factors in *Drosophila*. *Development* **126**, 5679-88.

García-Alvarez, B., de Pereda, J. M., Calderwood, D. A., Ulmer, T. S., Critchley, D., Campbell, I. D., Ginsberg, M. H. and Liddington, R. C. (2003). Structural determinants of integrin recognition by Talin. *Mol. Cell* **11**, 49-58.

Gassama-Diagne, A., Yu, W., ter Beest, M., Martin-Belmonte, F., Kierbel, A., Engel, J. and Mostov, K. (2006). Phosphatidylinositol-3,4,5-trisphosphate regulates the formation of the basolateral plasma membrane in epithelial cells. *Nat. Cell Biol.* **8**, 963-970.

Georges-Labouesse, E., Mark, M., Messaddeq, N., Gansmuller, A. (1998). Essential role of alpha6 integrins in cortical and retinal lamination. *Curr Biol*. **8**, 983-986.

Ghabrial, A., Luschnig, S., Adelstein, R. S. and Krasnow, M. A. (2003). Branching morphogenesis of the Drosophila tracheal system. *Annu. Rev. Cell Dev. Biol.* **19**, 623-647.

Ghassemi, S., Meacci, G., Liu, S., Gondarenko, A. A., Mathur, A., Roca-Cusachs, P., Sheetz, M. P. and Hone, J. (2012). Cells test substrate rigidity by local contractions on submicrometer pillars. *Proc. Natl. Acad. Sci. U S A* **109**, 5328-5333.

Ghatak, S., Morgner, J. and Wickström, S. A. (2013). ILK: a pseudokinase with a unique function in the integrin-actin linkage. *Biochem. Soc. Trans.* **41**, 995-1001.

Gingras, A. R., Ziegler, W. H., Frank, R., Barsukov, I. L., Roberts, G. C., Critchley, D. R. and Emsley, J. (2005). Mapping and consensus sequence identification for multiple vinculin binding sites within the talin rod. *J. Biol. Chem.* **280**, 37217-37224.

Gingras, A. R., Bate, N., Goult, B. T., Hazelwood, L., Canestrelli, I., Grossmann, J. G., Liu, H., Putz, N. S., Roberts, G. C., Volkmann, N. *et al.* (2008). The structure of the C-terminal actin-binding domain of talin. *EMBO J.* **27**, 458-469.

Gingras, A. R., Ziegler, W. H., Bobkov, A. A., Joyce, M. G., Fasci, D., Himmel, M., Rothemund, S., Ritter, A., Grossmann, J. G., Patel, B., *et al.* (2009). Structural determinants of integrin binding to the talin rod. *J. Biol. Chem*. **284**, 8866-8876.

Goh, K. L., Yang, J. T. and Hynes, R. O. (1997). Mesodermal defects and cranial neural crest apoptosis in alpha5 integrin-null embryos. *Development* **124**, 4309-4319.

Goksoy, E., Ma, Y. Q., Wang, X., Kong, X., Perera, D., Plow, E. F. and Qin, J. (2008). Structural basis for the autoinhibition of talin in regulating integrin activation. *Mol. Cell* **31**, 124-133.

Goldring, J. P. D. and Coetzer, T. H. T. (2003). Isolation of chicken immunoglobulins (IgY) from egg yolk. *Biochem. Mol. Biol. Ed*. **31**, 185-187.

Gonzalo, P., Moreno, V., Gálvez, B. G. and Arroyo, A. G. (2010). MT1-MMP and integrins: Hand-to-hand in cell communication. *Biofactors* **36**, 248-254.

Goult, B. T., Zacharchenko, T., Bate, N., Tsang, R., Hey, F., Gingras, A. R., Elliott, P. R., Roberts, G. C., Ballestrem, C., Critchley, D. R., Barsukov, I. L. (2013a). RIAM and vinculin binding to talin are mutually exclusive and regulate adhesion assembly and turnover. *J. Biol. Chem*. **288**, 8238-8249.

Goult, B. T., Xu, X. P., Gingras, A. R., Swift, M., Patel, B., Bate, N., Kopp, P. M., Barsukov, I. L., Critchley, D. R., Volkmann, N. *et al.* (2013b). Structural studies on full-length talin1

reveal a compact auto-inhibited dimer: implications for talin activation. *J. Struct. Biol.* **184**, 21-32.

Grabbe, C., Zervas, C. G., Hunter, T., Brown, N. H. and Palmer, R. H. (2004). Focal adhesion kinase is not required for integrin function or viability in Drosophila. *Development* **131**, 5795-5805.

Gratecos, D., Naidet, C., Astier, M., Thiery, J. P. and Sémériva, M. (1988). Drosophila fibronectin: a protein that shares properties similar to those of its mammalian homologue. *EMBO J.* **7**, 215-223.

Greutmann, M. and Tobler, D. (2012). Changing epidemiology and mortality in adult congenital heart disease: looking into the future. *Future Cardiol.* **8**, 171-177.

Grow, M. W. and Krieg, P. A. (1998). Tinman function is essential for vertebrate heart development: elimination of cardiac differentiation by dominant inhibitory mutants of the tinman-related genes, XNkx2-3 and XNkx2-5. *Dev. Biol.* **204**, 187-196.

Gunst, S. J. and Zhang, W. (2008). Actin cytoskeletal dynamics in smooth muscle: a new paradigm for the regulation of smooth muscle contraction. *Am. J. Physiol. Cell Physiol.* **295**, C576-C587.

Gupton, S. L. and Gertler, F. B. (2010). Integrin signaling switches the cytoskeletal and exocytic machinery that drives neuritogenesis. *Dev. Cell* **18**, 725-736.

Gustafsson, E. and Fässler, R. (2000). Insights into extracellular matrix functions from mutant mouse models. *Exp. Cell Res.* **261**, 52-68.

Haag, T. A., Haag, N. P., Lekven, A. C. and Hartenstein, V. (1999). The role of cell adhesion molecules in *Drosophila* heart morphogenesis: faint sausage, shotgun/DE-cadherin, and laminin A are required for discrete stages in heart development. *Dev. Biol.* **208**, 56-69.

Han, Z., Yi, P., Li, X. and Olson, E. N. (2006). Hand, an evolutionarily conserved bHLH transcription factor required for *Drosophila* cardiogenesis and hematopoiesis. *Development* **133**, 1175-1182.

Harburger, D. S. and Calderwood, D. A. (2009). Integrin signalling at a glance. *J. Cell Sci.* **122**, 159-163.

Harburger, D. S., Bouaouina, M. and Calderwood, D. A. (2009). Kindlin-1 and -2 directly bind the C-terminal region of beta integrin cytoplasmic tails and exert integrin-specific activation effects. *J. Biol. Chem*. **284**, 11485-11497.

Harden, N., Lee, J., Loh, H. Y., Ong, Y. M., Tan, I., Leung, T., Manser, E. and Lim, L. (1996). A Drosophila homolog of the Rac- and Cdc42-activated serine/threonine kinase PAK is a

potential focal adhesion and focal complex protein that colocalizes with dynamic actin structures. *Mol. Cell Biol*. **16**, 1896-1908.

Harpaz, N. and Volk, T. (2012). A novel method for obtaining semi-thin cross sections of the Drosophila heart and their labeling with multiple antibodies. *Methods* **56**, 63-68.

Harpaz, N., Ordan, E., Ocorr, K., Bodmer, R. and Volk, T. (2013). Multiplexin promotes heart but not aorta morphogenesis by polarized enhancement of slit/robo activity at the heart lumen. *PLoS Genet*. **9**, e1003597.

Hartenstein, V. and Mandal, L. (2006). The blood/vascular system in a phylogenetic perspective. *Bioessays* **28**, 1203-1210.

Haverslag, R., Pasterkamp, G. and Hoefer, I. E. (2008). Targeting adhesion molecules in cardiovascular disorders. *Cardiovasc. Hematol. Disord. Drug Targets* **8**, 252-260.

Hemmings, L., Rees, D. J., Ohanian, V., Bolton, S. J., Gilmore, A. P., Patel, B., Priddle, H., Trevithick, J. E., Hynes, R. O. and Critchley, D. R. (1996). Talin contains three actin-binding sites each of which is adjacent to a vinculin-binding site. *J. Cell Sci.* **109**, 2715-2726.

Henchcliffe, C., García-Alonso, L., Tang, J. and Goodman, C. S. (1993). Genetic analysis of laminin A reveals diverse functions during morphogenesis in Drosophila. *Development* **118**, 325-337.

Hogan, B. L. and Kolodziej, P. A. (2002). Organogenesis: molecular mechanisms of tubulogenesis. *Nat. Rev. Genet*. **3**, 513-523.

Hohenester, E., Hussain, S. and Howitt, J. A. (2006). Interaction of the guidance molecule Slit with cellular receptors. *Biochem. Soc. Trans*. **34**, 418-421.

Holtzman, N. G., Schoenebeck, J. J., Tsai, H. J. and Yelon, D. (2007). Endocardium is necessary for cardiomyocyte movement during heart tube assembly. *Development* **134**, 2379-2386.

Hozumi, K., Kobayashi, K., Katagiri, F., Kikkawa, Y., Kadoya, Y. and Nomizu, M. (2010). Syndecan- and integrin-binding peptides synergistically accelerate cell adhesion. *FEBS Lett.* **584**, 3381-3385.

Huang, C., Rajfur, Z., Yousefi, N., Chen, Z., Jacobson, K. and Ginsberg, M. H. (2009). Talin phosphorylation by Cdk5 regulates Smurf1-mediated talin head ubiquitylation and cell migration. *Nat. Cell Biol.* **11**, 624-630.

Humphries, J. D., Wang, P., Streuli, C., Geiger, B., Humphries, M. J. and Ballestrem, C. (2007). Vinculin controls focal adhesion formation by direct interactions with talin and actin. *J. Cell Biol.* **179**, 1043-1057.

Hynes, R. O. (1987). Integrins: a family of cell surface receptors. *Cell* **48**, 549-554.

Hynes, R. O. (2002). Integrins: bidirectional, allosteric signaling machines. *Cell* **110**, 673-687.

Hynes, R. O. (2007). Cell-matrix adhesion in vascular development. *J. Thromb. Haemost*. **5**, 32-40.

Israeli-Rosenberg, S., Manso, A. M., Okada, H. and Ross, R. S. (2014). Integrins and integrin-associated proteins in the cardiac myocyte. *Circ. Res.* **114**, 572-586.

Iruela-Arispe, L. and Davis, G. E. (2009). Cellular and Molecular Mechanisms of Vascular Lumen Formation. *Dev. Cell* **16**, 222-231.

Jacobs, J. R. and Goodman, C. S. (1989). Embryonic development of axon pathways in the *Drosophila* CNS. I. A glial scaffold appears before the first growth cones. *J. Neurosci.* **9**, 2402-2411.

Jacinto, A., Woolner, S. and Martin, P. (2002). Dynamic analysis of dorsal closure in Drosophila: from genetics to cell biology. *Dev. Cell* **3**, 9-19.

Jannuzi, A. L., Bunch, T. A., West, R. F. and Brower, D. L. (2004). Identification of integrin beta subunit mutations that alter heterodimer function in situ. *Mol. Biol. Cell* **15**, 3829-3840.

Jiang, G., Giannone, G., Critchley, D. R., Fukumoto, E. and Sheetz, M. P. (2003). Two-piconewton slip bond between fibronectin and the cytoskeleton depends on talin. *Nature* **424**, 334-337.

Jiao, Y., Feng, X., Zhan, Y., Wang, R., Zheng, S., Liu, W. and Zeng, X. (2012). Matrix metalloproteinase-2 promotes αvβ3 integrin-mediated adhesion and migration of human melanoma cells by cleaving fibronectin. *PLoS One* **7**, e41591.

Johnson, K. G., Ghose, A., Epstein, E., Lincecum, J., O'Connor, M. B. and Van Vactor, D. (2004). Axonal heparan sulfate proteoglycans regulate the distribution and efficiency of the repellent slit during midline axon guidance. *Curr. Biol.* **14**, 499-504.

Jones, T. A. and Metzstein, M. M. (2011). A novel function for the PAR complex in subcellular morphogenesis of tracheal terminal cells in Drosophila melanogaster. *Genetics* **189**, 153-164.

Jones, C. A., London, N. R., Chen, H., Park, K. W., Sauvaget, D., Stockton, R. A., Wythe, J. D., Suh, W., Larrieu-Lahargue, F., Mukouyama, Y. S. *et al.* (2008). Robo4 stabilizes the vascular network by inhibiting pathologic angiogenesis and endothelial hyperpermeability. *Nat. Med*. **14**, 448-453.

Jung, J. J., Inamdar, S. M., Tiwari, A., Ye, D., Lin, F. and Choudhury, A. (2013). Syntaxin 16 regulates lumen formation during epithelial morphogenesis. *PLoS One* **8**, e61857.

Keller, R. S., Shai, S. Y., Babbitt, C. J., Pham, C. G., Solaro, R. J., Valencik, M. L., Loftus, J. C., Ross, R. S. (2001). Disruption of Integrin Function in the Murine Myocardium Leads to Perinatal Lethality, Fibrosis, and Abnormal Cardiac Performance. *Am. J. Pathol.* **158**, 1079-1090.

Kishimoto, Y., Lee, K. H., Zon, L., Hammerschmidt, M. and Schulte-Merker, S. (1997). The molecular nature of Zebrafish swirl: BMP2 function is essential during early dorsoventral patterning. *Development* **124**, 4457-66.

Koh, W., Mahan, R. D. and Davis, G. E. (2008). Cdc42- and Rac1-mediated endothelial lumen formation requires Pak2, Pak4 and Par3, and PKC-dependent signaling. *J. Cell Sci*. **121**, 989-1001.

Knox, J., Moyer, K., Yacoub, N., Soldaat, C., Komosa, M., Vassilieva, K., Wilk, R., Hu, J., Vazquez Paz Lde, L., Syed, Q., *et al.* (2011). Syndecan contributes to heart cell specification and lumen formation during *Drosophila* cardiogenesis. *Dev. Biol*. **356**, 279-90.

Kreidberg, J. A., Donovan, M. J., Goldstein, S. L., Rennke, H., Shepherd, K., Jones, R. C. and Jaenisch, R. (1996). Alpha 3 beta 1 integrin has a crucial role in kidney and lung organogenesis. *Development* **122**, 3537-3547.

Kucera, T., Strilić, B., Regener, K., Schubert, M., Laudet, V. and Lammert, E. (2009). Ancestral vascular lumen formation via basal cell surfaces. *PLoS One* **4**, e4132.

Kusche-Gullberg, M., Garrison, K., MacKrell, A. J., Fessler, L. I. and Fessler, J. H. (1992). Laminin A chain: expression during Drosophila development and genomic sequence. *EMBO J.* **11**, 4519-4527.

Lai, Z. C., Fortini, M. E. and Rubin, G. M. (1991). The embryonic expression patterns of zfh-1 and zfh-2, two Drosophila genes encoding novel zinc-finger homeodomain proteins. *Mech. Dev.* **34**, 123-134.

Landry, M. C., Champagne, C., Boulanger, M. C., Jetté, A., Fuchs, M., Dziengelewski, C. and Lavoie, J. N. (2014). A functional interplay between the small GTPase Rab11a and mitochondria-shaping proteins regulates mitochondrial positioning and polarization of the actin cytoskeleton downstream of Src family kinases. *J. Biol. Chem*. **289**, 2230-2249.

Lee, H. S., Anekal, P., Lim, C. J., Liu, C. C. and Ginsberg, M. H. (2013). Two modes of integrin activation form a binary molecular switch in adhesion maturation. *Mol. Biol. Cell.* **24**, 1354-1362.

Lee, H.S., Bellin, R. M., Walker, D. L., Patel, B., Powers, P., Liu, H., Garcia-Alvarez, B., de Pereda, J. M., Liddington, R. C., Volkmann, N., Hanein, D., Critchley, D. R. and Robson, R. M. (2004). Characterization of an actin-binding site within the talin FERM domain. *J. Mol. Biol.* **343**, 771-784.

Lee, M. Y., Skoura, A., Park, E. J., Landskroner-Eiger, S., Jozsef, L., Luciano, A. K., Murata, T., Pasula, S., Dong, Y., Bouaouina, M. *et al.* (2014). Dynamin 2 regulation of integrin endocytosis, but not VEGF signaling, is crucial for developmental angiogenesis. *Development* **141**, 1465-1472.

Legate, K. R., Takahashi, S., Bonakdar, N., Fabry, B., Boettiger, D., Zent, R. and Fässler, R. (2011). Integrin adhesion and force coupling are independently regulated by localized PtdIns(4,5)2 synthesis. *EMBO J.* **30**, 4539-4553.

Lehmacher, C., Abeln, B. and Paululat, A. (2012). The ultrastructure of Drosophila heart cells. *Arthropod Struct. Dev.* **41**, 459-474.

Lei, L., Liu, D., Huang, Y., Jovin, I., Shai, S. Y., Kyriakides, T., Ross, R. S. and Giordano, F. J. (2008). Endothelial expression of beta1 integrin is required for embryonic vascular patterning and postnatal vascular remodeling. *Mol. Cell Biol*. **28**, 794-802.

Lenard, A., Ellertsdottir, E., Herwig, L., Krudewig, A., Sauteur, L., Belting, H. G. and Affolter, M. (2013). In vivo analysis reveals a highly stereotypic morphogenetic pathway of vascular anastomosis. *Dev. Cell* **25**, 492-506.

Leptin, M., Bogaert, T., Lehmann, R. and Wilcox, M. (1989). The function of PS integrins during Drosophila embryogenesis. *Cell* **56**, 401-408.

Levi, B. P., Ghabrial, A. S. and Krasnow, M. A. (2006). Drosophila talin and integrin genes are required for maintenance of tracheal terminal branches and luminal organization. *Development* **133**, 2383-2393.

Li, X., Graner, M. W., Williams, E. L., Roote, C. E., Bunch, T. A. and Zusman, S. (1998). Requirements for the cytoplasmic domain of the alphaPS1, alphaPS2 and betaPS integrin subunits during Drosophila development. *Development* **125**, 701-711.

Li, W. Z., Li, S. L., Zheng, H. Y., Zhang, S. P. and Xue, L. (2012). A broad expression profile of the GMR-GAL4 driver in Drosophila melanogaster. *Genet. Mol. Res*. **11**, 1997-2002.

Lin, G., Zhang, X., Ren, J., Pang, Z., Wang, C., Xu, N., Xi, R. (2013). Integrin signaling is required for maintenance and proliferation of intestinal stem cells in Drosophila. *Dev. Biol.* **377**, 177-187.

Liu, J., Zhang, L., Wang, D., Shen, H., Jiang, M., Mei, P., Hayden, P. S., Sedor, J. R. and Hu, H. (2003). Congenital diaphragmatic hernia, kidney agenesis and cardiac defects associated with Slit3-deficiency in mice. *Mech. Dev.* **120**, 1059-1070.

Liu, S., Thomas, S. M., Woodside, D. G., Rose, D. M., Kiosses, W. B., Pfaff, M. and Ginsberg, M. H. (1999). Binding of paxillin to alpha4 integrins modifies integrin-dependent biological responses. *Nature* **402**, 676-681.

Liu, J., He, X., Qi, Y., Tian, X., Monkley, S. J., Critchley, D. R., Corbett, S. A., Lowry, S. F., Graham, A. M. and Li, S. (2011). Talin1 regulates integrin turnover to promote embryonic epithelial morphogenesis. *Mol. Cell Biol.* **31**, 3366-3377.

Löer, B., Bauer, R., Bornheim, R., Grell, J., Kremmer, E., Kolanus, W., Hoch, M. (2008). The NHL-domain protein Wech is crucial for the integrin-cytoskeleton link. *Nat. Cell Biol.* **10**, 422-428.

Lubarsky, B. and Krasnow, M. A. (2003). Tube morphogenesis: making and shaping biological tubes. *Cell* **112**, 19-28.

Macabenta, F. D., Jensen, A. G., Cheng, Y. S., Kramer, J. J. and Kramer, S. G. (2013). Frazzled/DCC facilitates cardiac cell outgrowth and attachment during Drosophila dorsal vessel formation. *Dev. Biol.* **380**, 233-240.

MacMullin, A. and Jacobs, J. R. (2006). Slit coordinates cardiac morphogenesis in *Drosophila*. *Dev. Biol.* **293**, 154-164.

Mailleux, A. A., Overholtzer, M. and Brugge, J. S. (2008). Lumen formation during mammary epithelial morphogenesis: insights from in vitro and in vivo models. *Cell Cycle* **7**, 57-62.

Malan, D., Wenzel, D., Schmidt, A., Geisen, C., Raible, A., Bölck, B., Fleischmann, B. K. and Bloch, W. (2010). Endothelial beta1 integrins regulate sprouting and network formation during vascular development. *Development* **137**, 993-1002.

Margadant, C., Kreft, M., de Groot, D. J., Norman, J. C. and Sonnenberg, A. (2012). Distinct roles of talin and kindlin in regulating integrin α5β1 function and trafficking. *Curr. Biol.* **22**, 1554-1563.

Markwald, R., Eisenberg, C., Eisenberg, L., Trusk, T. and Sugi, Y. (1996). Epithelial-mesenchymal transformations in early avian heart development. *Acta. Anat. (Basel)* **156**, 173-186.

Marques, S. R., Lee, Y., Poss, K. D. and Yelon, D. (2008). Reiterative roles for FGF signaling in the establishment of size and proportion of the zebrafish heart. *Dev. Biol.* **321**, 397-406.

Martel, V., Racaud-Sultan, C., Dupe, S., Marie, C., Paulhe, F., Galmiche, A., Block, M. R. and Albiges-Rizo, C. (2001). Conformation, localization, and integrin binding of talin depend on its interaction with phosphoinositides. *J. Biol. Chem*. **276**, 21217-21227.

Martin, D., Zusman, S., Li, X., Williams, E. L., Khare, N., DaRocha, S., Chiquet-Ehrismann, R. and Baumgartner, S. (1999). wing blister, a new Drosophila laminin alpha chain required for cell adhesion and migration during embryonic and imaginal development. *J. Cell Biol.* **145**, 191-201.

Martin-Belmonte, F. and Mostov, K. (2007). Phosphoinositides control epithelial development. *Cell Cycle* **6**, 1957-1961.

Martín-Belmonte, F., Yu, W., Rodríguez-Fraticelli, A. E., Ewald, A. J., Werb, Z., Alonso, M. A. and Mostov, K. (2008). Cell-polarity dynamics controls the mechanism of lumen formation in epithelial morphogenesis. *Curr. Biol.* **18**, 507-513.

Martin-Bermudo, M. D. and Brown, N. H. (1996). Intracellular signals direct integrin localization to sites of function in embryonic muscles. *J. Cell Biol.* **134**, 217-226.

Martin-Bermudo, M. D., Dunin-Borkowski, O. M. and Brown, N. H. (1998). Modulation of integrin activity is vital for morphogenesis. *J. Cell Biol.* **141**, 1073-1081.

Mathew, S., Lu, Z., Palamuttam, R. J., Mernaugh, G., Hadziselimovic, A., Chen, J., Bulus, N., Gewin, L. S., Voehler, M., Meves, A. *et al.* (2012). β1 integrin NPXY motifs regulate kidney collecting-duct development and maintenance by induced-fit interactions with cytosolic proteins. *Mol. Cell Biol.* **32**, 4080-4091.

McCann, R. O. and Craig, S. W. (1997). The I/LWEQ module: a conserved sequence that signifies F-actin binding in functionally diverse proteins from yeast to mammals. *Proc. Natl. Acad. Sci. U S A* **94**, 5679-5684.

Meder, D., Shevchenko, A., Simons, K. and Füllekrug, J. (2005). Gp135/podocalyxin and NHERF-2 participate in the formation of a preapical domain during polarization of MDCK cells. *J. Cell Biol.* **168**, 303-313.

Medioni, C., Astier, M., Zmojdzian, M., Jagla, K. and Sémériva, M. (2008). Genetic control of cell morphogenesis during *Drosophila* melanogaster cardiac tube formation**. J. Cell Biol.** *182*, 249-61.

Medioni, C., Sénatore, S., Salmand, P. A., Lalevée, N., Perrin, L. and Sémériva M. (2009). The fabulous destiny of the Drosophila heart. *Curr. Opin. Genet. Dev.* **19**, 518-525.

Medioni, C., Bertrand, N., Mesbah, K., Hudry, B., Dupays, L., Wolstein, O., Washkowitz, A. J., Papaioannou, V. E., Mohun, T. J., Harvey, R. P. and Zaffran, S. (2010). Expression of Slit and Robo genes in the developing mouse heart. *Dev. Dyn.* **239**, 3303-3311.

Mentzer, S. J., Crimmins, M. A. and Herrmann, S. H. (1988). Functional domains of the CD11a adhesion molecule in lymphokine activated killer (LAK)-mediated cytolysis. *J. Clin. Lab Immunol.* **27**, 155-161.

Millard, T. H. and Martin, P. (2008). Dynamic analysis of filopodial interactions during the zippering phase of Drosophila dorsal closure. *Development* **135**, 621-626.

Miranti, C. K. and Brugge, J. S. (2002). Sensing the environment: a historical perspective on integrin signal transduction. *Nat. Cell Biol.* **4**, E83-E90.

Moes, M., Rodius, S., Coleman, S. J., Monkley, S. J., Goormaghtigh, E., Tremuth, L., Kox, C., van der Holst, P. P., Critchley, D. R. and Kieffer, N. (2007). The integrin binding site 2 (IBS2) in the talin rod domain is essential for linking integrin beta subunits to the cytoskeleton. *J. Biol. Chem.* **282**, 17280-17288.

Mohseni, N., McMillan, S. C., Chaudhary, R., Mok, J. and Reed, B. H. (2009). Autophagy promotes caspase-dependent cell death during Drosophila development. *Autophagy* **5**, 329-338.

Molina, M. R. and Cripps, R. M. (2001). Ostia, the inflow tracts of the Drosophila heart, develop from a genetically distinct subset of cardial cells. *Mech. Dev.* **109**, 51-59.

Mommersteeg, M. T., Andrews, W. D., Ypsilanti,A. R., Zelina, P., Yeh, M. L., Norden, J., Kispert, A., Chédotal, A., Christoffels, V. M. and Parnavelas, J. G. (2013). Slit-roundabout signaling regulates the development of the cardiac systemic venous return and pericardium. *Circ. Res.* **112**, 465-475.

Monkley, S. J., Zhou, X. H., Kinston, S. J., Giblett, S. M., Hemmings, L., Priddle, H., Brown, J. E., Pritchard, C. A., Critchley, D. R. and Fässler, R. (2000). Disruption of the talin gene arrests mouse development at the gastrulation stage. *Dev. Dyn.* **219**, 560-574.

Monkley, S. J., Pritchard, C. A. and Critchley, D. R. (2001). Analysis of the mammalian talin2 gene TLN2. *Biochem. Biophys. Res. Commun.* **286**, 880-885.

Monkley, S. J., Kostourou, V., Spence, L., Petrich, B., Coleman, S., Ginsberg, M. H., Pritchard, C. A. and Critchley, D. R. (2011). Endothelial cell talin1 is essential for embryonic angiogenesis. *Dev. Biol*. **349**, 494-502.

Montell, D. J. and Goodman, C. S. (1989). Drosophila laminin: sequence of B2 subunit and expression of all three subunits during embryogenesis. *J. Cell Biol.* **109**, 2441-2453.

Moorman, A., Webb, S., Brown, N. A., Lamers, W. and Anderson, R. H. (2003). Development of the heart: (1) formation of the cardiac chambers and arterial trunks. *Heart* **89**, 806-814.

Moreira, C. G., Jacinto, A. and Prag, S. (2013). Drosophila integrin adhesion complexes are essential for hemocyte migration in vivo. *Biol. Open* **2**, 795-801.

Morgan, M. R., Humphries, M. J. and Bass, M. D. (2007). Synergistic control of cell adhesion by integrins and syndecans. *Nat. Rev. Mol. Cell Biol.* **8**, 957-969.

Morgan, M. R., Hamidi, H., Bass, M. D., Warwood, S., Ballestrem, C. and Humphries, M. J. (2013). Syndecan-4 phosphorylation is a control point for integrin recycling. *Dev. Cell* **24**, 472-485.

Murakami, S., Umetsu, D,. Maeyama, Y., Sato, M., Yoshida S. and Tabata, T. (2007). Focal adhesion kinase controls morphogenesis of the Drosophila optic stalk. *Development* **134**, 1539-1548.

Narita, R., Yamashita, H., Goto, A., Imai, H., Ichihara, S., Mori, H. and Kitagawa, Y. (2004). Syndecan-dependent binding of Drosophila hemocytes to laminin alpha3/5 chain LG4-5 modules: Potential role in sessile hemocyte islets formation. *FEBS Lett*. **576**, 127-132.

Nemer, M. (2008). Genetic insights into normal and abnormal heart development. *Cardiovasc. Pathol.* **17**, 48-54.

Nusslein-Volhard, C., Wieschaus, E. and Kluding, H. (1984). Mutations affecting the pattern of the larval cuticle in Drosophila melanogaster I. Zygotic loci on the second chromosome. *Wilh. Roux's Arch. Dev. Biol.* **193**, 267-282.

Ocorr, K., Perrin, L., Lim, H. Y., Qian, L., Wu, X. and Bodmer, R. (2007). Genetic control of heart function and aging in Drosophila. *Trends Cardiovasc. Med.* **17**, 177-182.

Olson, E. N. (2006). Gene regulatory networks in the evolution and development of the heart. *Science* **313**, 1922-1927.

Owens, D. W., McLean, G. W., Wyke, A. W., Paraskeva, C., Parkinson, E. K., Frame, M. C. and Brunton, V. G. (2000). The catalytic activity of the Src family kinases is required to disrupt cadherin-dependent cell-cell contacts. *Mol. Biol. Chem*. **11**, 51-64.

Palacios, F., Tushir, J. S., Fujita, Y. and D'Souza-Schorey, C. (2005). Lysosomal targeting of E-cadherin: a unique mechanism for the down-regulation of cell-cell adhesion during epithelial to mesenchymal transitions. *Mol. Cell Biol*. **25**, 389-402.

Palmer, R. H., Fessler, L. I., Edeen, P. T., Madigan, S. J., McKeown, M. and Hunter, T. (1999). DFak56 is a novel Drosophila melanogaster focal adhesion kinase. *J. Biol. Chem*. **274**, 35621-35629.

Papagrigoriou, E., Gingras, A. R., Barsukov, I. L., Bate, N., Fillingham, I. J., Patel, B., Frank, R., Ziegler, W. H., Roberts, G. C., Critchley, D. R. and Emsley, J. (2004). Activation of a vinculin-binding site in the talin rod involves rearrangement of a five-helix bundle. *EMBO J.* **23**, 2942-2951.

Parsons, J. T. (2003). Focal adhesion kinase: the first ten years. *J. Cell Sci.* **116**, 1409-1416.

Patel, N. H. (1994). Imaging neuronal subsets and other cell types in whole-mount Drosophila embryos and larvae using antibody probes. *Methods Cell Biol.* **44**, 445-487.

Paul, J. D., Coulombe, K. L., Toth, P. T., Zhang, Y., Marsboom, G., Bindokas, V. P., Smith, D. W., Murry, C. E. and Rehman, J. (2013). SLIT3-ROBO4 activation promotes vascular network formation in human engineered tissue and angiogenesis in vivo. *J. Mol. Cell Cardiol.* **64**, 124-131.

Pedraza, L. G., Stewart, R. A., Li, D. M. and Xu, T. (2004). Drosophila Src-family kinases function with Csk to regulate cell proliferation and apoptosis. *Oncogene* **23**, 4754-4762.

Peng, H. B., Ali, A. A., Daggett, D. F., Rauvala, H., Hassell, J. R. and Smalheiser, N. R. (1998). The relationship between perlecan and dystroglycan and its implication in the formation of the neuromuscular junction. *Cell Adhes. Commun.* **5**, 475-489.

Perkins, A. D., Ellis, S. J., Asghari, P., Shamsian, A., Moore, E. D. and Tanentzapf, G. (2010). Integrin-mediated adhesion maintains sarcomeric integrity. *Dev. Biol.* **338**, 15-27.

Pfaff, M., Du, X. and Ginsberg, M. H. (1999). Calpain cleavage of integrin beta cytoplasmic domains. *FEBS Lett*. **460**, 17-22.

Pines, M., Fairchild, M. J. and Tanentzapf, G. (2011). Distinct regulatory mechanisms control integrin adhesive processes during tissue morphogenesis. *Dev. Dyn.* **240**, 36-51.

Pirraglia, C. and Myat, M. M. (2010). Genetic regulation of salivary gland development in *Drosophila melanogaster*. *Front Oral. Biol.* **14**, 32-47.

Pirraglia, C., Walters, J. and Myat, M. M. (2010). Pak1 control of E-cadherin endocytosis regulates salivary gland lumen size and shape. *Development* **137**, 4177-4189.

Pirraglia, C., Walters, J., Ahn, N. and Myat, M. M. (2013). Rac1 GTPase acts downstream of αPS1βPS integrin to control collective migration and lumen size in the Drosophila salivary gland. *Dev. Biol*. **377**, 21-32.

Playford, M. P. and Schaller, M. D. (2004). The interplay between Src and integrins in normal and tumor biology. *Oncogene* **23**, 7928-7946.

Prager-Khoutorsky, M., Lichtenstein, A., Krishnan, R., Rajendran, K., Mayo, A., Kam, Z., Geiger, B. and Bershadsky, A. D. (2011). Fibroblast polarization is a matrix-rigidity-

dependent process controlled by focal adhesion mechanosensing. *Nat. Cell Biol.* **13**, 1457-1465.

Price, L. S., Leng, J., Schwartz, M. A. and Bokoch, G. M. (1998). Activation of Rac and Cdc42 by integrins mediates cell spreading. *Mol. Biol. Cell* **9**, 1863-1871.

Prout, M., Damania, Z., Soong, J., Fristrom, D. and Fristrom, J. W. (1997). Autosomal mutations affecting adhesion between wing surfaces in Drosophila melanogaster. *Genetics* **146**, 275-285.

Qi, Y., Liu, J., Wu, X., Brakebusch, C., Leitges, M., Han, Y., Corbett, S. A., Lowry, S. F., Graham, A. M. and Li, S. (2011). Cdc42 controls vascular network assembly through protein kinase Cι during embryonic vasculogenesis. *Arterioscler. Thromb. Vasc. Biol*. **31**, 1861-1870.

Qian, L., Liu, J. and Bodmer, R. (2005). Slit and Robo control cardiac cell polarity and morphogenesis. *Curr. Biol.* **15**, 2271-2278.

Qin, J. and Wu, C. (2012). ILK: a pseudokinase in the center stage of cell-matrix adhesion and signaling*. Curr. Opin. Cell Biol.* **24**, 607-613.

Rainero, E. and Norman, J. C. (2013). Late endosomal and lysosomal trafficking during integrin-mediated cell migration and invasion: cell matrix receptors are trafficked through the late endosomal pathway in a way that dictates how cells migrate. *Bioessays* **35**, 523-532.

Ranganayakulu, G., Schulz, R. A. and Olson, E. N. (1996). Wingless signaling induces nautilus expression in the ventral mesoderm of the Drosophila embryo. *Dev. Biol.* **176**, 143-148.

Reed, B. H., McMillan, S. C. and Chaudhary, R. (2009). The preparation of Drosophila embryos for live-imaging using the hanging drop protocol*. J. Vis. Exp.* **25**, 1206.

Reifers, F., Walsh, E. C., Léger, S., Stainier, D. Y. and Brand, M. (2000). Induction and differentiation of the zebrafish heart requires fibroblast growth factor 8 (fgf8/acerebellar). *Development* **127**, 225-35.

Reim, I. and Frasch, M. (2010). Genetic and genomic dissection of cardiogenesis in the Drosophila model. *Pediatr. Cardiol.* **31**, 325-334.

Reiter, L.T., Potocki, L., Chien, S., Gribskov, M. and Bier, E. (2001). A systematic analysis of human disease-associated gene sequences in Drosophila melanogaster. *Genome Res.* **11**, 1114– 1125.

Reynolds, L. E., Wyder, L., Lively, J. C., Taverna, D., Robinson, S. D., Huang, X., Sheppard, D., Hynes, R. O. and Hodivala-Dilke, K. M. (2002). Enhanced pathological angiogenesis in mice lacking beta3 integrin or beta3 and beta5 integrins. *Nat. Med.* **8**, 27-34.

Ridley, A. J. (2011). Life at the leading edge. *Cell* **145**, 1012-1022.

Roberts, G. C. K. and Critchley, D. R. (2009). Structural and biophysical properties of the integrin-associated cytoskeletal protein talin. *Biophys. Rev.* **1**, 61-69.

Rodius, S., Chaloin, O., Moes, M., Schaffner-Reckinger, E., Landrieu, I., Lippens, G., Lin, M., Zhang, J. and Kieffer, N. (2008). The talin rod IBS2 alpha-helix interacts with the beta3 integrin cytoplasmic tail membrane-proximal helix by establishing charge complementary salt bridges. *J. Biol. Chem.* **283**, 24212-24223.

Roland, J. T., Bryant, D. M., Datta, A., Itzen, A., Mostov, K. E. and Goldenring, J. R. (2011). Rab GTPase-Myo5B complexes control membrane recycling and epithelial polarization. *Proc. Natl. Acad. Sci. U S A* **108**, 2789-2794.

Roote, C. E. and Zusman, S. (1995). Functions for PS integrins in tissue adhesion, migration, and shape changes during early embryonic development in Drosophila. *Dev. Biol.* **169**, 322-336.

Ross, R. S. (2002). The extracellular connections: the role of integrins in myocardial remodeling. *J. Card. Fail*. **8**, S326-S331.

Rørth, P. (2009). Collective cell migration. *Annu Rev Cell Dev Biol* **25**, 407-29.

Rudrapatna, V. A., Bangi, E. and Cagan, R. L. (2013). A Jnk-Rho-Actin remodeling positive feedback network directs Src-driven invasion. *Oncogene* [Epub ahead of print]

Rugendorff, A., Younossi-Hartenstein, A. and Hartenstein, V. (1994). Embryonic origin and differentiation of the Drosophila heart. *Roux's Arch. Dev. Biol*. **203**, 266-280.

Ruoslahti, E. and Pierschbacher, M. D. (1987). New perspectives in cell adhesion: RGD and integrins. *Science* **238**, 491-497.

Sacharidou, A., Koh, W., Stratman, A. N., Mayo, A. M., Fisher, K. E. and Davis, G. E. (2010). Endothelial lumen signaling complexes control 3D matrix-specific tubulogenesis through interdependent Cdc42- and MT1-MMP-mediated events. *Blood* **115**, 5259-5269.

Saga, S., Chen, W. T. and Yamada, K. M. (1988). Enhanced fibronectin receptor expression in Rous sarcoma virus-induced tumors. *Cancer Res.* **48**, 5510-5513.

Saltel, F., Mortier, E., Hytönen, V. P., Jacquier, M. C., Zimmermann, P., Vogel, V., Liu, W., Wehrle-Haller, B. (2009). New PI(4,5)P2- and membrane proximal integrin-binding motifs in the talin head control beta3-integrin clustering. *J. Cell Biol.* **187**, 715-731.

Santiago-Martínez, E., Soplop, N. H. and Kramer, S. G. (2006). Lateral positioning at the dorsal midline: Slit and Roundabout receptors guide Drosophila heart cell migration. *Proc. Natl. Acad Sci. U S A* **103**, 12442-12446.

Santiago-Martínez, E., Soplop, N. H., Patel, R. and Kramer, S. G. (2008). Repulsion by Slit and Roundabout prevents Shotgun/E-cadherin-mediated cell adhesion during Drosophila heart tube lumen formation. *J. Cell Biol.* **182**, 241-248.

Saraste, A. and Pulkki, K. (2000). Morphologic and biochemical hallmarks of apoptosis. *Cardiovasc. Res*. **45**, 528-537.

Schaller, M. D., Hildebrand, J. D. and Parsons, J. T. (1999). Complex formation with focal adhesion kinase: A mechanism to regulate activity and subcellular localization of Src kinases. *Mol. Biol. Cell* **10**, 3489-3505.

Schaller, M. D., Hildebrand, J. D., Shannon, J. D., Fox, J. W., Vines, R. R. and Parsons, J. T. (1994). Autophosphorylation of the focal adhesion kinase, pp125FAK, directs SH2-dependent binding of pp60src. Mol. Cell Biol. **14**, 1680-1688.

Schneider, M., Khalil, A. A., Poulton, J., Castillejo-Lopez, C., Egger-Adam, D., Wodarz, A., Deng, W. M. and Baumgartner, S. (2006). Perlecan and Dystroglycan act at the basal side of the Drosophila follicular epithelium to maintain epithelial organization. *Development* **133**, 3805-3815.

Schöck, F. and Perrimon, N. (2003). Retraction of the Drosophila germ band requires cell-matrix interaction. *Genes Dev.* **17**, 597-602.

Schultheiss, T. M., Burch, J. B. and Lassar, A. B. (1997). A role for bone morphogenetic proteins in the induction of cardiac myogenesis. *Genes Dev*. **11**, 451-62.

Serrels, A., Canel, M., Brunton, V. G. and Frame, M. C. (2011). Src/FAK-mediated regulation of E-cadherin as a mechanism for controlling collective cell movement: insights from in vivo imaging. *Cell Adh. Migr*. **5**, 260-365.

Seyres, D., Röder, L. and Perrin, L. (2012). Genes and networks regulating cardiac development and function in flies: genetic and functional genomic approaches. *Brief Funct. Genomics* **11**, 366-374.

Sheppard D. (2000). In vivo functions of integrins: lessons from null mutations in mice. *Matrix Biol.* **19**, 203-209.

Shindo, M., Wada, H., Kaido, M., Tateno, M., Aigaki, T., Tsuda, L. and Hayashi, S. (2008). Dual function of Src in the maintenance of adherens junctions during tracheal epithelial morphogenesis. *Development* **135**, 1355-1364.

Singhal, N. and Martin, P. T. (2011). Role of extracellular matrix proteins and their receptors in the development of the vertebrate neuromuscular junction. *Dev. Neurobiol.* **71**, 982-1005.

Small, E. M., Sutherland, L., Rajagopalan, K., Wang, S. and Olson, E. N. (2010). MicroRNA-218 regulates vascular patterning by modulation of Slit-Robo signaling. *Circ. Res.* **107**, 1336-1344.

Smith, S. J. and McCann, R. O. (2007). A C-terminal dimerization motif is required for focal adhesion targeting of Talin1 and the interaction of the Talin1 I/LWEQ module with F-actin. *Biochemistry* **46**, 10886-10898.

Smyth, N., Vatansever, H. S., Murray, P., Meyer, M., Frie, C., Paulsson, M. and Edgar, D. (1999). Absence of basement membranes after targeting the LAMC1 gene results in embryonic lethality due to failure of endoderm differentiation. *J. Cell Biol.* **144**, 151-160.

Song, X., Yang, J., Hirbawi, J., Ye, S., Perera, H. D., Goksoy, E., Dwivedi, P., Plow, E. F., Zhang, R. and Qin, J. (2012). A novel membrane-dependent on/off switch mechanism of talin FERM domain at sites of cell adhesion. *Cell Res.* **22**, 1533-1545.

Sonnenberg, A., Modderman, P. W. and Hogervorst, F. (1988). Laminin receptor on platelets is the integrin VLA-6. *Nature* **336**, 487-489.

Stark, K. A., Yee, G. H., Roote, C. E., Williams, E. L., Zusman, S. and Hynes, R. O. (1997). A novel alpha integrin subunit associates with betaPS and functions in tissue morphogenesis and movement during Drosophila development. *Development* **124**, 4583-4594.

Stephens, L. E., Sutherland, A. E., Klimanskaya, I. V., Andrieux, A., Meneses, J., Pedersen, R. A. and Damsky, C. H. (1995). Deletion of b1 integrins in mice results in inner cell mass failure and peri-implantation lethality. *Genes Dev*. **9**, 1883-1895.

Streuli, C. H. and Akhtar, N. (2009). Signal co-operation between integrins and other receptor systems. *Biochem. J.* **418**, 491-506.

Stevens, A. and Jacobs, J. R. (2002). Integrins regulate responsiveness to slit repellent signals. *J. Neurosci.* **22**, 4448-4455.

Strilić, B., Kucera, T., Eglinger, J., Hughes, M. R., McNagny, K. M., Tsukita, S., Dejana, E., Ferrara, N. and Lammert, E. (2009). The molecular basis of vascular lumen formation in the developing mouse aorta. *Dev. Cell* **17**, 505-515.

Syed, Q. R. (2012). Filopodial Activity of the Cardioblast Leading Edge in *Drosophila*. M.Sc. thesis. McMaster University, Canada.

Tadokoro, S., Shattil, S. J., Eto, K., Tai, V., Liddington, R. C., de Pereda, J. M., Ginsberg, M. H. and Calderwood, D. A. (2003). Talin binding to integrin beta tails: a final common step in integrin activation. *Science* **302**, 103-106.

Takahashi, F., Endo, S., Kojima, T. and Saigo, K. (1996). Regulation of cell-cell contacts in developing Drosophila eyes by Dsrc41, a new, close relative of vertebrate c-src. *Genes Dev*. **10**, 1645-1656.

Takahashi, M., Takahashi, F., Ui-Tei, K., Kojima, T. and Saigo, K. (2005). Requirements of genetic interactions between Src42A, armadillo and shotgun, a gene encoding E-cadherin, for normal development in Drosophila. *Development* **132**, 2547-2559.

Takala, H., Nurminen, E., Nurmi, S. M., Aatonen, M., Strandin, T., Takatalo, M., Kiema, T., Gahmberg, C. G., Ylänne, J. and Fagerholm, S. C. (2008). Beta2 integrin phosphorylation on Thr758 acts as a molecular switch to regulate 14-3-3 and filamin binding. *Blood* **112**, 1853-1862.

Tanaka-Matakatsu, M., Uemura, T., Oda, H., Takeichi, M. and Hayashi, S. (1996). Cadherin-mediated cell adhesion and cell motility in Drosophila trachea regulated by the transcription factor Escargot. *Development* **122**, 3697-3705.

Tanentzapf, G. and Brown, N. H. (2006). An interaction between integrin and the talin FERM domain mediates integrin activation but not linkage to the cytoskeleton. *Nat. Cell Biol.* **8**, 601-606.

Tanjore, H., Zeisberg, E. M., Gerami-Naini, B. and Kalluri, R. (2008). Beta1 integrin expression on endothelial cells is required for angiogenesis but not for vasculogenesis. *Dev. Dyn*. **237**, 75-82.

Tao, Y. and Schulz, R. A. (2007). Heart development in Drosophila. *Semin. Cell Dev. Biol.* **18**, 3-15.

Tao, Y., Wang, J., Tokusumi, T., Gajewski, K. and Schulz, R. A. (2007). Requirement of the LIM homeodomain transcription factor tailup for normal heart and hematopoietic organ formation in Drosophila melanogaster. *Mol. Cell Biol.* **27**, 3962-3969.

Tateno, M., Nishida, Y. and Adachi-Yamada, T. (2000). Regulation of JNK by Src during Drosophila development. *Science* **287**, 324-327.

Tawk, M., Araya, C., Lyons, D. A., Reugels, A. M., Girdler, G. C., Bayley, P. R., Hyde, D. R., Tada, M. and Clarke, J. D. (2007). A mirror-symmetric cell division that orchestrates neuroepithelial morphogenesis. *Nature* **446**, 797-800.

Terracio, L., Rubin, K., Gullberg, D., Balog, E., Carver, W., Jyring, R. and Borg, T. K. (1991). Expression of collagen binding integrins during cardiac development and hypertrophy. *Circ. Res*. **68**, 734-744.

Tokusumi, T., Russell, M., Gajewski, K., Fossett, N. and Schulz, R. A. (2007). U-shaped protein domains required for repression of cardiac gene expression in Drosophila. *Differentiation* **75**, 166-174.

Torgler, C. N., Narasimha, M., Knox, A. L., Zervas, C. G., Vernon, M. C. and Brown, N. H. (2004). Tensin stabilizes integrin adhesive contacts in Drosophila. *Dev. Cell* **6**, 357-369.

Tremuth, L., Kreis, S., Melchior, C., Hoebeke, J., Rondé, P., Plançon, S., Takeda, K. and Kieffer, N. (2004). A fluorescence cell biology approach to map the second integrin-binding site of talin to a 130-amino acid sequence within the rod domain. *J. Biol. Chem.* **279**, 22258-22266.

Treyer, A. and Müsch. A. (2013). Hepatocyte polarity. *Compr. Physiol.* **3**, 243-287.

Tsai, P. I., Kao, H. H., Grabbe, C., Lee, Y. T., Ghose, A., Lai, T. T., Peng, K. P., Van Vactor, D., Palmer, R. H., Chen, R. H., Yeh, S. R. and Chien, C. T. (2008). Fak56 functions downstream of integrin alphaPS3betanu and suppresses MAPK activation in neuromuscular junction growth. *Neural. Dev.* **3**, 26.

Tu, C., Ortega-Cava, C. F., Winograd, P., Stanton, M. J., Reddi, A. L., Dodge, I., Arya, R., Dimri, M., Clubb, R. J., Naramura, M. *et al.* (2010). Endosomal-sorting complexes required for transport (ESCRT) pathway-dependent endosomal traffic regulates the localization of active Src at focal adhesions. *Proc. Natl. Acad. Sci U S A* **107**, 16107-16112.

Turlo, K. A., Noel, O. D., Vora, R., LaRussa, M., Fassler, R., Hall-Glenn, F. and Iruela-Arispe, M. L. (2012). An essential requirement for β1 integrin in the assembly of extracellular matrix proteins within the vascular wall. *Dev. Biol.* **365**, 23-35.

Ulrich, F. and Heisenberg, C. P. (2009). Trafficking and cell migration. *Traffic* **10**, 811-818.

Vakaloglou, K. M., Chountala, M. and Zervas, C. G. (2012). Functional analysis of parvin and different modes of IPP-complex assembly at integrin sites during Drosophila development. *J. Cell Sci*. **125**, 3221-3232.

Valencik, M. L., Keller, R. S., Loftus, J. C. and McDonald, J. A. (2002). A lethal perinatal cardiac phenotype resulting from altered integrin function in cardiomyocytes. *J. Card. Fail.* **8**, 262-272.

van der Bom, T., Zomer, A. C., Zwinderman, A. H., Meijboom, F. J., Bouma, B. J. and Mulder, B. J. (2011). The changing epidemiology of congenital heart disease. *Nat. Rev. Cardiol.* **8**, 50-60.

van der Linde, D., Konings, E. E., Slager, M. A., Witsenburg, M., Helbing, W. A., Takkenberg, J. J., Roos-Hesselink, J. W. (2011). Birth prevalence of congenital heart disease worldwide: a systematic review and meta-analysis*. J. Am. Coll. Cardiol.* **58**, 2241-2247.

Vanderploeg, J., Vazquez Paz, L. L., MacMullin, A. and Jacobs, J. R. (2012). Integrins are required for cardioblast polarisation in Drosophila. *BMC Dev. Biol.* **12**, 8.

van der Neut, R., Krimpenfort, P., Calafat, J., Niessen, C. M., Sonnenberg, A. (1996). Epithelial detachment due to absence of hemidesmosomes in integrin beta4 null mice. *Nat Genet*. **13**, 366-369.

Vicente-Manzanares, M., Ma, X., Adelstein, R. S. and Horwitz, A. R. (2009). Non-muscle myosin II takes centre stage in cell adhesion and migration. *Nat. Rev. Mol. Cell Biol.* **10**, 778-790.

Wang, P., Ballestrem, C. and Streuli, C. H. (2011). The C terminus of talin links integrins to cell cycle progression*. J. Cell Biol.* **195**, 499-513.

Wang, H., Leavitt, L., Ramaswamy, R. and Rapraeger, A. C. (2010). Interaction of syndecan and alpha6beta4 integrin cytoplasmic domains: regulation of ErbB2-mediated integrin activation. *J. Biol. Chem*. **285**, 13569-13579.

Wang, J., Tao, Y., Reim, I., Gajewski, K., Frasch, M. and Schulz. R. A. (2005). Expression, regulation, and requirement of the toll transmembrane protein during dorsal vessel formation in Drosophila melanogaster. *Mol. Cell Biol.* **25**, 4200-4210.

Weber, G. F., Bjerke, M. A. and DeSimone, D. W. (2011). Integrins and cadherins join forces to form adhesive networks*. J. Cell Sci.* **124**, 1183-1193.

Wegener, K. L., Partridge, A. W., Han, J., Pickford, A. R., Liddington, R. C., Ginsberg, M. H. and Campbell, I. D. (2007). Structural basis of integrin activation by talin. *Cell* **128**, 171-182.

Weng, Z., Taylor, J. A., Turner, C. E., Brugge, J. S. and Seidel-Dugan, C. (1993). Detection of Src homology 3-binding proteins, including paxillin, in normal and v-Src-transformed Balb/c 3T3 cells*. J. Biol. Chem*. **268**, 14956-14963.

Whitelock, J. M., Melrose, J. and Iozzo, R. V. (2008). Diverse cell signaling events modulated by perlecan. *Biochemistry* **47**, 11174-11183.

Wickström, S. A., Lange, A., Montanez, E., and Fässler, R. (2010). The ILK/PINCH/parvin complex: the kinase is dead, long live the pseudokinase! *EMBO J.* **29**, 281-291.

Wieschaus, E., Nüsslein-Volhard, C. and Jürgens, G. (1984). Mutations affecting the pattern of the larval cuticle in Drosophila melanogaster: III. Zygotic loci on the X-chromosome and fourth chromosome. *Wilhem Roux Arch. Dev. Biol.* **193**, 296-307.

Wilcox, M., DiAntonio, A. and Leptin, M. (1989). The function of PS integrins in Drosophila wing morphogenesis. *Development* **107**, 891-897.

Willenborg, C., Jing, J., Wu, C., Matern, H., Schaack, J., Burden, J. and Prekeris, R. (2011). Interaction between FIP5 and SNX18 regulates epithelial lumen formation. *J. Cell Biol.* **195**, 71-86.

Williams, J. C., Weijland, A., Gonfloni, S., Thompson, A., Courtneidge, S. A., Superti-Furga, G. and Wierenga, R. K. (1997). The 2.35 A crystal structure of the inactivated form of chicken Src: a dynamic molecule with multiple regulatory interactions. *J. Mol. Biol*. **274**, 757-775.

Wolfenson, H., Lavelin, I. and Geiger, B. (2013). Dynamic regulation of the structure and functions of integrin adhesions. *Dev. Cell* **24**, 447-458.

Wong, K., Ren, X. R., Huang, Y. Z., Xie, Y., Liu, G., Saito, H., Tang, H., Wen, L., Brady-Kalnay, S. M., Mei, L. *et al.* (2001). Signal transduction in neuronal migration: roles of GTPase activating proteins and the small GTPase Cdc42 in the Slit- Robo pathway. *Cell* **107**, 209-221.

Wu, M. and Sato, T. N. (2008). On the mechanics of cardiac function of Drosophila embryo*. PLoS One* **3**, e4045.

Xing, B., Jedsadayanmata, A. and Lam, S. C. (2001). Localization of an integrin binding site to the C terminus of talin. *J. Biol. Chem.* **276**, 44373-44378.

Xu, W., Harrison, S. C. and Eck, M. J. (1997). Three-dimensional structure of the tyrosine kinase c-Src. *Nature* **385**, 595-602.

Xu, X., Yin, Z., Hudson, J. B., Ferguson, E. L. and Frasch, M. (1998). Smad proteins act in combination with synergistic and antagonistic regulators to target Dpp responses to the Drosophila mesoderm. *Genes Dev.* **12**, 2354-2370.

Yadav, S. S. and Narayan, G. (2014). Role of ROBO4 Signalling in Developmental and Pathological Angiogenesis. *Biomed. Res. Int.* 2014, 683025 [Epub ahead of print]

Yamashita, H., Goto, A., Kadowaki, T. and Kitagawa, Y. (2004). Mammalian and Drosophila cells adhere to the laminin alpha4 LG4 domain through syndecans, but not glypicans. *Biochem. J.* **382**, 933-943.

Yan, B., Calderwood, D. A., Yaspan, B. and Ginsberg, M. H. (2001). Calpain cleavage promotes talin binding to the beta 3 integrin cytoplasmic domain. *J. Biol. Chem*. **276**, 28164-28170.

Yang, J. T., Rayburn, H. and Hynes, R. O. (1993). Embryonic mesodermal defects in alpha 5 integrin-deficient mice. *Development* **119**, 1093-1105.

Yang, J. T., Rayburn, H. and Hynes, R. O. (1995). Cell adhesion events mediated by alpha 4 integrins are essential in placental and cardiac development. *Development* **121**, 549-560.

Yarnitzky, T. and Volk, T. (1995). Laminin is required for heart, somatic muscles, and gut development in the Drosophila embryo. *Dev. Biol*. **169**, 609-618.

Yates, L. A., Füzéry, A. K., Bonet, R., Campbell, I. D. and Gilbert, R. J. (2012). Biophysical analysis of Kindlin-3 reveals an elongated conformation and maps integrin binding to the membrane-distal β-subunit NPXY motif. *J. Biol. Chem.* **287**, 37715-37731.

Ye, F., Petrich, B. G., Anekal, P., Lefort, C. T., Kasirer-Friede, A., Shattil, S. J., Ruppert, R., Moser, M., Fässler, R. and Ginsberg, M. H. (2013). The mechanism of kindlin-mediated activation of integrin αIIbβ3. *Curr. Biol*. **23**, 2288-2295.

Yu, W., Datta, A., Leroy, P., O'Brien, L. E., Mak, G., Jou, T. S., Matlin, K. S., Mostov, K. E. and Zegers, M. M. (2005). Beta1-integrin orients epithelial polarity via Rac1 and laminin. *Mol. Biol. Cell* **16**, 433-445.

Yuan, L., Fairchild, M. J., Perkins, A. D. and Tanentzapf, G. (2010). Analysis of integrin turnover in fly myotendinous junctions. *J. Cell Sci.* **123**, 939-946.

Yue, J., Zhang, K. and Chen, J. (2012). Role of integrins in regulating proteases to mediate extracellular matrix remodeling. *Cancer Microenviron*. **5**, 275-283.

Yurchenco, P. D. (2011). Basement membranes: cell scaffoldings and signaling platforms. *Cold Spring Harb. Perspect. Biol.* **3**, a004911.

Zaidel-Bar, R., Ballestrem, C., Kam, Z. and Geiger, B. (2003). Early molecular events in the assembly of matrix adhesions at the leading edge of migrating cells. *J. Cell Sci*. **116**, 4605-4613.

Zaidel-Bar, R., Itzkovitz, S., Ma'ayan, A., Iyengar, R., and Geiger, B. (2007a). Functional atlas of the integrin adhesome. *Nat. Cell Biol.* **9**, 858–867.

Zaidel-Bar, R., Milo, R., Kam, Z., and Geiger, B. (2007b). A paxillin tyrosine phosphorylation switch regulates the assembly and form of cell-matrix adhesions. *J. Cell Sci.* **120**, 137–148.

Zemljic-Harpf, A., Manso, A. M. and Ross, R. S. (2009). Vinculin and talin: focus on the myocardium. *J. Investig. Med.* **57**, 849-855.

Zervas, C. G., Psarra, E., Williams, V., Solomon, E., Vakaloglou, K. M. and Brown, N. H. (2011). A central multifunctional role of integrin-linked kinase at muscle attachment sites. *J. Cell Sci.* **124**, 1316-1327.

Zhang, M., Liu, J., Cheng, A., Deyoung, S. M., Chen, X., Dold, L. H. and Saltiel, A. R. (2006). CAP interacts with cytoskeletal proteins and regulates adhesion-mediated ERK activation and motility. *EMBO J.* **25**, 5284-5293.

Zhang, H., Kim, A., Abraham, N., Khan, L. A., Hall, D. H., Fleming, J. T. and Gobel, V. (2012). Clathrin and AP-1 regulate apical polarity and lumen formation during C. elegans tubulogenesis. *Development* **139**, 2071-2083.

Zhao, X. and Guan, J. L. (2011). Focal adhesion kinase and its signaling pathways in cell migration and angiogenesis. *Adv. Drug. Deliv. Rev*. **63**, 610-615.

Zhao, Y., Malinin, N. L., Meller, J., Ma, Y., West, X. Z., Bledzka, K., Qin, J., Podrez, E. A. and Byzova, T. V. (2012). Regulation of cell adhesion and migration by Kindlin-3 cleavage by calpain. *J. Biol. Chem.* **287**, 40012-40020.

Zhong, T. P. (2005). Zebrafish genetics and formation of embryonic vasculature. *Curr Top Dev Biol* **71**, 53-81.

Ziegler, W. H., Gingras, A. R., Critchley, D. R. and Emsley, J. (2008). Integrin connections to the cytoskeleton through talin and vinculin. *Biochem. Soc. Trans.* **36**, 235-239.

Zovein, A. C., Luque, A., Turlo, K. A., Hofmann, J. J., Yee, K. M., Becker, M. S., Fassler, R., Mellman, I., Lane, T. F. and Iruela-Arispe, M. L. (2010). Beta1 integrin establishes endothelial cell polarity and arteriolar lumen formation via a Par3-dependent mechanism. *Dev. Cell* **18**, 39-51.

Supplemental methods information

APPENDIX A

Appendix A.1 – LanA is detected in multiple tissues in the *Drosophila* embryo

Whole-mount wildtype stage 17 embryos labeled with αLaminin A (LanA) were visualized by confocal microscopy. **(A-A'')** On the embryonic dorsal side, LanA is detected along both the apical (arrow) and basal (arrowhead) heart surfaces and segmentally between the somatic muscles (*). A' and A'' are maximum projections of 9µm, while A projects only the most dorsal 5 µm. **(B-B'')** Ventrally, LanA is detected in the central nervous system, primarily within the mesectodermal strand (v) or more laterally on glial cells (>; Montell and Goodman 1989). B is a 10µm ventral projection, B' is a 14 µm projection of tissue immediately dorsal to B, and B'' is a maximum projection of both B and B'. **(C-C'')** Lateral projection images (10-16 µm thick) of the embryo show αLanA along the lateral ectoderm (C), internal organs (C') and possibly the nerve cord (C''). These labeling patterns are consistent with those seen using broader polyclonal anti-lanA antibodies (Kusche-Gullberg *et al.* 1992, Montell and Goodman 1989), suggesting that this detects all LanA rich regions. Calibration: 10 microns.

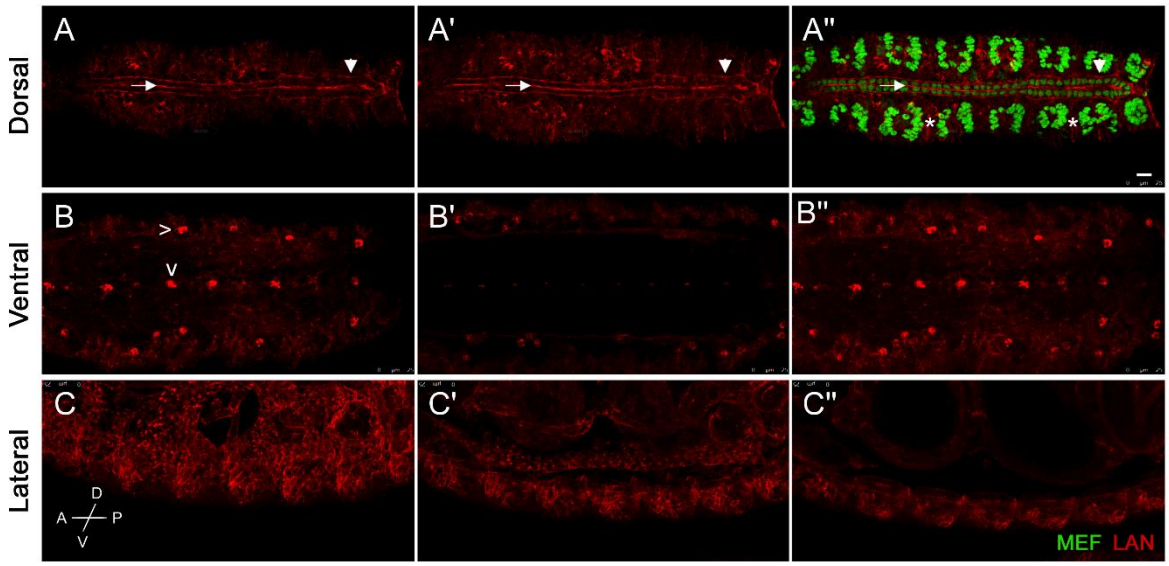
Dorsal
Ventral
Lateral
A
A'
A"
B
B'
B"
C
C'
C"
>
v
D
A
P
V
MEF LAN

Appendix A.2 – Genetic scheme to generate maternal and zygotic *rhea* null embryos

To generate embryos lacking both maternal and zygotic Talin, mitotic recombination was induced in the germ-line of $rhea^{79}/ovo^{D1}$ larvae. To do this, the following crosses were performed. Males carrying ovo^{D1}, a dominant female sterile allele, were crossed to females with a heat-shock inducible Flippase recombinase (FLPase) transgene (hsFLP). Males with both ovo^{D1} and hsFLP were crossed to $rhea^{79}$, FRT heterozygotes (FRT = FLPase recognition target). Larval progeny were heat-shocked to induce expression of FLPase. In ovo^{D1}, FRT/$rhea^{79}$, FRT larvae, FLPase triggered mitotic recombination at the FRT sites, generating mutant $rhea^{79}/rhea^{79}$ clones. These $rhea^{79}/ovo^{D1}$ heterozygous female adults had $rhea^{79}/rhea^{79}$ clones, and when such clones were present in the ovary, eggs with no maternal contribution were produced. Crossing these females with heterozygous $rhea^{79}$ males generated $rhea^{79}/rhea^{79}$ embryos lacking both maternal and zygotic Talin. Ovaries with the female sterile allele ovo^{D1} do not produce eggs, so all embryos collected were from $rhea^{79}/rhea^{79}$ female germ-line clone.

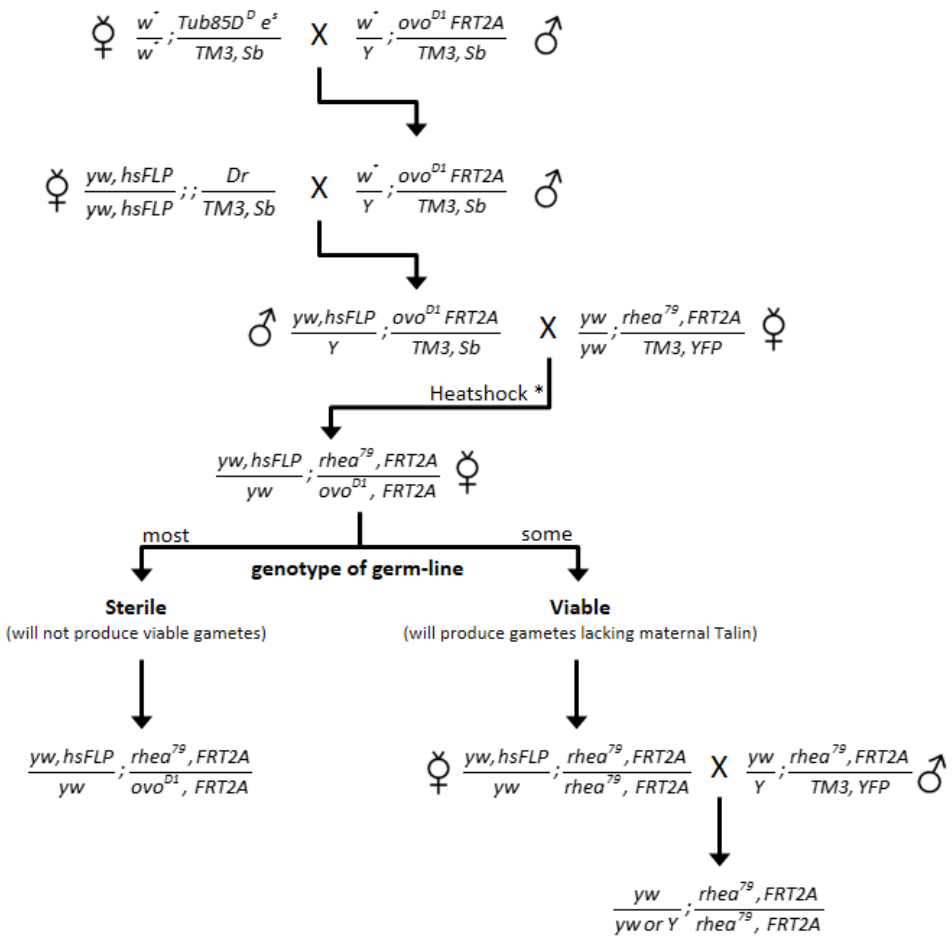

To differentiate from zygotic mutant embryos (with maternal Talin), germ-line clone derived embryos are termed: $\frac{rhea^{79}GLC}{rhea^{79}}$ or $rhea^{79}GLC/rhea^{79}$

* Heatshocks were performed on three consecutive days at the larval stage (1 hour per day)

Appendix A.3 – Genetic scheme to create strain for live imaging experiments

Embryos suitable for live imaging of the cardial cell nuclei and leading edge activity required several genetic elements within a single chromosome. tupGFP labels the cardioblast nuclei. Moesin-mcherry was expressed in cardioblasts under control of the dMEF promoter using the yeast derived Gal4-UAS system (Gal4 - transcription activator; UAS - Gal4-specific enhancer). The first series of crosses were used to select recombinant chromosomes harboring three genetic elements: dMEF-Gal4, tupGFP, and UAS-moesin-mcherry. Embryos with this chromosome were used for RNAi, mys^{1}, and $src42A^{E1}$ experiments (eg. Figure 3.6, D.4, Table 3.1). The second series of crosses were used to further recombine the $rhea^{79}$ allele onto this chromosome and then maintain the chromosome in a balanced stock. This was necessary as $rhea^{79}$, like the other necessary genetic elements, is on the third chromosome.

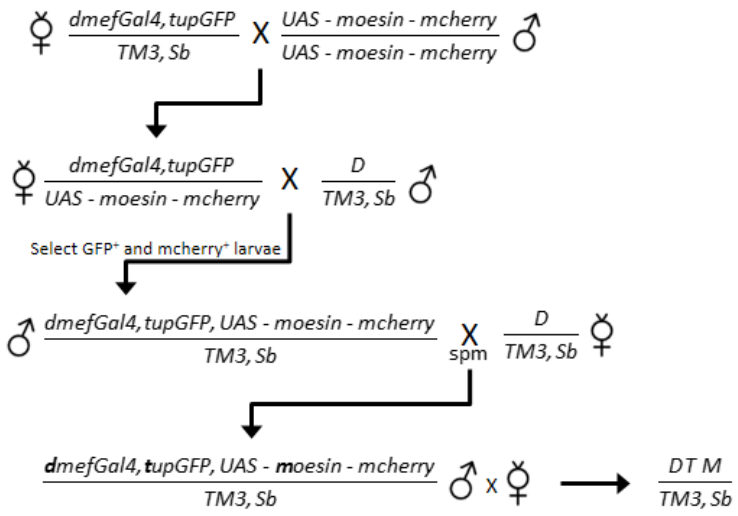

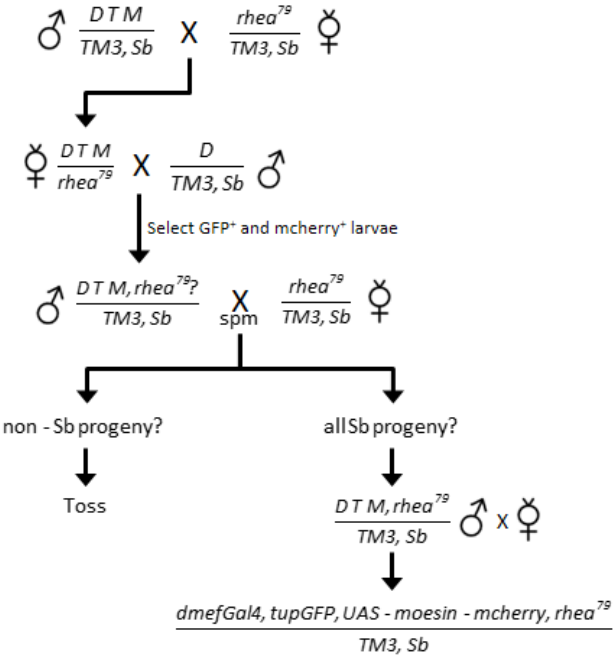

*spm = single pair mate (numerous putative recombinant males individually crossed)

Appendix A.4 – Genetic schemes to express Talin transgenes in *rhea*^{79} homozygous embryos

Strains carrying full length and modified Talin transgenes were outcrossed three times to a wildtype strain to eliminate potential modifying mutations which accumulated since the strain was originally created. Following this, a series of crosses were used to create stable strains that carried both the transgene and the *rhea*^{79} allele. Appropriate marked and balancer chromosomes were used to create stable stocks that allowed for accurate selection of the necessary chromosomes. These stable strains were crossed to *rhea*^{79} heterozygotes ("Experimental" cross) to produce *rhea*^{79} homozygous embryos carrying a single copy of the rescue transgene. Example genetic schemes are shown for transgenes on the X (**A**), second (**B**), and third (**C**) chromosomes.

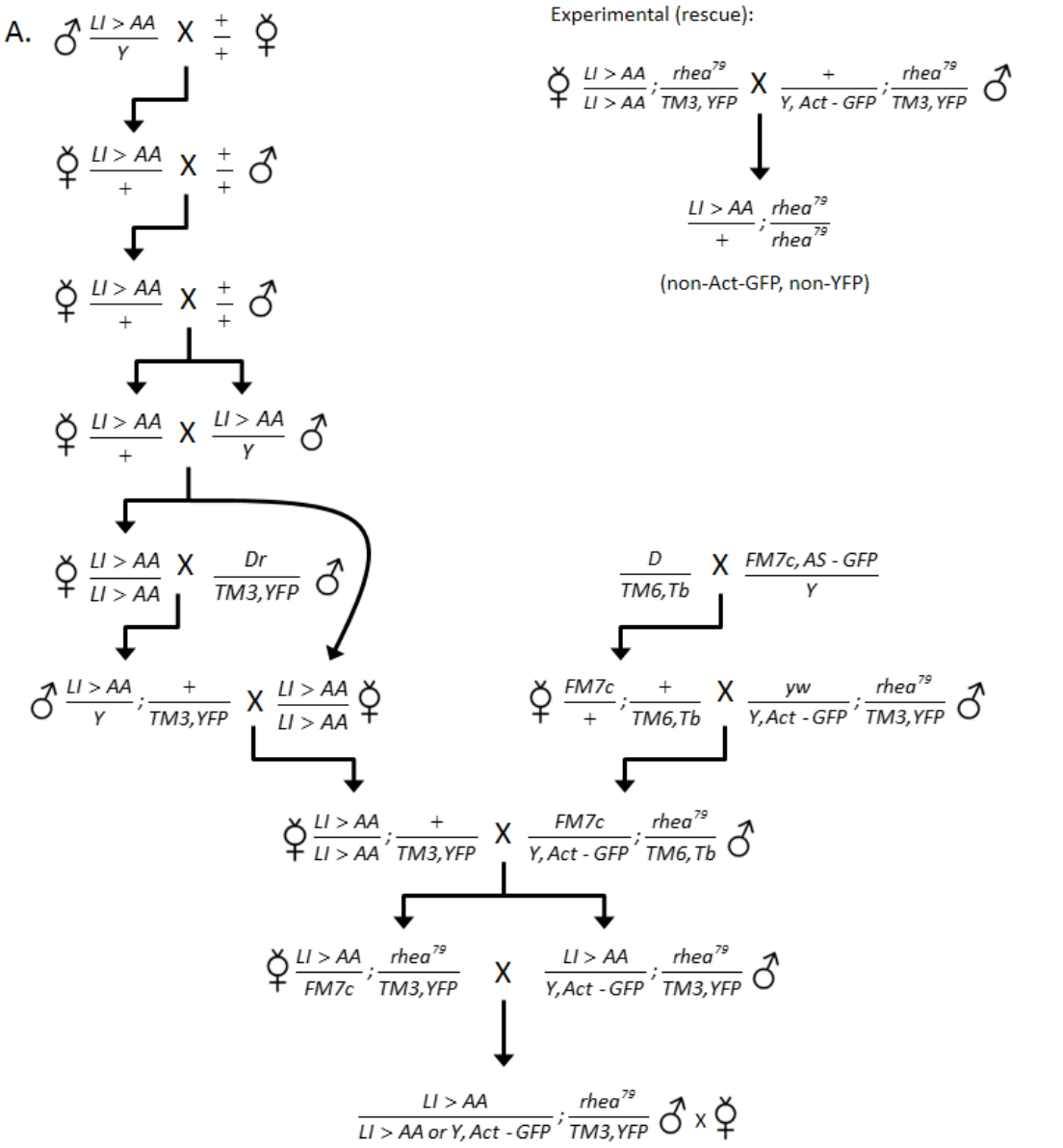
A.
LI > AA / Y X + / +
LI > AA / + X + / +
LI > AA / + X + / +
LI > AA / + X LI > AA / Y
LI > AA / LI > AA X Dr / TM3, YFP
LI > AA / Y ; + / TM3, YFP X LI > AA / LI > AA
LI > AA / LI > AA ; + / TM3, YFP X FM7c / Y, Act - GFP ; rhea79 / TM6, Tb
LI > AA / FM7c ; rhea79 / TM3, YFP X LI > AA / Y, Act - GFP ; rhea79 / TM3, YFP
LI > AA / LI > AA or Y, Act - GFP ; rhea79 / TM3, YFP x
Experimental (rescue):
LI > AA / LI > AA ; rhea79 / TM3, YFP X + / Y, Act - GFP ; rhea79 / TM3, YFP
LI > AA / + ; rhea79 / rhea79
(non-Act-GFP, non-YFP)
D / TM6, Tb X FM7c, AS - GFP / Y
FM7c / + ; + / TM6, Tb X yw / Y, Act - GFP ; rhea79 / TM3, YFP

*YFP = GMR>YFP

B.

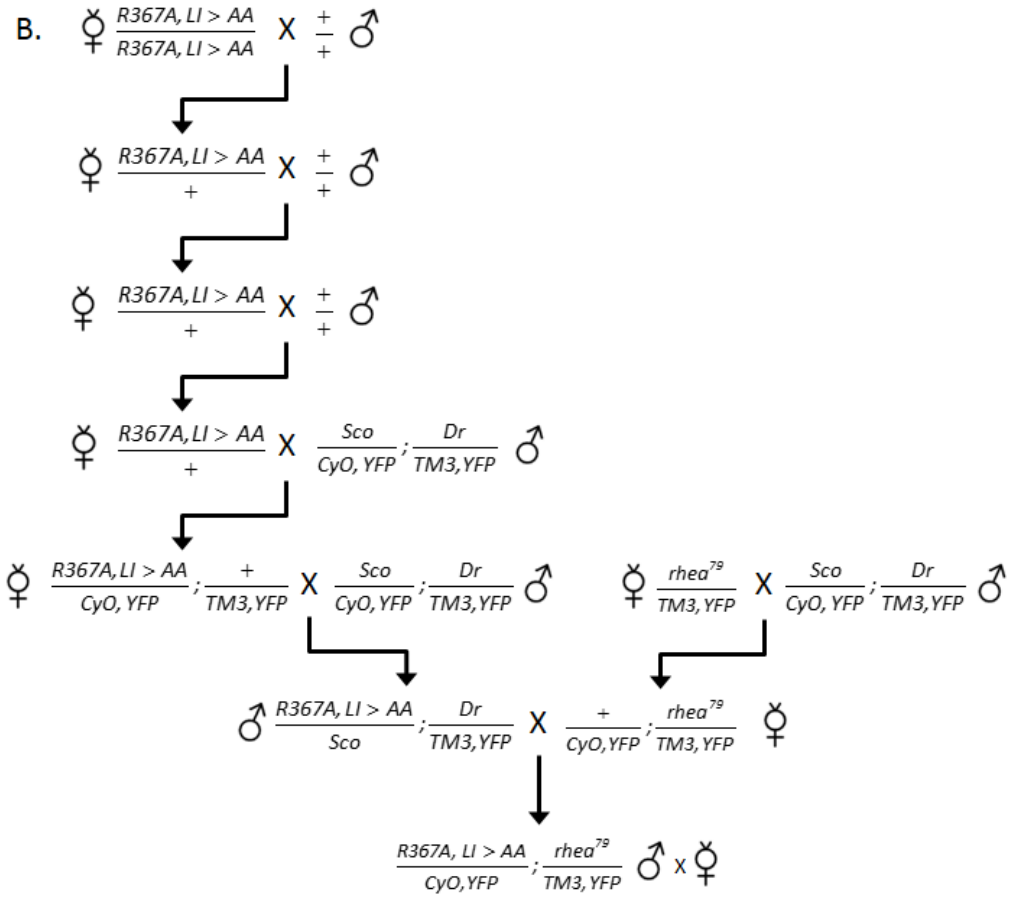

Experimental (rescue):

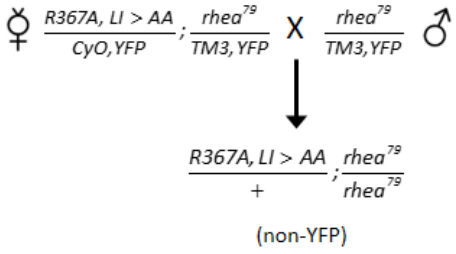

(non-YFP)

*YFP = GMR>YFP

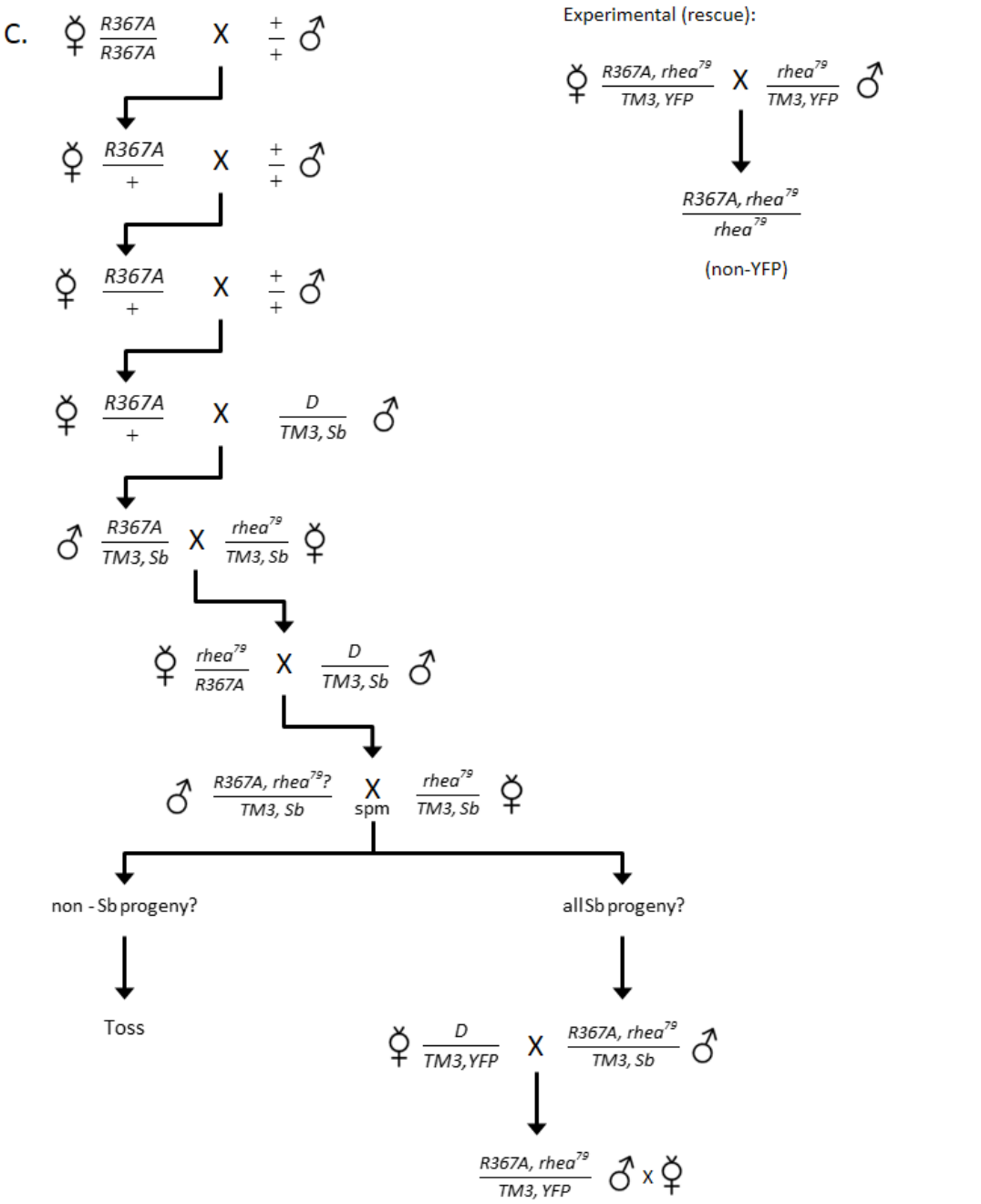

*rhea^{79} = rhea^{79}, FRT2A
*R367A is tagged with GFP
*spm = single pair mate (numerous putative recombinant males individually crossed)

Supplemental integrin information

APPENDIX B

Appendix B.1 – Heart phenotype in embryos homozygous for mutant alleles of integrin-related genes

Pericardial and cardioblasts are aligned in two bi-lateral rows along the midline in stage 17 wildtype embryos (**A, A'**). Robo is localized within the heart lumen, between the CB rows (**A''-A'''**). In *rhea*^{79} mutants, cardial cell alignment is usually unperturbed, although minor clumping is occasionally observed when subtle dorsal closure defects are present (**B-B'**). However, the space between CB rows is reduced and lower levels of Robo are detected apically (**B''-B'''**). Embryos homozygous for *vinc*^{1} (**C-C'''**), *stck*$^{3R\text{-}17}$ (**F-F'''**), and *fak56D*^{KG00304} (**G-G'''**) show few defects in the heart and Robo concentrates along the midline. *wech*^{K08815a} and *ilk*^{1} mutant embryos frequently had minor clumping or misalignment of pericardial and/or CBs, with Robo mislocalized away from the midline in these areas (**D-D'''** and **E-E'''**). In *src42A*^{E1} homozygotes, cardial cell alignment was normal, however there was frequent delayed or stalled migration of posterior heart cells (**H-H'**). When the heart did not properly form, Robo did not apicalize (**H''-H'''**).

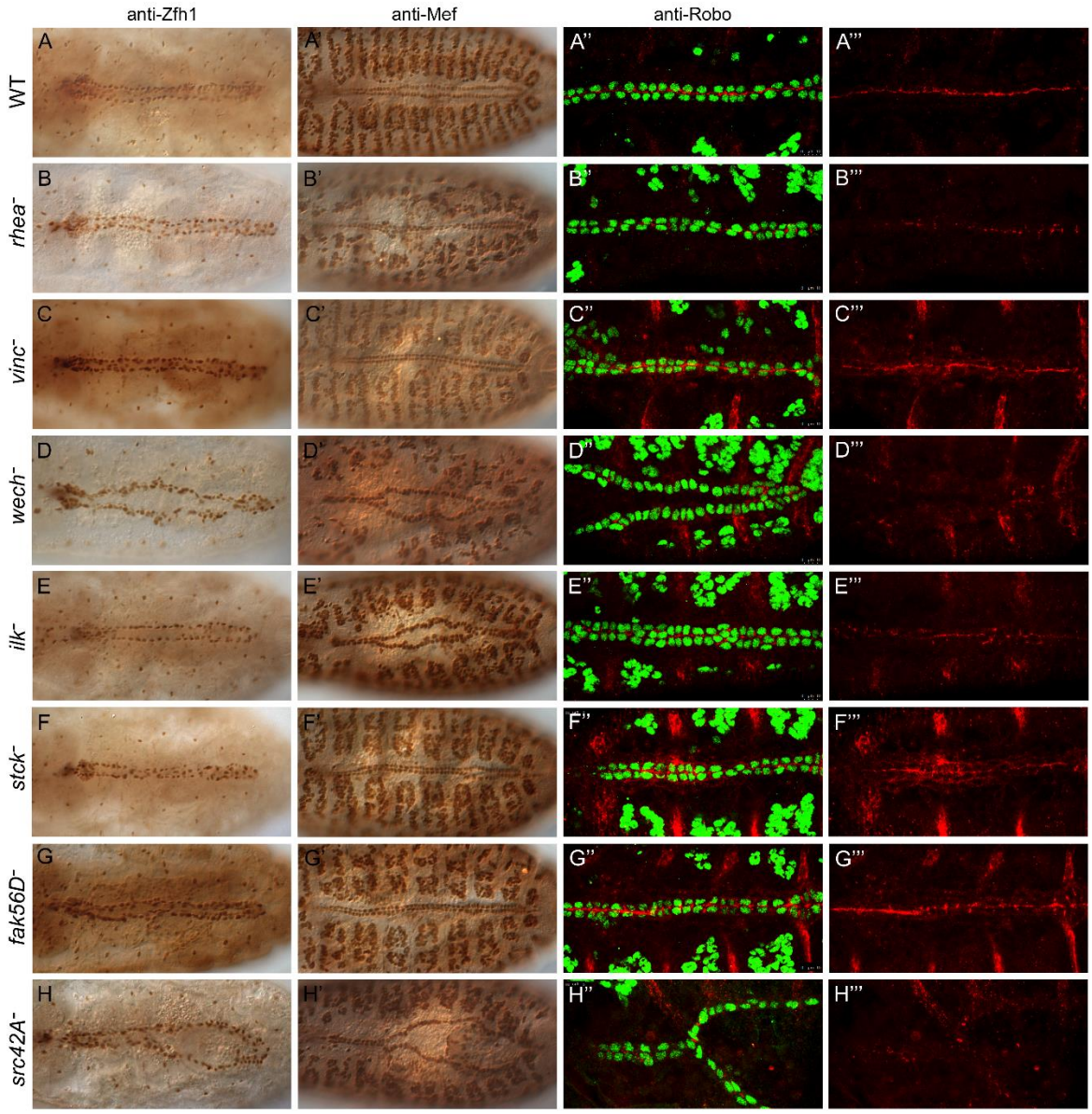
anti-Zfh1
anti-Mef
anti-Robo
WT
rhea-
vinc-
wech-
ilk-
stck-
fak56D-
src42A-
A
A'
A''
A'''
B
B'
B''
B'''
C
C'
C''
C'''
D
D'
D''
D'''
E
E'
E''
E'''
F
F'
F''
F'''
G
G'
G''
G'''
H
H'
H''
H'''

Supplemental Talin information

APPENDIX C

Appendix C.1 – Range of heart phenotypes in *rhea* zygotic and germ-line clone mutant embryos

Cardioblast and somatic muscle position (identified with αMEF) in stage 17 wildtype (**A**), zygotic null *rhea* (**B**), and germ-line clone null *rhea* embryos (**C**). In wildtype embryos, the contralateral CB rows align at the midline leaving a luminal space within the heart proper. Dorsal closure has complete and the segmental somatic muscles are situated close to the midline, immediately lateral to the heart. In most zygotic *rhea* mutants, the CBs and muscles are properly positioned, although there is a reduced luminal space within the heart proper (**B-B'**). Occasionally, dorsal closure does not complete (**B''**). In contrast, in *rhea* germ-line clone mutant embryos, the somatic muscles and cardioblasts are abnormally located due to disruptions in germ-band retraction and dorsal closure (**C-C'''**). Frequent phenotypes include dorsal protrusion of the gut (g; **C**), anterior or posterior displacement of the cardioblasts (**C, C'**), and severe displacement and disrupted structure of somatic muscles (**C-C'''**). Severe disruption in development often prevents confident identification of cell types (eg. in **C'''**). Calibration: 10 microns.

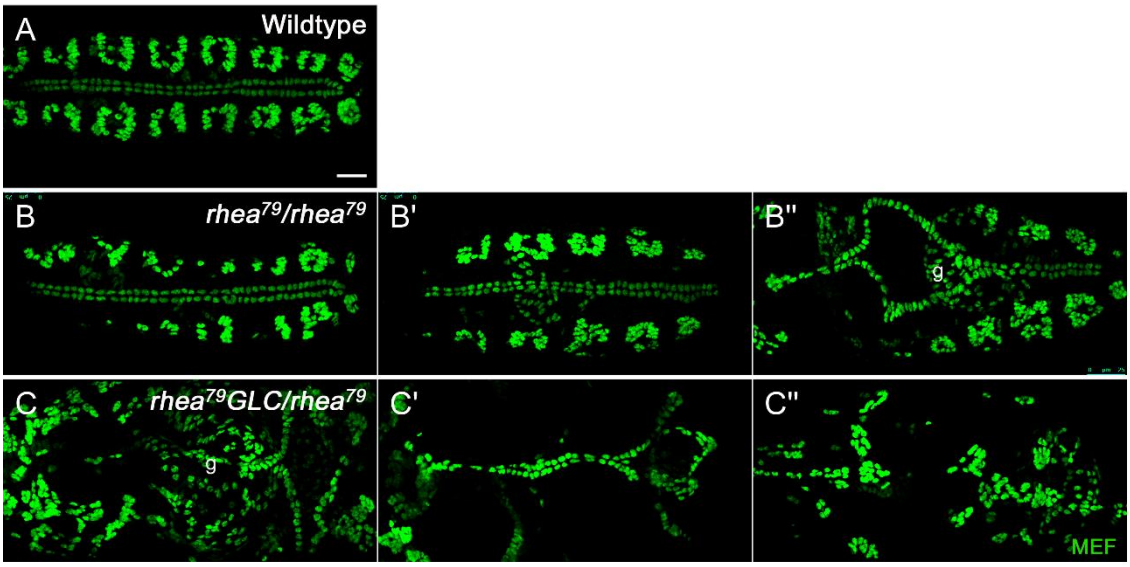
A
Wildtype
B
rhea79/rhea79
B'
B''
g
C
rhea79GLC/rhea79
g
C'
C''
MEF

Appendix C.2 – Talin localization is disrupted in *mys* (βPS1 integrin) mutants

In *mys* heterozygous embryos, Talin immunolabel is detected at high levels along the midline luminal surface and at lower levels basally (**A**). Talin is less concentrated along the heart midline and displays a more diffuse distribution pattern in zygotic *mys* mutant embryos (**B, C**). In *mys* germ-line clone embryos, there is no consistent apical or basal accumulation of Talin (**D**). Here and in following images, cardioblasts are labeled with αMEF. Calibration: 10 microns.

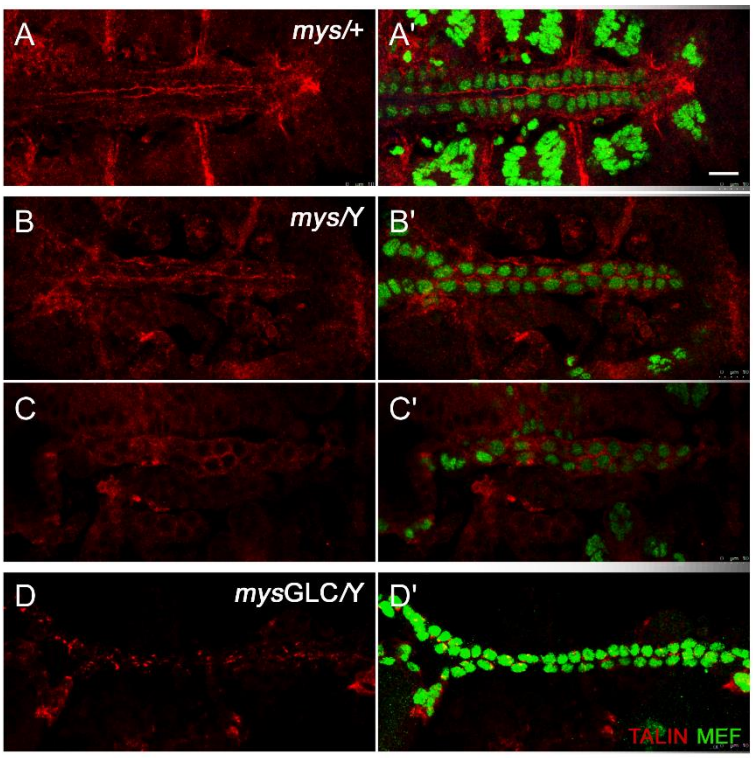
A
mys/+
A'
B
mys/Y
B'
C
C'
D
mysGLC/Y
D'
TALIN MEF

Appendix C.3 – CAP partially co-localizes with Talin along the apical and basal cardioblast surfaces

Cbl-associated protein (CAP; magenta) and Talin (red) immunolabel in stage 17 wildtype embryos. Both Talin and CAP are detected along the apical and basal cardioblast domains and are excluded from the lateral regions. However, in contrast to the broad and mostly continuous Talin distribution, CAP is restricted to discrete puncta which overlap with accumulated Talin. Panels in **B-B''** are enlargements of the boxed regions in **A-A''**. Images are maximum projections of a three micron stack.

Calibration: 10 microns in A, 5 microns in B.

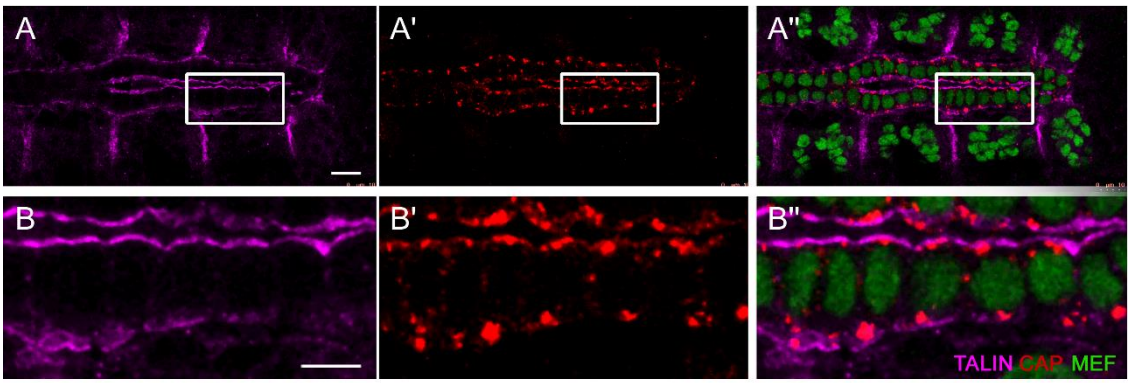
A
A'
A''
B
B'
B''
TALIN CAP MEF

Appendix C.4 – In *rhea* mutants, ectopic Dystroglycan lateral accumulations are devoid of junctional Discs-large

Dystroglycan and Discs-large double-labeled *rhea* heterozygous (**A**) or zygotic (**B**) or germ-line clone (**C**) *rhea* mutant embryos. Right panels are enlarged images of framed sections on the left. Arrows point to lateral pockets, while arrowheads indicate open pockets along the midline at tetra-cellular intersections. Note the absence of Dlg along Dg-rich membranes including the midline luminal domain in wildtype and the small ectopic pockets in mutants. Calibration: 10 microns.

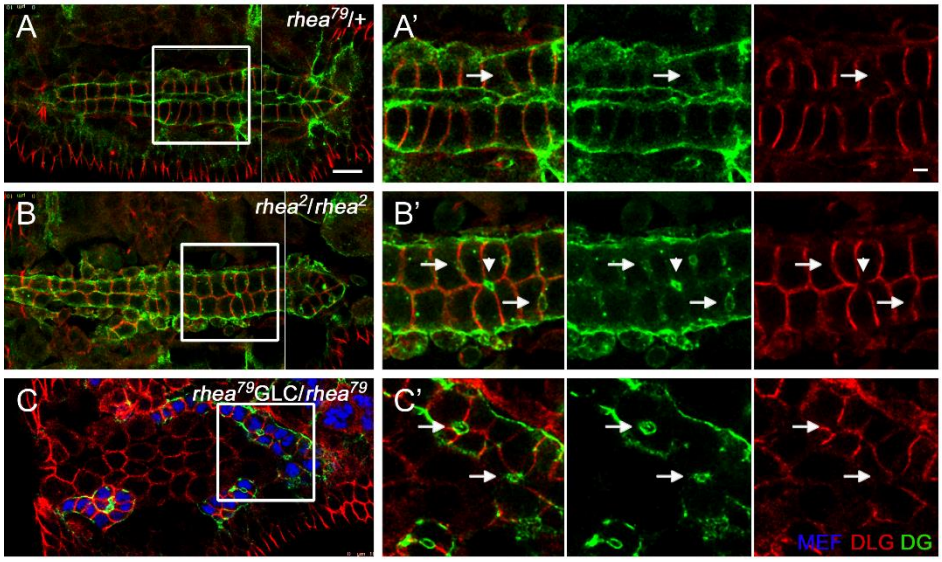
A
rhea79/+
A'
B
rhea2/rhea2
B'
C
rhea79GLC/rhea79
C'
MEF DLG DG

Appendix C.5 – Talin localization in *rhea* zygotic mutants expressing transgenic Talin rescue constructs

Talin localization in the heart of late stage *rhea* mutant embryos expressing full-length wildtype Talin^{GFP} or Talin^{GFP} with modified integrin binding sites. The Talin localization pattern was detected through immunolabeling with antibodies against Talin and GFP. In contrast to zygotic *rhea*^{79} embryos (**A**), embryos rescued with Talin^{WT} (**B**), Talin^{IBS1-} (R367A, **C**), or Talin^{IBS2-} (KS>DD, **D**) had high levels of Talin which was primarily distributed along the apical and basal cardioblast surfaces. Surrounding tissues also had GFP and Talin immunolabel, reflective of the ubiquitous expression of the rescue constructs. Similar to zygotic *rhea* mutants, embryos expressing transgenes harbouring mutations in both IBS1 and IBS2 (Talin$^{IBS1- IBS2-}$, **F**) or a single LI>AA mutation in the IBS2 (Talin^{IBS2b-}, **E**) had low levels of Talin accumulated in small puncta within the heart. All Talin label was imaged using identical settings. Calibration: 10 microns.

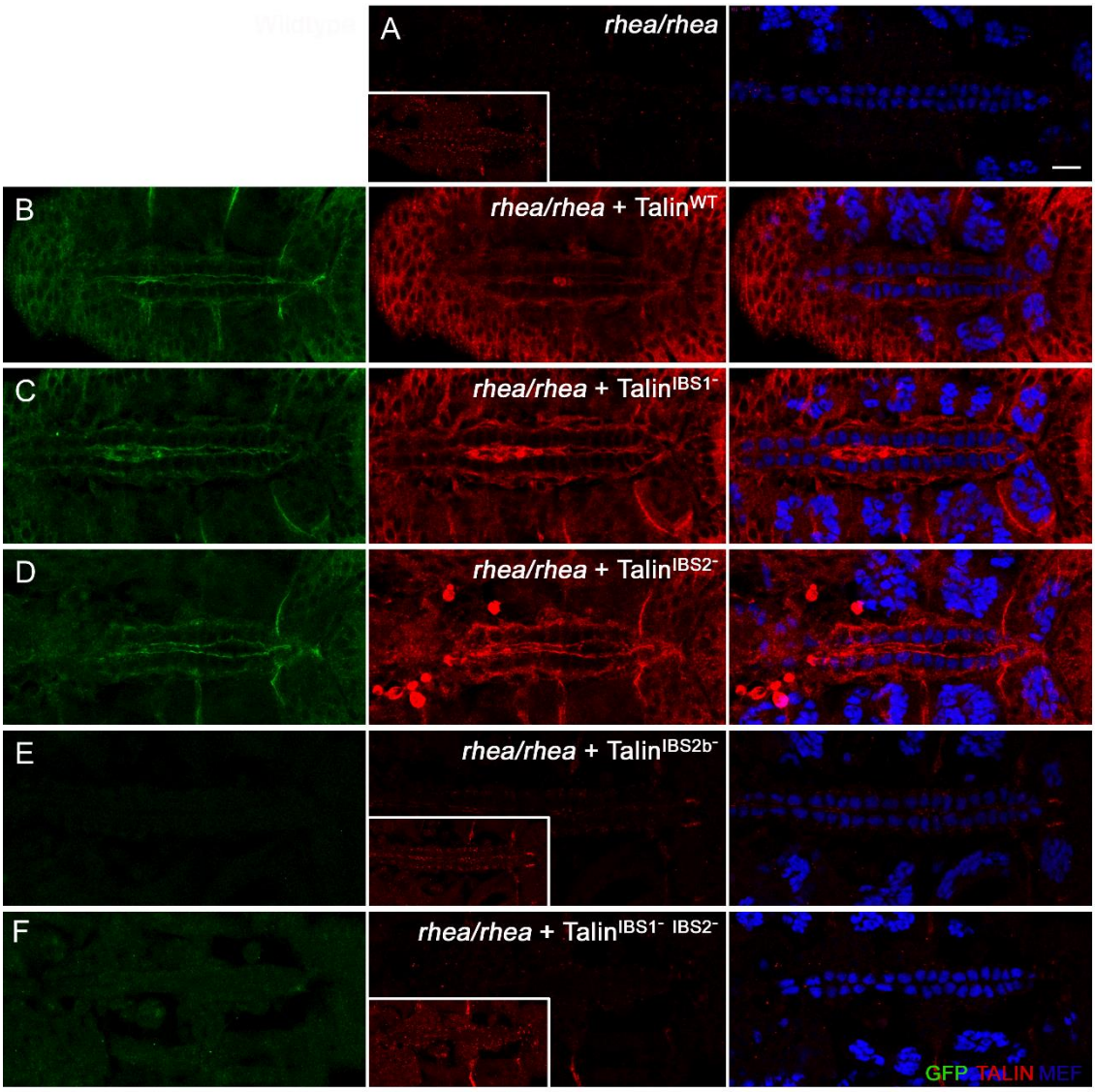
A
rhea/rhea
B
rhea/rhea + Talin^WT
C
rhea/rhea + Talin^IBS1-
D
rhea/rhea + Talin^IBS2-
E
rhea/rhea + Talin^IBS2b-
F
rhea/rhea + Talin^IBS1- IBS2-
GFP TALIN MEF

Appendix C.6 – Talin^{IBS2b-} and Talin$^{IBS1-, IBS2-}$ are unable to rescue heart development in *rhea* mutant embryos

(A-E) Frontal (**A, C**) and transverse (**B, D-E**) images of the heart in zygotic *rhea*^{79} mutants expressing Talin$^{IBS1- IBS2-}$ or Talin^{IBS2b-} transgenes. Similar to that observed in *rhea*^{79} zygotic mutants, βPS1 remains poorly localized within the heart (**A, C**), the distance between cardioblast rows remains narrow (arrow in **A, C**), and no open lumen forms at the midline (vertical arrow) between contralateral cardioblasts (**B, D-E**). Posterior is to the right in A and C, dorsal is to the top in B, D, and E. Calibration 10 microns.

(F-G) The average luminal width score and the number of seven-up cell blisters per embryo. No statistical difference is observed between zygotic *rhea*^{79} embryos and those expressing the Talin$^{IBS1- IBS2-}$ or Talin^{IBS2b-} transgenes. Error bars represent standard deviation.

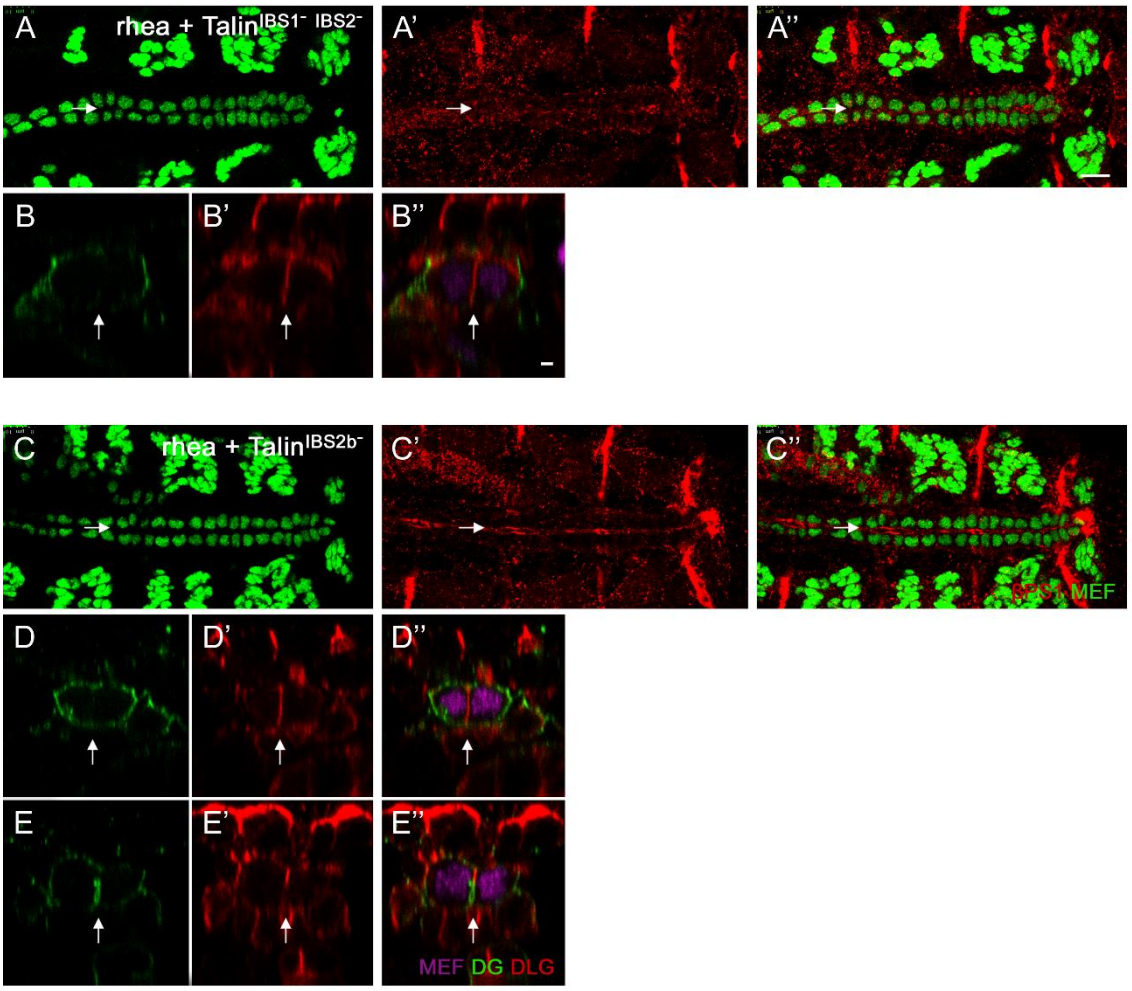
A
rhea + Talin IBS1- IBS2-
A'
A''
B
B'
B''
C
rhea + Talin IBS2b-
C'
C''
MEF
D
D'
D''
E
E'
E''
MEF DG DLG

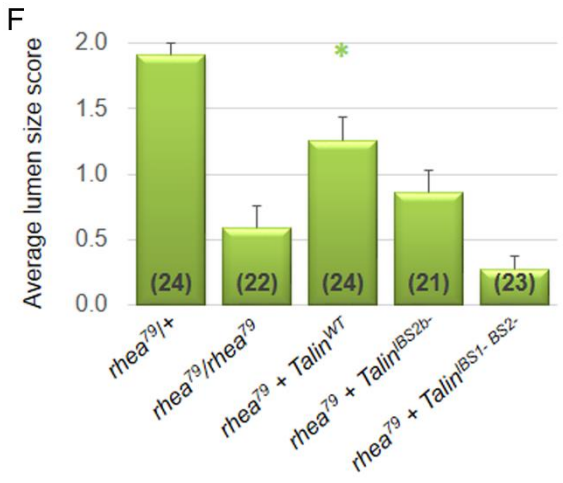
F
Average lumen size score
2.0
1.5
1.0
0.5
0.0
*
(24)
(22)
(24)
(21)
(23)
rhea79/+
rhea79/rhea79
rhea79 + TalinWT
rhea79 + TalinIBS2b-
rhea79 + TalinIBS1-, BS2-

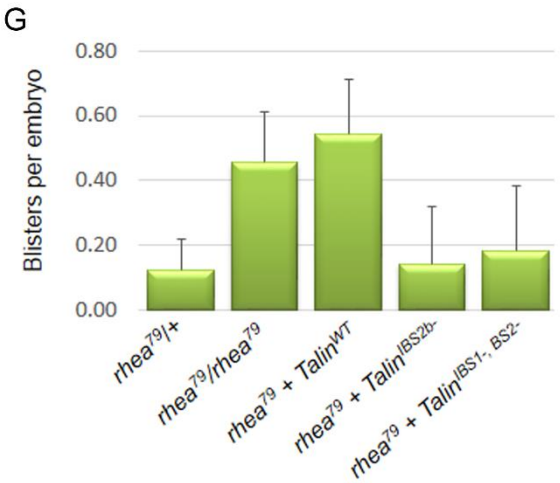
G
Blisters per embryo
0.80
0.60
0.40
0.20
0.00
rhea79/+
rhea79/rhea79
rhea79 + TalinWT
rhea79 + TalinIBS2b-
rhea79 + TalinIBS1-, BS2-

Src42A is required for cardioblast migration, but not lumen formation

APPENDIX D

D.1 Introduction

In the initial survey of genes encoding integrin adhesome proteins, late stage *src42A*^{E1} mutant embryos had delayed or stalled migration of posterior cardioblasts (CBs; Appendix B.1H). Since embryos lacking βPS1 or αPS3 exhibit aberrant CB migration followed by failed lumen formation (3.3.2 and 3.3.4), we hypothesized that Src may function downstream of integrins to modulate these events. Src is a non-receptor tyrosine kinase that can work in concert with Focal Adhesion Kinase (FAK) to activate signal transduction in a variety of contexts. Of relevance to this thesis, FAK-Src signaling promotes migratory cell behavior in both development and tumor progression, coordinating cell-cell and cell-ECM adhesion (eg. reviewed by Canel *et al.* 2013). Activated Src localizes to focal adhesions (Tu *et al.* 2010, Fincham *et al.* 2000) and phosphorylates several integrin adhesome proteins including FAK and Paxillin (Eide *et al.* 1995, Schaller *et al.* 1999, Weng *et al.* 1993). Cell migration is promoted by Src-dependent destabilization of the adherens junctions through increased E-cadherin (E-cad) endocytosis (Palacios *et al.* 2005, Canel *et al.* 2010, Serrels *et al.* 2011). Src also promotes cell migration by triggering focal adhesion turnover and modulating cytoskeletal dynamics (Playford and Schaller 2004, Landry *et al.* 2014, Bhoopathi *et al.* 2011, Rudrapatna *et al.* 2013). In this chapter, I explore the requirement for Src and FAK in *Drosophila* heart cardiogenesis. I demonstrate that while Src is required for proper heart formation, this is likely because of its involvement in surrounding tissues which impinge on the developing heart.

D.1.1 Src42A and Src64B

Drosophila has two Src genes, *src42A* and *src64B*, which are known to have overlapping and partially redundant roles in several, but not all, developmental processes. Embryos lacking *src42A*, but not *src64B*, had frequent delays in dorsal closure (Tateno *et al.* 2000, Takahashi *et al.* 2005). However, embryos expressing mutant alleles of both *src42A* and *src64B* had a more severe phenotype than single *src42A* mutants (Tateno *et al.* 2000). Similarly, development of *Drosophila* trachea, nervous system, and visual system is more severely disrupted in double mutants than in flies solely lacking *src42A* (Shindo *et al.* 2008, Takahashi *et al.* 2005). Embryos homozygous for the *src64B* mutant allele had no aberrant development of these tissues. These studies suggest that Src64B is able to partially compensate for Src42A. In contrast, Src42A is not able to compensate for Src64B in nurse cell formation. Flies with reduced Src64B function are viable to adulthood, however they are unable to properly form the ring canals that connect the oocyte to its surrounding nurse cells (Dodson *et al.* 1998). This phenotype is not enhanced when the gene dosage of *src42A* is reduced (Takahashi *et al.* 2005), suggesting that Src42A and Src64B are not functionally redundant in this process.

Vertebrate and *Drosophila* Src kinases have SH2 and SH3 protein binding motifs as well as a catalytic kinase domain (Boggon and Eck 2004). While null mutant alleles fully prevent Src function, other alleles or transgenic constructs may be designed to specifically abrogate either the protein binding regions or the kinase function. For example, a Src42A construct ($Src42A^{KR5\text{-}1}$ or simply $Src42A^{DN}$) harbouring a single amino acid substitution

within the ATP-binding site has no kinase activity (Takahashi *et al.* 1996, Chang *et al.* 1995). Furthermore, during *Drosophila* eye development this modified protein acts in a dominant negative fashion; the dominant rough eye phenotype in flies expressing $Src42A^{DN}$ is suppressed by wildtype Src42A in a dose-dependent manner (Takahashi *et al.* 1996). Within the C-terminal tail of Src is an autoinhibitory phosphorylation site (Tyrosine 527 in vertebrates, Tyrosine 511 in *Drosophila*; Cooper *et al.* 1986, Takahashi *et al.* 1996). When this tyrosine is phosphorylated, interactions among the SH2, SH3, and kinase domains maintain a conformation that prevents Src activity (Williams *et al.* 1997, Xu *et al.* 1997). A tyrosine to phenylalanine substitution prevents phosphorylation, yielding a constitutively active Src ($Src42A^{CA}$; Takahashi *et al.* 2005).

D.1.2 Fak56D

There is a single FAK in *Drosophila*, encoded by *fak56D*. Similar to vertebrate FAK and PYK2, Fak56D has a focal adhesion targeting domain, a binding site for the SH2 domain of Src, and a sequence-inferred tyrosine kinase domain (Fox *et al.* 1999, Fujimoto *et al.* 1999, Palmer *et al.* 1999). However, in contrast to the requirement for FAK in vertebrate development and integrin adhesions (reviews in Chatzizacharias *et al.* 2010 and Parsons 2003), flies lacking Fak56D are viable and fertile suggesting that the role of FAK is not fully conserved in *Drosophila* (Grabbe *et al.* 2004). Despite this, Fak56D is recruited to sites of integrin adhesion within the *Drosophila* embryo (Fujimoto *et al.* 1999). Fak56D overexpression produces wing blisters (Palmer *et al.* 1999), similar to those in flies

overexpressing αPS1 or αPS2 integrin (Brabant *et al.* 1996, Prout *et al.* 1997). Furthermore, several studies have used adhesion sensitized genetic backgrounds to demonstrate a role for Fak56D in integrin function. Reduced gene dosage of *fak56D* in *mys* (βPS1) heterozygotes produces abnormal phenotypes at neuromuscular junctions (Tsai *et al.* 2008) and within the optic axon stalk (Murakami *et al.* 2007). Similarly, halving the gene copy of *src42A* or *src64B* enhanced the NMJ phenotype in embryos devoid of Fak56D (Tsai *et al.* 2008). Here we use similar genetic approaches to test for a role in Src-FAK signaling in integrin-dependent *Drosophila* cardiogenesis.

D.2 Results and Discussion

D.2.1 Loss of Src42A, but not Src64B, results in incomplete cardioblast migration

In late stage wildtype embryos, CB migration has completed and the cells are aligned along the dorsal midline (Figure D.1A). In contrast, embryos homozygous for *src42A*^{E1} frequently exhibited an "open heart" phenotype, in which posterior CBs failed to reach the midline (Figure D.1B asterisks). To confirm this was not an allele-specific phenotype perhaps due to mutations elsewhere in the genome, several independent *src42A* mutant alleles were tested. Embryos carrying a *src42A* deletion (*src42A*$^{26\text{-}1}$) had a similar open heart phenotype (Figure D.1C). Embryos homozygous for a *src42A* hypomorphic allele had normal CB alignment, however transheteroallelic embryos for hypomorphic and null *src42A* alleles occasionally displayed stalled or delayed posterior CB migration (Figure D.1D-E). I hypothesized that *Src64B* may also be required for full CB

Figure D.1 – Loss of Src42A, but not Src64B, results in incomplete cardioblast migration

By stage 17, the two CB rows are aligned along the dorsal midline in wildtype embryos (**A**). In *src42A*^{E1} and *src42A*$^{26\text{-}1}$ null mutants, the posterior CBs fail to migrate to the midline (arrow) and the embryos exhibit an "open heart" phenotype (**B, C**; asterisks marks the open heart). The CBs in the *src42A*^{k10108} hypomorph migrate fully to the midline (**D**), although an open heart phenotype is observed in some *src42A*^{E1}/*src42A*^{k10108} mutants (**E**, asterisks). Embryos mutant for *src64B* (**F**) or with single gene copies of both *src42A* and *src64B* (**G**) have complete CB migration, but exhibit cell clumping (arrowhead). The CB nuclei here and in subsequent images are identified with αMEF immunolabel, unless otherwise noted.

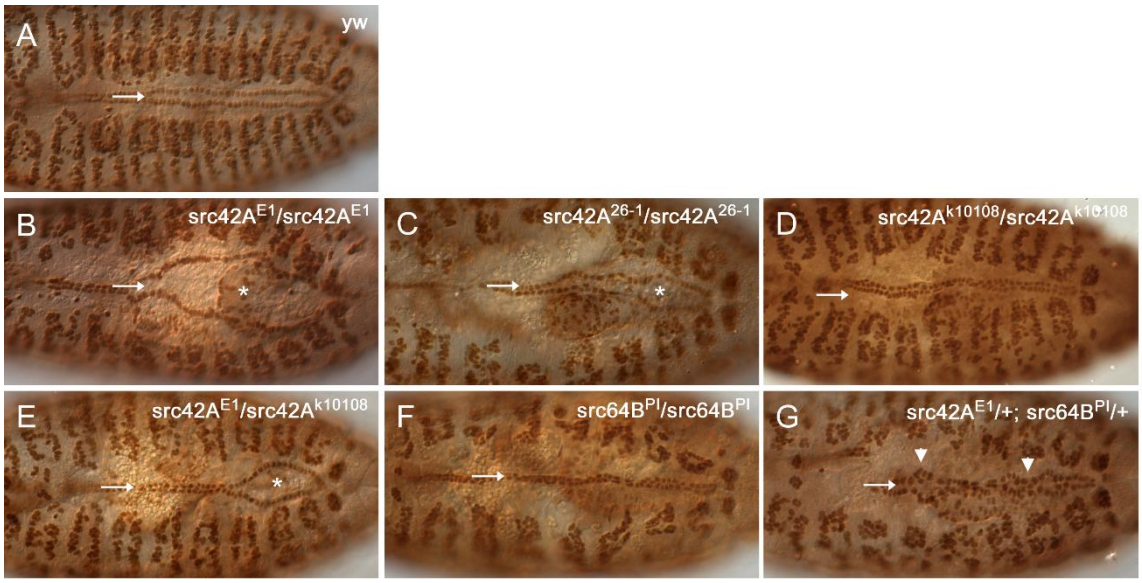
A
yw
B
src42A^{E1}/src42A^{E1}
C
src42A$^{26-1}$/src42A$^{26-1}$
D
src42A^{k10108}/src42A^{k10108}
E
src42A^{E1}/src42A^{k10108}
F
src64B^{PI}/src64B^{PI}
G
src42A^{E1}/+; src64B^{PI}/+

migration. The *src64B*^{PI} allele has two P-element insertions within an intron; *src64B*^{P1} mutants have greatly reduced, albeit not fully eliminated, Src64B expression (Dodson *et al.* 1988). Homozygous *src64B*^{PI} embryos had completed CB migration (Figure D.1F). Moreover, I generated embryos doubly heterozygous for *src42A* and *src64B*. In these embryos, there was frequent clumping and disorganization of CBs suggesting neighboring cell adhesion may be disrupted (Figure D.1G arrowheads). Despite this, both anterior and posterior CBs migrated fully to the midline (Figure D.1G arrow). Taken together, it appears that Src42A, but not Src64B is required for complete CB migration. However, it remains possible that Src42A and Src64B have partially overlapping functions in heart development and Src42A is able to compensate for a lack of Src64B.

D.2.2 Mutations in *fak56D* do not enhance the *src42A*^{E1} phenotype

In many tissues and developmental processes, Src forms a complex with FAK, which induces signaling downstream of integrins (Schaller *et al.* 1994). *fak56D* loss-of-function *Drosophila* embryos have no obvious heart phenotype (Figure D.2B-C). This is expected as flies of these genotypes are viable and healthy (Grabbe *et al.* 2004, Tsai *et al.* 2008). To determine if Fak56D modulates Src signaling within the heart, I reduced the *fak56D* gene dosage in *src42A*^{E1} sensitized backgrounds. Embryos homozygous for *fak56D*^{KG} and heterozygous for *src42A*^{E1} had normal heart assembly (Figure D.2D). Furthermore, *fak56D*^{KG} was unable to dominantly or recessively enhance the *src42A*^{E1}

Figure D.2 – Mutations in *fak56D* do not enhance the *src42A*^{E1} phenotype

Similar to wildtype embryos (**A**), *fak56D* mutant embryos have normal CB alignment and migration (**B, C**). Reducing the gene copy of *fak56D* to one or zero did not enhance the delay in CB migration in *src42A*^{E1} heterozygous or homozygous embryos (**D-F**).

.

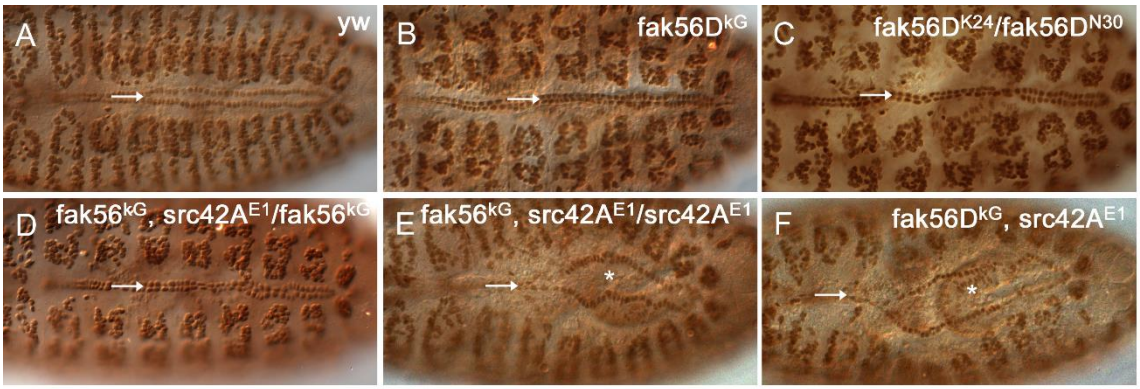
A
yw
B
fak56D^{kG}
C
fak56D^{K24}/fak56D^{N30}
D
fak56^{kG}, src42A^{E1}/fak56^{kG}
E
fak56^{kG}, src42A^{E1}/src42A^{E1}
F
fak56D^{kG}, src42A^{E1}

homozygous open heart phenotype (Figure D.2E-F). Therefore, Src42A, but not Fak56D is necessary for proper migration of the cardial cells in *Drosophila*.

D.2.3 Heart specific disruption of Src42A does not prevent cardioblast migration

While the data suggests that Src42A is required for heart development, it was unclear whether Src42A was required in the CBs themselves or if the mutant phenotype observed was due to disruptions in surrounding tissues (eg. the amnioserosa or ectoderm). Using the UAS-Gal4 system which allows temporal and spatial control of gene expression, I overexpressed wildtype (WT), constitutively active (CA), and dominant negative (DN) Src42A in the heart cardioblasts (and somatic muscles). To validate $Src42A^{WT}$ and $Src42A^{CA}$ constructs, I ectopically expressed them in the eye using GMR-Gal4 (Li *et al.* 2012) and observed eye defects similar to those published previously (Figure D.3 I-L; Pedraza *et al.* 2004). $Src42A^{DN}$ does not produce a severe eye phenotype (Figure D.3L, Takahashi *et al.* 1996), so this assay was unable to confirm the presence of the construct. However, ubiquitously expressed $Src42A^{DN}$ generates late pupal lethality (data not shown), consistent with it having a detrimental developmental effect.

Misexpression of Src42A in the heart tissue was not sufficient to disrupt CB migration (Figure D.3 A-D). Moreover, as in wildtype embryos, βPS1 integrin was primarily restricted to the apical or luminal surface of the CBs, with lower levels basally (Figure D.3E-H). However, embryos expressing dominant negative Src42A in the heart displayed frequent clumping of CBs (Figure D.3 D, H), suggesting a disruption in the adhesion

Figure D.3 – Disrupting the kinase activity of Src42A in the cardioblasts does not disrupt cell migration

(A-H) In wildtype stage 17 embryos, the two CB (green) rows are aligned along the dorsal midline (**A**) and βPS1 integrin localizes primarily along the apical CB surface (red, **E**). Embryos overexpressing wildtype or constitutively active Src42A in the CBs and somatic muscles had normal heart morphology (**B, C**). As in wildtype embryos (**E**), βPS1 localizes primarily along the apical surface of CBs, with lower levels present basally (**F, G**). In embryos expressing dominant negative Src42A in the heart and somatic muscles, CBs migrated to the midline (**D**). Despite moderate cell clumping (arrowheads in **D, H**), βPS1 integrin accumulated at apical CB surfaces (**H**). Arrows indicate the midline. Calibration: 10 microns.

(I-L) Validation of *src42A* mutant transgenes. Compared to eyes of wildtype embryos (**I**), flies overexpressing wildtype (**J**) or constitutively active (**K**) Src42A in the eye tissue (using GMR-Gal4) had reduced and misshapen eyes (consistent with Pedraza *et al.* 2004). Flies overexpressing dominant negative Src42A had eyes with no visible defects (consistent with Takahashi *et al.* 1996). Images are of the left eye. Calibration: 100 microns

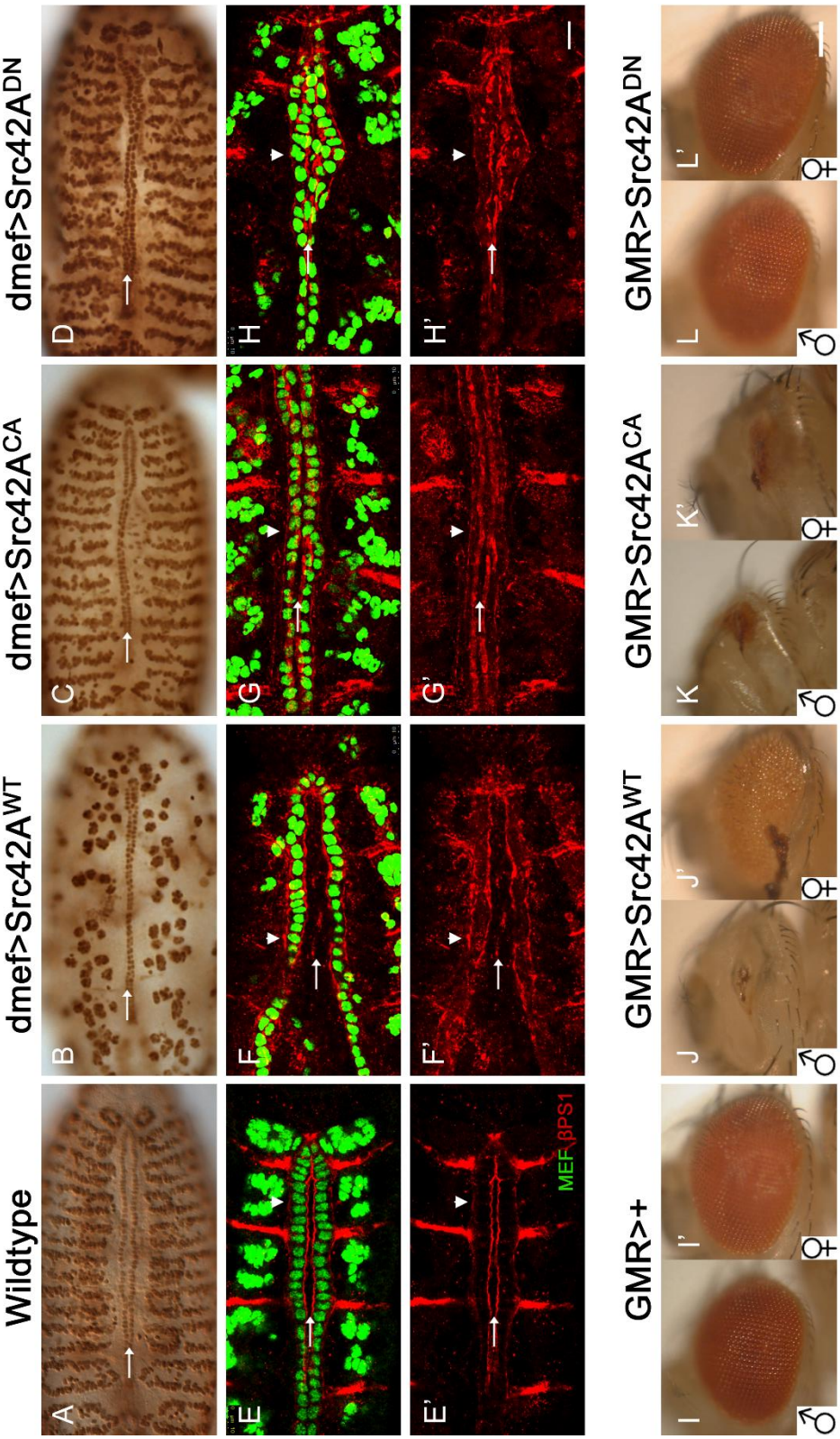
Wildtype
dmef>Src42A^WT
dmef>Src42A^CA
dmef>Src42A^DN
GMR>+
GMR>Src42A^WT
GMR>Src42A^CA
GMR>Src42A^DN
MEF βPS1

between neighboring cells. Thus, while it appears that Src42A does not function within the heart to stabilize βPS1 nor to regulate cardial cell migration, it may regulate E-cad mediated adhesion between neighboring cells. Such a role would be consistent with a Src kinase-dependent E-cad trafficking mechanism (Canel *et al.* 2010, Owens *et al.* 2000). Furthermore, although Src42A^{DN} acts in a dominant negative manner in the developing eye, it is unclear if it inhibits all Src function. The tyrosine to phenylalanine substitution in this construct disrupts the kinase domain (Chang *et al.* 1995), however it is possible that other protein-binding aspects of Src function remain intact and that these are sufficient for CB migration.

D.2.4 Src42A is required for leading edge membrane activity in the posterior heart

Our studies on integrin function in the heart demonstrated that integrins are required for the highly dynamic leading edge that migrating CBs extend (Figure 3.6). If Src42A is functioning downstream of integrins to control CB migration, lack of Src42A should result in a loss of membrane leading edge activity. Interestingly, while a reduction in leading edge activity was observed in the posterior of the heart in *src42A^{E1}* embryos, the CBs at the anterior of the heart retained a highly dynamic membrane activity similar to wildtype (Figure D.4 – compare B'' to B'). Cross-sectional imaging revealed that CBs with high membrane activity were polarized and extended a protrusion dorsally towards the midline (Figure D.4C, arrows) while cells with minimal activity were rounded and did not extend dorsally (Figure D.4C'). Thus, it appears that in the absence of Src42A, posterior CB

Figure D.4 – In *src42A* mutant embryos, cardioblasts with stalled migration lack leading edge membrane activity

The dynamic activity of the leading edge of migrating CBs was monitored in living embryos. Membrane actin was labeled with *dMEF-GAL4* regulated *UAS-moesin-mCherry* (red), while CBs were marked with *tup-GFP* (green). In wildtype embryos (**A**), both the anterior and posterior CBs extend highly dynamic processes towards the midline (arrowhead in **A'** and **A''**). In *src42A*^{E1} mutants, anterior CBs extend processes towards the midline (arrowhead in **B'**, cross-section in **C**), but posterior CBs remain rounded (**C'**) and do not extend such processes (**B''**, **C'**). Arrows mark the dorsal midline; posterior of the heart is to the right (**A, B**); dorsal at top (**C, C'**). Calibration: 10 microns.

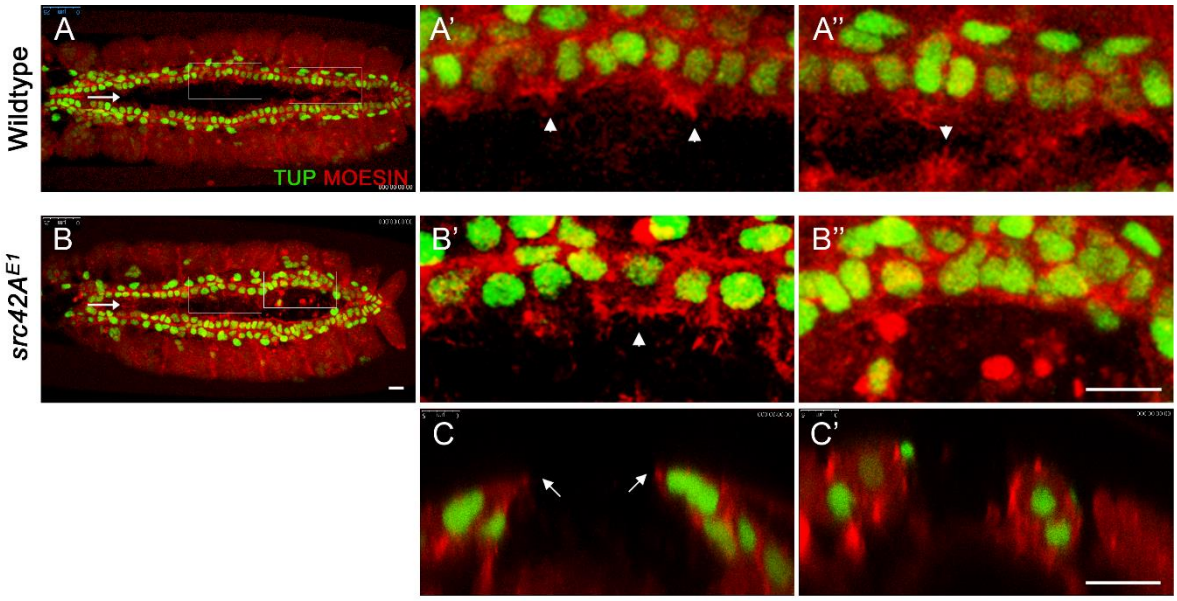
Wildtype
src42A^E1
A
A'
A''
B
B'
B''
C
C'
TUP MOESIN

leading edge activity is minimal, correlating with an inability of the CBs to fully migrate to the midline.

D.2.5 In *src42A*^{E1} embryos, amnioserosa cells at the midline inhibit cardioblast migration

While the data suggests that Src42A is required for heart development, it was unclear whether Src42A was required in the CBs themselves or if the mutant phenotype observed was due to disruptions in surrounding tissues (the amnioserosa or ectoderm). Furthermore, it was intriguing that only the posterior heart had aberrant cardial cell migration. Previous studies have documented that Src42A is required for dorsal closure (Tateno *et al.* 2000; Takahashi *et al.* 2005) and, consistent with this, a subset of *src42A* mutant embryos analyzed had incomplete dorsal closure (data not shown). Although somatic muscles positioned close to the midline suggested that dorsal closure was complete in most "open heart" *src42A* mutant embryos (Figure D.1), subtle phenotypes may not be readily apparent.

Therefore, to determine if the CB migration delay was due to disruptions in the amnioserosa, I labeled the amnioserosa using an antibody against Hindsight (Hnt), which is present in the nuclei of the amnioserosa and midgut cells (Figure D.5E), and the enhancer trap YET1, which expresses YFP in the amnioserosa perimeter cells (Figure D.5A). In wildtype embryos, the amnioserosa is visible at stage 15 and 16 (Figure D.5A, C, E), but has internalized and undergone apoptosis by stage 17 (Figure D.5G). Already in

Figure D.5 – Amnioserosa cells remain at the midline in late stage *src42A^{E1}* embryos

In wildtype embryos, the amnioserosa (red) is present at stage 15 (**A, E**) and 16 (**C**), but has internalized and undergone apoptosis by the end of embryogenesis (stage 17, **G**). In *src42A^{E1}* mutants, amnioserosa cells persist in the posterior region of the embryo even at late stages (**B, D, F, H**; arrowheads identify example amnioserosa cells; brightly red labeled cells in left of **H** are part of the midgut). In **A-D**, the outermost amnioserosa cells are marked with a YFP reporter construct (YET1). In **E-H** the nuclei of amnioserosa cells are labeled with αHindsight (HNT). Posterior of the heart is to the right. Calibration: 10 microns.

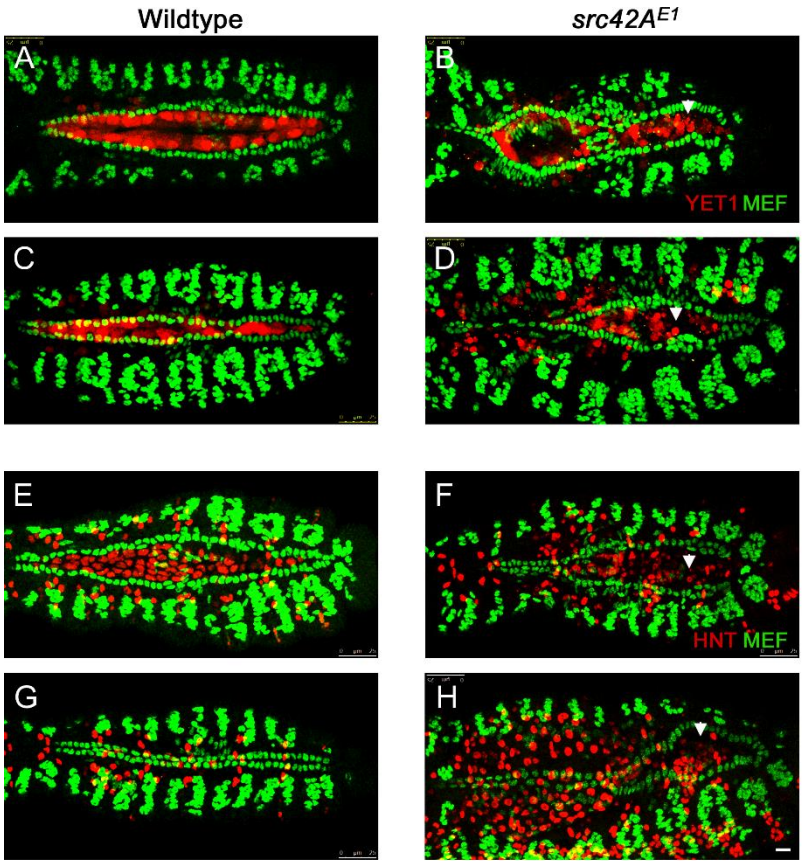
Wildtype
src42A^E1
A
B
YET1 MEF
C
D
E
F
HNT MEF
G
H

stage 15 and 16 embryos, there are few amnioserosa cells remaining near the posterior region of the heart. However, in *src42A*^{E1} embryos, the amnioserosa cells persist in the posterior region of the embryo, where the CB migration delay is observed (Figure D.5 B, D, F, H).

Transverse images of fixed wildtype embryos shows that as CB migration proceeds, the CBs move dorsally and eventually over the amnioserosa cells (Figure D.6A-A'). Once CB migration is complete, no amnioserosa cells are between the CBs; any remaining cells have internalized into the embryo and appear round, characteristic of cells entering apoptosis (Figure D.6A''; Saraste and Pulkki 2000). This is not the case in *src42A*^{E1} embryos: although the amnioserosa cells are rounded suggesting they are apoptotic, they persist at the dorsal midline (Figure D.6B-B''). Thus, it appears that the incomplete amnioserosa internalisation is a physical barrier to CB migration and the migration defects observed in *src42A* mutants may not be the result of a requirement of Src42A in the heart itself.

D.2.6 Src42A is not essential for lumen formation

In integrin *scb* (αPS3) or *mys* (βPS1) mutants, disruptions in cell migration and leading edge activity is correlated with the inability of the CBs to form a lumen. If Src42A is required in the heart itself, we would expect that *src42A* mutants would form no lumen between CB cells that were able to reach the midline. However, if the migration delays are due to disruptions in amnioserosa internalisation, contralateral CBs that meet at the

Figure D.6 – In *src42A*^{E1} embryos amnioserosa cell invagination from the dorsal midline is incomplete

In wildtype embryos, migrating CBs (green) move dorsally and eventually over the amnioserosa cells (red; **A-A'**). Following migration, no amnioserosa cells are between the CBs; any remaining cells have been internalized (**A''**). In contrast, late stage *src42A*^{E1} embryos are characterized by persistent amnioserosa cells at the midline (**B-B''**). Despite having the rounded shape characteristic of cells undergoing apoptosis, the amnioserosa cells do not internalize, but remain along the midline where the heart tube usually forms. CB nuclei (and flanking muscle nuclei in **A'** and **A''**) are labeled with αMEF (green), while YET1 marks the outermost amnioserosa cells (red). Dorsal is at the top; arrows mark the midline. Calibration: 10 microns.

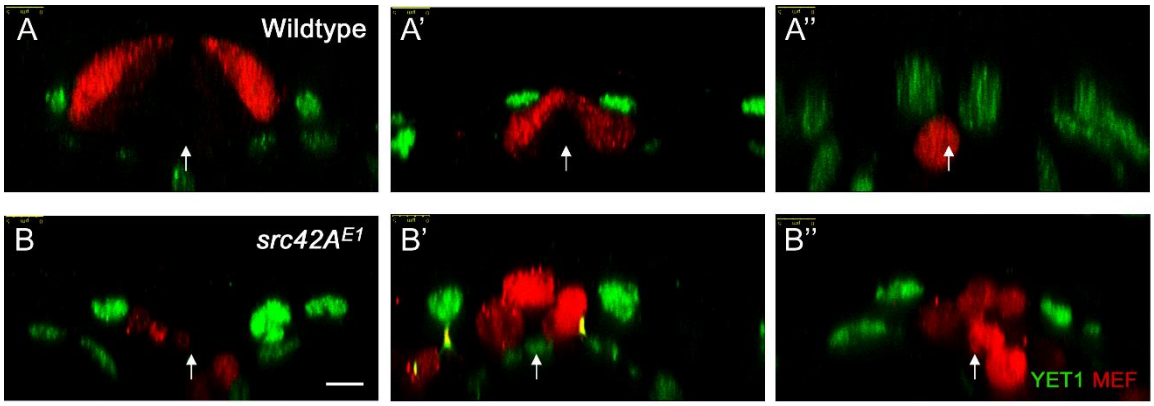
A
Wildtype
A'
A''
B
src42A^E1
B'
B''
YET1 MEF

midline would be able to form a lumen. Light level histology of embryo cross-sections was used to test these hypotheses. In late stage wildtype embryos, a lumen is visible between contralateral CBs (Figure D.7A). Dorsal closure has completed, as evidenced by the thick and continuous ectoderm layer dorsal to the heart (horizontal arrow). Any remaining amnioserosa cells have been internalized and are situated ventral to the heart (asterisks). In *src42A*^{E1} embryos, there are a range of phenotypes. Consistent with the confocal images described earlier, some embryos have amnioserosa cells remaining at the midline, precluding normal interactions between contralateral CBs (Figure D.7C). In many embryos, development is disrupted to such a point that identification of the CBs is impossible (eg. Figure D.7C). While dorsal closure succeeds, the layer of ectoderm is often thin and variable (Figure D.7B-D). However, despite these defects in the surrounding tissues, in regions of the embryo where contralateral CBs meet at the midline, a lumen, albeit small, often forms (Figure D.7D). As low levels of Src42A can be detected in late stage embryos (Shindo *et al.* 2008), it is possible that low levels of maternal Src42A are sufficient for lumen formation. However, taken together with the tissue-specific dominant negative data, it appears that Src42A is not required in the CBs to promote lumen formation. Rather, the heart defects observed in *src42A* mutants are due to disruptions in dorsal closure and amnioserosa internalisation.

Figure D.7 - Cardioblasts at the midline are capable of developing an open lumen between contralateral cells

In stage 17 wildtype embryos (**A**), contralateral cardioblasts ('c') are present at the dorsal midline and enclose a lumen (arrow). Dorsal to the heart is a thick and continuous ectoderm (horizontal arrow) and few if any amnioserosa cells remain ventrally (asterisks). In *src42A*^{E1} mutants, the ectoderm layer is thin and variable (horizontal arrow in **B-D**) and amnioserosa cells persist at or near the midline (asterisks; for some cells marked with an asterisks, identity is uncertain). The cardioblasts are not consistently present at the midline (eg. c? in **C**); however, when two contralateral cardioblasts are present, a small lumen often forms (arrow in **D**). Dorsal at top. Calibration: 10 microns.

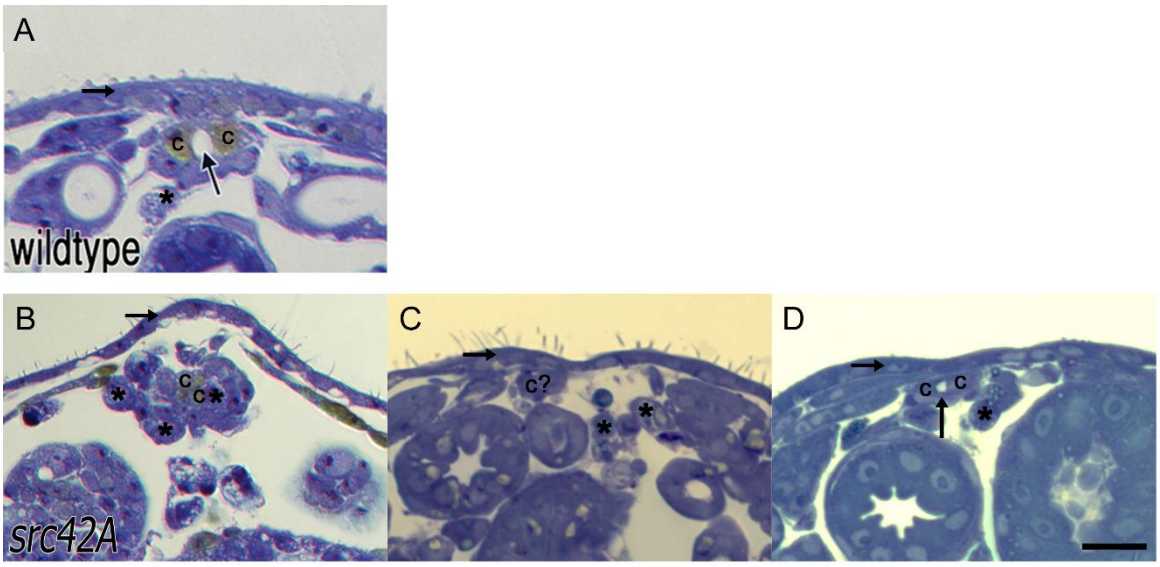
A
c
c
*
wildtype
B
c
c
*
*
*
src42A
C
c?
*
*
D
c
c
*

D.3 Conclusion

The transmembrane integrin heterodimer transduces signals into the cell through numerous cytoplasmic adhesome proteins. Two of these adhesome components, Src and FAK, play important roles in collective cell migration by coordinating integrins (cell-ECM adhesion), E-cad (cell-cell adhesion), and cytoskeletal dynamics. I have explored a putative role for Src-FAK signaling in *Drosophila* cardial cell migration and heart lumen formation. Src42A, but not Src64B or Fak56D, is essential for heart assembly. In particular, *src42A* mutant embryos have stalled migration of posterior CBs. These migration-defective CBs are unable to extend a dynamic membrane leading edge characteristic of motile cells. However, upon closer examination, CB migration in *src42A* mutant embryos appears to be physically inhibited by dorsal amnioserosa cells which fail to internalize. Cardial cells which do reach the midline are able to complete tubulogenesis and form an open lumen. Furthermore, heart tissue-specific disruption of Src42A activity does not perturb cardial cell migration nor βPS1 integrin luminal localization. Thus, in contrast to its role during dorsal closure, Src42A is likely not essential for integrin-mediated adhesion or signaling during tubulogenesis of the embryonic heart.

Recipe for common reagents

APPENDIX E

Solutions are stored at room temperature unless otherwise stated.

Fly food

Solution A (4 litre flask)

2400 ml	dH_2O
300 g	Sucrose
24 g	Sodium Potassium Tartrate tetrahydrate (Fisher S387-500)
3 g	Dipotassium orthophosphate dibasic (Fisher P288-500)
1.5 g	Sodium chloride (Sigma S3014-5kg)
1.5 g	Calcium chloride (Caledon 2520-1)
1.5 g	Magnesium chloride (Fisher BP214-500)
1.5 g	Ferric sulphate (MP Biomedical 158042)
54.5 g	Agar – 700B agar powder form (Moorhead and Company)

Solution B (2 litre flask)

600 ml	dH_2O
150 g	Yeast – Fleisc active dry yeast (Traynor's 2192)

Acid mix (Store at 4°C)

20.75 ml	85% phosphoric acid (Fisher 351290-500)
209 ml	Propionic acid – Fisher A258-500
to 500 ml	ddH_2O

Preparation notes:

Autoclave Solutions A and B on liquid cycle 1 (20 minutes) and mix immediately upon removal from autoclave. Cool (with constant stirring) to 55°C. Add 22ml 10% tegosept in absolute ethanol (methyl-4-hydroxybenzoate; Sigma H5501; store at 4°C) and 15ml acid mix. Pour into vials for stocks (Fisher AS519) or 16x100 mm pairwise tubes for crosses and weak stocks (Fisher 1496129) Plug with Rayon (Fisher 1264041) and store in a plastic bag at 4°C for up to one month.

Yeast Paste

- Yeast – Fleisc active dry yeast (Traynor's 2192)
- ddH_2O

Add water to yeast in 50 ml conical tube. Mix thoroughly until paste is homogenous and of toothpaste consistency. Store at 4°C.

Apple Juice Agar Plates

Solution A (4 litre flask)

3000 ml dH_2O

90 g Agar – 700B agar powder form (Moorhead and Company)

Solution B (2 litre flask)

1000 ml apple juice (eg. 2L Rougemont Royal Gala Apple Juice)

100 g Sucrose

Preparation notes:

Autoclave Solutions A and B on liquid cycle 1 (20 minutes) and mix immediately upon removal from autoclave. Cool (with constant stirring) to 45°C. Add 40 ml 10% tegosept in absolute ethanol (methyl-4-hydroxybenzoate; Sigma H5501). Pour into eight 1 L flasks (autoclaved on dry cycle 2). Store at 4°C until needed.

Pouring plates:

Microwave (previously prepared) agar for approximately five minutes, stirring every two minutes. Pour into 60x15 mm petri dishes (BD Falcon 353002; makes ~60 plates). Cool at room temperature until agar solidifies (~30 minutes). Cover with lids and store upside down at 4°C for up to one week.

10x Phosphate Buffer Saline (10xPBS)

1800 ml ddH_2O

7.68 g $NaH_2PO_4*H_2O$

35.82 g Na_2HPO_4

306.6 g NaCl

Adjust pH to 7.4 with NaOH pebbles. Pour into ten 1 L bottles (with caps loose). Autoclave on liquid cycle 1 (20 minutes).

PBT (ie. PBS + 0.1% Triton)

100 ml 10xPBS

900 ml ddH_2O

1 ml Triton-X 100 (Fisher BP 151-500)

PBS + 0.1% Tween 20

100 ml 10xPBS

900 ml ddH_2O

1 ml Tween 20 (Fisher BP 337-500)

Luria-Bertani (LB) media (with 0.1mg/mL ampicillin)

10 g	Tryptone
5 g	Yeast Extract
10 g	NaCl
to 1000 ml	ddH_2O

Autoclave on liquid cycle 1 (20 minutes). Cool to ~55°C. Add 1 ml 100 mg/ml ampicillin. Store at room temperature for up to six months.

Western reagents:

SDS-PAGE gel

6% resolving gel (for two gels)

5.3 ml	ddH_2O
2.0 ml	30% acrylamide mix (!)
2.5 ml	1.5M Tris (pH 8.8)
100 µl	10% sodium dodecyl sulphate (use 37°C waterbath to fully dissolve SDS)
8 µl	TEMED (!)
100 µl	10% ammonium persulfate (!) (make fresh every month)

10% resolving gel (for two gels)

4.0 ml	ddH_2O
3.3 ml	30% acrylamide mix (!)
2.5 ml	1.5M Tris (pH 8.8)
100 µl	10% sodium dodecyl sulphate (use 37°C waterbath to fully dissolve SDS)
4 µl	TEMED (!)
100 µl	10% ammonium persulfate (!) (make fresh every month)

Stacking gel (for two gels)

2.7 ml	ddH_2O
0.67 ml	30% acrylamide mix (!)
0.5 ml	1.0M Tris (pH 6.8)
40 µl	10% sodium dodecyl sulphate (use 37°C waterbath to fully dissolve SDS)
4 µl	TEMED (!)
40 µl	10% ammonium persulfate (!) (make fresh every month)

Preparation notes:

Add first four ingredients for both stacking and resolving gels in 15 ml conical tubes. Prepare gel casing. Degas resolving gel solution for ten minutes. Add TEMED and then ammonium persulfate to resolving gel mix. Immediately mix (gently by inverting tube) and pour gel. Add a thin layer of ddH_2O to prevent gel dehydration and wait for gel to polymerize (~20-30 minutes; until the water-gel separation is apparent). Remove water and add comb. Add TEMED and then ammonium persulfate to stacking gel mix. Immediately mix (gently by inverting tube) and pour on top of resolving gel. Allow gel to polymerize. Use gel immediately or wrap in saran and save for maximum one day at 4°C.

10x Running Buffer (for SDS-PAGE gels)

800 ml	ddH_2O
30.2 g	Tris base (Bioshop TRS001.1)
188 g	Glycine (Bioshop GLN001-500)
10 g	Sodium dodecyl sulphate (Sigma L6026-250g)

Stir until dissolved (likely overnight). Adjust volume to 1000 ml with ddH_2O.

Transfer Buffer

3 g	Tris base (Bioshop TRS001.1)
14.4 g	Glycine (Bioshop GLN001-500)
100 ml	Methanol (Caledon 6700-1)
to 1000 ml	ddH_2O

Time-lapse movies

APPENDIX F

The following time-lapse videos are supplemental to the still images presented in this thesis:

Movie 1 – Wildtype - as in Figures 3.6, 4.9, D.4
Movie 2 – *mys*^{1}/Y – as in Figure 3.6
Movie 3 – *mys*^{1}/+
Movie 4 – *rhea*^{79}/+ - as in Figure 4.9
Movie 5 – *rhea*^{79}/*rhea*^{79} (zygotic) – as in Figure 4.9
Movie 6 – *rhea*^{79}GLC/*rhea*^{79} (maternal and zygotic) – as in Figure 4.9
Movie 7 – *src42A*^{E1}/*src42A*^{E1} – as in Figure D.4